University of Almeria

ASSESSMENT OF SOLAR-DRIVEN PROCESSES AND OZONATION FOR DISINFECTION, DECONTAMINATION AND REUSE OF FRESH-CUT WASTEWATER

Leila Samira Nahim Granados

PhD Thesis

Almería, January 2020

University of Almeria

Departamento de Ingeniería Química

Doctorado en Biotecnología y Bioprocesos Industriales aplicados a la Agroalimentación , Medioambiente y Salud

ASSESSMENT OF SOLAR-DRIVEN PROCESSES AND OZONATION FOR DISINFECTION, DECONTAMINATION AND REUSE OF FRESH-CUT WASTEWATER

DESARROLLO Y APLICACIÓN DE PROCESOS FOTOQUÍMICOS Y FOTOCATALÍTICOS PARA LA DESINFECCIÓN, DESCONTAMINACIÓN Y REÚSO DE AGUAS PROCEDENTES DE LA INDUSTRIA DE IV GAMA

Memory presented for the title of Doctor:

Leila Samira Nahim Granados

Almería, January 2020

THESIS SUPERVISORS:

Dr. María Inmaculada Polo López
Research Fellow OPI
CIEMAT-PSA

Dr. José Antonio Sánchez Pérez
Full professor
University of Almeria

Tras mucho andar llegué hasta este precipicio

y sé que no, no es el final

sino el principio.

Agradecimientos

Llegados a este punto, es también importante mostrar el agradecimiento hacia todas y cada una de las personas que de una manera u otra han contribuido a que este momento llegue.

Para llegar al inicio de una Tesis doctoral es necesario el apoyo y esfuerzo de muchas personas. Académicamente, no quiero pasar por alto el esfuerzo de todo el personal educativo que ha contribuido a mi formación desde las primeras etapas hasta esta última… qué importante es contar con un sistema de educación pública a este nivel. Gracias. Dentro de estos profesionales, me gustaría destacar el papel de Antonio Romerosa y Manuel Serrano. Gracias por abrirme las puertas de la investigación y transmitirme vuestra pasión por ella.

Personalmente, es mi familia quien merece por mi parte el mayor de los agradecimientos. A mis abuelos y mis dos tíos, por ser mis segundos padres mientras ellos trabajaban por mi futuro. A mis tíos, además, por incentivar desde los inicios mi rendimiento académico y seguir apoyándome hasta ahora. A mi tía, por ser el mayor ejemplo de resilencia que conozco, por estar siempre. A mis primos, aunque somos pocos siempre hemos sabido mantenernos unidos, que orgullosa estoy de las personas en las que os estáis convirtiendo! A mi hermano, por ser mi compañero, amigo, por protegerme y apoyarme desde que llegue a este mundo, que regalo tenerte en mi vida. A mi cuñada, una más de la familia, eres muy importante para mí, que suerte la nuestra! Y como no, a mis padres. A vosotros os debo todo lo que soy. Gracias por sacrificaros por nosotros, nunca nos ha faltado nada... porque los valores no se compran y de eso hemos tenido de sobra. Por enseñarme el valor de las cosas y como conseguirlas: humildad, sacrificio y esfuerzo. Porque sois la mezcla perfecta, tú Papá, la exigencia, la ironía y la picardía… por enseñarme desde los inicios a intentar hacer las cosas mejor, mejor y mejor.Tú Mamá, la dulzura, la inocencia, la paciencia, el vivir por y para nosotros, mi apoyo. Gracias por darme esta familia, os quiero.

Como toda Tesis, ésta comienza con una decisión, muy difícil en mi caso, aunque creo que finalmente muy acertada. En este punto, quiero agradecer a

Pilar. Gracias Pilar por respetar mi decisión y darme esta oportunidad… esa fue la primera muestra de la gran persona que iba a descubrir, siempre con los valores por delante. Eres para mí todo un ejemplo, personal y profesional, podría enumerar muchos aspectos que admiro de tí pero voy a intentar resumirlos en dos: valentía y rigor científico.

Una vez dentro de esta nueva etapa, llegó el momento de descubrir las personas que se iban a encargar de ser mi guía durante ella. Inmaculada Polo y Jose Antonio Sánchez, mis directores. Pronto, fui consciente de lo afortunada que era por contar con su dirección. Esta tesis no hubiera sido posible sin vuestro apoyo y conocimiento. Jose Antonio, gracias, gracias por tu apoyo, consejos, por enseñarme a pensar ingenierilmente y confiar desde el minuto cero en mí. Inma, tú eres la energía de activación de esta tesis, esto no sería posible sin tí. Gracias por catalizar mis virtudes y desactivar mis defectos. Reúnes todos los nutrientes necesarios para hacer crecer exponencialmente a cualquier persona que pase por tus manos convirtiéndola no solo en un mejor profesional, si no también, en una mejor persona. Tengo tantísimo que agradecerte, que creo que se convierte en incontable por esta técnica, por lo que voy a intentar resumirlo tras n-diluciones seriadas: gracias por tu paciencia infinita, comprensión, exigencia y rigor científico, tu calidad y humildad tanto humana como profesional, por confiar siempre en mí, por tu sinceridad, por no perder nunca la sonrisa, por enseñarme tantísimas cosas del trabajo y de la vida… Eres el espejo donde mirarme.

Al grupo de investigación donde he tenido la suerte de desarrollar esta tesis doctoral, formado por grandes personas y profesionales. Nacho y Leo, gracias por vuestro apoyo y buena actitud. Sixto, gracias por tu profesionalidad, por confiar en mí, por estar siempre dispuesto a resolver una duda (y resolverla), por tu exigencia y saber hacer. Isa, gracias por tu cercanía, confianza, apoyo, ayuda, paciencia y profesionalidad. Soy consciente de lo difícil que es lidiar y ser la jefa de esta manada de leonas implicándote en ello, y tú has sido capaz de hacerlo. Eli e Isa, las dos técnicos de laboratorio, sin las cuales no sería posible llevar nuestro frenético ritmo de trabajo, gracias por vuestra ayuda y apoyo. Eli, tú has sido otro de mis grandes apoyos, mi tercera y cuarta mano y culpable de

apoyarme o hacerme desistir de muchos de mis locos planes experimentales. Gracias.

A todas mis compañeras de batallas solares durante estos 4 años. Laura, otro de mis apoyos durante mas de 2 años tanto personal como profesionalmente, eres todo un ejemplo para mí. María, a ti tengo muchísimo que agradecerte (podría tripitir agradecimientos): tú me enseñaste a dar mis primeros pasos laboralmente, con paciencia (y exigencia) has tratado siempre de ayudarme y enseñarme todo lo que estaba en tu mano. Personalmente, considero que ha sido una suerte conocerte, te aprecio y admiro a partes iguales. Alba, otro descubrimiento más bien tardío, pero no importa la espera si la dicha es buena. Tú también te has convertido en una persona fundamental para mí durante este último periodo, qué importante es tener cerca personas integras como tú. Ana, Melina, Azahara y Dennis, gracias por estar siempre ahí, ha sido un placer compartir tantas cosas con vosotros y sobretodo infinidad de risas muy necesarias en muchos momentos. Irene, tú has sido mi compañera (entre otros) de batallas, fiestas y confesiones. Gracias por tu apoyo durante todo este tiempo. Ilaria, gracias, por tus ganas de aprender, por tu buen ser y hacer, por confiar en mí y estar siempre ahí, vas a conseguir todo lo que te propongas…pequeño saltamontes. Y como no, qué haríamos en las plantas piloto sin nuestro apoyo. Agustín, tú eres el premio gordo de toda esta lotería… eres y seguramente serás de las mejores personas que la vida me dé la oportunidad de cruzarme, tienes un corazón enorme (y blanco)… y aunque no de sangre, para mí ya eres familia. Panchi, gracias por haber estado y estar siempre atento para echar una mano, por tu nobleza, paciencia y especial sentido del humor.

No puedo dejar de agradecer a todos y cada uno de los profesionales que desempeñan su labor en la PSA y hacen posible de una manera u otra que personas como yo puedan llevar a cabo su trabajo. De todos ellos, me gustaría destacar a aquellos con los que he podido tener un mayor trato personal y profesional: Carmela, Inés, Irene, Jesús Torrecillas, Pepe Luis, Marta y Carmen. Ha sido un placer conoceros y compartir con vosotros todo este tiempo, gracias!

Trabajar en este centro de referencia también me ha brindado la posibilidad de colaborar y conocer a decenas de investigadores de todas partes del mundo, de todos he aprendido algo, gracias. Entre ellos, algunos han dejado una huella especial: Margarita, Mercedes, Chus, Mohamed, Leonor, Teresa, Yeli y la versión valenciana y femenina de Zipi y Zape (Paula y Sara). Gracias a todos por tantísimos buenos momentos.

Moreover, this PhD stage gave me also the opportunity to stay during 3 months in the NIBEC research centre (Ulster University, Belfast) in the group of photocatalysis leaded by Dr. Tony Byrne. In these months, I felt at home and learned from all of them…thank you to the whole work group (Tony, Pilar, Patrick, Jeremy, Preetam, Stuart and Anukriti). Besides, in this research centre I found five wonderful people (Mariana, Rita, Bruno, Dilli and Daragh) with whom enjoying all the wonders of the city (including the yellow bus), thank you all.

Al personal de CIESOL, que ha colaborado científicamente en este trabajo. A Ana Agüera y todo su equipo. Ana, muchas gracias por todo, por tu gran profesionalidad, por estar siempre dispuesta a ayudarme y ser como eres. Ha sido un placer poder colaborar contigo durante todos estos años. A todo el equipo de trabajo que ha tenido que lidiar con mis muestras: Patricia, Eli, Marina, Ana.L y Ana.M. En especial, a tí Ana.M., un apoyo incondicional, mi compañera y amiga, una excelente profesional y persona. Gracias.

A los otros dos hermanos mayores que la vida me ha regalado: Franco y Gracia. Franco, tú has sido un ejemplo desde mis inicios en la investigación, me has enseñado, cuidado y protegido desde que te conozco. Gracias por cuidar y hacer mejor a tu hermanica. Gracia, otro regalo de la investigación, eres transparencia, nobleza y humildad. Has sido mi confidente, a quien acudir cuando las cosas van bien o no tan bien, uno de mis apoyos fundamentales. Gracias por todo.

Por último pero no menos importante, quiero agradecer a todos los amigos que durante estos años (y bastantes atrás) siguen a mi lado en las duras y en las maduras. Los de siempre: Victor, Nana, Laura, Mari Angeles, Mary, Laure,

Xoto, Yvan, Sandra, etc. Y los amigos que me regaló química: Ana, Reche, Luis, Cuti, Pepa, Zoe, Carmen, Pablo, Lucía y Encarni.

Thesis framework and scientific production

The research presented in this thesis has been developed in the framework of national project WATER4CROP (CTQ2014-54563-C3-3-R), supported by the Spanish Ministry of Economy and Competitiveness (MINECO).

The results shown in this memory have been published or are in process of being published in international journals with high scientific impact factor:

1. S. Nahim-Granados, M.I. Polo-López, J.A. Sánchez-Pérez. **Effective solar processes in fresh-cut wastewater disinfection: inactivation of pathogenic *E. coli* O157:H7 and *Salmonella enteritidis**. *Catalysis Today.* **313**, 79-85, 2018. IF: 4.888

2. S. Nahim-Granados, I. Oller, S. Malato, J.A. Sánchez-Pérez, M.I. Polo-López. **Commercial fertilizer as effective iron chelate (Fe^{3+}-EDDHA) for wastewater disinfection under natural sunlight for reusing in irrigation**. *Applied Catalysis B: Environmental.* **253**, 286–292, 2019. IF: 14.229

3. S. Nahim-Granados, G. Rivas-Ibáñez, J.A. Sánchez-Pérez, I. Oller, S. Malato, M.I. Polo-López. **Fresh-cut wastewater disinfection and decontamination by ozonation at pilot scale**. *Water Research.* **170**, 115304, 2020. IF: 7.913

4. S. Nahim-Granados, G. Rivas-Ibáñez, J.A. Sánchez-Pérez, I. Oller, S. Malato, M.I. Polo-López. **Solar driven processes to reclaim wastewater from fresh-cut industry: techno-economical assessment of pathogens and organic microcontaminants removal at pilot plant scale.** *Applied Catalysis B: Environmental.* Submitted. IF: 14.229

5. S. Nahim-Granados, G. Rivas-Ibáñez, J.A. Sánchez-Pérez, I. Oller, S. Malato, A. Agüera, P. Plaza-Bolaños, M.I. Polo-López. **Chemical and microbial risk assessment of fresh-cut wastewater reclamation for reuse in agriculture**. In preparation.

Moreover, **9 Oral and 5 Poster communications** have been presented by the PhD candidate in different International Conferences.

Furthermore, the PhD candidate has collaborated with other researchers, from which is co-author of the following publications in journals with high scientific impact factor:

1. M.I. Polo-López, <u>S. Nahim Granados</u>, P. Fernández Ibáñez. **Homogeneous Fenton and Photo-Fenton Disinfection of Surface and Groundwater** (<u>Chapter</u> 169), in Applications of Advanced Oxidation Processes (AOPs) in Drinking Water Treatment, Eds. A. Gil et al. The Handbook of Environmental Chemistry, Springer International Publishing AG, 2018, ISBN: 978-3-319-76881-6.

2. M. I. Polo-López, M. Castro-Alférez, <u>S. Nahim-Granados</u>, S. Malato, P. Fernández-Ibáñez. *Legionella jordanis* **inactivation in water by solar driven processes: EMA-qPCR versus culture-based analyses for new mechanistic insights**. *Catalysis Today.* **287**, 15–21, 2017. IF: 4.667

3. Luigi Rizzo, Teresa Agovino, <u>S. Nahim-Granados</u>, M. Castro-Alferez, P. Fernández-Ibáñez, M.I. Polo-Lopez. **Tertiary treatment of urban wastewater by solar and UV-C driven advanced oxidation with peracetic acid: Effect on contaminants of emerging concern and antibiotic resistance**. *Water Research.* **149**, 272-281, 2019. IF: 7.913

4. A.B. Martínez-Piernas, <u>S. Nahim-Granados</u>, M.I. Polo-López, P. Fernández-Ibáñez, S. Murgolo, G. Mascolo, A. Agüera. **Identification of transformation products of carbamazepine in lettuce crops irrigated with Ultraviolet-C treated water**. *Environmental Pollution.* **247**, 1009-1019, 2019. IF: 5.714

5. Y. Aguas, M. Hincapié, A.B. Martínez-Piernas, A. Agüera, P. Fernández-Ibáñez, <u>S. Nahim-Granados</u>, M. I. Polo-López. **Reclamation of Real Urban Wastewater Using Solar Advanced Oxidation Processes:**

An Assessment of Microbial Pathogens and 74 Organic Microcontaminants Uptake in Lettuce and Radish. *Environmental Science & Technology.* **53**, 9705-9714, 2019. IF: 7.149

6. L.C. Ferreira, M. Castro-Alférez, <u>S. Nahim-Granados</u>, M.I. Polo-López, M.S. Lucas, G. Li Puma, P. Fernández-Ibáñez. **Inactivation of water pathogens with solar photo-activated persulfate oxidation.** *Chemical Engineering Journal.* **381**, 122275, 2020. IF: 8.355

7. S.G. Michael, I. Michael-Kordatou, <u>S. Nahim-Granados</u>, M.I. Polo-López, J. Rocha, A.B. Martínez-Piernas, P. Fernández-Ibáñez, A. Agüera, C.M. Manaia, D. Fatta- Kassinos. **Superiority of UV-C/H$_2$O$_2$ over solar/H$_2$O$_2$ oxidation for the removal of antibiotic resistance determinants and toxicity from urban wastewater.** *Chemical Engineering Journal.* Under revision. IF: 8.355

INDEX OF CONTENTS

INDEX OF FIGURES

INDEX OF TABLES

ABBREVIATIONS

ACN	Acetonitrile
ADI	Acceptable daily intake
AOP	Advanced oxidation process
ATZ	Atrazine
AZX	Azoxystrobin
BOD_5	Biological oxygen demand
BPF	Buprofezin
C_a	Chlorophyll a
CAT	Catalase
C_b	Chlorophyll b
CEC	Contaminant of emerging concern
CECT	Spanish Type Culture Collection
CFU	Colony forming unit
C_I	Investment cost
C_M	Maintenance cost
C_O	Operational cost
COD	Ordinary legislative procedure
COT	Committee on Toxicity of Chemicals in Food, Consumer Products and the Environment
CPC	Compound parabolic collector
DAD	Diode array detector
DALY	Disability-adjusted life year

DBP	Disinfection by-product
DIC	Dissolved inorganic Carbon
DL	Detection limit
DNA	Dexoxyribonucleic acid
DOC	Dissolved organic carbon
DOM	Dissolved organic matter
EDDHA	Ethylenediamine-N',N'-bis 2-hydroxyphenylacetic acid
EDDS	Ethylendiamine-N',N'-disuccinic acid
EDG	Electron-donating group
EDI	Estimated daily intake
EDTA	Ethylendiaminetetracetic acid
EFSA	European Food Safety Authority
EQS	Environmental quality standards
EU	European Union
EU WFD	European Union Water Framework Directive
FAO	Food and Agriculture Organization
FCWW	Fresh-cut wastewater
FDA	The Food and Drug Administration
G %	Germination rate
HI	Hazard index
HPLC	High performance liquid chromatography
HQ	Hazard quotient
I	Inhibition

IFPA	International Fresh-Cut Produce Association
IMD	Imidacloprid
ISO	International Organization for Standardization
IW	Isotonic water
LOD	Limit of detection
LOQ	Limit of quantification
LPS	Lipopolysaccharides
LRV	Log reduction value
MLR	Maximum residue level
NSE	No significant effects
NTA	Nitrilotriacetic acid
NTU	Nephelometric turbidity unit
OD	Optical density
OM	Organic matter
OMC	Organic microcontaminant
PAC	Powered activated carbon
PCM	Procymidone
PHS	Priority hazardous substances
POP	Persistent organic pollutant
PS	Priority substance
PSA	Plataforma Solar de Almería
QMRA	Quantitative microbial risk assessment
Q_{uv}	Cumulative UV energy

RD   Real Decree

RGI   Relative growth index

ROS   Reactive oxygen species

rpm   Revolutions per minute

S   Stimulation

SDGs   Sustainable development goals

SFCWW   Synthetic fresh-cut wastewater

SOD   Superoxide dismutase

SPE   Solid phase extraction

SZ   Simazine

TBY   Terbutryn

TC   Total carbon

TDC   Total dissolved carbon

THM   Trihalomethane

TMX   Thiamethoxam

TSS   Total suspended solids

U.S.   United States

UN   United Nations

UNESCO   United Nations Educational, Scientific and Cultural Organization

UPLC   Ultra performance liquid chromatography

UV   Ultraviolet

w/v   Weight/volume

WHO   World Health Organization

WW   Wastewater

WWTP   Wastewater treatment plant

SUMMARY / RESUMEN

SUMMARY

The world is undergoing global socio-economic changes that involve important environmental problems like water scarcity where agriculture plays a critical role due to its high consumption of freshwater resources. The intensification of water stress generates new water-food challenges to current and future sustainability agriculture. Therefore, the implementation of emerging technologies in order to respond to these pressures in water-scarce countries is crucial. In this regard, agro-food industrial wastewater (WW) reuse for agriculture represents an unconventional water supply, improving the water use efficiency. Among the different agro-food industries, the fresh-cut produce industry stands out for its rapid development in the last years due to the trend of demand for healthy, nutritious and fresh food marketed as 'ready-to-eat'. This industry is one of the major water consumers in the agro-food sector due to the high water volumes (up to 40 m^3/ton of raw product) required mainly during the vegetables wash stage.

The consumption of fresh-cut products is an important route of foodborne pathogens transmission when a proper disinfection treatment is not applied in the production process. In fact, several worldwide outbreaks attributed to the consumption of raw-eat vegetables have been reported over the past few years. In spite of the microbiological risk, the wastewater generated by this industry is also an important source of organic microcontaminants (OMCs) (mainly pesticides) which are not yet regulated. To avoid the associated risk with pathogens, the most common strategy in this industry is the use of chlorine compounds as a sanitizing agent during the washing step. Nevertheless, the commonly hyper-chlorination practice linked with the high quantity of dissolved organic matter in this water matrix leads to the generation of unhealthy disinfection by-products (DBPs) and has resulted in the forbiddance of the chlorination practice in some European countries. Moreover, the chlorination process does not efficiently degrade chemical contaminants and it therefore does not control their accumulation during the processing stage.

Consequently, the search and evaluation of new or alternative water treatments able to reduce simultaneously the microbiological and organic chemical contamination without DBPs formation in this industry has grown recently.

The general aim of this study is to investigate the use of solar-driven technologies (solar photo-Fenton and H_2O_2/solar) and a conventional process (ozone) for the improvement of fresh-cut wastewater (or washing water) to reach the chemical and microbiological quality established on wastewater reuse guidelines for irrigation in agriculture. In this study, the selected targets were two human bacterial pathogens (*E. coli* O157:H7 and *S. enteritidis*) as model of microbial contamination and a mix of OMCs (atrazine, azoxystrobin, buprofezin, imidacloprid, procymidone, simazine, thiamethoxam and terbutryn) as model of chemical contamination (pesticides).

Firstly, a synthetic fresh-cut wastewater (SFCWW) recipe was formulated to be used along this study as a tool to avoid water characteristics fluctuations of real matrices and therefore to perform more realistic comparisons between different treatments and experimental conditions. Although the solar processes have proven to be effective for disinfection of different types of water matrices, the high turbidity (100 NTU) of SFCWW makes necessary to study the disinfection capability of solar processes in this particular water matrix. In line with this, the disinfection capability of four solar processes (solar photo-inactivation, H_2O_2/solar, Fe/solar and solar photo-Fenton) was studied at laboratory scale and under controlled conditions in a solar simulator. The results obtained clearly indicate their capability to disinfect SFCWW in short treatment times (> 5 Log Reduction value (LRV) in < 45 min) in all cases. The best disinfection efficiency was obtained for the H_2O_2/solar process using 20 mg/L of oxidant and requiring less than 20 min of treatment regardless of the year season, making this process a promising option to disinfect fresh-cut wastewater. Nevertheless, the low disinfection capability shown by the iron/solar processes (mainly explained by iron speciation at SFCWW pH, i.e., 6.25) indicates the need to use alternatives iron sources which let improving the disinfection efficiency.

In this context, the assessment of different iron sources (mainly iron chelates and iron complexes) that allow the iron kept in solution longer, increasing the process efficiency is a key research topic in the last years. In this study, the use of a commercial iron fertilizer (Fe^{3+}-EDDHA) employed to remediate iron chlorosis in agriculture has been investigated for the first time as a bactericidal agent in solar water disinfection processes in comparison with the conventional use of iron salts. The study was carried out at laboratory scale (200 mL), under natural solar radiation, with reagent concentrations ranged from 0.5 to 5 mg/L of iron and in two water matrices with different complexity: isotonic water (IW) and SFCWW. The results showed a clear improvement of the solar disinfection efficiency when using the new iron source (45 min) in comparison with the conventional one (iron salts) that required 90 min of treatment time. Moreover, an inactivation mechanism was proposed to explain both, the loss of bacterial viability and the different resistant of each bacterial strain to be inactivated (*S. enteritidis* showed higher resistance than *E. coli* O157:H7). Briefly, the mechanism proposed was mainly attributed to changes in the cell membrane permeability when Fe^{3+}-EDDHA is present and on structural damages caused by hydroxyl radicals (HO$^•$) for Fe^{3+}-EDDHA/H_2O_2/solar process.

These promising disinfection results were latter on investigated simultaneously with OMCs decontamination at pilot plant scale in SFCWW to determine the capability of these solar processes to be applied at pre-industrial scale. For this purpose, solar experiments (H_2O_2/solar, Fe^{3+}-EDDHA/solar and Fe^{3+}-EDDHA/H_2O_2/solar) were conducted under natural sunlight using tubular reactors of 60 L treatment capability provided with Compound Parabolic Collector. The experimental results obtained showed high efficiency to reduce the microbiological contamination (>5-LRV in 60 min) and moderate efficiency to reduce the OMCs load (from 20 to 40 %) for all the solar processes studied.

Ozone and peroxone processes (ozone with added H_2O_2) at pilot plant scale (10 L) were also investigated as conventional advanced oxidation processes (AOPs). The capability of both processes for the simultaneous disinfection and

decontamination of SFCWW under several operational conditions: natural SFCWW pH (6.25) and basic pH (11), two different initial ozone productions (0.09 and 0.15 gO_3/Lh) and the addition of 20 mg/L of H_2O_2 have been investigated. The results obtained shown that the highest efficiency for OMC removal (85 %) and pathogen inactivation (> 5-LRV) were obtained with the simplest condition, i.e., ozonation treatment at natural pH requiring the following ozone doses: < 10 and < 30 mgO_3/L for SFCWW disinfection and decontamination, respectively.

In summary, the purification results obtained have significant implications due to the solar processes as well as the ozonation process investigated have demonstrated to allow safe wastewater reclamation for irrigation purpose.

Once the treatment capacity of the selected processes were investigated at pilot scale, irrigation tests in an experimental greenhouse using two raw eaten vegetables (radish and lettuce) were performed to investigate the application of treated SFCWW for agriculture purpose, demonstrating also the reduction of the water-footprint of this industry. The irrigation tests were done using the best operational conditions obtained for each solar treatment (H_2O_2/solar and Fe^{3+}-EDDHA/H_2O_2/solar) and ozonation (at natural pH). In addition, untreated SFCWW spiked with target contaminants (used as positive control) and mineral water with a total absence of target contaminants (used as negative control) were also investigated in this study. In general, the analysis of harvested crop samples irrigated with treated SFCWW revealed a complete absence of pathogens, i.e., below the limit of detection (LOD), of 1 CFU/99 g in lettuce and <1 CFU/8 g in radish for all the treatments evaluated and both crops. For OMCs, in all processes in comparison with the results ontained with untreated SFCWW a clear reduction on their uptake by crops was observed. In particular, the crops irrigated with ozonated SFCWW shown the highest reduction of OMCs uptake by crops: 95 and 92 % in lettuce and radish, respectively. In the case of solar processes, the reduction of OMCs uptake varied from 64 to 77 % in lettuce and from 43 to 59 % in radish, for all the solar processes evaluated. Nevertheless,

lettuce crops irrigated with treated SFCWW by the solar process that incorporate the iron micronutrient (Fe^{3+}-EDDHA/H_2O_2/solar) showed twice chlorophyll content than those irrigated by ozonated and H_2O_2/solar treated water. Therefore, in view of the results, the physiologic benefit of crops by the employ of Fe^{3+}-EDDHA as iron source to reuse treated water by solar processes was also confirmed. In general, the results obtained support the suitability of the solar processes studied to reduce both: the crops contamination (microbiological and chemical) and the iron chlorosis risk.

Finally, a techno-economic, environmental and health risk evaluation of the global processes was done to determine the implementation viability of the studied processes (ozonation, H_2O_2/solar and Fe^{3+}-EDDHA/H_2O_2/solar) including chlorination as a reference of the more widely applied disinfection process in this type of industry. The environmental evaluation was performed by ecotoxicity studies using different tests applied to the treated SFCWW: *Vibrio fischeri* test to evaluate the impact discharges and *Lactuca sativa* test to determine the suitability for crops irrigation. The results obtained with *V. fischeri* showed non-acute toxicity for solar treated SFCWW, slight acute toxicity for ozonated SFCWW and acute toxicity for chlorinated SFCWW. The results obtained with *Lactuca sativa* tests showed in general non-significant effects for ozonated and solar treated SFCWW and an inhibition grown effect with chlorinated SFCWW. Therefore, these results confirm the suitability of ozone and solar processes for subsequent SFCWW reuse and exacerbate the non-suitability of the chlorination process for the same purpose.

The economic analysis for the simultaneous disinfection and decontamination of SFCWW at the best operational conditions founded shown treatment costs of ca. 1.15 €/m³ for ozonation and ca. 1.60 €/m³ for Fe^{3+}-EDDHA/H_2O_2/solar process. These treatment costs are almost twice of the obtained for chlorination (ca. 0.70 €/m³), which is, at industrial scale, the main barrier for changing to other alternative process.

Lastly, a chemical and microbiological health risk assessment of the crops irrigated with treated SFCWW (by ozone and solar processes) and untreated SFCWW was performed using: i) the estimation of the hazard index (HI) as a tool to estimate the dietary risk assessment for the combined exposure of the chemical contaminants and ii) the quantitative microbial risk assessment (QMRA) based on dose-response models and Monte Carlo simulations using the software FDA-iRISK®. The results obtained from the dietary risk assessment of the OMC residues in lettuce and radish showed that any of the vegetables irrigated with treated or untreated SFCWW entail a significant health risk, being lower the risk associated with treated SFCWW. In the case of the QMRA, the crops irrigated by untreated SFCWW represent an important infection risk for the consumer whereas the crops irrigated by the treated SFCWW demonstrated a reduction of more than 4 orders of magnitude the infection risk associated to the consumption of raw vegetables.

RESUMEN

El mundo está experimentando cambios socioeconómicos globales que generan importantes problemas medioambientales como la escasez de agua dulce donde la agricultura juega un papel clave debido a su alto consumo de recursos hídricos. La intensificación de la escasez de agua genera nuevos desafíos para una agricultura sostenible, tanto actual como futura. Por lo tanto, la implementación de tecnologías emergentes para responder a estas presiones en países con escasez de agua es crucial. En esta línea, el uso de aguas residuales procedentes de industrias agroalimentarias con el fin de su regeneración y reutilización en agricultura representa una alternativa viable, además de ser una fuente de agua no convencional que favorece el uso más eficiente de los recursos hídricos. Entre las diferentes industrias agroalimentarias, la industria de IV gama ha experimentado un importante crecimiento en los últimos años debido al interés por el consumo de vegetales saludables, nutritivos, procesados y envasados listos para su consumo en fresco. Esta industria presenta uno de los mayores consumos de agua del sector agroalimentario principalmente como

consecuencia de los altos volúmenes de agua requeridos en la etapa de lavado de vegetales (hasta 40 m^3 por tonelada de producto).

Por otro lado, el consumo de productos de IV gama es una importante ruta de transmisión de patógenos si no se aplica un adecuado tratamiento de desinfección durante el proceso de producción. De hecho, en los últimos años se han publicado numerosos brotes epidémicos atribuidos al consumo de estos productos. Además del conocido riesgo microbiológico, este agua residual es también una importante fuente de microcontaminantes orgánicos (OMCs, por sus siglas en inglés) (principalmente plaguicidas), los cuales carecen de ninguna regulación. La estrategia más empleada para disminuir el riesgo microbiológico asociado con estos productos es el uso de compuestos clorados como agentes desinfectantes en la etapa de lavado. Sin embargo, la generación de subproductos de desinfección tóxicos como consecuencia del empleo de cantidades excesivas de cloro en estas matrices de agua con alto contenido orgánico, ha dado lugar a la prohibición en algunos países europeos del empleo de compuestos clorados en la industria de IV gama. Además, la cloración no evita la acumulación de OMCs durante el proceso industrial debido a su baja efectividad en la degradación de los mismos. Por ello, recientemente ha aumentado el interés en la búsqueda y evaluación de nuevos y/o alternativos tratamientos de agua capaces de reducir simultáneamente la contaminación microbiológica y química asociada a esta industria sin la generación de subproductos de desinfección.

El objetivo general de este estudio es evaluar la capacidad de tratamiento de varias tecnologías solares (foto-Fenton solar y H$_2$O$_2$/solar) y un proceso convencional (ozonización) aplicados al agua residual (agua de lavado) de la industria de IV gama con objeto de alcanzar los límites de calidad establecidos en las regulaciones de reutilización de agua residual en agricultura. En este estudio, se han seleccionado y utilizado dos bacterias patógenas humanas como modelos de contaminación microbiana transmitida por alimentos (*Escherichia coli* O157:H7 y *Salmonella enteritidis)* y una mezcla de ocho OMCs (atrazine,

azoxystrobin, buprofezin, imidacloprid, procymidone, simazine, thiamethoxam y terbutryn) como modelos de contaminación química (pesticidas).

En primer lugar, se desarrolló una receta sintética de agua para su uso a lo largo de todo el estudio experimental como modelo de matriz de agua residual de la industria de IV gama (en adelante SFCWW, por sus siglas en inglés 'synthetic fresh-cut wastewater'), evitando así las fluctuaciones físico-químicas del agua industrial. Esto permite por tanto realizar análisis comparativos más precisos entre los tratamientos y condiciones experimentales investigados en este estudio. Los procesos solares han mostrado su eficiencia en la desinfección de diferentes tipos de matrices acuosas, no obstante, el alto valor de turbidez (100 NTU) de SFCWW requiere investigar experimentalmente su capacidad de desinfección y descontaminación en esta particular matriz de agua. En este estudio, la capacidad de desinfección de cuatro procesos solares (foto-inactivación solar, H_2O_2/solar, Fe/solar y foto-Fenton solar) se ha investigado a escala de laboratorio en un simulador solar con condiciones controladas de radiación y temperatura. Los resultados obtenidos muestran claramente su capacidad para desinfectar SFCWW en cortos periodos de tiempo (reducciones >5 log en < 45 min). El mayor rendimiento de desinfección se obtuvo con el proceso H_2O_2/solar con 20 mg/L de oxidante, donde independientemente de las condiciones ambientales (estación del año) tras 20 min de tratamiento se alcanza una desinfección completa. Todo esto convierte al proceso H_2O_2/solar en una prometedora alternativa para desinfectar agua residual procedente de la industria de IV gama. Sin embargo, los procesos solares Fe/solar y foto-Fenton mostraron una baja capacidad de desinfección como consecuencia de la precipitación del hierro al pH de la matriz de agua (6.25), poniendo de manifiesto la necesidad del uso de fuentes alternativas de hierro que permitan una mayor estabilidad del mismo en disolución a pH cercanos a la neutralidad, mejorando la capacidad de desinfección.

En línea con esto, la búsqueda y evaluación de fuentes alternativas de hierro que permitan incrementar la cantidad de hierro disponible en disolución (quelatos y complejos) y por tanto la eficiencia del proceso homogéneo, se ha convertido en

una importante línea de investigación en los últimos años. En este trabajo experimental, se ha investigado por primera vez el uso de un fertilizante de hierro comercial (Fe^{3+}-EDDHA), comúnmente empleado en agricultura para prevenir y remediar la clorosis de hierro. Su uso como agente bactericida en procesos de desinfección solar de agua se ha analizado en comparación con el proceso convencional de foto-Fenton con sales de hierro. El estudio se llevó a cabo a escala de laboratorio (200 mL), bajo radiación solar natural, con concentraciones de hierro de 0.5 a 5 mg/L y en dos matrices de agua de distinta complejidad: solución isotónica y SFCWW. Los resultados obtenidos mostraron una mayor eficiencia de desinfección solar con Fe^{3+}-EDDHA (45 min de tratamiento) en comparación con foto-Fenton convencional con sales de hierro (90 min de tratamiento). Además, se ha propuesto el mecanismo de inactivación bacteriana mediante el proceso solar Fe^{3+}-EDDHA para explicar tanto la pérdida de viabilidad como la diferente resistencia a la inactivación de ambas bacterias (*S. enteritidis* mostro mayor resistencia que *E. coli* O157:H7). Brevemente, el mecanismo de inactivación propuesto está basado principalmente en cambios de permeabilidad de la membrana bacteriana en presencia de Fe^{3+}-EDDHA y en daños estructurales causados por los radicales hidroxilo generados en el proceso Fe^{3+}-EDDHA/H_2O_2/solar.

A continuación, se evaluó la capacidad de estos prometedores procesos solares para la desinfección y descontaminación simultánea de SFCWW a escala planta piloto para determinar su posible aplicación a escala preindustrial. Para ello, se evaluaron los procesos H_2O_2/solar, Fe^{3+}-EDDHA/solar y Fe^{3+}-EDDHA/H_2O_2/solar bajo radiación solar natural y en reactores tubulares provistos de un colector parabólico compuesto con una capacidad de tratamiento de 60 L de agua. En general, todos los procesos solares estudiados mostraron una alta eficiencia para reducir la contaminación microbiológica (>5-log en 60 min) mientras que la reducción de OMCs fue moderada (reducciones del 20 al 40 % de la carga inicial).

Además, también se investigó la capacidad de tratamiento (descontaminación y desinfección simultánea en SFCWW) a escala piloto (10 L) del proceso de

ozonización y peroxone (ozono con adición de H_2O_2) como referencia de procesos de oxidación avanzada (POA) convencionales en aguas residuales y de la industria agroalimentaria. En este estudio, se investigaron las siguientes condiciones de operación: dos producciones distintas de ozono (0.09 y 0.15 gO_3/Lh) al pH natural de SFCWW (6.25) y pH básico (11), además de la adición de 20 mg/L de H_2O_2. La condición de tratamiento más sencilla, es decir ozonación a pH natural, mostró la mayor eficiencia de desinfección (>5-log) y degradación de OMCs (85%) requiriendo para ello bajas dosis de ozono: <10 y <30 mgO_3/L, respectivamente. En resumen, los resultados obtenidos en procesos solares y ozono tienen implicaciones significativas ya que han demostrado ser capaces de alcanzar un alto nivel de purificación del agua objetivo, el cual permite su posterior reutilización para riego agrícola.

Una vez demostrada la capacidad de tratamiento de los procesos seleccionados a escala piloto y con el objeto de investigar la posible aplicación del agua tratada para riego agrícola, se llevaron a cabo ensayos de riego de dos vegetales de típico consumo en crudo (rábano y lechuga) en un invernadero experimental. Estos ensayos se realizaron con SFCWW tratada mediante las mejores condiciones de operación obtenidas previamente para cada tratamiento (H_2O_2/solar, Fe^{3+}-EDDHA/H_2O_2/solar y ozono a pH natural). Además, también se llevaron a cabo controles de riego positivo (SFCWW fortificada con los contaminantes objetivo) y negativo (agua mineral ausente de contaminación). En general, los resultados del análisis de muestras vegetales regados con SFCWW tratada (cualquier proceso) revelaron una total ausencia de contaminación microbiológica (Límite de Detección; < 1 CFU/99 g de lechuga y < 1 CFU/8 g de rábano) en ambos vegetales. En cuanto a los OMCs, los vegetales regados por todos los procesos mostraron una menor absorción de OMCs que las muestras del control positivo. En particular, los vegetales regados con SFCWW tratada con ozono mostraron una mayor reducción en la absorción de OMCs: 95 y 92 % en lechuga y rábano, respectivamente. En el caso de los procesos solares, las reducciones observadas variaron del 64 al 77 % en lechuga y del 43 al 59 % en rábano. Sin embargo, las lechugas regadas con agua tratada por el proceso solar

que incorpora el micronutriente Fe^{3+}-EDDHA (Fe^{3+}-EDDHA/H_2O_2/solar) mostraron el doble de contenido de clorofila que las regadas con agua tratada por ozono o el proceso H_2O_2/solar. Por lo tanto, estos resultados confirman el beneficio del uso de Fe^{3+}-EDDHA como fuente de hierro para la fisiología del cultivo y para el propio tratamiento solar del agua. En general, los resultados respaldan la capacidad de los procesos estudiados para reducir tanto la contaminación (microbiológica y química) como el riesgo de clorosis férrica.

Finalmente, con el objeto de determinar la viabilidad de implementación de los procesos estudiados (ozonización, H_2O_2/solar y Fe^{3+}-EDDHA/H_2O_2/solar) se llevó a cabo una evaluación del proceso global desde el punto de vista tecno-económico, ambiental y de seguridad alimentaria, incluyendo en este estudio la cloración como referencia del proceso de desinfección más empleado en este tipo de industria. La evaluación ambiental se realizó mediante el estudio de la ecotoxidad del agua tratada con: *Vibrio Fischeri* como organismo referencia para la evaluación específica del posible impacto de su vertido y *Lactuca sativa* para determinar su idoneidad para el riego de vegetales. Los resultados de los tests con *V. fischeri* mostraron ausencia de toxicidad aguda para el agua tratada por procesos solares, leve toxicidad agua para el agua ozonizada y toxicidad aguda para el agua clorada. En el caso de *Lactuca sativa*, no se observaron efectos significativos para el agua tratada por procesos solares u ozonada, mientras que se observó un efecto de inhibición para el agua clorada. Por tanto, estos resultados confirman la idoneidad de la aplicación de los procesos solares estudiados y el ozono para la regeneración de SFCWW y resalta la no idoneidad del proceso de cloración para este mismo objetivo.

Los resultados de la estimación del coste de tratamiento para la desinfección y eliminación simultanea de OMCs en SFCWW para las mejores condiciones de tratamiento fueron ≈1.15 €/m^3 para el proceso de ozonación y ≈1.60 €/m^3 para el proceso Fe^{3+}-EDDHA/H_2O_2/solar. Estos costes de tratamiento son aproximadamente el doble del estimado para el proceso de cloración

($\approx 0.70\,\text{€}/\text{m}^3$), siendo el coste de los procesos a escala industrial la principal barrera para la aplicación de estos procesos alternativos.

En último lugar, se llevó a cabo una evaluación de riesgos químicos y microbiológicos de los vegetales regados con SFCWW sin tratar y tratada (por ozono y procesos solares). Para ello, se evaluó el riesgo en una dieta alimentaria del consumo combinado de los OMCs objeto de estudio y empleando como herramienta para esta estimación el conocido como índice de riesgo (HI, por sus siglas en inglés). Los resultados obtenidos mostraron que ninguno de los vegetales analizados (regados con SFCWW sin tratar o tratada) constituye un riesgo para la salud humana, siendo la probabilidad menor en los vegetales regados con agua tratada. Por otro lado, la evaluación cuantitativa del riesgo microbiológico (QMRA, pos sus siglas in inglés) se estimó haciendo uso del software FDA-iRISK® en base a modelos de dosis-respuesta y simulaciones de Monte Carlo. En este caso, los vegetales regados con SFCWW sin tratar presentan un importante riesgo de infección para el consumidor, mientras que en los vegetales regados con agua tratada este riesgo de infección se reduce más de 4 órdenes de magnitud.

CHAPTER 1
INTRODUCTION

1. INTRODUCTION

In this chapter, a general overview of the water scarcity situation worldwide has been reviewed. The impact of the agro-food industrial activity on this situation has been also widely enlightened due to it is the central key of investigation in this research. Also the current situation regarding to water legislation in terms of water pollutants limitations for wastewater reclamation has been summarized.

Finally, the most common treatment technologies applied to solve or remediate the water stress focusing on the agro-food industry have been extensively revised which served as the starting point of this research for the study of new water treatments.

1.1. Water scarcity: current overview

Water is crucial element for the life. It is very well known, that the Earth`s surface, unlike what its name indicates, is covered by water in 70 % of its extension. In spite of this large volume available, only the 2.5 % is freshwater of which the easily accessible freshwater represents just a 1 % [Shiklomanov, 1993]. The low water availability linked with several factors that decrease the water accessibility and simultaneously increase its demand has generated worldwide water stress. Nowadays, it has been estimated that around one-third of the world population (2 billion of people) are under conditions of high water stress and around two-thirds (4 billion of people) are under this stress during at least one month of the year as is represented in Figure 1.1.
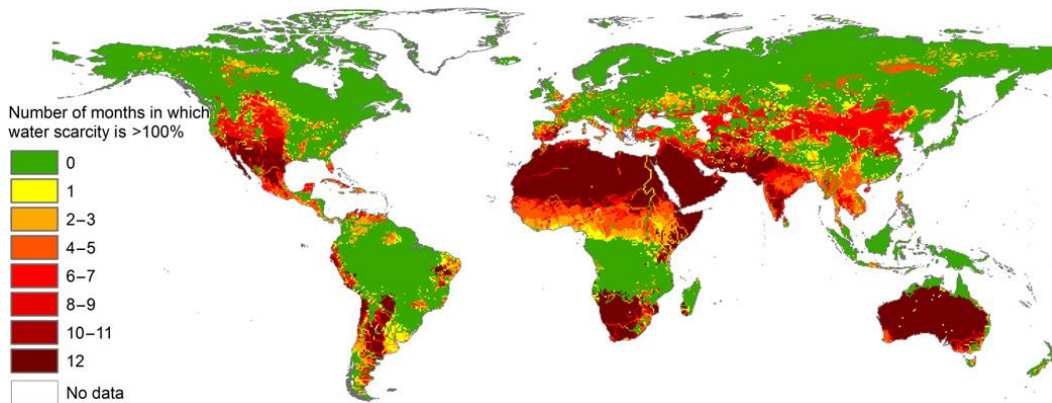
Figure 1.1. Number of months per year with severe water scarcity [Mekonnen and Hoekstra, 2016].

The factors that intensify global water stress are very well known and scientific communities and governances has recently being straighter forced to consider this problematic situation as one of the humanity future global challenges. In fact, a non-optimistic future appears if the human behaviour and the anthropogenic activities are not modified to be in harmony with a sustainable environment. As a motivational example of the important social and economic worldwide implications of the increased water scarcity, it can be mentioned the water-conflicts in low and middle-income countries that have drastically increased from 94 to 263 in the current decade [UNESCO, 2019]. In line with

this, it is expected that water scarcity and their related conflicts will intensify the current trend of displacement of poor and marginalized people and therefore exacerbating the current global and humanitarian crisis. In all this scenario, and supporting this statement in 2015 was published the '2030 Agenda for Sustainable Development Goals' by the United Nations, forcing to address different challenges including the water scarcity and sanitation as Goal 6, among others priority challenges [UN, 2016].

The main socio-economic and environmental factors affecting freshwater scarcity are briefly summarized as follows:

i) The global climate change intensifies the climate conditions of each area being this phenomenon summarized in the widely accepted paradigm '*dry gets drier, wet gets wetter*' [Hu *et al.,* 2019]. Thus, the water stress is being exacerbated in the dry areas which are becoming drier and therefore increasing the climate inequalities.

ii) The global water demand is increasing almost 1 % per year since 1980 and a similar increase rate is expected until 2050 which means that the water demand will be at least 20 % higher [Burek *et al*., 2016]. This demand increase is mainly linked with the socio-economic development and the continuous population growth in low and middle-income countries. Moreover, the continuous population grew and the urbanization expansion by migration from rural areas to cities will also increase the industrial and domestic water use and therefore the water pollution. The population growth rises up the water demand in two ways: directly (drinking water and sanitation) and indirectly (water-intensive services such as agriculture). The major water use, is the indirect one like its use for food production, being the daily drinking water requirement per person (2 to 4 litres) almost insignificant respect to the water volume needed to produce the daily food requirement for a person (2000 to 5000 litres) [FAO WATER, 2010].

iii) The water pollution represents one of the main factors that decrease the fresh-water sources availability. The sources of pollution are very wide and extend but most of them came from anthropogenic activities, including domestic, agriculture and industry, which if not properly treated and managed, an

uncontrolled amount of pollutants (including both chemical and microbiological contaminants) reach surfaces and groundwater, transforming it into non-useful water-bodies, and very difficult to restore it [FAO, 2017].

1.2. Water pollutants: types and sources

Polluted water drastically impact on human health and their well-being. It is estimated that one-tenth of the global burden diseases can be attributed to the polluted water representing an important global threat as it is depicted in Figure 1.2 [WHO, 2004].
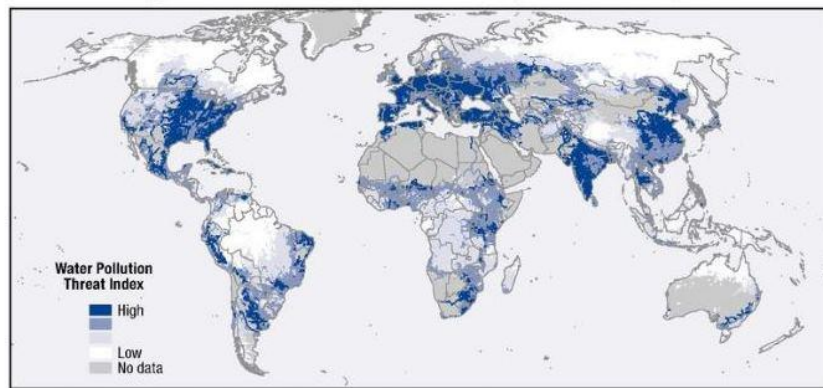
Figure 1.2. Global distribution of water pollution hazard in 2010 [Sadoff *et al.*, 2015].

Water pollutants can be classified into two main groups: microbial and chemical contaminants. The water microbiological pollutants are diverse but the general concern is focused on those that can affect the economy as the fungal pathogens that affect crop yield, and mainly in those that affect the human health known as waterborne pathogens. These lasts can be classified as excreta-related pathogens (bacteria, helminths, protozoa and viruses) and vector-borne pathogens as *Plasmodium* spp and *Wuchererua bancrofti.* The main sources of water microbiological contamination are the cattle raising and the human wastewater generated in households, hospital and office buildings [FAO, 2011].

Regarding chemical pollutants, they can be classified in two categories, macropollutants which occurs at mg/L levels and are mainly inorganic salts, heavy metals and nutrients (nitrogen and phosphorus species) and, organic

micropollutants or microcontaminants (OMCs) which are synthetic and natural organic contaminants typically detected at trace levels (ng/L to μg/L) [Sousa *et al.*, 2018]. The discharge from agriculture, industrial activities and municipal sewage treatment plants are the main sources of chemical pollution in water bodies [Schwarzenbach *et al.*, 2010].

The continuous production and development of chemical compounds for human activities employment is generating persistent disposal of these contaminants in the aquatic environment. Although the public data about the number of chemical compounds are scarce representing less than 5 % of them, it is estimated that at least 100000 different chemicals are in use and at least 1000 new chemical are developed every day [OECD, 2018]. The global industrialization and the population grown give rise up the chemical production, which is estimated to continuous grown exponentially as it is observed in Figure 1.3.
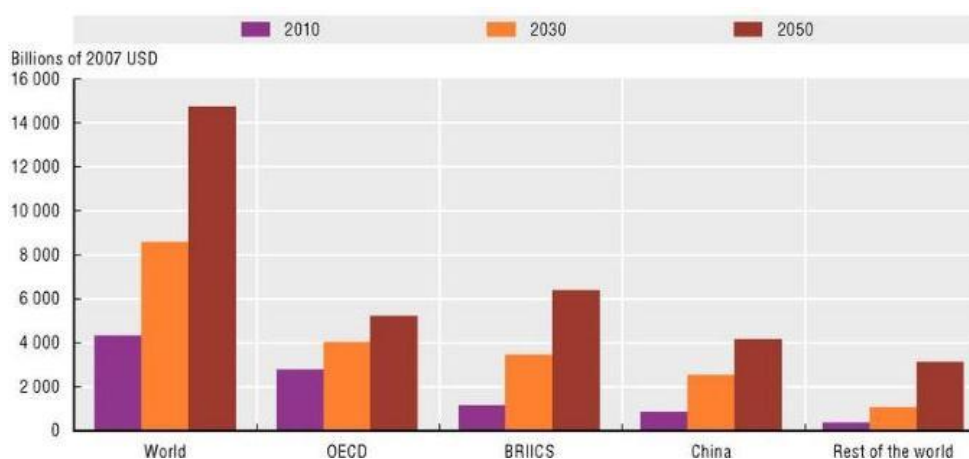
Figure 1.3. Projected chemicals production by region [OECD, 2012].

The water microcontaminants classification is diverse but in general, they can be classified in 7 groups: industrial chemicals, chlorination-by products, personal care products, hormones, pharmaceuticals, surfactants or detergents and pesticides [Luo *et al.*, 2014]. The physicochemical properties of some of these OMCs confer resistance to be degraded by both natural and conventional municipal WWTPs processes being poorly removed and therefore becoming part of the environment. Many of these OMCs may involve toxic effects on aquatic ecosystems and human health even at such low concentrations. The toxic effects

can be short-term or long-term effects due to the bioaccumulation potential of the persistent ones [Schwarzenbach *et al.*, 2006]. The scarce knowledge about their potential health and environmental risks had led to the labelling of some substances as contaminants of emerging concern (CECs). The CECs are OMCs not covered by any water quality regulation but recently recognized as potential hazards. These compounds might be new substances that have been recently detected in the environment or substances that have been present for a longer time and detected recently as a result of the development of more sensitive analytical methods. Examples of some CECs include microplastics, manufactured nanomaterials, personal care products, industrial and household chemicals, pharmaceuticals, pesticides, and their transformation products.

1.3. Water legislation

The concern about the potential negative interactions of pollutants (OMCs and waterborne pathogens) with the environment and human health in the last two decades, has led to the European regulatory administration to undertake efforts for the development of water quality policies to respond to the new uncertainties created in the context of water quality and scarcity, including OMCs monitoring, protection of water resources and wastewater reclamation to reduce future risks, among other aspects.

In particular, and focused on the studies carried out in this research, unfortunately there is no specific regulation related with the reclamation and reuse of water in the agro-food industry. Therefore, to set the proper parameters in the experimental methodology and limits regarding pollutants discharge after the evaluation of several water purification process, the current legislation of the European Union Water Framework Directive (EU WFD), the current stablished reclaimed water quality based on Spanish RD 1620/2007 and the currently EU Proposal 2018/0169 (COD) have been considered as key water policies requirements and they are explained in detail in next sub-sections.

1.3.1. European Union Water Framework Directive (EU WFD)

The evolution of the European legislation on water quality protection against OMCs over the last two decades is summarized in Figure 1.4. In the year 2000 a European policy (Directive 2000/60/EC), namely the European Union Water Framework Directive (EU WFD) was implemented. The objective of this directive was the protection of the aquatic environment by the identification and classification of substances or group of substances that can represent a risk to the aquatic environment, labelling as priority substances (PSs) to study their potential effect to define annual averages and maximum concentration values for a substance or group of substances that can interfere in the environment and establish European Environmental Quality standards (EQS) [EC, 2000]. After that, several amendments, decisions and directives have been published until the last, in the year 2018.

In 2001 and based on the collected information about the production, use volumes, potential hazards and environmental occurrence of PSs, the first list of 33 PSs that must be monitored was published including a new subclassification as priority hazardous substances (PHS) of 13 of them. The PHSs are defined as '*substances or a group of substances that are toxic, persistent and liable to bioaccumulate*' [EC, 2001]. The definition of PHS is very similar than the substances labelling as Persistent Organic Pollutants (POPs) listed in the same year in the Stockholm convention and selected with the aim to eliminate or restrict their production and usage [Stockholm Convention, 2008]. The information of this convention was later ratified by the European Commission Regulation No 850/2004 [EC, 2004].

In 2008, an amended of the EU WFD directive was published (Directive 2008/105/EC), where the EQS as maximum concentrations values for the 33 PSs and 8 other pollutants as a tool to monitor the water chemical quality and make decisions to maintain a good ecological and chemical water status were defined [EC, 2008]. In 2013, the 2008 Directive was updated (Directive 2013/39/EU), expanding the number of PS to 45 (Table 1.1), and stablishing

more restrictive EQS and proposing a watch list of substances to be temporary monitored in the field of water policy [EC, 2013].

Directive 2000/60/EC – EU Water Framework Directive (EU WFD)
• Achieve good ecological and chemical status of water
• Identify priority substances/group of substances (PSs) with significant risk to or via the aquatic environment
• Set EU Environmental Quality Standards (EQS) with annual average value (AA-EQS) and maximum allowable concentration (MAC-EQS)

Decision 2455/2001/EC
• Set the first list of 33 PSs that must be monitored at Community level including priority substances (PHSs)

Directive 2008/105/EC – amended EU WFD 2000/60/EC
• The first list of EQS (AA-EQS, MAC-EQS) for the 33 PSs and 8 other certain pollutants
• Monitoring of the PSs in surface water

Directive 2013/39/EU
• Update of directive 2008/105/EC
• Development of new water treatment solutions
• Recommendation of the monitoring of 45 PSs and a set of 8 other certain pollutants with EQS
• Proposal of a first Watch List of substances for Union-wide monitoring in the field of water policy

Decision 2015/495/EU
• Establishment of the first Watch List of 17 organic compounds defined as 10 substances/group of substances, contaminants of emerging concern (CECs)

Decision 2018/840/EU – repealed Decision 2015/495/EU
• Establishment of the second Watch List of 15 organic compounds defined as 8 substances/group of substances, contaminants of emerging concern (CECs)

The Stockholm Convention on Persistent Organic Pollutants (POPs)
• Signed in 2001, the treaty ratified in 2004
• Elimination or restriction of the production and usage of POPs

European Commission Regulation № 850/2004
• Adaptation of The Stockholm Convention to EU legislation
• 180 parties (179 states and the EU except Italy)

Figure 1.4. Schematic evolution of the European legislation on water quality protection against OMCs over the last two decades [Pietrzak *et al.*, 2019].

Table 1.1. List of PSs according to the Directive 2013/39/EU and their classification.

No.	Name of priority substance [3]	Class	Subclass	PHS
1	Alachlor	Pesticide	Chloroacetanilides	
2	Anthracene	-	-	X
3	**Atrazine**	**Pesticide**	**Triazines**	
4	Benzene	Industrial compound	Multiple aplications	
5	Brominated diphenylethers	Industrial compound	Flame retardants	X*
6	Cadmium and its compounds	-	-	X
7	Chloroalkanes, C_{10-13}	Industrial compound	Multiple applications	X
8	Chlorfenvinphos	Pesticide	Organophosphorus	
9	Chlorpyrifos (Chlorpyrifos-ethyl)	Pesticide	Organophosphorus	
10	1,2-dichloroethane	Industrial compound	Solvents	
11	Dichloromethane	Industrial compound	Solvents	
12	Di(2-ethylhexyl)phthalate (DEHP)	Industrial compound	Plasticizers	X
13	Diuron	Pesticide	Phenylureas	
14	Endosulfan	Pesticide	Organochlorines	X
15	Fluoranthene	-	-	
16	Hexachlorobenzene	Pesticide	Organochlorines	X
17	Hexachlorobutadiene	Pesticide	Organochlorines	X
18	Hexachlorocyclohexane	Pesticide	Organochlorines	X
19	Isoproturon	Pesticide	Phenylureas	
20	Lead and its compounds	-	-	
21	Mercury and its compounds	-	-	X
22	Naphthalene	-	-	
23	Nickel and its compounds	-	-	
24	Nonylphenols	Industrial compound	Multiple applications	X*
25	Octylphenols [6]	Industrial compound	Multiple applications	
26	Pentachlorobenzene	Industrial compound	Solvents	X
27	Pentachlorophenol	Pesticide	Organochlorines	
28	Polyaromatic hydrocarbons (PAH) [7]	-	-	X
29	**Simazine**	**Pesticide**	**Triazines**	
30	Tributyltin compounds	Pesticide	Organotin	X*
31	Trichlorobenzenes	Industrial compound	Solvents	
32	Trichloromethane (chloroform)	Industrial compound	Solvents	
33	Trifluralin	Pesticide	Dinitroanilines	X
34	Dicofol	Pesticide	Organochlorines	X
35	Perfluorooctane sulfonic acid and its derivatives (PFOS)	Industrial compound	Multiple applications	X
36	Quinoxyfen	Pesticide	Quinolines	X
37	Dioxins and dioxin-like compounds	-	-	X*
38	Aclonifen	Pesticide	Diphenyl ethers	
39	Bifenox	Pesticide	Diphenyl ethers	
40	Cybutryne	Pesticide	Triazines	
41	Cypermethrin [10]	Pesticide	Pyrethroids	
42	Dichlorvos	Pesticide	Organophosphorus	
43	Hexabromocyclododecanes (HBCDD)	Industrial compound	Flame retardants	X*

Table 1.1. (Continue) List of PSs according to the Directive 2013/39/EU and their classification.

No.	Name of priority substance [3]	Class	Subclass	PHS
44	Heptachlor and heptachlor epoxide	Pesticide	Organochlorines	X
45	**Terbutryn**	**Pesticide**	**Triazines**	

*Indicate that only some substances of the groups are identified as PHSs.
In bold type, the pesticides selected in this research from this list.

The proposed watch list was launched two years later (Decision 2015/495/EU) by the establishment of the first watch list of 17 organic compounds including 10 substances or groups of substances considered as CECs. The objective of this watch list was to increase the monitoring of these substances as a tool to obtain more evidences of their potential exposure hazards [EC, 2015]. Finally, the last Decision was repealed 3 years later by the Decision 2018/840/EU taking into account the data gathered in this period and updating the watch list to 15 organic compounds as 8 substances or groups of substances including pharmaceuticals, steroid hormones and pesticides (Table 1.2) [EC, 2018].

Table 1.2. Watch list of substances to be monitored in water according to the Decision 2018/840/EU and their classification.

Substance	Class	Subclass
17-α-ethinylestradiol (EE2)	Steroid hormones	Estradiol derivates
17-β-estradiol (E2)		Estradiol derivates
Estrone (E1)		Estrone derivates
Erythromycin	Pharmaceuticals	Macrolide antibiotics
Clarithromycin		Macrolide antibiotics
Azithromycin		Macrolide antibiotics
Amoxicillin		Penicillin antibiotics
Ciprofloxacin		Fluoroquinolone antibiotics
Imidacloprid	Pesticides	Neonicotinoids
Thiacloprid		Neonicotinoids
Thiamethoxam		Neonicotinoids
Clothianidin		Neonicotinoids
Acetamiprid		Neonicotinoids
Metaflumizone		Semicarbazones
Methiocarb		Carbamates

In bold type, the pesticides selected in this research from this list.

It is important to mention the significance of pesticides in the European water regulation lists, where represent more than 50 % of the substances. Logically,

agriculture is the main source of pesticides in the aquatic environment although, as previously mentioned, the inability of WWTPs to remove OMCs converts them in another important introduction pathway. The regular pesticides discharge into the environment, even at low concentrations, may generate their accumulation in the aquatic compartments [Pietrzak *et al.*, 2019]. The physic-chemical properties of pesticides, carefully designed for its application, like water solubility and their recalcitrant behaviour, join with their worldwide intensive use convert them in important water pollutants.

Spain is one of the countries with the highest employment of pesticides in the EU, 76941 tonnes of pesticides were sold in Spain in the year 2016, which represent almost 20 % of the global sales in the EU. Moreover, the trend in the last decades is an increase in the pesticides sales as a result of agriculture expansion. In Spain a pesticides sales increase of 5 % was observed from 2011 to 2016. Nevertheless, this trend was not equally significant for the different pesticides families: a considerable consumption increase was reported for fungicides and herbicides (24 and 10 %) whereas sales decreases for insecticides and acaricides [EUROSTAT, 2019]. These differences are not casual and are linked with the notable increase of the biological and integrated pest control implementation as a consequence of the recent pesticides concern. This data indicate the possible higher environmental impact of fungicides and herbicides in a near future, a tendency that should be taken into account in the elaboration of future regulations.

Pesticides accumulation in European water bodies causes potential toxicological effects on aquatic ecosystems and human water supplies. The data recollected in the context of the EU WFD indicate that almost 50 % of the European water bodies are in risk due to pesticides presence which threatens the freshwater biodiversity [Malaj *et al.*, 2014]. Moreover, as fresh and groundwater are the main water supplies for human consumption and irrigation, pesticides pollution also represents an important threat to human health.

1.3.2. Reclaimed wastewater quality policies

In spite of the increase wastewater reuse around the world, the EU did not adopt any guidelines or regulation for wastewater reuse until the year 2016. In this year, the European Commission published the '*Guidelines on Integrating Water Reuse into Water Planning and Management in the context of the WFD*', where regulations on minimum quality requirements for reusing water in agricultural irrigation and aquifer recharge was included complementing the European water policy (WFD and urban wastewater treatment directive) [EEA, 2016]. In 2017, the Joint Research Center (JRC) of the European Commission published a report considering the 'Minimum quality requirements for water reuse in agricultural irrigation and aquifer recharge', where through a risk management framework and based again in the two more important applications of wastewater reuse (agriculture and aquifer recharge) aimed to establish the basis of the future EU reuse policy [Alcalde-Sanz and Gawlik, 2017]. Finally, in 2018 the EU published a proposal for a regulation of the European Parliament and of the Council on minimum requirements for wastewater reuse in agriculture (Proposal 2018/0169 (COD)) considering microbiological and physical-chemical parameters established after an evaluation on health and environmental risk assessment. This proposal was amended and approved by the European Parliament (Committee on the Environment, Public Health, and Food Safety) in January of 2019 [COD, 2019].

As urban wastewater needs to be treated before used for irrigation and the level of purification can vary according to the type of crops to be irrigated, in this regulation a 'fit-for-purpose' strategy has been defined including the appropriate treatment, the minimum quality parameters (microbiological and physical-chemical values), the irrigation method that vary depending on its intended agricultural use and the degree of human contact (Table 1.3 and 1.4). Moreover, in this document the minimum frequency of analysis and the monitoring validation of the reclaimed water for agricultural irrigation are also established.

Table 1.3. Classes of reclaimed water quality respect to the allowed agricultural use and irrigation method, Proposal 2018/0169(COD).

Minimum reclaimed water quality class	Crop category	Irrigation method
A	All food crops, including root crops consumed raw and food crops where the edible part is in direct contact with reclaimed water	All irrigation methods
B	Food crops consumed raw where the edible part is produced above ground and is not in direct contact with reclaimed water, processed food crops and non-food crops including crops to feed milk or meat-producing animals	All irrigation methods
C		Only irrigation methods that do not lead to direct contact between the crop and the reclaimed water. For example, drip irrigation
D	Industrial, energy, and seed crops	All irrigation methods

Table 1.4. Reclaimed water quality requirements for agricultural irrigation, Proposal 2018/0169(COD).

Class	Indicative appropriate treatment	Limit value				
		E. coli (CFU/100 mL)	BOD$_5$ (mg/L)	TSS (mg/L)	Turbidity (NTU)	Other
A	Secondary treatment, filtration, and disinfection	≤ 10 or below detection limit	≤ 10	≤ 10	≤ 5	*Legionella* spp.: ≤ 1000 CFU/L when there is a risk of aerosolization in greenhouses (≤ 90 % of samples)\n\nIntestinal nematodes (*helminth eggs*): ≤ 1 egg/L when irrigation of pastures or forage (≤ 90 % of samples)\n\n*Salmonella*; absent (100 % of samples)
B	Secondary treatment and disinfection	≤100	According to Council Directive 91/271/EEC (Annex I, Table 1)\n\nBOD$_5$: 25mg/L\n\nTSS: 35-60 mg/L		-	
C	Secondary treatment and disinfection	≤1000			-	
D	Secondary treatment and disinfection	≤10000			-	

As a consequence of the lack of a common European policy for wastewater reuse during the last decades, some European countries like Spain adopted its own reuse legislation. The Spanish reuse policy was published in 2007 by a Royal Decree (Spanish Royal Decree 1620/2007) [RD, 2007]. The reuse legislation was adopted for 13 different purposes which can be divided into 5 categories: recreational, industrial, environmental, urban and agricultural irrigation. In the agricultural case, three water quality criteria were stablished mainly depending

on the contact with the reclaimed water and crop consumption as shows Table 1.5.

Table 1.5. Reclaimed water quality for agricultural irrigation established by the Spanish Royal Decree 1620/2007.

Agricultural uses	Maximum admitted threshold				
	Intestinal nematodes (egg/10 L)	*E. coli* (CFU/100 mL)	TSS (mg/L)	Turbidity (NTU)	Other
Quality 1: a) Crop irrigation with an application method which allows **direct contact** of reclaimed water with the edible part of the **crop consumed uncooked**.	1	100	20	10	*Legionella* spp.: 1000 CFU/L if there is a risk of aerosolization. Presence/Absence tests of pathogens.
Quality 2: a) Crop irrigation with an application method which allows **direct contact** of reclaimed water with the edible part of **crop which is not consumed fresh** but after processing. b) Fodder irrigation for milk or meat-producing animals. c) Aquaculture	1	1000	35	No fixed limit	*T. saginata* and *T. solium:* 1 egg / L if the fodder is used for feeding milk or meat-producing animals. Presence/Absence tests of pathogens.
Quality 3: a) Localized irrigation of **woody crops** preventing the contact of effluent with fruits consumed by humans. b) Irrigation of ornamental crops, greenhouses without direct contact of effluent with produced. c) Irrigation of industrial non-food crops, nurseries, fodder for silo, cereals and oleaginous seeds.	1	10000	35	No fixed limit	*Legionella* spp.: 100 CFU/L.

Finally, and although it is important to highlight the efforts of the European authorities in the last decade for stablish community guidelines with the aim to decrease the human and environmental risks related with wastewater reuse in agriculture, several gaps remaining unknown like emergent risks that have not been included in the regulation or still under investigation by the research

community [Rizzo *et al.,* 2018a]. In this regard, six of these gaps can be highlighted as follow:

- The regulation should include a list of chemicals and their relevant toxicity values including WFD priority chemicals and other organic pollutants (CECs).

- Monitoring of new disinfection-by-products (DBPs) and potential toxic oxidation intermediates formed during the water treatments.

- Monitoring of microbial regrowth risk during reclaimed water storage.

- Monitoring the potential antibiotic resistance spread (including both antibiotic resistance bacteria and genes, ARBs and ARGs) in the environment and their potential transference to crops by establishing monitoring of an antibiotic-resistant indicator in reclaimed water.

- Proposals of community monitoring programs to study the potential translocation to crops, bioaccumulation, and persistence in the environment of the contaminants (CECs, DBPs, ARGs).

- Include a special program of dissemination and information for farmers to overcoming the concern about the risk related to the use of reclaimed water, which is one of the greatest barriers for its application.

The presence of all these gaps and several unanswered questions about wastewater reuse in agriculture have generated a growing interest in the scientific community and therefore, the number of research publications about this topic has grown almost exponentially in the last two decades generating more than 125 research documents per year as is shown in Figure 1.5. And it is expected that this trend will continue in the next decades as a result of worldwide water reuse extension, development of new advanced treatments for this purpose and an increase in the number of research tools available for risks evaluation.

Although quality regulations to water reuse have been established, crops irrigation with reclaimed water still remains as a controversial practice, mainly because zero risks does not exist and therefore this practice leads to a potential exposition of the consumers to microbial and chemical pollutants with their associated risks to human health: infectious diseases and exposition to OMCs [Ikehata *et al.*, 2013].
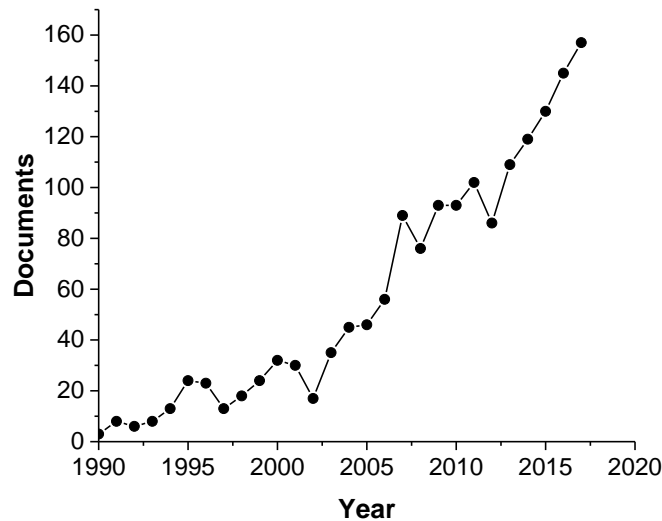
Figure 1.5. Frequency of reports by year (1990 - 2017), dealing with wastewater reuse. The search was based on Scopus database using as keywords 'wastewater reuse' and including articles, reviews, books, and book chapters.

In this regard, a risk analysis of the water reuse scenario to assess disease and food-safety risks focused on human health by the use of this analysis tool internationally recognized it is an appropriate strategy to estimate the damage or injury that can be expected from the consumer exposure to the pollutants. The risk analysis can be used as a prospective or retrospective tool, i.e; to anticipate an exposure before appropriate measures or with the data provided from a real exposure scenario. The prospective analysis is the most used as a prevention tool due to the absence of real exposure data.

Although the number of microbial risk analyzes performed in real scenarios is scarce, the translocation of microbial pollutants to crops and their human health impact is widely known whereas regarding OMCs, still limited information

concerning the occurrence, uptake or fate and the possible human health impacts through the food-crop chain. Therefore, more experimental studies are needed to evaluate the microbial and chemical risks associated with water reuse using real data [Qadir and Scott, 2009].

1.4. Water consumption in the agro-food industry

It is very well known that the main water demanding activities are the agriculture followed by the industry. Recently, the industry related with the fresh-cut produce has grown exponentially demanding high amounts of water for its process performance. In this research study, it has been linked both activities in order to implement a strategy to treat and reuse WW from agro-food industries in agriculture will allow closing the water circle within the system ensuring process water sustainability, continuous water availability and environmental protection through reducing the water footprint of these industries [Inyinbor *et al.*, 2019].

1.4.1. Fresh-cut produce industry

The agro-food industries play a key role in the worldwide economic development being their importance in developing nations even more crucial due to these industries represent an efficient tool to combat the poverty and eradicate hunger, which are the two main problems in these regions [Inyinbor *et al.*, 2019].

Over recent decades, the worldwide demand for fresh vegetables has increased due to their nutritional value and beneficial health effects. Nutritionists, researchers, and even governmental campaigns encourage the daily consumption of fresh fruits and vegetables as fundamental bases of a diet rich in antioxidants and vitamins. Their daily consumption is linked with the prevention of a grand array of well-known, chronic and some non-communicable diseases such as metabolic and degenerative disorders, diabetes, obesity, cancer, and cardiovascular, among others. The impact of these diseases is high being responsible for causing almost 2.7 million deaths annually [WHO, 2005]. At the same time, significant changes in people's lifestyle, particularly in metropolitan

areas, where the frenetic routine not allow lengthy meal preparation times, forces the consumers to look for practical, healthy products, easy to prepare and consume.

The food industry responds to these consumer needs with the minimally processed or fresh-cut products. These fresh-cut products are defined as '*any fresh fruit or vegetable or combination of their physically altered from its original form, but remaining in a fresh state*'. Fresh-cut products are mainly marketed as 'ready-to-eat' saving time and facilitating the consumption in catering, home and even on the run, of products that still maintaining freshness. As these products have responded to the consumer needs, their consumption has undergone a sharp increase in the last decades, encouraging the rapid development of the so-called fresh-cut produce industry in developed countries [Chinnici *et al.*, 2019].

In particular, in Spain this is the food category with the higher growth. The increase in purchase and consumption of these products was more than 50 % higher in 2018 than the previous year as shown in Figure 1.6. These data are surprising since it is consumed an average of 6.67 kg/year of fresh-cut products per person, being the green salad most present in the household's Spanish menu than the famous and popular pizza [MAPA, 2019].
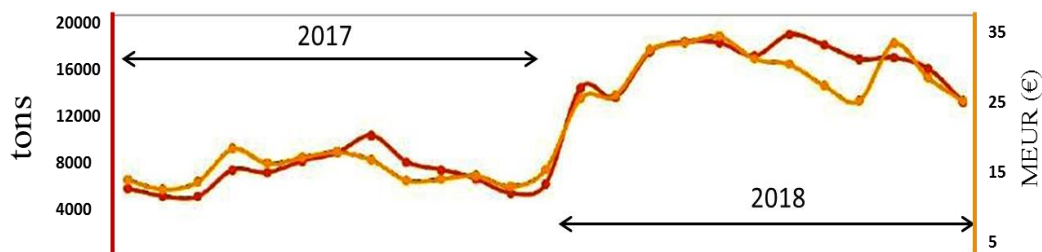
Figure 1.6. Monthly evolution of expenses (orange) and purchases (red) of fresh-cut products in Spain during the years 2017 and 2018 [MAPA, 2019].

These industries consume huge volumes of water (mainly in washing steps), and as most of the water is not used as an ingredient also generate large wastewater volumes. Although water demand depends on the specific activity of each industry (frequency of water refilling washing tanks, product/water ratio, etc.), the water consumption can be up to 40 m^3/ton of raw product processed. Most

of the wastewater generated by these industries is biodegradable and rich in organic materials and nutrients. However, excessive levels of phosphorous (phosphates) can be present as treatment residues when large quantities of phosphoric acid are used in the chlorination process. These high phosphate concentrations can lead to an anaerobic effluent due to the alteration of the nutrient ratio required for a subsequent biological treatment and hence can also represent an environmental issue [BREF, 2006]. Moreover, the agro-food wastewater usually contains by-products from the use of chemical disinfection techniques and organic microcontaminants (OMCs) (mainly pesticides residues used on the source crop) which increase the risks and environmental concerns.

1.4.1.1. Manufacture of fresh-cut products

The manufacture of the 'ready-to-eat' fresh-cut products involves several processing steps or unit operations which are schematized in Figure 1.7 and briefly described below [Gil *et al.,* 2006]:
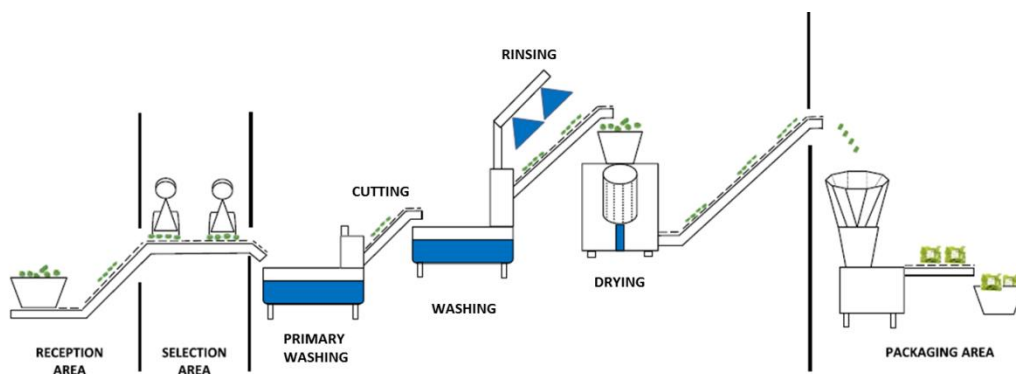
Figure 1.7. Scheme of processing steps in a fresh-cut company [Castro-Ibañez *et al.,* 2017].

i) <u>Raw material reception, selection and storage</u>: This step is crucial due to the inspection and selection of good quality raw vegetables to yield standard and good quality fresh-cut products. The vegetables quality criteria are checked in both ways: visual (product freshness and absence of necrotic tissues, insects and microbial diseases, among others) and through analytical studies to comply with regulations like nitrate or pesticides residues content, according to EC, No 1881/2006 and maximum residue levels (MRLs) fixed by European

Commission, respectively. After that, the product is directly moved to the processing area or storage appropriately (≈4 °C) till use (less than 2 days).

ii) <u>Primary washing</u>: In this step, the caked-on dust or dirt from the vegetables are removed. The procedure like type of washing system or contact time vary for each company although it is reported a high efficiency for baths with air injection or a gentle agitation that aid in the removal of soils from vegetables surface. Nevertheless, two parameters are common for all installations: the water temperature (≈4 °C) and the use of potable water quality (Council Directive 98/83/EC). This step accounts for ca. 20 % of the total water consumed in the process line.

iii) <u>Cutting and grading:</u> Before the cutting step, a manual sorting and trimming to remove vegetables with physiological defects including putrescence and unwanted plant parts (seeds, stems and cores) are carried out to avoid latter dispersion in the processing line. Size reduction is performed by cutting the vegetables into uniform, smaller and standard size and shape parts using high-speed machines with stainless steel sharp blades of food grade. As example, iceberg lettuce is cut in 6 mm pieces size. After that, and to provide standardization and uniformity of the end-product, a new sorting using shaker screen sizers is performed to eliminate undersized small pieces.

iv) <u>Washing/rinsing</u>: Immediately after cutting, the vegetable pieces are washed in cold potable quality water alone or with the presence of a sanitizer. This step is crucial in the processing of this type of products due to allow to remove free cellular contents (exudates) released in the cutting step which combined with the product cooling avoid a potential microbiological proliferation in the damaged tissue prolonging the product shelf-life. In this processing step, is very important the control of four parameters: product residence time, an adequate ratio between water and product quantity, the water temperature and the concentration of the sanitizer, when employed. Also, this step is by far the higher water consumer, around 60 % of the total volume of water used in the processing line.

In the case that a sanitizer is added in the washing bath; a subsequent rinsing stage is incorporated in the product processing line. The objective of this step is to clean the product and eliminate residual concentrations of sanitizer or sub-products generated in the process. The rinse system can also vary between different plants although the most widely used design consists on a conveyor belt where the products are sprayed with clean water as they proceed on. When apply, this step is ca. 20 % of the total water used in the processing line.

v) <u>Drying and packaging</u>: After washing and/or rinsing a dewatering step by centrifugation is applied, where the time and speed of the process are adjusted for each product type to avoid cellular injuries and in some special cases (too delicate products) forced air in a semi-fluidized bed is used. Finally, the product is packaging aseptically. The packaging material more widely use are polymeric films and the internal atmosphere of the package is modified with the aim to achieve adequate shelf-life of fresh-cut products by decreasing aerobic respiration rate without induction of the anaerobic one.

Once the ready-to-eat product is prepared, it is stored and transported holding an appropriate temperature to avoid microbial proliferation and extend the product shelf-life. Finally, the product is distributed to the terminal market facilities (retailers, wholesalers, foodservice operations and distribution centers, among others), from where the fresh-cut product will reach the final consumer.

1.4.1.2. Microbial risk associate to fresh-cut industry

There are several factors along the manufacture of fresh-cut products that determine a high probability of microbial contamination, being the main factor of risk the raw consumption. The vegetables can become contaminated during any of the production chain steps between farms to consumer. The main sources of contamination are briefly explained below:

i) During the primary production, where multiple cross-contamination may occurs by direct contact of vegetables with water (irrigation, floods or splash), the internalisation of microorganism in the vegetables from the soil and the poor

hygienic practices in the harvest process. Therefore, the application of Good Agricultural Practices (GAPs) and Good Manufacturing Practices (GMPs) that ensure the safety and hygiene in the production are highly recommended. These practices are frequently included in food law rules as the Codex Alimentarius (CAC/RCP 53–2003) or the European community regulations (EU Regulation 852/2004).

ii) During the industrial processing, the application of complex unit operations (explained above) provide opportunities for cross-contamination whereby just a few contaminated products may cause the contamination of a large proportion of end-products [Castro-Ibañez *et al.*, 2017]. The main contamination points usually becomes from human handling, contaminated equipment surfaces and water. The manual grading of vegetables performed previously to the cutting step represents a microbial source when exhaustive control and hygienic practices are not applied. After that, in the cutting step, the moisture present due to the primary washing and the liquid losses by the vegetables (exudates promote the microorganism's dissemination that may reach utensils (trimming knives and slicers) and equipment surfaces. These conditions linked with the physical modifications in the products (punctures, cuts and plant tissue wounding) converts the cutting step in one of the key microbial contamination point of the fresh-cut production chain. Another crucial contamination step is the washing process; due to water is a good vehicle for a wide distribution of microbial contamination [Doyle and Erickson, 2008]. In fact, an experimental study performed by Wachtel and Charkowski in 2002 demonstrated the capability of the microbial spread during this step. In this study, an inoculated lettuce piece with microbial pathogens was mixed with a large number of clean pieces, and their storage in chilled water for 24 h lead to the contamination of the 100 % of lettuces pieces [Wachtel and Charkowski, 2002].

Among the different marketed products of the fresh-cut industry, shredded leafy vegetables (lettuce, spinach and chard) and salad mixed are by far the most marketed products representing more than 80 % of the market. Therefore, these types of products are considered the highest priority vegetables in terms of health

safety according to the Food and Agriculture Organization (FAO) and the World Health Organization (WHO) [FAO/WHO, 2008]. The role of these products as pathogens vehicles is confirmed due to the global increase of fresh-cut product consumption which is linked with a remarkable increase in the number of fresh-produce outbreaks as it is shown in Figure 1.8. The outbreak reports linked to salad and leafy vegetables are distributed unequally in the different world-regions being almost three times higher in U.S.A. (223 cases) respect to the EU (74), although the increase in the number of cases was similar in the last decade [Callejón *et al.*, 2015].

Although the size of the outbreaks provoked by these products may vary from just few people to thousands, medium and/or larger outbreaks incidents are common as a consequence of the wide market of these products and the fact related with one contamination point can led to thousands contaminated end-products [Harris *et al.*, 2003]. An example of a recent incident is the multistate outbreak linked with chopped lettuce reported in U.S.A. in 2018, where 210 people from 36 states were infected, 96 people hospitalized and 5 deaths [CDC, 2018].
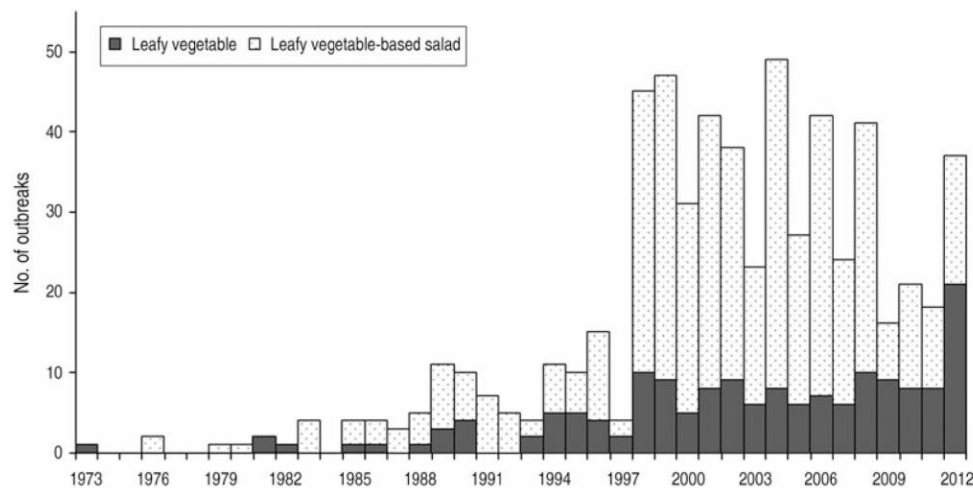
Figure 1.8. Leafy vegetable-associated outbreaks, including leafy vegetable-based salads, in U.S.A. between 1973 and 2012 [Herman *et al.*, 2015].

Nevertheless, apart from the consumption of the raw vegetables, other socio-economic reasons may favor the outbreaks increase:

- An increase in the product exportation and in the complexity of the production chain.

- The intensive agriculture has generated high proximity between farms field and animals (wild or in a farm), which are the main potential source of primary contamination [Lynch *et al.*, 2009].

- Increase of the number of vulnerable consumers, mainly immune-compromised population such as childrens and the elderly [Santos *et al.*, 2012].

The mentioned fresh-produce associated outbreaks are caused by a wide spectrum of microorganisms, including parasites, fungi, viruses and bacteria. However, the most commonly infections outbreaks are attributed to norovirus (NoV) and the coliform bacteria *E. coli* O157:H7 and *Salmonella spp.* [Kaczmarek *et al.*, 2019]. This fact is easily visible graphically in Figure 1.9, where a classification for the number of fresh-produce foodborne outbreaks based on the pathogen responsible in U.S.A. in a period of 14 years (1998-2012) is shown [Wadamori *et al.*, 2017]. In the case of the EU, the pattern of outbreaks was analogous to U.S. in most of the microorganism types, differing only in the prevalence of *E. coli*, which is significantly lower [Callejón *et al.*, 2015].
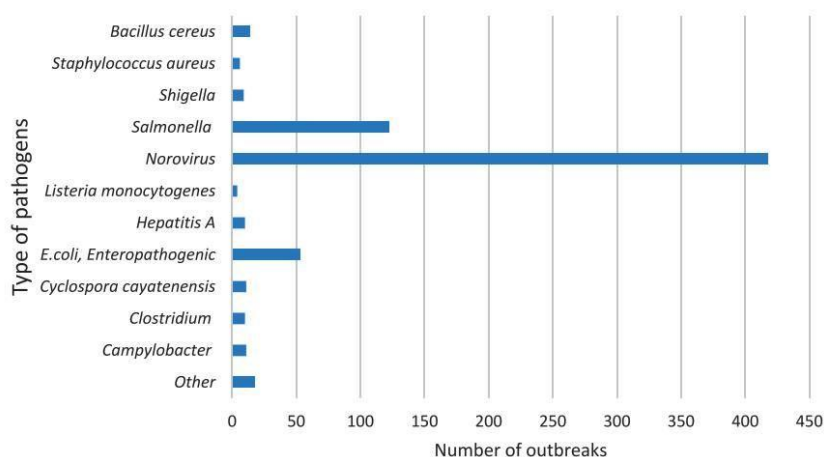
Figure 1.9. Reported pathogens responsible for fresh-produce foodborne outbreaks in U.S.A. between 1998-2012 [Wadamori *et al.,* 2017].

Taking into account that most of the NoV outbreaks reported occur by human contamination (food handlers) in the food service establishments, the other two coliform bacteria (*E. coli* O157:H7 and *Salmonella spp)* which provoke high infections number can be considered as the main sources of food-borne pathogens contamination during production chain of fresh-products [Callejón *et al.*, 2015]. Both are inhabitants of animal guts, facultative anaerobic, Gram-negative bacteria, non-sporulated microorganisms and highly infective (low infection dose) being even potentially lethal in vulnerable consumers (with a low immune response). The ingestion of food contaminated by *Salmonella spp.* usually presents an incubation period of 18-72 hours known their infection as Salmonellosis which symptoms are chills, abdominal pain, fever, nausea, diarrhea and vomiting [Harris *et al.*, 2003]. In the case of *E. coli* O157:H7, this bacteria is the dominant serotype of the Shiga toxin-producing *E. coli* strain more known as *E. coli* STEC. As the name indicated these *E. coli* strains are able to produce Shiga toxins (Stx) which are one of the most potent bacterial toxins. The most common infection incubation period for this pathogen varies from 2 to 5 days and the related symptoms can vary from asymptomatic and normal diarrhea to more severe symptoms like bloody diarrhea know as hemorrhagic colitis (HC) and hemolytic uremic syndrome (HUS), for which this strain is also known as Enterohemorrhagic *E. coli* (EHEC) [EFSA, 2011].

1.4.2. Agriculture

Agriculture is by far the largest water consumer, using almost 70 % of the water withdrawals volumes, although this percentage varied in each country in relation to the climate and being higher in arid or semiarid countries as shown in Figure 1.10.

The water requirement for vegetables cultivation varies significantly for each type of crop. Among them, the vegetables associated with the fresh-cut industry, i.e., short-term salad crops such as lettuce and radish present high water requirements due to these crops are very sensitive to lack of water and thus have to be watered very frequently. The estimated irrigation water needed for the

cultivation of a lettuce ton in a country with a Mediterranean climate like Spain is ca. 54 m³ [Perrin *et al.*, 2014]. According to the Spanish government, in Spain there is 32400 hectares of lettuce cultivation and an associated lettuce production of 843600 ton per cultivation cycle [BME, 2019]. Therefore, taking into account these data, the water consumption estimated only for a cycle of lettuce production in Spain is more than 4.0 x 10⁷ m³ which led to a high water foot-print of the industries related with these type of crops as is the case of the fresh-cut industry.
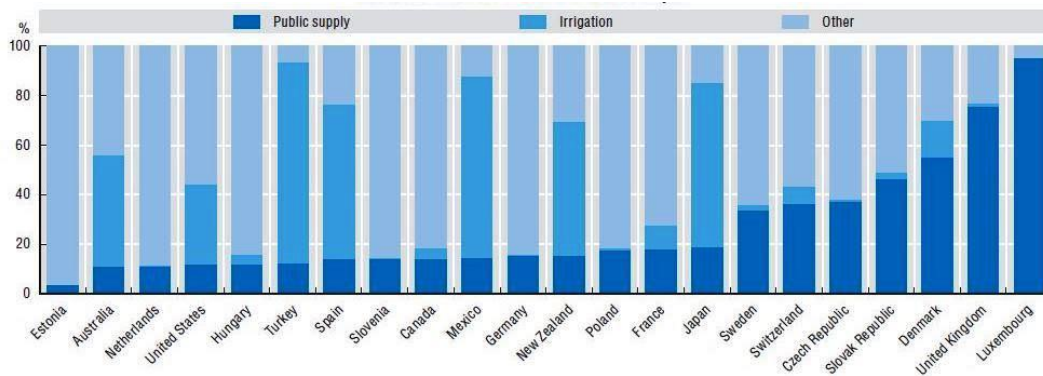
Figure 1.10. Freshwater abstractions by major primary uses in 22 countries [OECD, 2015].

On the other hand, water withdrawn for irrigation are globally increasing and it is estimated that will increase ca. 1 1% in 2050 specially in lower-income countries [FAO, 2015]. Hence, investments on infrastructures and water technologies that allow the employ of alternative water resources (like urban or industrial wastewater) improving their availability for irrigation purposes to guarantee future water availability and food production worldwide are needed. This sustainable water alternative has been included in one of the 17 Sustainable Development Goals (SDGs) adopted by the United Nations (UN) which objectives, among others, is tackling climate change and environmental protection. Specifically, in one of the specific targets (6.3) of the sixth goal (Clean water and sanitization) it is specifically reported: '*By 2030 improve water quality by reducing pollution, eliminating dumping and minimizing release of hazardous chemicals*

and materials, halving the proportion of untreated wastewater and substantially increasing recycling and safe reuse globally' [UN, 2016].

The main sources of wastewater generation are urban wastewater treatment plants (UWWTPs) and industrial activities. Urban wastewater reuse is not a new practice and represents an important non-conventional irrigation source, whether treated or not. Currently, the total land irrigated with raw or partially diluted urban wastewater in fifty countries is approximately 10 % of total irrigated land (20 million hectares) and only about 525000 ha are irrigated with reclaimed water (with a tertiary treatment) [FAO WATER, 2010]. The countries that report the highest volume of treated wastewater used for irrigation are: Qatar, Kuwait, United Arab Emirates, Cyprus, and Israel, all of them arid regions [Mateo-Sagasta and Burke, 2010]. This practice is also important in other Mediterranean countries like Spain, Italy, Greece, and Malta. Nevertheless, in these countries the use of non-conventional sources of water such as tertiary treated wastewater for irrigation still represent a minor source (about 1 %). In the case of Spain, only ca. $0.35 \cdot 10^9$ m^3 of reclaimed water per year is used respect to the total agricultural water withdrawal per year ($22 \cdot 10^9$ m^3), thus in Spain the reclaimed water used for irrigation represent almost 1.6 % of the total irrigation water [Drewes *et al.,* 2017; FAO-AQUASTAT, 2016].

The use of reclaimed water as an alternative water source for irrigation purposes has also important cost benefits, due to the reduction of freshwater abstraction, transmission, treatment, and distribution, as well as the reduction of wastewater discharge in rivers and coastal systems. In addition, the recycling of water nutrients is of great importance on the irrigation reuse scheme. This is the case of nitrogen and phosphorus, two of the more important fertilizers used for crops production, and which fabrication process is an energy-intensive and costly process [Johnston *et al.,* 2014]. Thus, recycling the phosphorus and nitrogen content from wastewater reduced the energy demands, the useful life of phosphate rock reserves, save the cost of fertilizers and reduce discharge into streams and rivers avoiding the eutrophication of water which strongly affects the ecosystem [FAO, 2015].

Nevertheless, in order to take benefits of the wastewater reuse, important efforts and investment by the regional authorities are needed in terms of promotion of sustainable and decentralized technological solutions for harvesting, treating and storage of wastewater.

Regarding the industrial sector, as was mentioned previously the fresh-cut industry present a high water consumption and wastewater generation with high nutrient content. Therefore, the implementation of a suitable water treatment to achieve a wastewater quality that complains with the reuse regulations at the end of the industrial process seems to be a plausible option to decrease the water foot-print of this industry through wastewater reuse for agriculture.

1.5. Water disinfection processes in fresh-cut industry

The washing step is one of the main processing operations involved in the microorganism propagation during the industrial production chain of fresh-cut produce. Therefore, water disinfection management is critical to avoid the dissemination of foodborne pathogens.

In this regard, the most common strategy to circumvent cross-contamination events is the employ of a sanitizer agent in the washing step. According the to FDA (Food and Drug Administration), sanitize is defined as '*to treat clean produce by a process that is effective in destroying or substantially reducing the numbers of microorganisms of public health concern, and also to reduce other undesirable microorganisms, without adversely affecting the quality of the product or its safety for the consumer*' [FDA,1998]. Any sanitizer has to be authorized by the regulation of each country. In Spain, the Real Decree 140/2003 established the authorized products for water treatment intended for human consumption (potable water) or to be used in the food industry. In the European Union, this statement is according to the REACH regulation (CE) nº 1907/2006.

Among the different sanitizers, chlorine has been widely used in food processing industries in the 20th century for spray, flume or wash waters disinfection [Kaczmarek *et al.*, 2019]. These compounds are the most used due to their

stability, low cost, good disinfection effectiveness against a wide microbial spectrum and their low impact on the sensorial and nutritional quality of the vegetables [Van Haute *et al.*, 2013].

Although there are other chlorine products with high antimicrobial activity, the industrial products most used as source of chlorine are sodium hypochlorite solutions due to they are cheaper and more stable than other compounds such as chlorine dioxide (ClO_2) which has to be generated in-situ. During chlorination process, several parameters have to be considered to reach the highest disinfection process performance:

-The range of chlorine concentration, which vary from 50 to 200 mg/L of total chlorine according to FDA; while the International Fresh-Cut Produce Association (IFPA) recommended a maximum total chlorine concentration of 100-150 mg/L.

-The water pH, recommended in the range 6 to 7 to favor the chemical state of chlorine in solution as hypochlorous acid ($HOCl^-$) which is the form with the highest antimicrobial power.

-The residual free chlorine is the excess of the added chlorine that does not react with the water matrix maintaining its form as hypochlorous acid and therefore also its bactericidal power. The IFPA recommended a residual concentration of 2 to 7 mg/L to avoid a microbial build-up and cross-contamination during the washing process [Delaquis *et al.*, 2004]. This parameter is directly related with the chlorine water demand, the concentration of chlorine that quickly reacts with the organic and inorganic components of the water matrix generating combined chlorine compounds with less microbial activity. Some EU countries have established the concentration of chlorine allowed to be used in fresh-cut products processing. For example, in UK, the maximum concentration of total chlorine and residual free chlorine approved are 100 and 10 mg/L, respectively [CFA, 2010].

However, the efficacy of chlorine treatment as a sanitizer agent in fresh-produce industries, even using high chlorine concentrations, is limited to 1 or 2-log

microbial reductions [Van Haute *et al.*, 2013]. The reduced effectiveness is attributed to the high chlorine water demand, which occurs due to the physic-chemical characteristics of the wash water, i.e., high organic and inorganic concentrations and high quantity of suspended solids (generally pieces of vegetable tissues) [Kaczmarek *et al.*, 2019]. As a consequence, a continuous addition of sodium hypochlorite until an excessive dose ($\geq$ 200 mg/L of total chlorine) is a usual practice, so-called hyper-chlorination. The excess of chlorine has several drawbacks, being the most important the production of adverse effects in the sensorial quality of the fresh-products and the generation of harmful disinfection by-products (DBPs) [Delaquis *et al.*, 2004].

The type of DBPs generated can be inorganic or organic compounds. The inorganic DBPs with higher health concern due to its potential toxicity are the toxic elemental chlorine (gas Cl_2) that affects the respiratory system of workers [Van Haute *et al.*, 2013] and the generation of chlorates (ClO_3^-) that are nephrotoxic compounds. The chlorates accumulated during the washing step are transferred to the fresh-cut products in an estimate rate of 2.5-10 % (depending on the vegetable) [Garrido *et al.*, 2019] and this represents an important health risk for consumers. In the EU, the maximum residue level (MRL) allowed for chlorate in food is 0.01 mg/kg, although recent studies on leafy vegetables have shown chlorate concentrations of 0.2 - 0.3 mg/kg in the end-products [Garrido *et al.*, 2019; Gil *et al.,* 2019].

The harmful chlorinated organic compounds generated as a consequence of wash water chlorination may be from different chemical families: acids like dichloroacetic acid (DCAA) and trichloroacetic acid (TCAA), mono- or dichloramines and trihalomethanes (THMs). Among these compounds, the trihalomethanes are the DBP family that has been generated more health concern due to these compounds are classified by the International Agency for Research on Cancer (IARC) and the WHO as carcinogenic to humans even at very low concentrations (100 μg/L established in drinking water) [Gómez-López *et al.*, 2014]. In this context, the European Authorities has not be positioned regarding the approval or banned of the use of chlorine compounds in

fresh-cut industry and left each member state to decide independently, which had led to the prohibition of their employ in some European countries including Switzerland, Belgium, Germany, Denmark and the Netherlands [Castro-Ibáñez *et al.*, 2017].

This recently modifications had led to an increase in the search of alternative water disinfection treatments covering similar action spectrum of chlorination but reducing undesired post-treatment toxic effects [Bilek and Turantaş, 2013]. In this regard, a wide range of disinfection alternative treatments to chlorination based on biological substances, chemical agents and physical removal of microorganisms are currently under investigation [Meireles *et al.*, 2016; Artés-Hernández *et al.*, 2017] and they will be widely explained in next section.

1.6. Alternative water purification processes

It is important to highlight that most of the water treatments applied or under investigation for remediation of wash water in the fresh-cut industry are mainly focused on the inactivation of food-borne pathogens, nevertheless this wastewater are usually polluted by OMCs (mainly pesticides), which removal should be considered as target contaminants for the evaluation of new or alternative process for this industry, taking into in mind their potential as reclaimed water for agriculture.

Regarding main alternative disinfection processes to chlorine in the fresh-cut industry, they can be divided on three categories: use of biological substances, chemical agents and physical removal. The advantages and disadvantages of these biological, physical and chemical processes are summarized in Figure 1.11. It can not be noted that, from the fresh-cut industry point of view, alterations of the organoleptic properties are one of the main drawbacks to apply a new water treatment in the industry. Therefore, treatments combinations have been evaluated during last years as a strategy to improve the individual treatment capability for disinfect wash water.
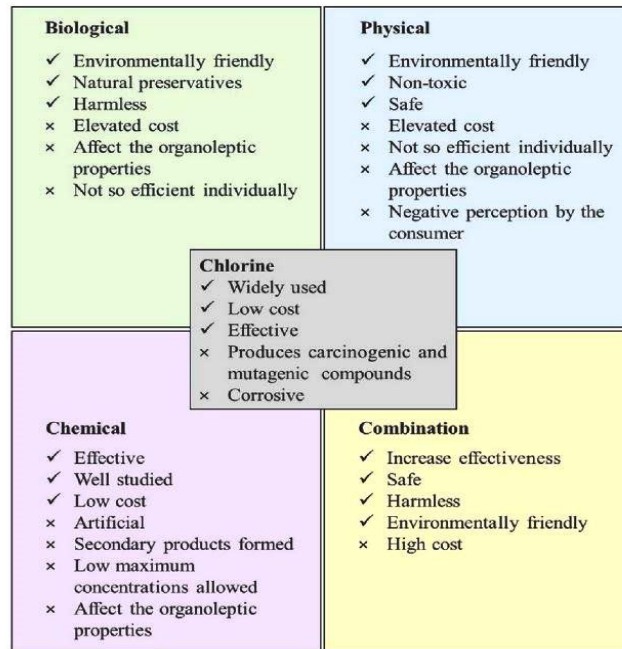
Figure 1.11. Advantages (✓) and disadvantages (x) of chlorination and other water disinfection processes [Meireles *et al*., 2016].

The potential biological-based treatment alternatives can be summarized in the use of three biological substances: bacteriocins [Arevalos-Sánchez *et al*., 2012], phytochemicals [Belleti *et al*., 2008] and lytic bacteriophages [Spricigo *et al*., 2013]. The disinfection mechanisms by these biological processes are based on disruption and malfunctioning of the outer bacterial membrane altering the permeability (bacteriocins and phytochemicals) or provoking the microbial lysis (lytic bacteriophages).

Regarding the physical-based alternatives, they can be classified as non-irradiation and irradiation processes. The most important non-irradiation physical treatments are the application of high pressure [Rendueles *et al.,* 2011], ultrasound [Elizaquível *et al*., 2012], pulsed light [Agüero *et al*., 2016], cold plasma [Schnabel *et al*., 2019] and radiation, including Ultraviolet-C (UV-C) [Ignat *et al*., 2015] and Ultraviolet-A (UV-A) radiation by using proper lamps. In fact, the use of UVC and UVA radiation usually is investigated in combination with chemical agents, to improve its water disinfection performance. Several studies have been recently reported using UV-A lamps as source light with

several compounds like gallic acid [Cossu *et al.*, 2016], ferulic acid [Cossu *et al.*, 2018], benzoic acid [Ding *et al.*, 2018], ZnO [Ercan *et al.*, 2016] and propylparaben [Ding *et al.*, 2019] showing promising results. In the case of UV-C, this has been also investigated jointly with chemical agents, including heterogeneous photocatalysis (UV-C/TiO$_2$) and photo-chemical processes (UV-C/H$_2$O$_2$ and UV-C/PAA) [Selma *et al.*, 2008b; Hadjok *et al.,* 2008; Collazo *et al.*, 2019].

A schematic representation of the main mechanisms involved in the bacteria inactivation by physical methods is presented in Figure 1.12. This is based mainly on DNA alterations, oxidation of vital components by the Reactive Oxygen Species generated (ROS) or physical disruptions through heat or force. Among all these processes, UV-C is the most promising technology to be implemented in commercial installations due to their efficiency against a wide range of microorganisms and the no-residue generation. Nevertheless, those making use of a UVC-lamp (low Hg pressure, maximum 254 nm) as a photon source have high process costs which represents the main obstacle to their commercial application.
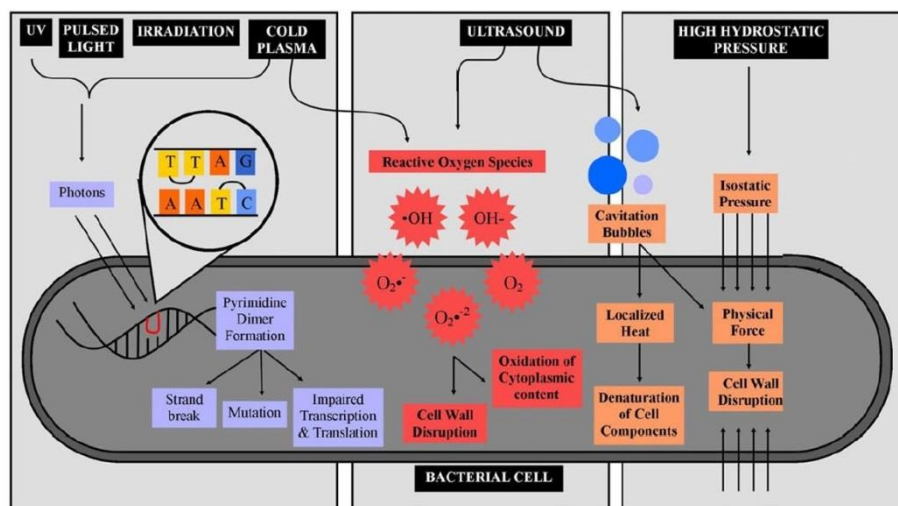
Figure 1.12. Schematic representation of the disinfection mechanisms by physical methods [Bhilwadikar *et al.*, 2019].

Finally, several chemical disinfection alternatives to chlorine has been also widely investigated such as ozonation [Selma *et al.*, 2007], electrolyzed water

[Gil *et al*., 2015], essential oils [Burt, 2004], organic acid compounds [Park *et al*., 2011], peracetic acid (PAA) [Lee and Huang, 2019], hydrogen peroxide [Huang *et al*., 2012], and the recently trend to the employ of persulfate salts as oxidant agent [Qi *et al*., 2019].

On the other hand, Advanced Oxidation Processes (AOPs) have widely proven to be effective for disinfect different types of water matrices. AOPs are chemical process or physicochemical processes widely investigated for disinfection and decontamination of wastewaters. These processes are based on the generation of non-selective hydroxyl radicals (HO$^{\bullet}$), the strongest Reactive Oxygen Species (ROS) after fluoride (E$_0$: 2.80 V) which generates accumulative damages on cells leading to its inactivation. The main disinfection mechanisms for the chemical methods are summarized in Figure 1.13. These inactivation mechanisms are based on cellular components oxidation and alteration of the cytoplasmic conditions by the effect of: 1) ROS generated; 2) chlorine active species (electrolyzed water) and; 3) hydrophobic or lipophilic compounds.
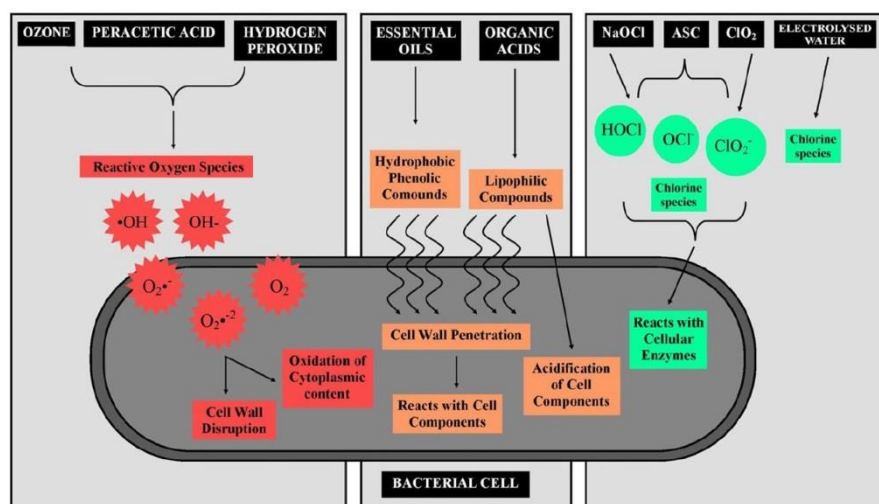
Figure 1.13. Schematic representation of the main disinfection mechanisms by chemical methods [Bhilwadikar *et al*., 2019].

Among all the disinfection processes previously mentioned, the use of radiation and ozonation are the most promising treatment alternatives to be implemented in the fresh-cut industry due to their efficiency against a wide range of microorganisms and the no-residue generation [Selma *et al*., 2008a]. In this

context, the use of an environmentally friendly source of energy such as natural solar radiation may drastically reduce the cost of UVC water treatment. Therefore, in this research, both ozonation and AOPs driven by natural sunlight as source of photons have been investigated for the simultaneous removal of bacteria and OMCs (pesticides) from fresh-cut wastewater, which have not been yet investigated.

1.6.1. Ozonation

Ozone was discovered in the 17th and 18th centuries. In 1795, Van Mauren (a Dutch chemist) suspect to the presence of a non-known compound with a characteristics odor during a strong storm with electric discharges. In 1840, 45 years later, the German-Swiss chemist Christian Friedrich Schönbein finally discovered the ozone molecule. This chemist also gave the name of this molecule which comes from the Greek word 'ózein' which means 'to smell'. Once discovered, its chemical structure as O_3 was confirmed 32 years later and its resonance structure a few decades later (1952) [Beltran, 2003].
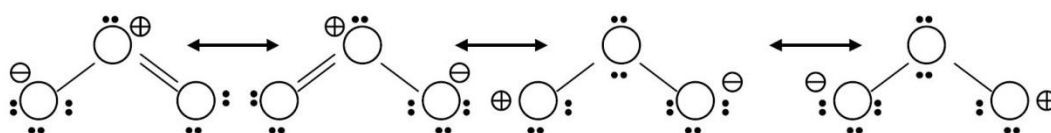
Figure 1.14. Resonance structures of ozone molecule.

The ozone molecule is composed of three oxygen atoms with a sp^2 hybridation which should form an equilateral triangle (angle of 120º between the orbitals) with an oxygen nucleus in its center. However, in the O_3 molecule, this angle is lower (116º 49") which was explained due to the ozone molecule is a hybrid resonance structure formed by the four possible structures that are shown in Figure 1.14. According to the bond length, the two first resonance structures are the most important although the other two also contribute to some extent generating the mentioned bond angle lower than 120º as a consequence of the

electrostatic attraction between the adjacent oxygen atoms with opposite charges. The electronic configuration of the molecule makes ozone highly reactive to oxidize compounds (standard redox potential of 2.07 V) and also confers it a weak polarity (0.53 Debye). Moreover, the positively and negatively charged oxygen atoms in some resonance structures confer to ozone an electrophilic and a nucleophilic character, respectively.

1.6.1.1. Chemistry of aqueous ozone

Because of its high reactivity, ozone may react in water through different electrophilic reactions types. Theoretically and based on its electronic configuration this compound could also be involved in nucleophilic reactions but this nucleophilic behaviour is not yet confirmed in aqueous systems [Beltran, 2003]. The ozone reactions in an aqueous medium can be classified in three types: cycloadditions, electrophilic substitutions and electron-transfer reactions. The organic water constituents mainly react directly and selectively with molecular ozone through the two first reaction types also known as direct ozone reactions [Beltran, 2003; Von Sonntag, 2012].

i) Direct Ozone reactions

These reactions are based on an initial ozone electrophilic attack, and therefore the water constituents with the presence of electron-rich moieties (unsaturations, π bonds with delocalized electrons, electron-rich heteroatoms as sulfur or nitrogen and electron-donating group (EDG)) in their structure are susceptible to be involved in these reactions being finally oxidized.

The cycloadditions reactions occur typically in the presence of unsaturated organic compounds, such as alkenes which are oxidized generating H_2O_2 and two carbonyl compounds. This reaction mechanism is known as Criegee mechanism (Figure 1.15). Briefly, it consists of three steps: 1) a 1,3-dipolar addition to the double bound generating a trioxolane (ozonide) which is an unstable intermediate; 2) the decomposition of ozonide generating a carbonyl compound and a dipolar ion also known as a zwitterion; and 3) the dipolar ion

reacts with a water molecule generating hydroxyhydroperoxide which finally is decomposed in H_2O_2 and another carbonyl compound [Wei *et al.*, 2017].
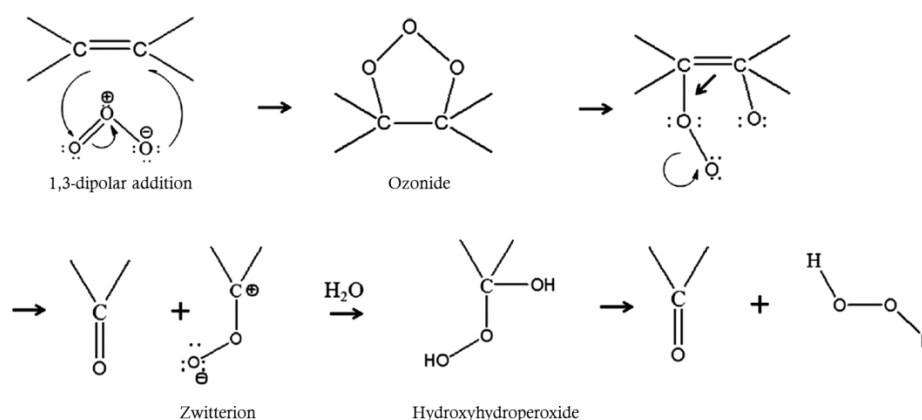
Figure 1.15. Criegee mechanism of ozone direct reaction.

On the other hand, aromatic and polyaromatic compounds substituted with an EDG as -OH or -NH$_2$ group, are especially susceptible to react with ozone. This reaction mechanism is simple and is shown in Figure 1.16. Briefly, it consists in an electrophilic attack of ozone to a nucleophilic position, mainly at para- and ortho- ring positions, giving rise to a molecular oxygen release and the hydroxylation of the parent compound.
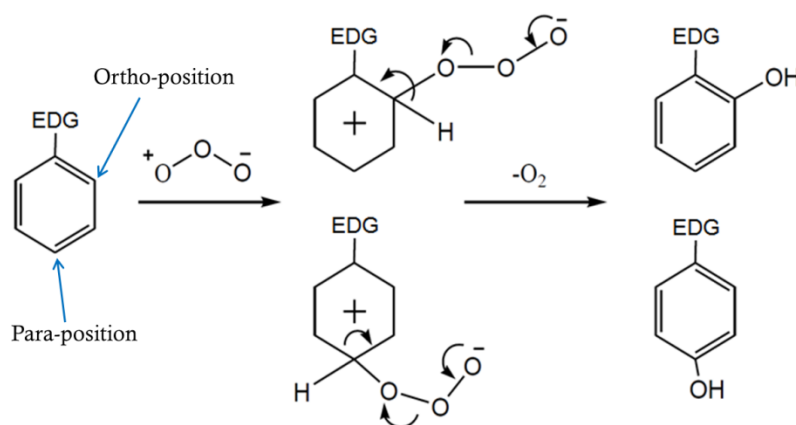
Figure 1.16. Electrophilic substitution reaction of an aromatic compound with an EDG and ozone.

Both direct reactions are selective and therefore depending on the chemical structure of the organic compound, the rate constants can vary more than ten orders of magnitude (from 0.1 to 10^{10} $M^{-1}s^{-1}$).

ii) Electron transfer Ozone reactions

The high standard redox potential of the ozone molecule (2.07 V) make also possible electron transfer reactions with the water constituents. The main electron transfer reactions of aqueous ozone are the reactions involved in their radical chain decomposition. The reactions involved in the decomposition of ozone in water, initially proposed by Joseph Weiss in 1934, have been modified over the years, being the mechanism present below the most accepted recently [Merényi *et al.*, 2010]. This mechanism involves the generation of reactive oxygen species (ROS), mainly HO˙, by several reactions (Eq 1.1-1.13) explained in the following general mechanisms and steps: i) Initiation step (Eq.1.1-1.2) where superoxide anion radical ($O_2^{\bullet-}$) and hydroperoxyl radical ($HO_2^{\bullet}$) are generated; ii) radical chain (Eq. 1.3-1.11) where hydroxyl radicals (HO˙) are generated and hydroperoxyl radical ($HO_2^{\bullet}$) are regenerated; and iii) termination step where reactions with matrix constituents, such as dissolved organic matter (DOM) (Eq. 1.12) or reactions between radicals (Eq. 1.13) can occur.

$$O_3 + OH^- \rightarrow HO_4^- \qquad k_1 = 70\ M^{-1}s^{-1} \qquad\qquad \text{Eq. 1.1}$$

$$HO_4^- \leftrightarrow O_2^{\bullet-} + HO_2^{\bullet} \qquad k_2 \approx 10^7\ s^{-1} \qquad\qquad \text{Eq. 1.2}$$

$$HO_2^{\bullet} + O_2^{\bullet-} \rightarrow HO_2^- + O_2 \qquad k_3 = 10^8\ M^{-1}s^{-1} \qquad \text{Eq. 1.3}$$

$$HO_2^- + O_3 \rightarrow HO_5^- \qquad k_4 > 2.8 \times 10^6\ M^{-1}s^{-1} \qquad \text{Eq. 1.4}$$

$$HO_5^- \leftrightarrow HO_2^{\bullet} + O_3^{\bullet-} \qquad k_5 > 10^7\ s^{-1} \qquad\qquad \text{Eq. 1.5}$$

$$HO_5^- \rightarrow 2\ O_2 + OH^- \qquad k_6 \approx k_5 \qquad\qquad\qquad \text{Eq. 1.6}$$

$$HO_2^{\bullet} \leftrightarrow O_2^{\bullet-} + H^+ \qquad k_7 = 3.2 \text{ x } 10^5 \text{ s}^{-1} \qquad \text{Eq. 1.7}$$

$$O_3 + O_2^{\bullet-} \rightarrow O_3^{\bullet-} + O_2 \qquad k_8 = 1.6 \text{ x } 10^9 \text{ M}^{-1}\text{s}^{-1} \qquad \text{Eq. 1.8}$$

$$O_3^{\bullet-} \rightarrow O_2 + O^{\bullet-} \qquad k_9 = 1.94 \text{ x } 10^3 \text{ s}^{-1} \qquad \text{Eq. 1.9}$$

$$O^{\bullet-} + H_2O \rightarrow HO^{\bullet} + OH^- \qquad k_{10} = 9.6 \text{ x } 10^7 \text{ s}^{-1} \qquad \text{Eq. 1.10}$$

$$HO^{\bullet} + O_3 \rightarrow O_2 + HO_2^{\bullet} \qquad k_{11} = 2.0 \text{ x } 10^9 \text{ M}^{-1}\text{s}^{-1} \qquad \text{Eq. 1.11}$$

$$DOM + HO^{\bullet} \rightarrow O_2^{\bullet-} + P \qquad k_{12} \approx 10^8 - 10^{10} \text{ M}^{-1}\text{s}^{-1} \qquad \text{Eq. 1.12}$$

$$HO^{\bullet} + HO_2^{\bullet} \rightarrow O_2 + H_2O \qquad k_{13} = 3.7 \text{ x } 10^{10} \text{ M}^{-1}\text{s}^{-1} \qquad \text{Eq. 1.13}$$
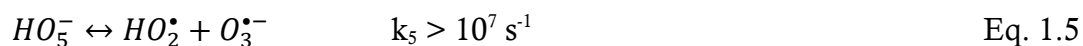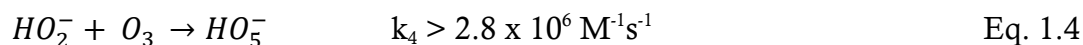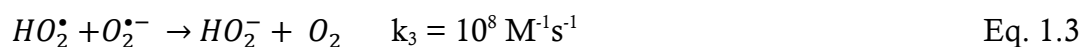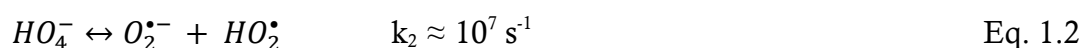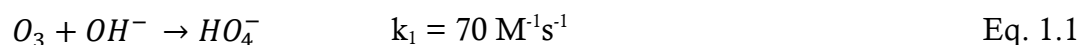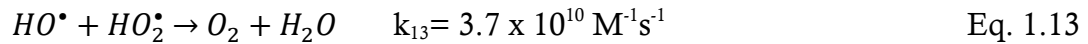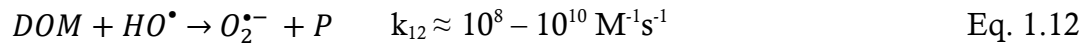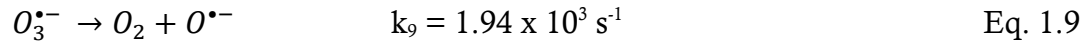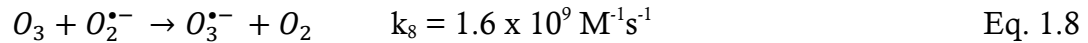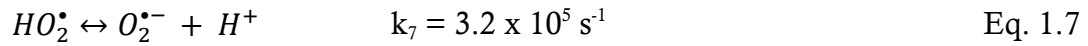
The predominant reaction-path in water ozonation depends on the water pH which affects the O_3 decomposition kinetics. At pH lower than 8, the direct and selective oxidation by O_3 seems to be the predominant pathway. At pH > 8, the O_3 decomposition kinetic is accelerated (higher concentration of OH^-), favoring, therefore, the indirect and fast oxidation of organic compounds mainly by the $HO^{\bullet}$ generated which has a stronger oxidant character (E°= 2.80V). The $HO^{\bullet}$ generation during water ozonation has generated a debate in the scientific community about the consideration of this process as an AOP or not, although based on the general definition of an AOP, ozonation should be considered as one of them.

Complex water matrices usually contain several constituents that can interfere in the ozone decomposition reactions (initiating, promoting or inhibiting the $HO^{\bullet}$ generation). As was presented in the Eq. 1.12, the DOM can act as a scavenger of the radicals generated ending the chain reaction. Nevertheless, some dissolve organic compounds, such as electron-rich aromatic moieties, can acts as radical chain promoters through electron transfer reactions with ozone although it is difficult to estimate the ratio of DOM that acts promoting or inhibiting the chain reaction [Pocostales *et al.*, 2010; Von Gunten *et al.,* 2003].

Other water constituents that can interfere in the radicals generation are some inorganic anions. These ions act as radical chain inhibitors or HO• scavengers. Some of the most important anions are chloride, bromide, nitrite, carbonate and bicarbonate. Such as, nitrite reacts fast with molecular ozone in a 1:1 molar ratio and it is estimated that consume ca. 3.43 gO_3 per g of NO_2-N [Rizzo *et al.*, 2019]. Among all of these inorganic ions, the reaction between bromide and ozone is the one that more concern generates due to giving rise to the formation of the toxic byproduct bromate which is a potential human carcinogen. Regarding water legislation, although there is not a specific guideline for its presence in wastewater, the parametric value of bromate is already established for drinking water quality and environmental standard in a limit value of 10 and 50 μg/L, respectively [WHO, 2011]. Bromate formation during ozonation depends on several factors such as T, pH and dissolved organic carbon (DOC), but is mainly linked with the initial bromide concentration and the specific ozone doses applied. Previous studies have reported that the bromide concentration found in urban wastewater varies between μg/L to a few mg/L. The molar bromate yields after ozonation, applying the most usual specific ozone doses for wastewater treatment, (from 0.4 to 0.6 gO_3/g DOC) was found to be in the range of 3 to 5 %. Therefore, a bromide concentration of <0.1 mg/L should not generate a bromate concentration higher than the allowed values. If the bromide concentration is higher, the water treatment by ozonation is not recommended [Soltermann *et al.*, 2017; Rizzo *et al.*, 2019].

Overall, if the water matrix intended to treat contains organic contaminants with low reactivity towards molecular ozone (ozone-recalcitrant compounds) and also high quantity of inorganic ions which inhibit their degradation by indirect ozone reactions, water ozonation will not be effective. These water characteristics are common in most of the wastewater matrices, and for this reason the search and study of ozone-based processes able to improve the generation of HO• and therefore also their efficiency is required.

In the regard, it is well described that the generation of HO• by ozone decomposition (indirect pathway) can be significantly accelerated by H_2O_2

addition (peroxone process), trough O_3 reaction with the H_2O_2 conjugate base (HO_2^-) (Eq. 1.14).

$$H_2O_2 \leftrightarrow H^+ + HO_2^- \hspace{4cm} \text{Eq. 1.14}$$

Nevertheless, contrary to what was commonly accepted, recent studies have demonstrated that the $HO^\bullet$ generation yield in the peroxone process is near to 0.5 instead to 1, i.e., twice O_3 molecules are required to generate one $HO^\bullet$ [Merenyi *et al.*, 2010; Fischbacher *et al.*, 2013]. The proposed mechanistic interpretation for the low yield observed are based on an adduct formation (HO_5^-) (Eq. 1.4) which can decompose trough 2 different ways (Eq. 1.5-1.6), of which only one yields $HO^\bullet$ (Eq. 1.5). Therefore, according to these latest findings, the benefits of adding H_2O_2 may be only based on a faster ozone decomposition into $HO^\bullet$ and not on higher radical yields.

The faster $HO^\bullet$ generation by peroxone process can increase the removal efficiencies of the ozone-recalcitrant organic compounds and also has proven to be able to inhibit the bromate formation in some extend, being a promising ozone-based process alternative [Mao *et al.*, 2018].

1.6.1.2. Ozone generation applied in water treatment

The high reactivity of ozone molecule also converts it in an unstable gas. For this reason ozone has to be generated in situ. There are several techniques to generate ozone such as phosphorous contact, photochemical techniques (oxygen radiolysis and photolysis by UV irradiation with wavelengths <220 nm), electrochemical generation in aqueous solution or the application of an electric discharge to an oxygen flow, only the last one are able to produce ozone in industrial quantities (>2 kg/h) and therefore is today the most widely used for commercial ozone production [Wei *et al.*, 2017]. This last technique is known as corona discharge generation and is an evolution of one of the first ozone generators which was invented by Werner von Siemens in 1857 [Pekárek *et al.*,

2008]. A schematic illustration of the ozone generation process by corona discharge is represented in Figure 1.17.
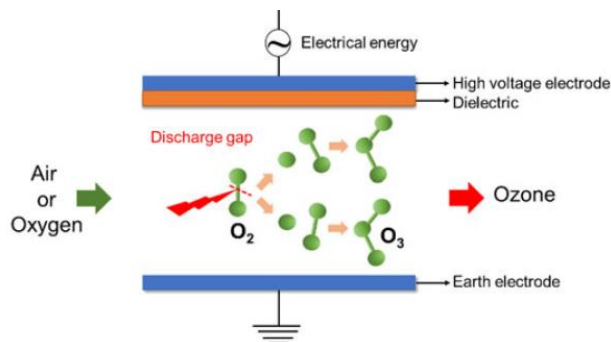
Figure 1.17. Schematic ozone generation process by corona discharge [Deng *et al.*, 2019]

In general, the corona generators are composed by a power supply, two electrodes (high voltage and earth) and a dielectric material which may be glass, ceramic, or quartz. The ozone generation consists in the application of a high voltage through a narrow gap filled with oxygen. In these conditions, the electrons present collide with oxygen molecules excite them from the ground state (O_2) to negative ion state (O^-), i.e., the oxygen molecule is splitted, and after that, the negative oxygen ions immediately react with other oxygen molecule giving ozone (O_3) [Wei *et al.*, 2017].

The high oxidation potential of both, molecular ozone and ROS generated during its decomposition in water, converts ozonation in one of the most powerful water disinfectant agents and with a wide antimicrobial spectrum. However, there is a controversy on which oxidant specie is more responsible of bacteria inactivation by ozone process due to some authors reported that the direct oxidation of molecular constituents by O_3 is the main inactivation mechanism whereas others have suggested that are the ROS generated. There is not an agreement about this topic but the recent research seems to indicate that the major contribution of one oxidant or another will mainly depend on the water matrix characteristics which are the determinant parameter on the stability and generation of O_3 and ROS, respectively.

Due to its high disinfection capability, until a few decades ago ozonation was applied with the only porpuse of water disinfection. The first industrial application of ozone for water treatment (drinking water disinfection) was in Nice in the year 1906, where ozone was applied to disinfect more than 20000 m^3 per day of river water [Loeb *et al.*, 2012].

Recent and interesting ozone applications, are it use as chlorine alternatives to disinfect swimming pool waters due to ozone are also able to oxidize dissolve organic carbon resulting in cleaner waters or its use to disinfect irrigation water for plant disease management due to its capability to also inactivate viruses and fungi [Hansen *et al.*, 2016].

On the other hand, the high reactivity towards organic compounds showed by aqueous ozone application join with the growing concern about the environmental and health risk associated with water microcontaminants has led to the decision of some countries to include ozonation as a tertiary process in UWWTPs to remove OMCs prior to their discharged into water bodies or its reuse in agricultural irrigation. Several research studies have been performed to evaluate the capability and drawbacks of this application [Rizzo *et al.*, 2019]. Among these studies, stands up one study at large-pilot scale in a municipal WWTP of Switzerland performed by Margot et al. and published in 2013. In this study, the removal of more than 70 OMCs (from different families) present in urban wastewater was investigated during more than one year concluding that low ozone doses for OMCs removal is a viable option due to OMCs removals of ca. 80 % were attained [Margot *et al.*, 2013].

In fact, Switzerland is the most representative example in terms of urban wastewater legislation for OMCs removal and therefore, environment protection. The last Swiss water legislation, which entered into force in 2016, require the upgrade of some selected WWTPs and at least the removal of 80 % of the OMCs present in the raw wastewater. To that purpose, several WWTPs are being improved either with ozonation or powered activated carbon (PAC) [Rizzo *et al.*, 2019].

Finally, water ozonation has been applied during decades for many and varied industrial applications [Rice *et al.*, 1996], being in the last years, of special interest its application in food industries, like in fresh-cut industry as was mentioned above. In this context, over the latest years, the interest in ozonation as a chlorination replacement treatment in food processing industries has increased, being recently declared 'Generally Recognized As Safe' (GRAS status) for food contact. Its use has been approved in many countries due to its high biocidal efficacy in a wide antimicrobial spectrum, high penetrability and decomposition without leaving residues [Smetanska *et al.*, 2013; Hassenberg *et al.*, 2007]. In contrast, no information is currently available about the use of the peroxone treatment for water treatment in the food industry.

The ozonation process has some important advantages compared with chlorine that make it a viable option for its application in fresh-cut industries; some of them are [Tomas and Tiwari, 2013]:

- This system is able to generate the disinfectant demand 'in situ' eliminating the need to store and transport it.

- Ozone is an antimicrobial agent stronger than hypochlorite (3000 times), a key factor to explain the broad spectrum of ozone disinfection. Unlike chlorine, ozone is able to inactivate cysts-forming protozoan parasites and bacterial or fungal spores.

- It spontaneous aqueous decomposition into oxygen (a non-toxic residue) is one of the biggest advantages due to reduce the generation of the worrying chlorine DPBs and reduce the risk of residue formation on the food-contact surfaces.

- Ozone save water due to no-residues is left avoiding therefore the standard practice of product rinses to remove them from the products. Moreover, ozone suppressed the increase of DOC in the washing water delaying the water replacement reducing the industrial water footprint.

- Reduce the environmental impact of the industry due to generate more 'clean' wastewater, i.e., with less conductivity, turbidity, organic matter and organic contaminants than the generated as a result of chlorine application.

1.6.2. Solar water treatments

The interest in the application of AOPs as alternative technology for water purification (elimination of both organic contaminants and microorganisms) has grown significantly in the last decades due to their high oxidant capability and non-selectivity which allow the complete mineralization of wide range of organic compounds (into carbon dioxide, water and inorganic ions) and the inactivation of a broad-spectrum microorganisms [Malato *et al.*, 2009].

Among all the AOPs, are especially important the photochemical and photocatalytic processes based on the contaminant oxidation by the radicals generated as a result of the radiation absorption by a photo-sensible compound or a photo-catalyst. The production of radiation by commercial UV lamps is expensive which leads to an increasing interest in the use of an alternative source of photons. In this regard, the use of the inexhaustible and free solar radiation ($\lambda > 300$ nm, Figure 1.18) as source of photons in photochemical or photocatalytic processes make them economically and environmentally sustainable processes.
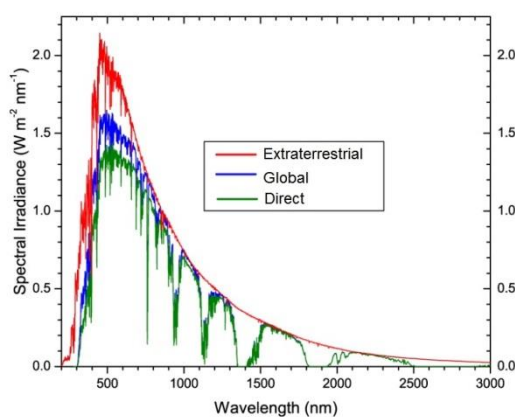
Figure 1.18. Solar spectra for extraterrestrial radiation (ASTM E-490), global and direct radiation with an air mass of 1.5 on a sun-facing 37° tilted surface (ASTM G-173-03) [ASTM, 2014 ; ASTM, 2005].

1.6.2.1. Photo-reactors

The reactors more used for solar water treatment are based on compound parabolic collector (CPC) systems. These reactors were developed in the 80s with the aim to concentrate the solar radiation using a fixed dispositive as a combination between high concentration parabolic collectors and fixed flat systems. The main advantages of its use for solar water treatment are its lower cost than solar tracking collectors, the capability to collect both diffuse and direct radiation with a high optical performance and its combination with tubular reactors allowing to work with a turbulent flow that favors the efficiency of the photocatalytic processes [Blanco, 2002].

These reactors are based on static collectors with a solar concentration factor of 1. CPC photo-reactors are formed by a reflective surface where two parabolic mirrors are connected with an absorber tube in the focus. The reflector design allows to collect the incident radiation and to distribute the reflected light homogeneously around the absorber tubes (Figure 1.19) where the water is recirculated under turbulent flow conditions using centrifugal pumps.
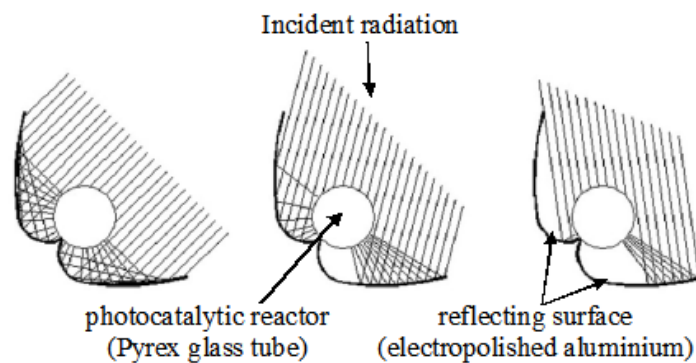
Figure 1.19. Diagram of solar radiation collection and distribution in CPC reactors [Blanco, 2002].

The reflectors are made by anodized aluminum sheets due to its high UV reflectivity and resistance to high solar radiations and adverse weather conditions whereas the material commonly used for the absorber tube is

borosilicate-glass as a compromise between the price and the transmissivity in the UV range [Blanco *et al.*, 1999].

The efficiency of the use of these photo-reactors for water treatment has been widely proven by several disinfection and decontamination studies [Malato *et al.*, 2009].

1.6.2.2. Solar photo-Fenton process

Fenton process is one of the AOPs most studied for water treatment due to is able to generate a high quantity of hydroxyl radicals by a reaction between iron and the oxidant H_2O_2 which is decomposed into H_2O and O_2 and therefore without generating chemical residues. Moreover, iron is omnipresent in the environment being the fourth most abundant element in the Earth's surface in several oxidation states, although in aqueous solution is mainly present as ferrous (Fe^{2+}) or ferric iron (Fe^{3+}) forming hexacoordinated complexes with lewis-base ligands (as water molecules) present in the aqueous system.

The Fenton reaction was discovered in 1894 by Henry John Horstman Fenton, who oxidizes tartaric acid in aqueous solution by addition of ferrous iron and H_2O_2 [Fenton, 1894]. The mixture of dissolve iron and H_2O_2 is called Fenton or Fenton-like reagent for the use of ferrous and ferric iron, respectively. The global Fenton reaction in an acid medium, dark and in absence of organic compounds is the H_2O_2 oxidation into molecular oxygen and water catalysed by iron (Eq. 1.15).

$$2\ H_2O_2 \xrightarrow{Fe} O_2 + H_2O \qquad\qquad\qquad \text{Eq. 1.15}$$

The Fenton or thermal Fenton reaction pathway is a radical chain reaction, known as Haber-Weiss mechanism, which main reactions are presented in Eq. 1.16-1.23 [Malato *et al.*, 2009].

$$Fe^{2+} + H_2O_2 \rightarrow Fe^{3+} + HO^- + HO^\bullet \qquad k_{16} = 53\text{-}76\ \text{M}^{-1}\text{s}^{-1} \qquad \text{Eq.1.16}$$

$$Fe^{2+} + HO^\bullet \rightarrow Fe^{3+} + HO^-$$
$k_{17} = 2.6\text{-}5.8 \times 10^8 \ M^{-1}s^{-1}$ Eq. 1.17

$$Fe^{2+} + HO_2^\bullet \rightarrow Fe^{3+} + HO_2^-$$
$k_{18} = 0.75\text{-}1.5 \times 10^6 \ M^{-1}s^{-1}$ Eq. 1.18

$$Fe^{2+} + HO_2^\bullet + H^+ \rightarrow Fe^{3+} + H_2O_2$$
$k_{19} = 1.3 \times 10^6 \ M^{-1}s^{-1}$ Eq. 1.19

$$Fe^{3+} + H_2O_2 \rightarrow Fe^{2+} + HO_2^\bullet + H^+$$
$k_{20} = 0.0001\text{-}0.01 \ M^{-1}s^{-1}$ Eq. 1.20

$$Fe^{3+} + HO_2^\bullet \rightarrow Fe^{2+} + O_2 + H^+$$
$k_{21} = 1.2 \times 10^6 \ M^{-1}s^{-1}$ Eq. 1.21

$$Fe^{3+} + O_2^{\bullet-} \rightarrow Fe^{2+} + O_2$$
$k_{22} = 0.05\text{-}1.9 \times 10^9 \ M^{-1}s^{-1}$ Eq. 1.22

$$HO^\bullet + H_2O_2 \rightarrow H_2O + HO_2^\bullet$$
$k_{23} = 1.7\text{-}2.5 \times 10^{-7} \ M^{-1}s^{-1}$ Eq. 1.23
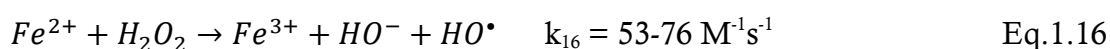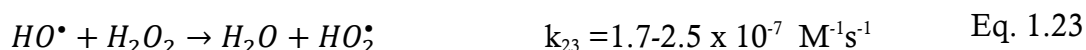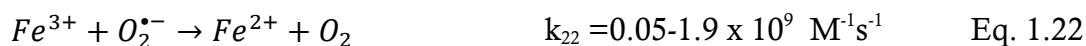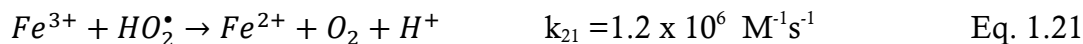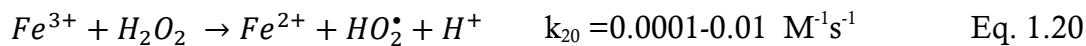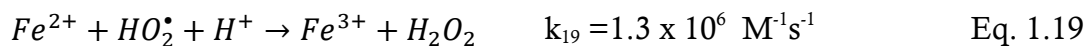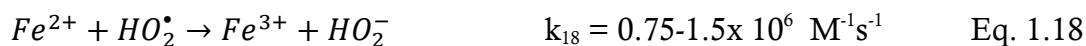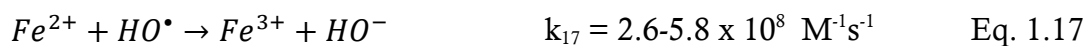
Furthermore, a number of radical-radical reactions (Eq. 1.24-1.26) and equilibriums (Eq. 1.27-1.32) also accurs:

$$2HO^\bullet \rightarrow H_2O_2$$
$k_{24} = 5\text{-}8 \times 10^9 \ M^{-1}s^{-1}$ Eq. 1.24

$$2HO_2^\bullet \rightarrow H_2O_2 + O_2$$
$k_{25} = 0.8\text{-}2.2 \times 10^6 \ M^{-1}s^{-1}$ Eq. 1.25

$$HO_2^\bullet + HO^\bullet \rightarrow H_2O + O_2$$
$k_{26} = 1.4 \times 10^{10} \ M^{-1}s^{-1}$ Eq. 1.26

$$HO_2^\bullet \leftrightarrow O_2^{\bullet-} + H^+$$
$k_{27} = 3.55 \times 10^{-5} \ M^{-1}s^{-1}$ Eq. 1.27

$$HO^\bullet \leftrightarrow O^{\bullet-} + H^+$$
$k_{28} = 1.02 \times 10^{-12} \ M^{-1}s^{-1}$ Eq. 1.28

$$HO_2^\bullet + H^+ \leftrightarrow H_2O_2^{\bullet+}$$
$k_{29} = 3.16\text{-}3.98 \times 10^{-12} \ M^{-1}s^{-1}$ Eq. 1.29

$$H_2O_2 \leftrightarrow HO_2^- + H^+$$
$k_{30} = 2.63 \times 10^{-12} \ M^{-1}s^{-1}$ Eq. 1.30

$$[Fe]^{3+} + H_2O_2 \leftrightarrow [(Fe(HO_2)]^{2+} + H^+$$
$k_{31} = 3.1 \times 10^{-3} \ M^{-1}s^{-1}$ Eq. 1.31

$$[(Fe(HO_2)]^{2+} + H_2O_2 \leftrightarrow [(Fe(HO)(HO_2)]^+ + H^+$$
$k_{32} = 2 \times 10^{-4} \ M^{-1}s^{-1}$ Eq. 1.32
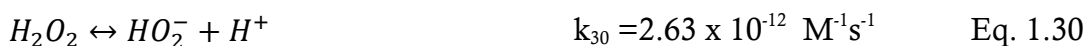
If organic compounds are present, they are oxidized by the $HO^\bullet$ generated by different electrophilic reactions: hydrogen abstraction from C-H, N-H or O-H bonds, electron transfer reactions and electrophilic additions to double bonds or aromatic rings.

Nonetheless, the Fenton process is limited by the reactions of ferrous iron regeneration (Eq. 1.20-1.22). This limitation can be overcome by irradiation with wavelengths up to 580 nm (can be solar radiation) in the so-called photo-Fenton process. In this process, the photo-reduction of ferric iron to ferrous iron (Eq. 1.33-1.34) give rise to a reduction-oxidation catalytic cycle where the iron is constantly reduced and oxidized resulting in a more efficient process due to the continuous generation of $HO^\bullet$ [Malato *et al.*, 2009].

$$[Fe(H_2O)]^{3+} + hv \rightarrow Fe^{2+} + HO^\bullet + H^+ \qquad \text{Eq. 33}$$

$$[Fe(OH)]^{2+} + hv \rightarrow Fe^{2+} + HO^\bullet \qquad \text{Eq. 34}$$
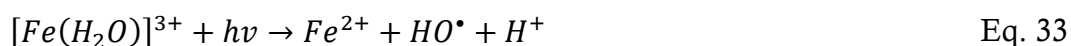
The photo-reduction of Fe^{2+} is generated by a change in the electron distribution of the aqua-complex, i.e., an internal redox process between the ligand and the metal through a charge-transfer absorption (CT), which is allowed and intense in the visible spectrum. There are different CT processes, in this case as the molecular orbitals of the ligand are full, the charge transfer occurs from these full ligand orbitals to empty or not totally filled metal orbitals, therefore through a ligand-to-metal charge-transfer (LMCT) resulting in the metal reduction.

Factors affecting photo-Fenton process

There are several factors that affect the photo-Fenton process efficiency, the most important are pH, temperature, inorganic chemical compounds and concentration of reagents (iron and H_2O_2).

As the iron ions in an aqueous medium are forming hexacoordinate complexes with water and/or hydroxyl ligands depending on the pH of the media, this factor is key in their acid-base equilibrium formation. Among both, ferric iron species are more critical due to its hydroxides complexes tend to precipitate decreasing the process efficiency, and they are formed at lower pH values than those of ferrous iron. For pH values <2.3, the predominant iron complex is $[Fe(H_2O)_6]^{3+}$ which present a low reaction rate with H_2O_2 and so decrease the

process efficiency [Gallard *et al.*, 1998]; and for values >3.5 hydroxide complexes like [Fe(H$_2$O)$_4$ (OH)$_2$]$^+$ and [Fe(H$_2$O)$_3$ (OH)$_3$] begins to form. These ferric iron hydroxide complex formed have very low solubility in water and tend to precipitate. Its precipitation process consists on polymerization reactions of dimers and oligomers with loss of water molecules until the formation of insoluble iron hydroxides as goethite or hematite in not stoichiometric quantities [Flynn, 1984]. The hydroxide precipitate formed contains water and presents a cationic character, properties that explain their industrial use as chemical coagulants. Finally, when pH value is between both conditions, i.e., 2.3<pH< 3.5, the precipitation process did not take place and the dominant iron complex in solution is [Fe(H$_2$O)$_5$(OH)]$^{2+}$ which has the higher absorption coefficient in the solar spectrum being hence, the most photoactive iron aqua-complex. For these reasons, pH value of 2.8 is the optimum one for the photo-Fenton process [Pignatello, 1992].

The effect of the inorganic water constituents is also considerable. Ions commonly present in wastewater have negative effects on the process efficiency due to a scavenger effect with the radicals generated and the formation of iron compounds with less reactivity or solubility. The inorganic ions with high detrimental effect are phosphates, carbonates, bicarbonates, sulfates and chloride of which the effect of phosphates, carbonates and bicarbonates are the strongest.

The detrimental effects of phosphates are based mainly on their scavenger effect and iron precipitation through iron complex formation (Eq. 1.35-1.36) [Lu *et al.*, 1997].

$$Fe^{2+} + H_2PO_4^- \rightarrow FeH_2PO_4^+ \qquad\qquad \text{Eq. 1.35}$$

$$Fe^{3+} + H_2PO_4^- \rightarrow FeH_2PO_4^{2+} \qquad\qquad \text{Eq. 1.36}$$

In the case of carbonates and bicarbonates, they act as scavengers of HO$^•$ by reaction with them, which lead to the generation of the very low reactive carbonate radicals (Eq. 1.37-1.38).

$$HCO_3^- + HO^\bullet \rightarrow CO_3^{\bullet-} + H_2O \qquad \text{Eq. 1.37}$$

$$CO_3{}^{2-} + HO^\bullet \rightarrow CO_3^{\bullet-} + OH^- \qquad \text{Eq. 1.38}$$

Finally, the behaviour of sulfate and chloride ions is similar. Both generate sulfate or chlorine radicals by direct reaction with the $HO^\bullet$ and form iron complexes which although are less photo-actives than the aqua-complexes, absorb photons generating also the corresponding radicals (Eq. 1.39-1.47).

$$Fe^{2+} + Cl^- \leftrightarrow FeCl^+ \qquad \text{Eq. 1.39}$$

$$Fe^{3+} + Cl^- \leftrightarrow FeCl^{2+} \qquad \text{Eq. 1.40}$$

$$Fe^{3+} + 2Cl^- \leftrightarrow FeCl_2^+ \qquad \text{Eq. 1.41}$$

$$Cl^- + HO^\bullet \rightarrow [ClHO]^- \qquad \text{Eq. 1.42}$$

$$FeCl^{2+} + h\upsilon \rightarrow Cl^\bullet + Fe^{2+} \qquad \text{Eq. 1.43}$$

$$FeCl_2^+ + h\upsilon \rightarrow Cl^\bullet + FeCl^+ \qquad \text{Eq. 1.44}$$

$$Fe^{3+} + SO_4{}^{2-} \leftrightarrow FeSO_4^+ \qquad \text{Eq. 1.45}$$

$$FeSO_4^+ + h\upsilon \rightarrow Fe^{2+} + SO_4^{\bullet-} \qquad \text{Eq. 1.46}$$

$$SO_4^{2-} + HO^\bullet \rightarrow SO_4^{\bullet-} + HO^- \qquad \text{Eq. 1.47}$$

Although the photochemical reactions of the complexed formed are able to generate sulfate and chlorine radicals, these radicals are weaker oxidants than $HO^\bullet$, the overall efficiency of the photo-Fenton process decrease considerably. Moreover, a high concentration of chlorine in water presents another important drawback due to can generate toxic and undesired chlorinated compounds [Kiwi *et al.*, 2000].

As for all the endothermic reactions, an increase of temperature enhance the photo-Fenton kinetics (mainly the initial thermal-Fenton process) but its increase

to values upwards 45 ˚C lead to a lower efficiency due to iron precipitation and higher decomposition kinetics of H_2O_2. Thus, in a compromise decision, the optimum temperatures for the process will be between 40 and 45 ˚C.

As expected in a chemical or photochemical reaction, the reagent concentrations also influence on the treatment efficiency. The process efficiency increase by increasing the iron concentration, but its increases can generate additional turbidity decreasing the light penetration and the process efficiency. This phenomenon is more significant when the treatment is applied at circumneutral pH due to iron precipitation. Besides, the efficiency also depend on the reactor configuration and the photon flux. Another important factor to take into account is the intended use of the treated water, as there are legislations that establish environmental limit of iron emissions. Specifically in Andalucia (Decree 109/2015), a daily emission limit of 3.3 and 2.2 mg/L are stablished for wastewater discharge in coastal or transitional waters and surface waters, respectively. Therefore, the iron concentration should be selected carefully considering all these factors. Regarding H_2O_2, its concentration also depends on several factors. One of the most important is the iron concentration selected due to have to be enough to avoid a process limitation but not in large excess to avoid a scavenger effect. The water matrix intended to treat also influence because the H_2O_2 react with the organic matter decreasing its concentration. Finally, the H_2O_2 concentration also has to be chosen depending on the type of target pollutants. If the goal of the treatment is the water disinfection its concentration should be non-lethal by itself as it would be chemical disinfection. In general, if the treatment objective is the simultaneous disinfection and decontamination of urban wastewaters or industrial wastewater with similar characteristics, mild oxidation conditions (up to 20 and 50 mg/L of iron and H_2O_2) have been reported as the best operational conditions [Giannakis *et al.*, 2016b].

Solar photo-Fenton like process at neutral pH

The need to operate at acidic pH to keep iron in solution and improve the photo-Fenton process efficiency is the main drawback of this process due to this operating condition increases both the cost of treatment (acidification and neutralization) and the environmental impact of the water treatment (high salinity and CO_2 generation) [Gallego-Schmid *et al.*, 2019; Arzate *et al.*, 2019]. To deal with these drawbacks, and considering that iron can form complexes with several Lewis bases (especially organic polydentate ligands), in the last years, the search and evaluation of complexing agents that allow keeping iron in solution as a tool to increase the capability of photo-Fenton at neutral pH have been encouraged as it is observed in Figure 1.20.
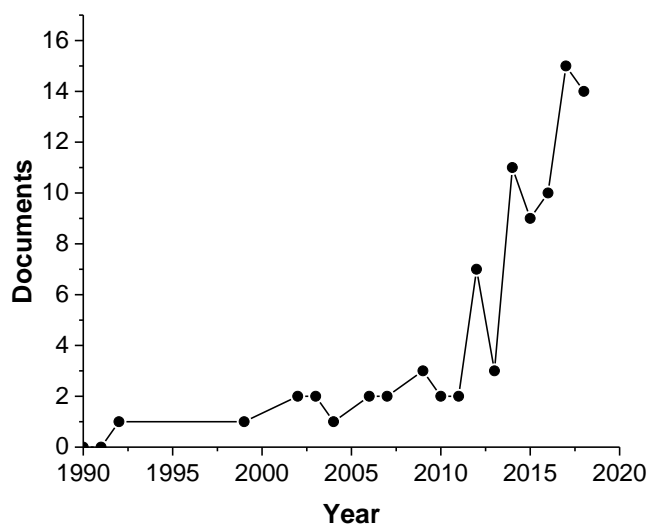
Figure 1.20. Frequency of reports by year (1990 - 2018), dealing with applications of photo-Fenton treatment using complexing or chelating agents. The search was based on Scopus database using as keywords 'iron chelate', 'iron complex', 'photo-Fenton', 'near-neutral', and 'like-photo' including articles, reviews, books, and book chapters.

Each iron complex presents different light absorption properties depending on the organic ligand, which determines the quantum yield of the photo-reduction process. In general, these ferric iron complexes absorb light in the near UV and visible regions, using a wider fraction of the solar spectrum (up to 580 nm), and exhibiting higher quantum yields than the aqua-complexes. Therefore, when the

photo-Fenton process is solar-driven, the contribution of these complexes to the photo-reduction is greater [Clarizia *et al.*, 2017].

The ferric iron complexes can be formed with dissolved organic matter sometimes already present in the water matrix intended to treat with common functional groups as carboxylate and polycarboxylate groups, i.e., oxalate, malate, citrate, etc. Nevertheless, in most cases, their quantity is insufficient to complex all the iron needed for the water treatment and for this reason the most common strategy to work at neutral pH is the addition of the complexing agent.

Several types of iron chelating agents have been reported in the literature to enhance water disinfection and decontamination at near-neutral pH by photo-Fenton through keeping iron in solution. The employ of simple and very well-known conjugate bases of natural organic acids, such as ascorbic, oxalic, tartaric, citric, gluconic or caffeic acid as complexing agent has been studied in several works due to their complex capability, natural character and high biodegradability. Among them, Fe-oxalate and Fe-citrate complexes have been thoroughly investigated, although their optimal working pH can be extended up to 5 or 6 and therefore the system still need operating at acid pH [Clarizia *et al.*, 2017].

Other natural complexing agents investigated are the polyphenols which are in a significant fraction in industrial wastewaters from the processing of natural products as olive mill wastewater. Thus the reusing of them to increase the photo-Fenton treatment capability constitutes an economically and environmentally attractive strategy [Davididou *et al.*, 2019; Ruíz-Delgado *et al.*, 2019].

On the other hand, the employ of synthetic chelating agents based on aminopolicarboxylic acids, which allow to operate in a wide pH range without it modification, like Nitrilotriacetic acid (NTA), Ethylendiaminetetracetic acid (EDTA) and Ethylendiamine-N',N'-disuccinic acid (EDDS) has been encouraged in the last years. Among then, the use of the Fe^{3+}-EDDS chelate stands out due to its biodegradability and higher efficiency for OMCs removal.

Nevertheless, its disinfection capability is limited in comparison with other complexing agents or other solar treatments [Klamerth *et al.*, 2012; García-Fernández *et al.*, 2019].

A summary of the parameters and results obtained by different decontamination and/or disinfection photo-Fenton studies reported in literature using complexing or chelating agents is shown in Table 1.6.

On the other hand, the use of synthetic iron fertilizers based on aminopolycarboxylic acids is commonly used in Mediterranean agriculture as iron chelating agent to increase the iron bioavailability for plants and to avoid the well-known iron chlorosis, plant disease that reduces the crop yield. Among the different iron-chelating agents authorized by EC Regulation No. 2003/2003 and subsequent amendments, Ethylenediamine-N',N'-bis 2-hydroxyphenylacetic acid (EDDHA) is the most efficient to prevent and remedy iron chlorosis under neutral and alkaline soil conditions due to its high stability in a wide range of pH (3-10) [Biasone *et al.*, 2013]. Currently, 80 % of fertilizers used in agriculture are synthetic iron chelates with 56-79 % of EDDHA. In this line, a recent study reported the use of Fe^{2+}-EDDHA/H_2O_2 as Fenton treatment for degradation of polychlorinated biphenyls (PCBs) in contaminated soils with very promising results [Ma *et al.*, 2018]. Moreover, the effect of the sub-products generated by photodecomposition has been previously investigated resulting non-toxic for crops [Hernández-Apaolaza and Lucena, 2011]. Therefore, its use as possible iron-chelate for water treatment and further reuse in agriculture by solar-driven processes seems to be a plausible option to tackling two important problems in the Mediterranean agriculture: water scarcity and iron chlorosis.

Table 1.6. Reports of photo-Fenton treatment application using complexing or chelating agents.

Reference	Iron source and reagents concentrations	Water matrix	Source of light	Target	Results
Cho *et al.*, 2004	Oxalate $[Fe^{3+}]= 0.5$ mM $[H_2O_2]= 2$ mM	Phosphate buffer solution	Lamp	*E.coli*	4-LRV in 50 min
Cho and Yoon, 2008	Oxalate $[Fe^{3+}]= 0.5$ Mm $[H_2O_2]= 2$ mM	Phosphate buffer solution	Lamp	*C. parvum* and *B. subtilis*	2-LRV in 300 min
Klamerth *et al.*, 2012	EDDS $[Fe^{3+}]= 0.09$ mM $[H_2O_2]= 1.5$ mM	Municipal wastewater	Sunlight	OMCs, total bacteria and total coliforms	88 % of OMCs removal in 8 min, 2-LRV of total bacteria and 3-LRV of total coliforms in 200 min
Perini *et al.*, 2013	Citrate and oxalate $[Fe^{3+}]= 6.4$ µM $[H_2O_2]= 320$ µM	Ultrapure water	Lamp	Ciprofloxacin	Citrate: 60 % Oxalate: 20 % in 10 min
De Luca *et al.*, 2014	EDTA, NTA, oxalic acid (OA) tartaric acid (TA) $[Fe^{3+}]= 0.089$ mM $[H_2O_2]= 0.294$ mM	Ultrapure water	Lamp	Sulfamethoxazole	EDTA: 75 % in 75 min NTA: 80 % in 120 min TA: 10 % in 60 min OA: 65 % in 120 min
Papoutsakis *et al.*, 2015	EDDS $[Fe^{3+}]= 0.025$ mM $[H_2O_2]= 0.88$ mM	Municipal wastewater	Sunlight	Phenol, bisphenol A, sulfamethoxazole, carbamazepine and pyrimethanil	40 % of OMCs removal with 3 kJ/L
Aurioles-López *et al.*, 2016	Acetylacetonate $[Fe^{3+}]= 0.09$ mM $[H_2O_2]= 0.3$ mM	Distilled water	Sunlight	*Fusarium solani*	> 5-LRV with 1.77 kJ/L
Ruales-Lonfat *et al.*, 2016	Citrate $[Fe^{3+}]= 0.01$ mM $[H_2O_2]= 0.3$ mM	Natural water	Lamp	*E.coli*	> 5-LRV in 60 min
Bianco *et al.*, 2017	EDDS $[Fe^{3+}]= 1.6$ µM $[H_2O_2]= 1$ mM	Distilled water	Sunlight	*Enterococcus faecalis*	> 5-LRV with 22.5 kJ/L
De la Obra *et al.*, 2017	EDDS $[Fe^{3+}]= 0.1$ mM $[H_2O_2]= 1.5$ mM	Municipal wastewater	Sunlight	Carbamazepine, flumequine, ibuprofen, ofloxacin and sulfamethoxazole	>90 % removal in < 1 kJ/L
Villegas-Guzman *et al.*, 2017	Citric, ascorbic, tartaric and caffeic acid $[Fe^{3+}]= 0.09$ µM $[H_2O_2]= 0.73$ mM	Synthetic wastewater	Lamp	*E.coli*	> 5-LRV in 70 min for all the complexing agents
Davididou *et al.*, 2019	Olive mill WW and EDDS $[Fe^{3+}]= 0.035$ mM $[H_2O_2]= 0.58$ mM	Distilled water	Sunlight	Saccharin	OMW: 90 % removal with 25 kJ/L EDDS: 90 % removal with 2 kJ/L
Dong *et al.*, 2019	NTA $[Fe^{3+}]= 0.178$ mM $[H_2O_2]= 4.54$ mM	Municipal wastewater	Lamp	Carbamazepine, crotamiton and ibuprofen	>92 % removal in 120 min
García-Fernández *et al.*, 2019	EDDS $[Fe^{3+}]= 0.1$ mM $[H_2O_2]= 0.3$ mM	Municipal wastewater	Sunlight	*E.coli* and *E.faecalis*	> 5-LRV with 29 kJ/L
López-Vinent *et al.*, 2020	EDDS $[Fe^{3+}]= 0.18$ mM $[H_2O_2]= 4.41$ mM	Municipal wastewater	Lamp	Propranolol	60 % in 60 min
Miralles-Cuevas *et al.*, 2019	EDDS $[Fe^{3+}]= 0.1$ mM $[H_2O_2]= 1.5$ mM	Simulated freshwater	Sunlight	Antipyrine, carbamazepine, caffeine, ciprofloxacin, sulfamethoxazole	>90 % removal with 3 kJ/L

Table 1.6. (Continue) Reports of photo-Fenton treatment application using complexing or chelating agents.

Reference	Iron source and reagents concentrations	Water matrix	Source of light	Target	Results
Ruíz-Delgado *et al.*, 2019	OMW $[Fe^{3+}]= 0.1$ mM $[H_2O_2]= 1.47$ mM	Natural water	Sunlight	Chlorfenvinphos Diclofenac Pentachlorophenol Terbutryn	80 % removal of in 120 min
Serna-Galvis *et al.*, 2019	Citric acid $[Fe^{3+}]= 0.09$ mM $[H_2O_2]= 1.47$ mM	Hospital wastewater	Lamp	*Klebsiella pneumoniae*	> 5-LRV in 300 min
Soriano-molina *et al.*, 2019	EDDS $[Fe^{3+}]= 0.1$ mM $[H_2O_2]= 1.5$ mM	Municipal wastewater	Sunlight	45 OMCs	>80 % removal in 15 min
Cuervo Lumbaque *et al.*, 2019	EDDS $[Fe^{3+}]= 0.28$mM $[H_2O_2]= 5$ mM	Simulated municipal wastewater	Sunlight	Diazepam,dipyrone, fluoxetine, furosemide, nimesulide, paracetamol, progesterone, and propranolol	>90 % removal in 110 min

LRV: Log-reduction value

kJ/L: units of Q_{UV} parameter (accumulated solar UV-irradiance per unit of time and volume.

1.6.2.3. Photo-inactivation assisted with H_2O_2

H_2O_2 is an oxidant widely used for water treatment due to has a reduction potential of around 1.4 V at near-neutral pH [Giannakis *et al.*, 2016a] and is cheap, safe, easy to handle and does not generate residues as it easily decomposes to water and oxygen. Although H_2O_2 has been used as antimicrobial agent (at high concentrations, 3 % - 90 %) for about 200 years, in the last decades highlights its use as oxidant agent to generate HO˙ in AOPs, included Fenton or photo-Fenton processes, peroxone process and UVC based processes, among others. Its combination with longwave irradiation sources, like sunlight, showed low HO˙ generation efficiencies, as expected due to the high energy required for the cleavage of the O-O bond into HO˙ and therefore, their dissociation will be generated only under shortwave wavelengths (<290 nm) which are in a very small extent in the solar spectrum [Malato *et al.*, 2009].

Nevertheless, a synergistic disinfection effect by combination of near-UV light and H_2O_2 for phages and *E. coli* inactivation was reported 30 years ago [Ananthaswamy and Eisenstark, 1976; Hartman and Eisenstark, 1980]. The solar water treatment studies assisted with H_2O_2 reported in literature is shown in Figure 1.21. Although a growing trend for the application of this solar process is

observed, the number of research items still being very low as only 62 studies were reported in the last 3 decades according to Scopus database.

Regarding the inactivation mechanism of this process, briefly it is believed that around the 20 % of the low H_2O_2 concentrations (0.3-3 mM) added to the water matrix intended to treat is able to diffuse into the bacterial cell (little and uncharged molecule) which in presence of solar radiation and intracellular iron generate $HO^{\bullet}$ by internal photo-Fenton reactions. Therefore, it is believed that the general bacterial inactivation mechanism by H_2O_2/solar process is based on internal damages by a synergistic effect between the photo-oxidative damages induced by solar radiation and the generated by the internal photo-Fenton reactions [Giannakis *et al.*, 2016a].
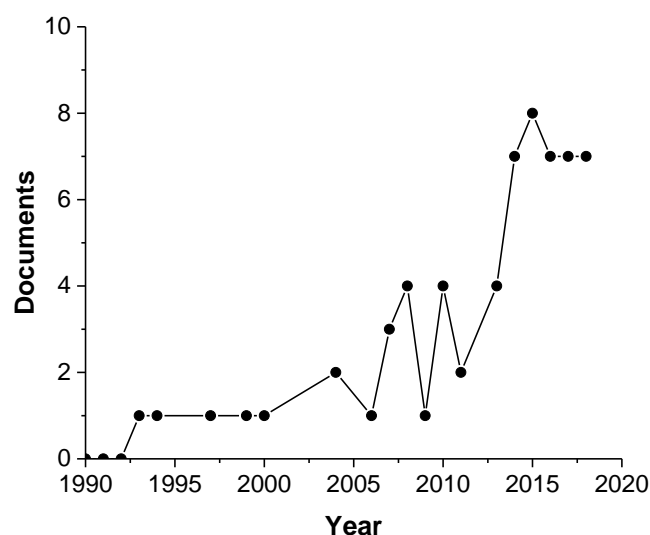
Figure 1.21. Frequency of reports by year (1990 - 2018), dealing with photo-inactivation assisted with H_2O_2. The search was based on Scopus database using as keywords 'solar/H_2O_2 ', 'sunlight/H_2O_2', 'UV-A/H_2O_2', ' hv/H_2O_2', 'H_2O_2/hv','H_2O_2/sunlight' and 'H_2O_2/solar' including articles, reviews, books, and book chapters.

The main cases of solar/H_2O_2 process application in water treatment reported in this decade are presented in Table 1.7. As a consequence of the low oxidation potential of H_2O_2/solar process in comparison with other photo-chemical processes, most of them are focused on water disinfection and present the data of organic contaminants removal as a complementary insight of the process application.

Table 1.7. Reports of H_2O_2/solar treatment application in water treatment.

Reference	[H_2O_2]	Water matrix	Source of light	Target	Results
Rincón and Pulgarin, 2006	0.3 mM	Ultrapure water	Lamp	*E. coli*	6-LRV in 135 min
Sichel *et al.*, 2009	1.65 mM	Well water	Sunlight	*Fusarium solani*	3-LRV in 180 min
Polo-López *et al.*, 2011	0.3 mM	Distilled water and Simulated municipal wastewater	Sunlight	Spores of *Fusarium equiseti*	3-LRV in 120 and 300 min
Sphuler *et al.*, 2010	0.3 mM	Ultrapure water	Lamp	*E. coli*	6-LRV in 180 min
Sciacca *et al.*, 2011	0.88 mM	Surface water with high turbidity (76-78 NTU)	Sunlight	*Salmonella sp.* and total coliforms	3-LRV in 180 min
Bandala *et al.*, 2012	140 mM	Ultrapure water	Sunlight	*Ascaris eggs*	0.5-LRV in 120 min
García-Fernandez *et al.*, 2012	0.29 mM	Distilled water	Sunlight	*E. coli* and *F. solani*	*E. coli*: > 5-LRV (1 kJ/L) *F. solani*: > 3-LRV (15 kJ/L)
Ortega-Gomez *et al.*, 2012	3.52 mM	Saline water	Lamp	*E. faecalis*	> 5-LRV in 120 min
Polo-López *et al.*, 2012	0.3 mM	Simulated municipal wastewater	Sunlight	*F. solani* spores	3-LRV in 22 kJ/L
Agullo-Barcelo *et al.*, 2013	1.47 mM	Municipal wastewater	Sunlight	*E. coli*, Sulphite-reducing clostridia (SRC), somatic coliphages (SOMCPH) and F-specific RNA phages (FRNA)	*E. coli:* > 5-LRV (17.5 kJ/L) SRC and SOMCPH: 2-LRV (35 kJ/L) FRNA: > 5-LRV (35 kJ/L)
Ortega-Gómez *et al.*, 2013	1.47 mM	Simulated municipal wastewater	Sunlight	*E. faecalis*	4-LRV in 100 min
Polo-López *et al.*, 2013	0.3 mM	Distilled water	Sunlight	*Phytophthora capsici*	3-LRV in 60 min
Eleren *et al.*, 2014	1.47 mM	Humic surface water	Lamp	*E. coli* and *B. subtilis* spores	*E. coli:* > 5-LRV in 60 min *B. subtilis:* > 4-LRV in 120 min
Polo-López *et al.*, 2014	0.29 mM	Municipal wastewater	Sunlight	*F. solani* spores	> 2-LRV with 27.5 kJ/L
Ferro *et al.*, 2015a	0.59 mM	Municipal wastewater	Sunlight	Multi-drug resistant (MDR)-*E.coli*	> 5-LRV with 8 kJ/L
Ferro *et al.*, 2015b	0.59 mM	Municipal wastewater	Sunlight	AR *E. coli* , *E. faecalis*, Carbamazepine (CBZ), Flumequine (FLU), and Thiabendazole (TBZ)	AR *E. coli* > 5-LRV in 120 min AR *E. faecalis* > 5-LRV in 240min CBZ: 12% removal FLU:94 % removal TBZ: 50 % removal in 90 min
Fiorentino *et al.*, 2015	1.47 mM	Municipal wastewater	Sunlight	MDR *E.coli*	> 5-LRV in 90 min
Ndounla and Pulgarin, 2015	0.29 mM	Natural water	Sunlight	Total coliforms-*E.coli* and *Salmonella spp*.	> 4-LRV in 120 min
Ng *et al.*,2015	2 mM	Saline water	Lamp	*E.coli*	> 4-LRV in 120 min
Formisano *et al.*, 2016	2.94 mM	Municipal wastewater	Sunlight	*E. coli* and *Enterococci*	*E. coli* : > 3-LRV in 120 min *Enterococci*: > 2-LRV in 120 min

Table 1.7. (Continue) Reports of H_2O_2/solar treatment application in water treatment.

Reference	[H₂O₂]	Water matrix	Source of light	Target	Results
Topac and Alkan, 2016	0.29 mM	Simulated domestic WW	Lamp	*E. coli*	> 4-LRV in 15 min
Abeledo-Lameiro *et al.*, 2017	1.47 mM	Distilled water	Sunlight	*Cryptosporidium parvum*	80 % reduction in 300 min
Aguas *et al.*, 2017	1.18 mM	Municipal wastewater	Sunlight	*Curvularia sp.*	> 2-LRV with 22.5 kJ/L
Alkan *et al.*, 2017	1.47 mM	Domestic wastewater with high turbidity (158 NTU)	Lamp	*E. coli*	> 5-LRV in 60 min
Polo-López *et al.*, 2017	1.47 mM	Distilled water	Sunlight	*Legionella jordanis*	> 5-LRV in 15 min
Giannakis *et al.*, 2018	0.59 mM	Simulated municipal wastewater	Lamp	Antibiotic Resistant Bacteria (ARB)-*E. coli*	> 5-LRV in 90 min
Moreira *et al.*, 2018	0.59 mM	Municipal wastewater	Sunlight	ARB *Faecal coliform* and ARB *Enterococci* Sulfamethoxazole, carbamazepine and diclofenac	ARB *Faecal coliform:* > 4-LRV in 12.5 kJ/L ARB *Enterococci*: > 2-LRV with 20 kJ/L Sulfamethoxazole: 45 % removal with 235 kJ/L Carbamazepine: 40 % removal with 235 kJ/L Diclofenac: >95 % removal with 20 kJ/L
Aguas *et al.*, 2019	0.59 mM	Municipal wastewater	Sunlight	*E. coli, Salmonella spp.*,total coliforms and *Enterococcus spp.* 74 OMCs	*E. coli:* > 3-LRV in 150 min *Salmonella:* > 2-LRV in 105 min Total coliforms: > 3-LRV in 180 min *Enterococcus spp:* > 2-LRV in 285 min OMCs: 56 % removal in 300 min
García-Fernandez *et al.*, 2019	0.3 mM	Municipal wastewater	Sunlight	*E. coli* and *E.faecalis*	*E. coli*: > 2-LRV with 12.5 kJ/L *E. faecalis*: > 2-LRV with 25 kJ/L
Rizzo *et al.*, 2018b	0.59 mM	Municipal wastewater	Sunlight	Chloramphenicol	65 % removal with 250 kJ/L
Kowalska *et al.*, 2020	0.59 mM	Distilled water	Sunlight	Carbamazepine, diclofenac and trimethoprim	Carbamazepine: >75 % removal in 300 min Diclofenac: >75 % removal in 90 min Trimethoprim: >75 % removal in 300 min
Maniakova *et al.*, 2020	0.59 mM	Municipal wastewater	Sunlight	Carbamazepine, diclofenac and trimethoprim	Carbamazepine: 45 % removal Diclofenac: >97.5 % removal Trimethoprim: 44 % removal in 240 min or 12.1 kJ/L
Serna-Galvis *et al.*, 2019	1.47 mM	Distilled water	Lamp	ARB *Klebsiella pneumoniae*	3-LRV in 180 min

LRV: Log-reduction value

kJ/L: units of Q_{UV} parameter (accumulated solar UV-irradiance per unit of time and volume.

CHAPTER 2

OBJECTIVES AND EXPERIMENTAL PLAN

2. OBJECTIVES AND EXPERIMENTAL PLAN

2.1. Objectives

The general aim of this study is to investigate the use of solar-driven technologies (solar photo-Fenton and H_2O_2/solar) and a conventional process (ozone) for the improvement of fresh-cut wastewater (or washing water) to reach the chemical and microbiological quality established on wastewater reuse guidelines for irrigation in agriculture. In this study, the targets selected were two human bacterial pathogens (*E. coli* O157:H7 and *S. enteritidis*) as model of microbial contamination and a mix of organic microcontaminants (OMCs) (atrazine, azoxystrobin, buprofezin, imidacloprid, procymidone, simazine, thiamethoxam and terbutryn) as model of chemical contamination (pesticides) in this type of industry.

The specific objectives of this work are:

1. To develop a synthetic fresh-cut wastewater (SFCWW) recipe that allows a realistic comparison between treatments under standardized conditions and to evaluate the disinfection performance of solar photo-inactivation, H_2O_2/solar, Fe/solar and solar photo-Fenton at laboratory scale and under controlled conditions as alternative treatments to chlorination process.

2. To investigate the disinfection capability of a commercial iron micronutrient (Fe^{3+}-EDDHA) as a new iron source for solar water disinfection at near-neutral pH in comparison with the use of conventional iron salts in two water matrices (SFCWW and isotonic water (IW)) under natural solar radiation and at laboratory scale.

3. To assess the up-scaling (60 L) of solar photo-inactivation, H_2O_2/solar, Fe^{3+}-EDDHA/solar and Fe^{3+}-EDDHA/H_2O_2/solar for the simultaneous disinfection and decontamination (5 OMCs) of SFCWW using solar reactors provided with CPC collectors.

4. To evaluate the capability of ozone and peroxone processes for the treatment of SFCWW to reduce its microbiological and chemical contamination (6 OMCs) at pilot scale (10 L) and at different operational conditions.

5. To assess the reuse of treated SFCWW *in vivo* by irrigation tests at pilot scale (30 m^2 experimental greenhouse) to investigate the fate of chemical contaminants and bacteria in two raw-eaten vegetables, i.e., radish and lettuce crops.

6. To evaluate the techno-economic, environmental and health risk viability of the global process: from the treatment capability to the reuse of treated SFCWW for crops irrigation.

2.2. Experimental plan

The experimental plan developed to meet the objectives of this work is explained below.

Objective 1: To develop a synthetic fresh-cut wastewater (SFCWW) recipe that allows a realistic comparison between treatments under standardized conditions and to evaluate the disinfection performance of solar photo-inactivation, H_2O_2/solar, Fe/solar and solar photo-Fenton at laboratory scale and under controlled conditions as alternative treatments to chlorination process. Chapter 4 explains in detail the experimental study performed to accomplish with this objective. In summary it consisted on the following tasks:

(i)   Development of a synthetic fresh-cut wastewater model, performing the following steps:

- Revision of the scientific literature to select the most representative physic-chemical parameters of real and simulated fresh-cut wastewater.

- Sampling and analysis of real fresh-cut wastewater samples from two different crop processing lines.

- Proposition and development of a fresh-cut wastewater chemical model based on the collected data from literature and laboratory analysis of real samples.

(ii)   Assessment of the disinfection capability of solar photo-inactivation, H_2O_2/solar (10 mg/L), Fe/solar and solar photo-Fenton (2.5 mg/L of Fe^{2+} or Fe^{3+} and 5 mg/L of H_2O_2) processes in a 700 mL open reactor within SFCWW and under controlled temperature (<30 ºC) and constant solar irradiance (30 W/m^2) using a solar simulator.

(iii)   Experimental study of the H_2O_2 concentration and UV-irradiance effects on bacterial inactivation by the H_2O_2/solar process in SFCWW under

controlled conditions. This partial objective was achieved performing the following steps:

- Performance of a series of H_2O_2/solar water disinfection experiments in a 700 mL open reactor at three H_2O_2 concentrations (5, 10 and 20 mg/L) and five solar UV-irradiances levels (10, 20, 30, 40 and 50 W/m^2).

- Analysis of the inactivation kinetic constants obtained by response surface methodology.

<u>Objective 2:</u> To investigate the disinfection capability of a commercial iron micronutrient (Fe^{3+}-EDDHA) as a new iron source for solar water disinfection at near-neutral pH in comparison with the use of conventional iron salts in two water matrices (SFCWW and isotonic water (IW)) under natural solar radiation and at laboratory scale. Chapter 5 explains the experimental study performed to reach this objective, briefly:

(i)   Analysis of the physic-chemical characteristics and photostability of Fe^{3+}-EDDHA in solution (100 mg/L of commercial product in ultrapure water (UW)). Study carried out in a 700 mL open reactor and in a solar simulator under constant solar UV-irradiance (30 W/m^2).

(ii)   Assessment of the disinfection capability of Fe/solar and solar photo-Fenton processes with the commercial iron micronutrient (Fe^{3+}-EDDHA) in comparison with an iron salt ($Fe(NO_3)_3$) commonly employed in photo-Fenton studies. This study was carried out in two water matrices (IW and SFCWW) within a 200 mL-reactor and under natural solar radiation.

- Performance of Fe/solar disinfection experiments at three iron concentrations (0.5, 2.5 and 5 mg/L) and comparison with solar photo-inactivation results.

- Performance of solar photo-Fenton disinfection experiments at three reagents concentrations (0.5:1, 2.5:5 and 5:10 mg/L of iron:H_2O_2) and comparison with H_2O_2/solar results (1, 5 and 10 mg/L).

(iii)   Proposal of the bacterial inactivation mechanisms by Fe^{3+}-EDDHA solar processes, performing the following steps:

- Revision of scientific literature.

- Measurement of hydroxyl radicals generation during the solar photo-Fenton process (2.5:5 mg/L of iron:H_2O_2) in ultrapure water (UW) and a solar simulator under constant solar UV-irradiance (30 W/m^2).

Objective 3: To assess the up-scaling (60 L) of solar photo-inactivation, H_2O_2/solar, Fe^{3+}-EDDHA/solar and Fe^{3+}-EDDHA/H_2O_2/solar for the simultaneous disinfection and decontamination (5 OMCs) of SFCWW using solar reactors provided with CPC collectors. The experimental study performed to achieve this objective is shown in chapter 6, briefly it consist in the following taks:

(i)   Studying the treatment capability of solar photo-inactivation and H_2O_2/solar processes testing five oxidant concentrations: 2.5, 5, 10, 20 and 40 mg/L.

(ii)   Studying the treatment capability of Fe^{3+}-EDDHA/solar process testing three iron chelate concentrations: 2.5, 5, and 10 mg/L.

(iii)   Studying the treatment capability of Fe^{3+}-EDDHA/H_2O_2/solar process testing three reagents (Fe^{3+}-EDDHA:H_2O_2) concentrations: 0.5:2.5; 2.5:20; and 5:40 mg/L.

(iv)   Analysis of the post-treatment bacterial regrown of each solar process.

Objective 4: To evaluate the capability of ozone and peroxone processes for the treatment of SFCWW to reduce its microbiological and chemical contamination

(6 OMCs) at pilot scale (10 L) and at different operational conditions. Chapter 7 explains the experimental study carried out to reach this objective, briefly:

(i) Studying the treatment capability of the ozonation process ($0.09 \ gO_3/Lh$) at natural (6.25) and basic (11) water pH.

(ii) Studying the treatment capability of the peroxone process ($0.09 \ gO_3/Lh$ with 20 mg/L of H_2O_2) at natural (6.25) and basic (11) water pH. Additionally, the treatment capability of the peroxone process at natural pH was also tested at higher O_3 generation ($0.15 \ gO_3/Lh$ and 20 mg/L of H_2O_2).

(iii) Analysis of the OMCs removal results and correlation with their chemical structure.

Objective 5: To assess the reuse of treated SFCWW in vivo by irrigation tests at pilot scale (30 m^2 experimental greenhouse) to investigate the fate of chemical contaminants and bacteria in two raw-eaten vegetables, i.e., radish and lettuce crops. In Chapter 8, the water reuse tests and the samples analysis performed are fully described, briefly:

(i) Performance of negative (mineral water) and positive (non-treated water) irrigation controls. Analysis of bacteria and OMCs fate in crops and peat.

(ii) Analysis of the treated water feasibility for reuse in vegetable irrigation by monitoring bacterial regrown during storage.

(iii) Performance of four irrigation assays with treated SFCWW water by ozonation, H_2O_2/solar and Fe^{3+}-EDDHA/H_2O_2/solar processes at the best operational condition and reagent concentrations obtained along the previous objectives of this work. Analysis of bacteria and OMCs fate in crops and peat.

(iv)   Determination of chlorophyll content in lettuce crops irrigated with treated SFCWW as key parameter to determine the risk of iron chlorosis disease.

Objective 6: To evaluate the techno-economic, environmental and health viability of the global processes: from the treatment capability to the reuse of treated SFCWW for crops irrigation. The study performed to achieve this objective is shown in chapter 9, briefly:

(i)   Estimation of the wastewater treatment cost for ozonation and solar processes and comparison with chlorination cost.

(ii)   Analysis of treated SFCWW ecotoxicity using *Lactuca sativa* and *Vibrio fisheri* as tests.

(iii)   Evaluation of the chemical and microbiological health risk assessment of crops irrigated with treated SFCWW.

CHAPTER 3
MATERIALS AND METHODS

3. MATERIALS AND METHODS

In this research, a multi-disciplinary approach has been performed, and therefore a number of laboratory procedures, methodologies and facilities have been used to carry out the experimental plans. All of them are fully described in this chapter.

All the experimental procedures have been carried out at CIEMAT-Plataforma Solar de Almeria (Almeria, Spain), by the access to both the 'Laboratory of Solar Treatment of Water' and the 'Water Treatment Facilities'. Also, in particular, the sophisticated OMCs analytical methodologies have been performed in collaboration with the research group FQM374 "Análisis ambiental y tratamiento de aguas" belonging to the University of Almeria (UAL) and the research centre CIESOL which is a Joint Centre of the UAL-CIEMAT.

3.1. Chemicals

The chemicals employed along all the procedures were used as received from the manufacturer and they are summarized in Table 3.1.

Table 3.1. Chemicals used in this research.

Compound	Brand	Use to/as
Sodium chloride	Sigma Aldrich	prepare isotonic water, SFCWW and Nutrient-Broth I
Malt extract	AppliChem Panreac	organic matter content in SFCWW
Kaolin powder	Millipore®, Germany	turbid agent in SFCWW
Sodium hydroxide	J. T. Burker	adjust pH of SFCWW
Ammonium chloride	Sigma-Aldrich, USA	ionic content in SFCWW
Magnesium sulphate anhydrous		
Sodium bromide	Merck, Germany	
Sodium fluoride		
Sodium nitrate	Riedel-de-Haën, Germany	
Calcium chloride dehydrate		
Sodium sulphate anhydrous	J.T Baker, USA	
Potassium chloride		
Phosphate-buffered saline	Oxoid	isotonic medium for bacterial suspension
Beef extract / Peptone	Panreac, Spain	to prepare Nutrient-Broth I
Iron sulfate heptahydrate	Panreac, Spain	source of iron
Iron nitrate nonehydrate		
Sequestrene 138 Fe G100	Syngenta, Spain	
1,10-phenanthroline	Merck, Germany	spectrophotometric iron measurement
Hydrogen peroxide (35% w/v)	Sigma Aldrich, USA	oxidant in experiments and cleaning of reactors
Titanium (IV) Oxysulfate	Riedel-de-Haën, Germany	spectrophotometric measurement of H_2O_2
Bovine liver catalase	Sigma-Aldrich, USA	eliminate residual H_2O_2 concentration.
Pesticides	Sigma-Aldrich, Spain	target OMCs
Methanol / Acetonitrile	Riedel-de-Haen™, Chromasolv™	prepared stock solution of OMCs
Phenol	Merck, Germany	to determine the HO˙ generation.
Benzene	Panreac, Spain	determine the HO˙ generation
Potassium bromate	Reagent Plus, Sigma-Aldrich, Spain	determine the bromate generation in ozonation experiments
Potassium indigotrisulfonate	Sigma Aldrich, Spain	spectrophotometric measurement of ozone in solution
Zinc sulphate heptahydrate	Panreac, Barcelona, Spain	positive control in toxicity test of *Lactuca sativa*
Acetone	Riedel-de-Haen™, Chromasolv™	chlorophyll extraction procedure
Monosodium phosphate	Sigma Aldrich, Spain	spectrophotometric measurement of ozone in solution

3.2. Microbial targets: description and samples enumeration

The microbial analysis were performed in a microbiology laboratory with a biosafety level II equipped with four laminar flow cabinets (Telstar Bio-II-A) where all water samples were handling to ensure sterile conditions (Figure 3.1 (a)). Moreover, all the solutions, materials and culture medias were autoclaved (Figure 3.1 (b)) during 15 min at 121 ºC to sterilize them prior to use. Waste solutions and materials were also autoclaved before disposal for safety reasons.
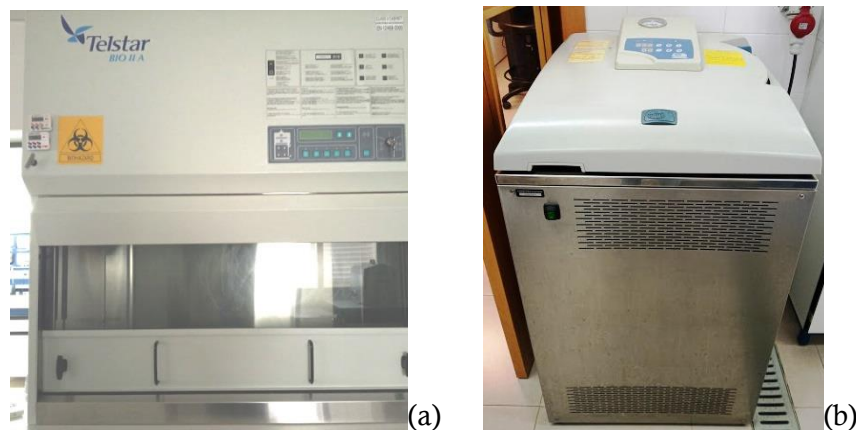
Figure 3.1. Laminar flow cabinet (a); and autoclave (b).

Bacteria strain classification and description

Two bacterial strains have been tested in this study as model of foodborne pathogens on the fresh-cut industry, *Escherichia coli* O157:H7 and *Salmonella enteritidis*. Both strains are classified as Bacteria (Domain and Kingdom), Proteobacteria (Phylum), Gammaproteobacteria (Class), enterobacterales (Order), Enterobacteriaceae (Family). The specific characteristics of each bacterium are detailed as follow:

i) *Escherichia coli* O157:H7. Genus: *Escherichia*; Specie: *Escherichia coli* O157:H7. This bacterium is Prokariotic cell, unicellular, gram-negative, facultative anaerobes, rod-shaped, non-spore forming, animal parasite, and habitant in human and animal intestine, somatic (O), with antigen 157 and flagellated (H)

with antigen 7. Moreover it is a chemoorganotrophic organism (respiratory and fermentative metabolism) and produces a Shiga toxin (STEC, shiga toxin-producing *E. coli*).

ii) *Salmonella enteritidis*. Genus: *Salmonella*; Specie: *Salmonella enterica*; Subspecie: *enterica*; serovar Enteritidis. This bacterium is Prokariotic, unicellular, gram-negative, facultative anaerobes, rod-shaped, non-spore forming, animal parasite, habitant in human and animal intestine, motile via flagella and a chemoorganotrophic organism. Moreover the name of the subspecie *Salmonella Enteritidis* come from the Greek noun 'enteron' which mean gut and from the termination '-idis' which mean inflammation, therefore the name of this subspecie mean gut inflammation which is one the main symptoms associated with its infection.

Bacteria stock preparation

E. coli O157:H7 (CECT 4972) and *Salmonella subsp. enteritidis* (CECT 4155) were obtained from the Spanish Type Culture Collection (CECT) as a freeze-dried culture. The dried pellet was rehydrated with 0.2 – 0.3 mL of Nutrient-Broth I (containing 5 g/L of NaCl and 10 g/L of beef extract and peptone) and Tryptone Soya Broth (TSB) (OXOID) for *E. coli* O157:H7 and *S. enteritidis*, respectively. After that, an aliquot of the suspension (50-100 μL) was transferred into a sterile vial containing 5 mL of the specific broth medium (Nutrient Broth I for *E.coli* and TSB for *S. enteritidis*). Both suspensions were incubated in a rotary shaking incubator (Heidolph Unimax 1010- Inkubator 1000) at 37 °C and 100 rpm for 20 h (Figure 3.2). The turbid suspensions obtained were transferred to cryobeads sterile vials (Deltalab®, Spain) for their long-term storage at -5 °C.

Inoculum preparation

The stock cryovials were slowly thawed until reach room temperature (25 °C) and one drop was streaked onto a Petri dish of a generic medium (Luria Bertani agar) and incubated for 20 h at 37 °C in an incubator (Blinder), obtaining stock dishes with the desired isolated bacteria colonies. These stock dishes were

preserved under refrigeration during 1 week and used to prepare the daily fresh liquid cultures. These liquid cultures were prepared by transferring a single colony from the Petri dish (using a loop) to a sterile vial containing 14 mL of the specific liquid broth medium for each bacteria and incubated in the rotary shaking incubator with the same conditions explained above to obtain the bacterial stationary phase concentration ($\sim 10^9$ CFU/mL). The bacterial suspensions obtained were centrifuged for 10 min at $900 \times g$ and the bacterial pellets were re-suspended in phosphate-buffered saline (PBS) solution and directly diluted into the water matrix to obtain the initial concentration desired (10^6 CFU/mL) in the samples.

Figure 3.2. Rotary shaking incubator.

Bacterial enumeration in water samples

Water samples from solar experiments were serial diluted (10-fold) in PBS and enumerated using the standard plate counting method. To do so, sample volumes of 50 and 500 μL were spread on ChromoCult® Coliform Agar (Merck KGaA, Darmstadt, Germany) and Salmonella Shigella Agar (Scharlau®, Spain) Petri dishes and incubated at 37 °C during 24 and 48 h for *E. coli* O157:H7 and *S. enteritidis*, respectively. Colonies were counted after the incubation time. The detection limit (DL) of this technique is 2 CFU/mL. The agar mediums used are selective for each bacterium. This selectivity is based on the presence of certain substrates which participate in enzymatic reactions generating specific colored

colonies for each bacterium. In the case of *S. enteritidis*, the agar medium contains sodium thiosulfate as sulphur source for the production of hydrogen sulphide, detected as colonies with a black centre formation. For *E. coli*, ChromoCult® contains Salmon-GAL and X-glucuronide which are cleave by the enzimes ß-D-galactosidase and ß-D-glucoronidase of *E. coli* generating a dark blue-violet colour colonies. Nevertheless, our specific strain (*E. coli* O157:H7) lacks the ß-D-glucoronidase enzyme and therefore the colonies of *E. coli* O157:H7 present a salmon-red coloration (Figure 3.3).
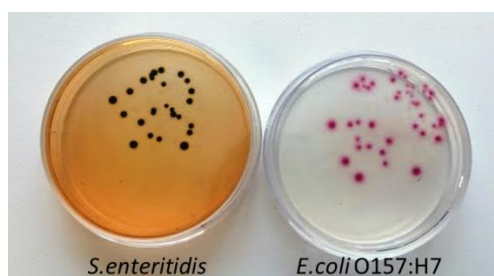
Figure 3.3. *S. enteritidis* and *E. coli* O157:H7 colonies in selective agar Petri dishes.

Moreover, to decrease the detection limit with the aim to fit with the limit established in guidelines for wastewater reuse (10-100 CFU/100mL), the membrane filtration method was also used. In this case, 100 mL of sample was filtered using a Microfil®filtration system (Millipore, USA) (Figure 3.4) using cellulose nitrate filters (0.45 μm, Sartorius Stedim, Spain) and following the similar culture media procedure as described previously.

Figure 3.4. Microfil®filtration system.

Bacterial enumeration in crops and peat samples

The fate of both bacteria in lettuce leaves, radish and peat were also enumerated using the standard plate counting method previously described. The procedure of crops and peat analysis was performed according to literature [Bichai *et al.*, 2012; Ferro *et al.*, 2015b]. Briefly, it consists on the following steps (Figure 3.5):

- For lettuce leaves the extraction procedure was the same: 3 ± 0.5 g of each sample was cut in small (<1 cm^2) pieces, mixed with 20 mL of isotonic solution (0.9 % NaCl w/v) in a Stomacher bag and homogenized in a Stomacher 400 (Seward, UK) at 260 rpm for five min. The limit of detection (LOD) was 1 CFU/3 g.

- In the case of radish fruit, the procedure was the same as leaves but the sample size was the weight of each radish fruit unit harvested. The LOD was 1 CFU/8 g.

- For peat samples, 5 ± 0.5 g of the mixed peat was collected and mixed with 45 mL of isotonic water in a 100 mL container and homogenized by manual stirring. The LOD was 1 CFU/5 g.
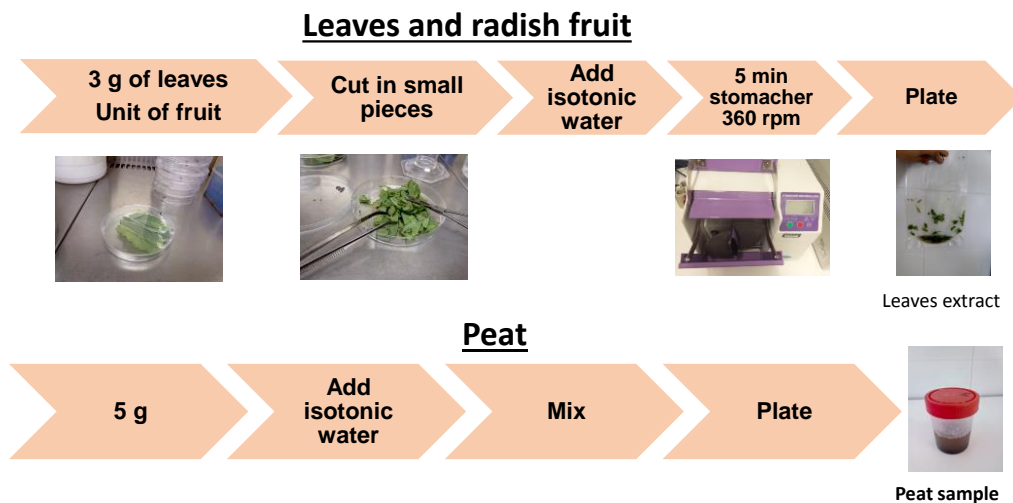
Figure 3.5. Schematic procedure to quantify the microbial fate in crops and peat.

3.3 Organic microcontaminants (OMCs): description and analytical measurements

The 8 OMCs used in this study were selected according to the following criteria: i) their use for farmers during vegetables cultivation, ii) their detection in wastewater from agro-food industries [Campos-Mañas, *et al.*, 2019] and iii) their presence on the latest European directives as priority substances (PSs). The description of each OMC selected are presented below [Lewis *et al.*, 2016]. The physic-chemical properties of each OMC in solution at pH 7 and 20 °C is summarized in Table 3.2, and their structure and UV-absorption spectra on aqueous solution at 10 mg/L are shown in Figure 3.6.

__Atrazine__ (ATZ) is a triazine herbicide that has not been approved by EU for its use. It is a priority substance in water since 2008 (2008/105/EC). It used to control broad-leaved weeds and grasses and it has a selective and systemic action (inhibits photosynthesis, photosystem II) with residual and foliar activity.

__Azoxystrobin__ (AZX) is a strobilurin fungicide of broad-spectrum approved for use at EU level. It used mainly for fungal infections in cereals and it has a systemic translaminar and protectant action (respiration inhibitor) having additional curative and eradicant properties.

Table 3.2. Physic-chemical properties of OMCs in solution at pH 7 and 20°C.

OMCs	Formula	Molecular mass (g/mol)	Water solubility (mg/L)	pKa/ Log K_{ow}	Aqueous photolysis/ hydrolysis (DT_{50}, days)
Atrazine	$C_8H_{14}ClN_5$	215.7	35	1.7/2.7	2.6/86
Azoxystrobin	$C_{22}H_{17}N_3O_5$	403.4	6.7	0.9/2.5	8.7/ stable
Buprofezin	$C_{16}H_{23}N_3OS$	305.4	0.46	6.7/4.93	33/378
Imidacloprid	$C_9H_{10}ClN_5O_2$	255.7	610	11.1/0.57	0.2/ stable
Procymidone	$C_{13}H_{11}C_{l2}NO_2$	284.1	2.46	3.5/3.3	8/24.7 (fast hydrolysis at basic pH)
Simazine	$C_7H_{12}ClN_5$	201.7	5	1.6/2.3	1.9/96
Terbutryn	$C_{10}H_{19}N_5S$	241.4	25	4.3/3.7	0.5/ stable
Thiamethoxam	$C_8H_{10}ClN_5O_3S$	291.7	4100	0.4/-0.13	2.7/ stable

Buprofezin (BPF) is a thidiazine acaricide approved for it use at EU level (only in some countries, included Spain). It is used for whitefly and other insect control. Its mode of action is mainly by contact and stomach (inhibitors of chitin biosynthesis, moulting inhibitor).

Imidacloprid (IMD) is a neonicotinoid insecticide approved for use in the EU with certain restrictions for flowering crops. It is a priority substance in water since 2015 (2015/495/EU). It is used to control sucking and soil insects with a systemic, contact and stomach action (acetylcholine receptor agonist).

Procymidone (PCM) is a dicarboximide fungicide that has not been approved by EU for its use. It is widely used in horticulture as a seed dressing, pre-harvest spray or post-harvest dip for the control of various fungal diseases. Moderately systemic fungicide (inhibition of osmotic signal transduction), with protective and curative properties.

Simazine (SZ) is a triazine herbicide that has not been approved by EU for its use, except in Spain. Priority substance in water since 2008 (2008/105/EC). It is used to control broad-leaved weeds and grasses and it has a selective and systemic action (inhibits photosynthesis, photosystem II) with residual and foliar activity.

Terbutryn (TBY) is a triazine herbicide that has not been approved by EU for its use. Priority substance in water since 2013 (2013/39/EU). It is used to control broad-leaved weeds and grasses and it has a selective and systemic action (inhibits photosynthesis, photosystem II), absorbed through roots and foliage and translocated with residual and foliar activity.

Thiamethoxam (TMX) is a neonicotinoid pesticide approved for use at EU level and used to control a wide range of common pests. Priority substance in water since 2015 (2015/495/EU). Its mode of action is systemic with contact and stomach action (acetylcholine receptor agonist).
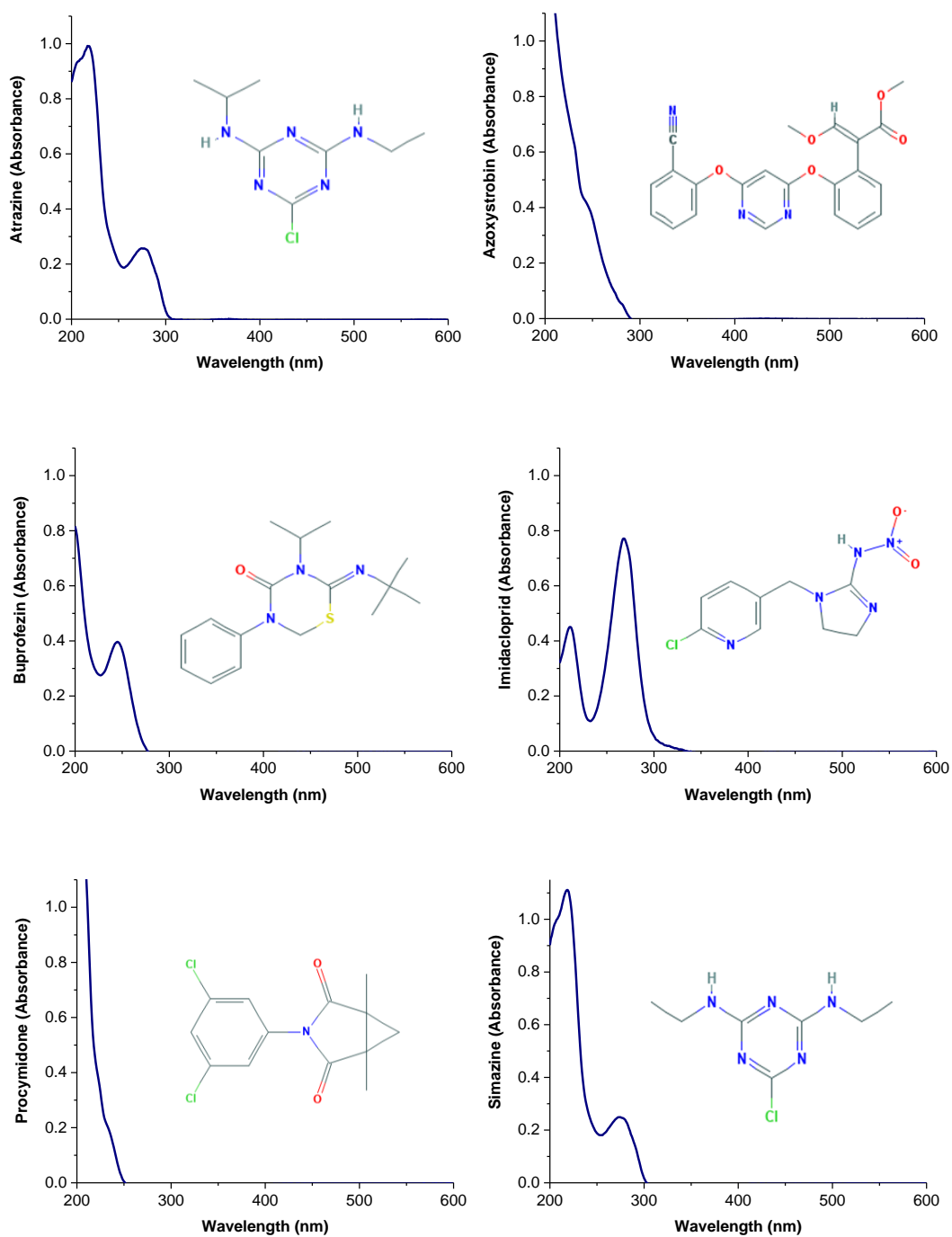
Figure 3.6. Structure and UV-absorption spectra of each OMC in aqueous solution at 10 mg/L.
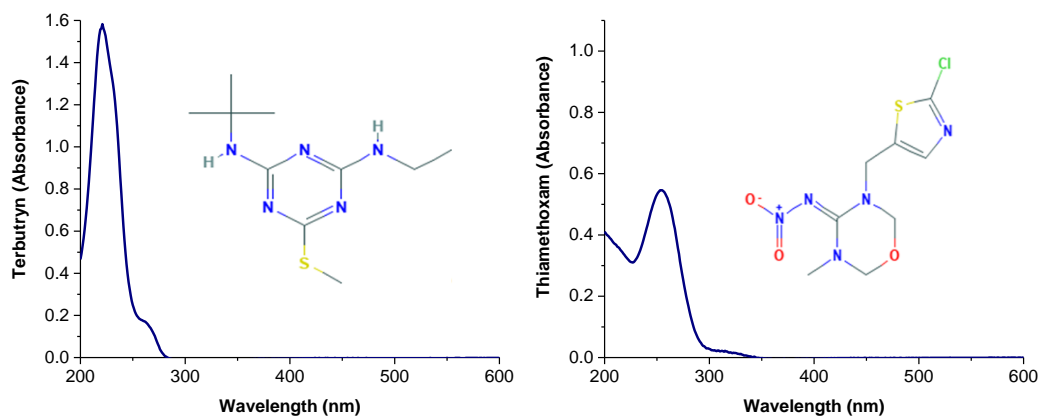
Figure 3.6. (Continued) Structure and UV-absorption spectra of each OMC in aqueous solution at 10 mg/L.

These pesticides were quantified by different analytical techniques depending on the matrix as will be explained later.

OMCs monitoring during water treatments: UPLC- UV-DAD

Degradation of the target OMCs (atrazine, azoxystrobin, buprofezin, imidacloprid, procymidone, simazine, terbutryn and thiamethoxam), spiked at 100 μg/L each, during the studied water treatments were monitored by Ultra-Performance Liquid Chromatography with ultraviolet-diode array detection (UPLC-UV-DAD).

The UPLC technique is based on the use of normal-sized columns (10–25 cm long) but, unlike HPLC columns, they are packed with smaller particles (<2 μm). The small particles require a high pressure to work (in the 6000–15000 psi range) being this the reason of the denomination 'ultra' of this technique. The increased surface area of UPLC columns increase significantly their efficiency allowing faster separations without any reduction of the resolution between compounds. In addition, the sharpness of the peaks contributes to improve sensitivity and reduce detection limits.

In general, UPLC-UV-DAD technique is based on the pumping of a mobile phase (also known as eluent), containing the analytes, through a stationary phase (chromatographic column) where these analytes will be separated based on their

interaction with the stationary phase (mainly based on their physic-chemical properties, i.e., polarity) and finally, they are led to a UV-DAD detector.

The most widely used liquid chromatography (LC) separation technique for pesticides is reverse-phase chromatography, which is based on a non-polar stationary phase, the more commonly employed column is C18, and the use of a polar mobile phase (usually a mixture between water and an organic solvent). Therefore, analytes with less polarity (more hydrophobic substances) are retained in the non-polar stationary phase and detected later than hydrophilic substances. Depending on the complexity of the compound mixture intended to separate, two different elution methods can be applied:

- **Isocratic elution**, where the mobile phase does not change during the analysis and it is usually applied for simple separations of only one or two compounds.

- **Gradient elution**, where the mobile phase composition changes during the analysis. It is applied to more complex mixtures, i.e., the separation and simultaneous analysis of several contaminants, because changes in the mobile phase polarity throughout the analysis allow an improved separation of the analytes.

Once the analytes are separated, they pass through a flow cell in the UV-DAD detector, where they generate a signal which is related to the absorption properties and concentration of the analytes. The analog signal generated is recorded and digitized by the software against analysis time, generating Gaussian peaks. Finally, for the quantification, a linear relationship between the contaminant concentration and the peak area obtained by means of calibrations with standard solutions is used. In this study, the calibration curves for the 8 target OMCs were obtained simultaneously using the gradient elution method and are presented in the Eq 3.1-3.8.

$$C_{Atrazine} \left(\frac{mg}{L}\right) = \frac{peak\ area}{0.7062} \qquad R^2 = 0.999 \qquad\qquad \text{Eq. 3.1}$$

$$C_{Azoxystrobin} \left(\frac{mg}{L}\right) = \frac{peak\ area}{0.5739} \qquad R^2 = 0.995 \qquad\qquad \text{Eq. 3.2}$$

$$C_{Buprofezin} \left(\frac{mg}{L}\right) = \frac{peak\ area}{0.2017} \qquad R^2 = 0.998 \qquad\qquad \text{Eq. 3.3}$$

$$C_{Imidacloprid} \left(\frac{mg}{L}\right) = \frac{peak\ area}{0.4775} \qquad R^2 = 0.998 \qquad\qquad \text{Eq. 3.4}$$

$$C_{Procymidone} \left(\frac{mg}{L}\right) = \frac{peak\ area}{0.5424} \qquad R^2 = 0.999 \qquad\qquad \text{Eq. 3.5}$$

$$C_{Simazine} \left(\frac{mg}{L}\right) = \frac{peak\ area}{0.7804} \qquad R^2 = 0.998 \qquad\qquad \text{Eq. 3.6}$$

$$C_{Terbutryn} \left(\frac{mg}{L}\right) = \frac{peak\ area}{0.7888} \qquad R^2 = 0.996 \qquad\qquad \text{Eq. 3.7}$$

$$C_{Thiamethoxam} \left(\frac{mg}{L}\right) = \frac{peak\ area}{0.3174} \qquad R^2 = 0.997 \qquad\qquad \text{Eq. 3.8}$$

The chromatographic system employed in this study consisted of an Agilent 1260 (Palo Alto, CA, USA) chromatograph, a quaternary solvent pump, an autosampler, a thermostatic column oven and an UV-DAD detection system (Figure 3.7). The chromatographic column used for the analytical separation was a C18 reversed-phase column (XDB-C18, 1.8 μm, 4.6x50 mm from Agilent) and the whole system control and data evaluation was conducted via a PC interface provided with the Agilent ChemStation® software.
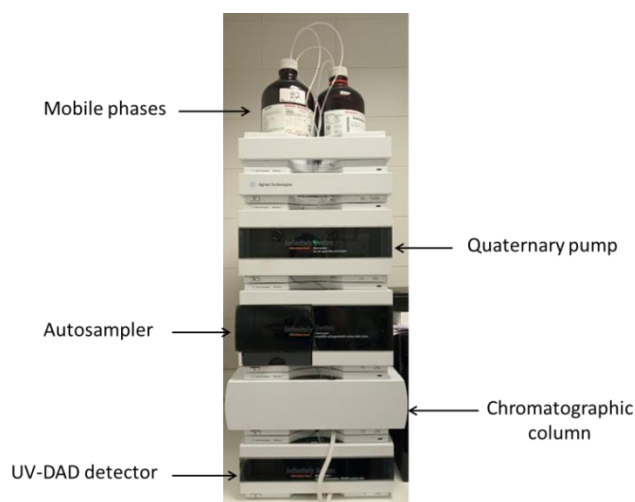
Figure 3.7. Photograph of the UPLC-UV-DAD system (Agilent 1260).

Before injection, water samples were prepared by filtering 4.5 mL of sample through a 0.22 μm syringe-driven nylon filter (Millex), and then, 0.5 mL of acetonitrile (ACN) (HPLC grade, Panreac, Spain) was passed through the filter to remove residual adsorbed compounds, obtaining a final mixture of ACN:water similar to the initial percentage of the mobile phase.

The eluents used were ACN and ultrapure water, the flow rate 1 mL/min and a sample injection volume of 100 μL. The working method of 11.5 min of duration consisted on: 0.5 min of isocratic conditions (90 % H_2O:10 % ACN), followed by 5.5 min of a linear gradient up to 100 % ACN, then 100 % ACN during 1.5 min, returning to the initial conditions in 1 min, with a final post-time of 3 min. Detection wavelength used for the analytes identification is showed in Table 3.3.

This table also shows the retention times and LOD and limits of quantification (LOQ) obtained with this method. In general, the analytes were efficiently separated with quantification limits lower than 5 μg/L (except for azoxystrobin) and therefore their quantification by UPLC-UV-DAD allowed an efficient monitoring of their degradation during the water treatments, since at least 95 % of removal could be detected.

Table 3.3. Chromatographic conditions used for detection and quantification of each OMC.

OMC	Retention time (t_r, min)	Detection wavelength (λ, nm)	Limit of quantification (LOQ, µg/L)	Limit of detection (LOD, µg/L)
Atrazine	4.2	230	2	0.9
Azoxystrobin	5.4	214	20	0.8
Buprofezin	7.0	250	5.0	3.2
Imidacloprid	3.4	273	2.2	1
Procymidone	5.8	214	3.6	1.2
Simazine	4.2	230	2.0	0.8
Terbutryn	5.6	230	1.9	0.6
Thiamethoxam	3.0	250	3.0	1.2

OMCs monitoring in real wastewater samples from a fresh-cut industry: SPE extraction and HPLC-QqLIT-MS/MS analysis

A High Performance Liquid Chromatograph coupled to a mass spectrometry system equipped with a hybrid quadrupole/linear ion trap tandem mass analyzer (HPLC-QqLIT-MS/MS) was used for pesticides screening in four real wastewater samples collected at different washing intervals from two processing lines in the fresh-cut industry 'Verdifresh' (Annex A). These analysis were performed in the "Environmental Analysis" functional unit of the Solar Energy Research Center (CIESOL).

This chromatographic technique are similar than the explained previously for UPLC-UV-DAD, being only different the detection method, which allow much lower quantification limits with higher capability of confirmation of targets in complex water samples. The basic principle of LC coupled to mass spectrometry involves the conversion of the analytes to gas phase ions by an electrospray ionization source. Then a sequential and multistage isolation of precursor ions according to their specific mass-to-charge ratio (m/z) is performed in the first quadrupole (Q1) and there are fragmented in the second quadrupole (Q2). Finally, in the third quadrupole (Q3), the product ions formed in Q2 are detected. This technique is based on the trapping of the fragments generated in Q2 converting the ions detected and their abundance into electrical signals. In the QqLIT systems two quadrupoles, precede a linear ion-trap (IT) mass

analyzer (Figure 3.8), improving significantly the ion trap performance by enhancing the full-scan sensitivity while maintain the complete triple quadrupole operational modes.
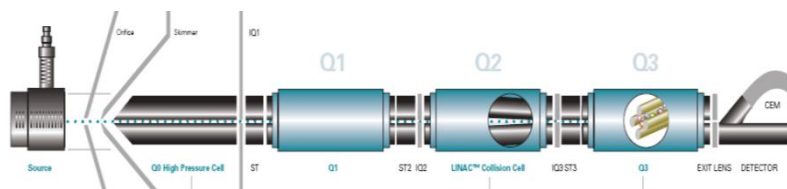
Figure 3.8. Schematic representation of a QqLIT- MS/MS analyzer.

In our case, the analysis of the real wastewater samples from a fresh-cut industry were performed by a pesticides-multiresidue method (33 different pesticides) using a 1200 HPLC system (Agilent Technologies, Wilmington, DE, USA) coupled to a hybrid quadrupole/linear ion trap (QqLIT) mass spectrometer (5500 Q-TRAP®, Sciex, Foster City, CA, USA) (Figure 3.9).

Figure 3.9. Photograph of HPLC-QqLIT-MS/MS equipment.

A solid phase extraction (SPE) procedure was applied to the samples with the aim to avoid matrix interferences and preconcentrate the targets. Prior to extraction, samples were vacuum filtered through 0.45-μm PTFE (Whatman, Buckinghamshire, UK) and the pH was adjusted to 8 with 20 % NH_4OH. Then, 50 mL of sample was extracted by SFE using Oasis HLB (6 cc, 200 mg; Waters, Miliford, MA, USA) cartridges. SPE cartridges were previously conditioned with 6 mL of MeOH and 5 mL of Milli-Q water at pH 8. After loading the sample, cartridges were dried with N_2 for 30 min. The elution of the analytes was

performed with 2 x 4 mL of MeOH collected in glass tubes. The eluted sample was dried under a gentle N_2 stream and reconstituted with 1 mL of MeOH. Prior to injection, 1:10 dilution was applied to the extract with ACN:Milli-Q water (10:90, v/v). An aliquot of the organic extract was stored in the freezer (-20ºC) till analysis.

The HPLC method consisted on the sample chromatographic separation with a Kinetex C18 column (150×4.6 mm, 2.6-µm particle size, Phenomenex, Torrance, CA, USA). Eluent A was Milli-Q water (0.1 % formic acid) and eluent B was MeOH, which were used in an optimised gradient as follows: initial conditions, 20 % B for 0.5 min; within 3 min, linear gradient from 20 % to 50 % B; within 7 min, from 50 % to 90 % B and within 9.5 min from 90 % to 100 % B. The gradient was kept at 100 % B for 4.5 min and at 14.01 min the initial conditions were reached again and maintained constant for a re-equilibration time of 7 min. The total run time was 21 min. The sample injection volume was 10 µL and the flow rate was 0.5 mL/min.

This system was equipped with a TurboIon Spray source, which operate in positive (+ESI) and negative (-ESI) electrospray ionization modes in the same run. The working source settings were: 550°C of source temperature; ion spray voltage (IS), 5500 V (+ESI) and -5500 V (-ESI); CAD gas, medium; ion source gas 1 (ISG1), 50 psi; ion source gas 2 (ISG2), 50 psi and curtain gas, 25 (arbitrary units). N_2 was used as nebuliser, curtain and collision gas. The precursor ion, ionisation mode and MS/MS parameters: declustering potential (DP); collision energy (CE); entrance potential (EP) and cell exit potential (CXP) were optimised for each compound by injection of individual standard solutions in MeOH (10 µg/L). Analyzes were done using the multiple reaction monitoring (MRM) mode being the detection window at 40 s and the target scan time (TST) at 0.5 s. Confirmation of the analytes in the samples was carried out according to the European Union (EU) guidelines for pesticide residue analysis SANTE/11813/2017 [SANTE, 2017], which includes the presence of two SRM transitions (two product ions) at the correct retention time (RT) and the correct

SRM1/SRM2 ratio. Data were acquired using Analyst Software 1.6.2 and processed with MultiQuant 3.0.1 software (Sciex). The LOD and LOQ were from 10 to 500 ng/L.

OMCs in vegetables and peat: QuEChERs extraction and HPLC-QqLIT-MS/MS analysis

Samples obtained from reuse irrigation assays (lettuce leaves, radish fruit and peat) were also analyzed by HPLC-QqLIT-MS/MS with a previous QuEChERs extraction.

QuEChERs extraction is a Quick, Easy, Cheap, Effective, Rugged, and Safe method which name is adopted based on the acronyms of these characteristics. This method is based on a simple experimental layout which uses low amounts of sample and organic solvents in agreement with the green chemistry principles and it has been demonstrated being effective for the detection and quantification of a broad spectrum of compounds in different matrices [Payá *et al.*, 2007].

The procedure consists on a salting-out extraction with an organic solvent (mainly ACN), followed by a dispersive solid-phase extraction (d-SPE) clean-up with sorbents. Due to the fact that the effectivity of the extraction depends on the target analyte properties and the matrix composition, some modifications of the basic procedure were standardized to allow the extraction a wide range of analytes with different properties. One of the most used variant is the buffered citrate QuEChERS with which sample pH values between 5.0 and 5.5 are obtained as a compromise between the quantitative extraction and protection of alkali and acid-labile compounds. The salting-out extraction step is based on an equilibrium between an aqueous and an organic layer, usually ACN, due to this organic solvent has shown to extract a broadest range of organic compounds without co-extraction of large amounts of lipophilic material. In this step, the addition of some salts to improve the efficiency of the extraction is also performed: $MgSO_4$, acting as a dehydrating agent which contributes to remove water traces; and NaCl, used as liquid–liquid partitioning salt to induce phase separation and thus increase the selectivity of the extraction. The buffer reagents

sodium citrate tribasic dihydrate and sodium citrate dibasic sesquihydrate were also added in a 2:1 ratio (w/w) with the aim explained previously. After the extraction, a d-SPE step was performed. This procedure is a clean-up step using several combinations of porous sorbents and salts to remove co-extracted matrix interfering substances, which may interfere in the subsequent analyzes. Different combinations of sorbents have been proposed, being the combination between Primary Secondary Amine and octadecyl silica (C18) the most used. Primary Secondary Amine is added to remove organic acids, sugars, fatty acids and some pigments, while C18 is effective to remove non-polar interferences, such as lipids.

In this study, the citrate variant of the QuEChERS extraction procedure based on the European Standard Method EN Code 15662 published by CEN (European Committee for Standardization) [CEN, 2007], was applied to the extraction of the OMCs in all the samples evaluated, although with some little modifications were done depending of the matrices analyzed. The procedure is summarized in Figure 3.10 and it is briefly described as follow:

The extraction method for lettuce leaves and radish fruits consisted on weighting a portion of 10 g of sample, previously cut and crushed, into a 50 mL polypropylene centrifuge tube, where 10 mL of ACN and the appropriate quantity of an extraction surrogate standard solution of Caffeine-C_{13} (250 μL/L) at 1 μg/L, were added. This tube was shaken vigorously in a vortex for 3 min. Following this, 4 g of anhydrous $MgSO_4$, 1 g of NaCl, 1 g of sodium citrate tribasic dehydrate and 0.5 g of sodium citrate dibasic sesquihydrate were added. Then, the tube was shaken again during 2 min and centrifuged (3500 rpm, 2054 *g*) for 5 min. After that, the d-SPE clean-up mixture was applied. To this aim, a 5 mL aliquot of the upper organic phase of the extract was transferred to a 15 mL centrifuge tube and cleaned up by the addition of 750 mg of anhydrous $MgSO_4$, 125 mg of C18 and 125 mg of Primary Secondary Amine. The tube was then shaken for 30 s and centrifuged (3500 rpm) for 5 min. Then, the upper layer

of the extract was transferred to a screw-cap vial, adding 10 μL of ACN at 1 % of formic acid per mL of extract.

For peat extraction, the method was the same as for lettuce, changing only the first step of the extraction method where only 1 g of sample was weighed, rehydrated with 4 mL of Milli-Q water and spiked with the extraction surrogate at 50 μg/L.

Finally and before the sample injection, 100 μL of the final extract was evaporated to dryness under gentle N_2 stream and reconstituted in 100 μL of ACN:H_2O (10:90, v/v).

The working source settings were: 550 °C; ESI, 4500 V; CAD gas, medium; ISG1, 50 psi; ISG2, 40 psi and curtain gas, 25 a.u. The conditions for the MRM were: detection window at 40 s and target scan time (TST) at 0.5 s.

The HPLC method consist on a chromatographic separation carried out using a XDB C18 50 x 4.6 mm and 1.8 μm particle size analytical column (Agilent Technologies). The mobile phase consisted of ACN (solvent B) and 0.1 % formic acid in MilliQ water (solvent A). The initial proportion of solvent B was 10 %, which was kept constant for 1 min, increased to 50 % within 4 min, increased to 100 % within 10 min, kept constant for 4 min and reduced to 10 % in 0.1 min. The total analysis run time was 14.1 min and the post-run equilibration time was 4 min. The injection volume was 10 μL and the flow rate was kept constant at 0.4 mL/min.

The criteria for analytes confirmation were the same explained below. Moreover, matrix-matched calibration curves (with sample dilutions ranged from 1:10 to 1:10000, according to the sample matrix and compound concentration) were used for the analytes quantification in order to minimize matrix affects and obtain accurate results. In crop samples, the LOD and LOQ were from 0.01 to 0.1 ng/g, whereas in peat they ranged from 0.1 to 0.5 ng/g.
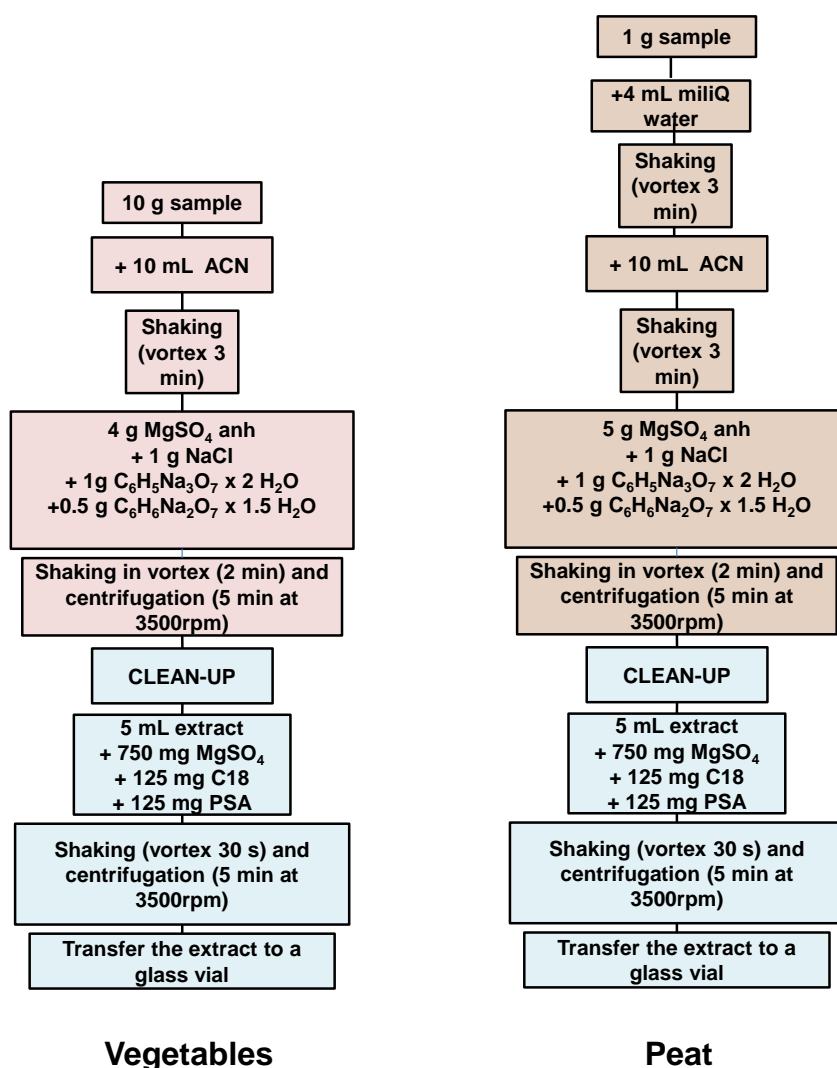
Figure 3.10. Schematic representation of the QuEChERS extraction methods applied for the different matrices studied.

3.4. Water matrices

3.4.1. Isotonic water

This water matrix was used to investigate the processes efficiency without any other chemical interactions, i.e., organic and inorganic compounds commonly present in real water matrices. The isotonic water was prepared by dissolving NaCl 0.9 % (w/v) in sterile demineralized water to avoid osmotic bacterial stress. Its main physic-chemical characteristics are: conductivity < 10 mS/cm, pH ≈5.5 and DOC < 0.5 mg/L.

The demineralized water was obtained from a water treatment plant located at PSA facilities, which consist on several steps. Briefly, the water was filtered by Silex® and after that it was chlorinated and filtered again (5 μm). Then, a process of inverse osmosis takes place (polyamide membranes) and finally an electro-deionization stage favour the removal of ions not retained by inverse osmosis.

3.4.2. Synthetic fresh-cut wastewater (SFCWW)

This water matrix was developed in this research as model of wastewater from the fresh-cut industry. Detailed information on recipe development and the main physic-chemical characteristics are widely explained in Chapter 4.1, section 4.1.1. (Results and Discussion) and Annex. The synthetic fresh-cut wastewater was prepared by adding the following concentration of reagents to demineralized water: malt extract (55 mg/L), sodium hydroxide (5 μL of a solution 2 M), kaolin (125 mg/L), sodium chloride (160 mg/L), ammonium chloride (0.7 mg/L), magnesium sulphate anhydrous (49 mg/L), sodium bromide (13 mg/L), sodium fluoride (0.6 mg/L), sodium nitrate (65 mg/L), calcium chloride dehydrate (145 mg/L), sodium sulphate anhydrous (10 mg/L) and potassium chloride (205 mg/L). Its main remarkable characteristics are the high turbidity (100 NTU) and DOC (25.4 mg/L).

3.5. Reactors

Along the experimental studies of this research, four different reactors have been used: a simulated-solar reactor (at lab-scale), 2 solar reactors (at lab-scale and at pilot-plant scale) and an ozonation reactor at pilot-plant scale, all of them available at PSA facilities. Their main characteristics are described below.

3.5.1. Lab-scale reactors

3.5.1.1. 700 mL Simulated-solar reactor

The solar experiments under controlled conditions were performed using a solar simulator SUNTEST XLS+ (Atlas Material Testing Solutions) and an open glass

vessel reactor of 19 cm of diameter with an irradiate surface of 0.0284 m^2 (Figure 3.11).
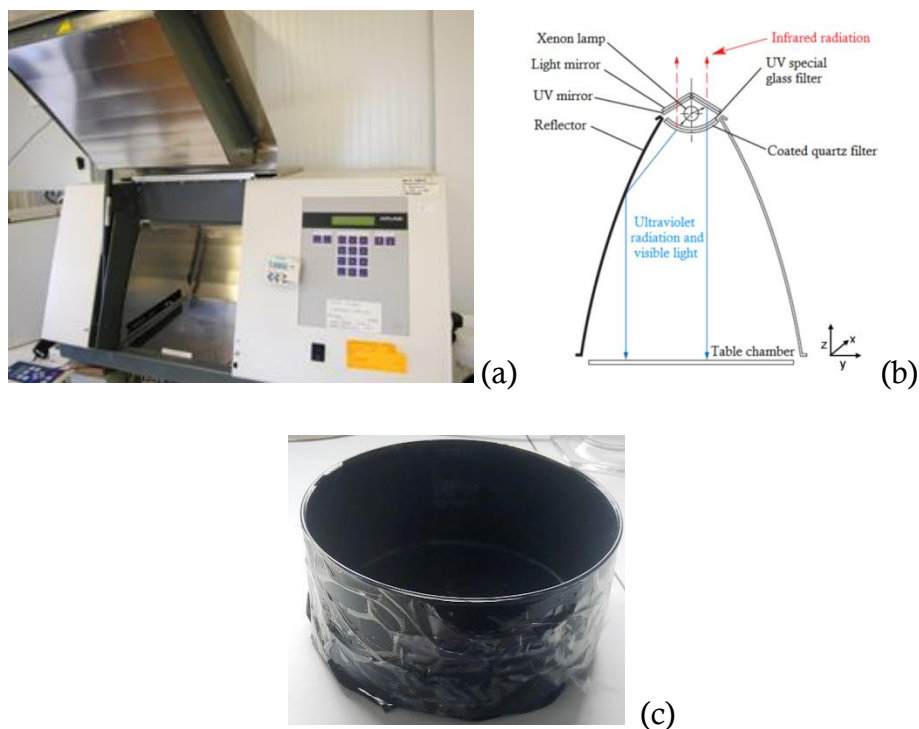
Figure 3.11. Photographs of the solar simulator system (a), diagram of the internal chamber (b) and 700 mL Simulated-solar reactor (c).

The total water volume of the reactor was 700 mL (8 cm of water high), which are entirely illuminated. The outside surface of the reactor is lined with black plastic to consider a one-dimensional radiation gradient due to the radiation came from the top. To ensure a homogenous suspension along the experiment the reactor was placed on a magnetic agitator (set at 450 rpm).

Artificial solar radiation was provided by the solar simulator SUNTEST XLS+. The irradiance system consists on a Xenon lamp and several specific filters that simulates the solar global radiation spectrum (daylight). The irradiance generated by the lamp is constant and its value can be established by select a set point in the equipment configuration in the range of 300 to 800 nm providing the desired value with a coefficient of variation of 5 %.

The table chamber's dimensions are 330 x 330 mm being the walls of the chamber covered by reflectors to redirect the radiation to the solar reactor which is located on the table sample. The distance between the lamp and the table sample is 26 cm.

3.5.1.2. 200 mL-solar reactor

Solar experiments at lab-scale and under natural sunlight were performed in bottles of 250 mL DURAN-glass (Schott, Germany) made of borosilicate glass that permits the transmission of 90 % of UVA range. The water volume was 200 mL and an illuminated surface area of 0.0095 m^2. The bottles were covered by glass cups (Schott, Germany) to allow that the solar radiation entry from all directions. The reactors were placed on a magnetic agitator (set at 450 rpm) to ensure a homogenous suspension along the experiments (Figure 3.12).

The use of this reactor for solar experiments has several advantages due to allow to work with small water volumes and consequently small reagents consumptions, it permits to carried out several operational conditions simultaneously (including test replicates) avoiding daily fluctuations and it has not dark parts, i.e., there is absence of uninterrupted solar incident radiation on water sample during the solar treatments.

Figure 3.12. 200 mL-solar reactor exposed to natural sunlight.

3.5.2. Pilot plant reactors

3.5.2.1. Ozonation reactor

The ozonation pilot plant consists on a column reactor with an inlet O_3 diffuser for batch operation with a maximum capacity of 20 L (Anseros PAP-pilot plant, Anseros Klaus Nonnenmacher GmbH, Germany). The reactor is equipped with an oxygen generator which concentrate atmospheric oxygen using molecular sieves (Anseros SEP100), a corona-discharge ozone generator (Anseros COM-AD02), two non-dispersive UV analyzers (BMT 964) to measure inlet and outlet ozone gas concentration, a flow-meter for inlet air regulation and an ozone destroyer to remove residual ozone and avoid it releases to the atmosphere. A diagram and a photograph of the ozonation reactor are show in Figure 3.13.

The operational conditions of the ozone pilot plant used in this study was 10 L of total volume of water, a constant inlet air flow of 0.06 Nm^3/h and two different initial ozone production of 0.9 and 1.5 gO_3/h, resulting from the ozone generator working at 10 % or 20 % power, respectively.

(a)

(b)
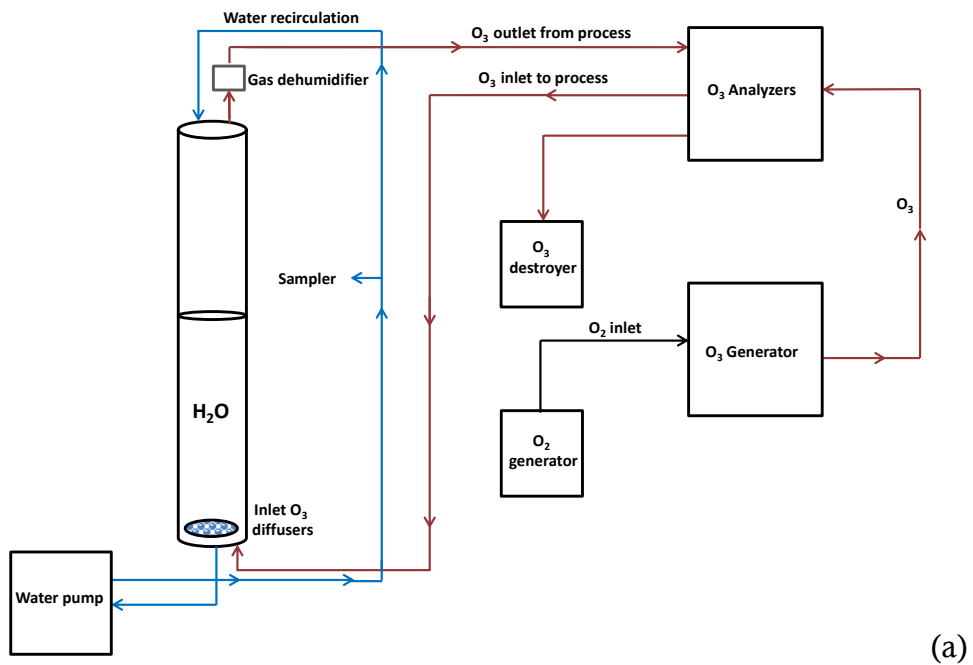
Figure 3.13. Diagram (a) and photograph of the ozonation pilot plant (b)**.**

3.5.2.2. Solar Compound Parabolic Collector (CPC) reactor

The CPC photo-reactor used in this study consist on two modules of CPC mirrors placed on an anodized-aluminium platform titled at 37° from the horizontal plane and south-facing. This inclination is selected to match with the local latitude at Plataforma Solar de Almería (latitude: 37º84' N, longitude: 2º34' W) and to recover the maximum UV radiation during the year (+10 %). The CPC mirror modules are made of highly reflective anodized aluminium sheet (MiroSun, Alanod, Germany) with a concentration factor 1 and a UVA reflectivity of 87 %. Each module has 10 borosilicate-glass tubes (1500 mm x 50 mm and 2.5 mm thick) with a total irradiated surface of 4.5 m² and 75 % of total irradiated water volume (45 L out of 60 L). The water is recirculated through the tubes by a centrifugal pump (150 W, Mod.NH-200 PS PanWorld, USA) with a flow rate of 30 L/min. The pH and water temperature are monitored throughout the experiments by sensors (CRISON, Spain) placed in the dark piped-system, which values are continuously recorded by a software acquisition data (PROASIS, DESIN Instruments, S.A.).

A general diagram of the solar CPC reactor used is shown in Figure 3.14. The dark blue line indicates the water flow recirculation during solar experiments in batch conditions.
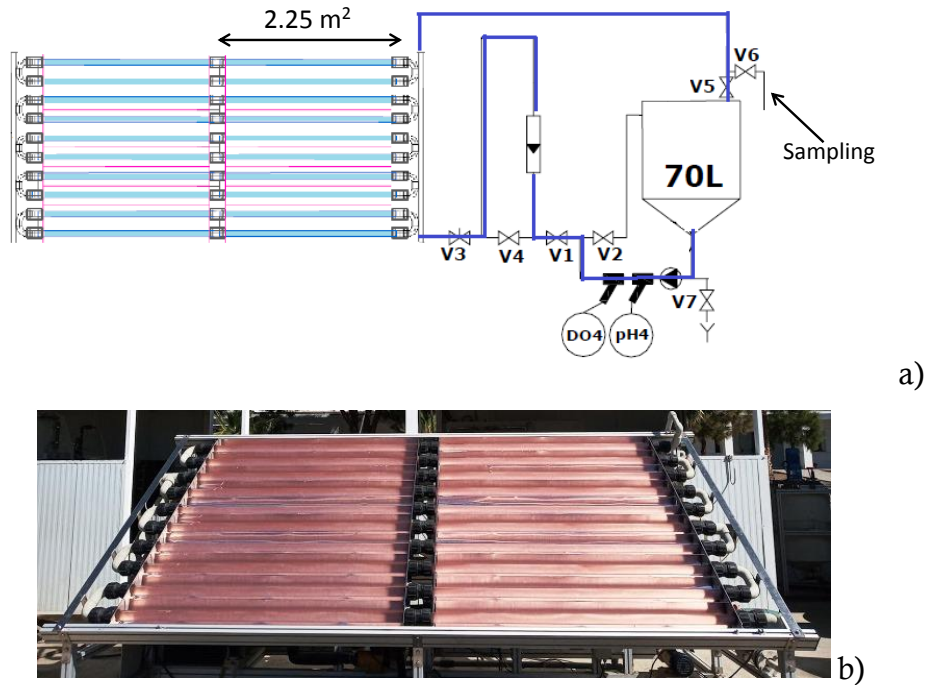
Figure 3.14. Diagram (a) and photograph (b) of the solar CPC reactor.

3.6. Solar radiation measurements

3.6.1. Solar radiation devices

The incident natural solar radiation was recorded by using different pyranometers available at the solar radiation station of the 'Laboratory of Solar Treatment of Water' at PSA. This station accounts for 5 pyranometers (2 for global and 3 for UV measurements), they are located at 3 meters high and close to the solar CPC reactors (area for solar tests). All pyranometers are connected by a data logger to a computer that registers the data during the day (every min) in terms of solar energy incident irradiation per unit area (W/m^2).

The global radiation is measured by a pyranometer Model CMP-6, Kipp & Zonen (Netherlands) which has a semi-sphere that receives both diffuse and direct radiation, a spectral response ranged from 310 to 2800 nm and high

sensitivity (14.7 $\mu V/W/m^2$). The solar UV radiation is measured with a pyranometer Model (CUV-5) which spectral response ranged from 280 to 400 nm and a sensitivity of 300 $\mu V/W/m^2$ (Figure 3.15).

Besides, they are placed on the horizontal plane and also titled 37º (similar to the CPC reactor inclination), in order to use the proper radiation data depending on the system under investigation. In particular in this study, data from the UV pyranometer located horizontally was used for analysis of results obtained with 200 mL-solar reactor; while UV pyranometer title 37º was used for analysis of results from solar CPC reactor tests.
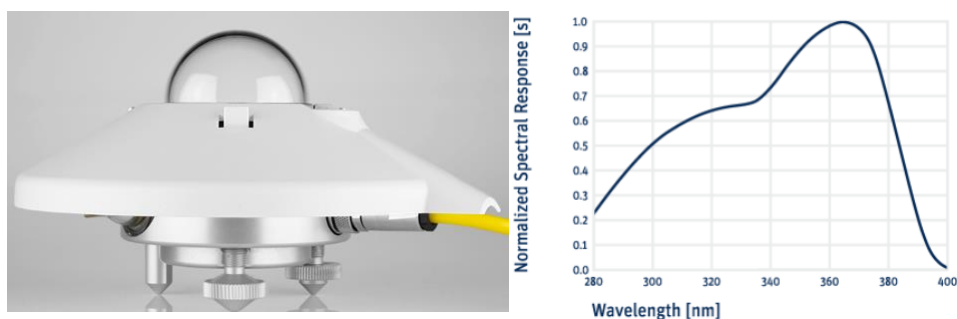
Figure 3.15. UV pyranometer located at PSA facilities and its spectral response.

Moreover, a portable UV-A radiometer model PMA2111 (Solar Light Co., Inc, Philadelphia) (Figure 3.16), was used to measure the irradiance received in the 700 mL Simulated-solar reactor during experiments performed under simulated solar radiation. The detector of this radiometer is suitable for measuring diffused radiation or radiation from extended sources and provides fast and accurate measurements in the range from 320 to 400 nm with a high resolution (0.01 W/m^2).

Figure 3.16. Portable UV-A radiometer.

Finally, a Spectrometer (AvaSpec-ULS2048) was used to measure the UV transmittance of water samples. This spectrometer collects the radiation from an angle of 180° using a cosine corrector CC-UV/VIS sensor especially suited for measurements in the 200 – 800 nm range.

3.6.2. Solar radiation analysis

All the experiments under natural sunlight were performed at PSA facilities. The weather of this location is usually sunny (≤300 days/year). The average solar irradiance (global, UV horizontal and UV at 37°) measured by the pyranometers explained above at PSA in the time frame used in this experimental study (from 10:30 am to 15:30 pm) divided in quarterly periods during 2017 are shown in Figure 3.17. As it is showed, the differences between seasons are lower in the incident radiation measured at 37 °C, as it was explained above. The UV values recorded in this period ranged from a minimum of 23.4 ± 2.5 W/m^2 to a maximum of 44 ± 5.1 W/m^2.

Solar UV-dose and the Q_{UV} parameters have been used as a tool to normalize the data of solar experiments obtained in this experimental study. This allows the evaluation and comparison of experimental results from different days and seasons. Solar UV-dose (Wh/m^2) was calculated as the product between the solar radiation collected by the pyranometers (UV, W/m^2) and the treatment time (t, h) (Eq.3.9). Q_{UV} parameter represents the cumulative UV energy during exposure time per unit of volume of treated water (kJ/L) (Eq. 3.10).

$$UV\ dose = UV x\ t \qquad\qquad\qquad \text{Eq. 3.9}$$

$$Q_{UV} = \sum_{n} \overline{UV}_{n-1} \frac{A_r}{V_t}\left(t_n - t_{n-1}\right) \qquad\qquad \text{Eq. 3.10}$$

Where, t_n the experimental time for the sample n, $\overline{UV}_{n-1}$ is the average of the solar UV-A irradiance in the period (t_n -t_{n-1}), A_r is the illuminated surface of the reactor and V_t is the total volume of the reactor.
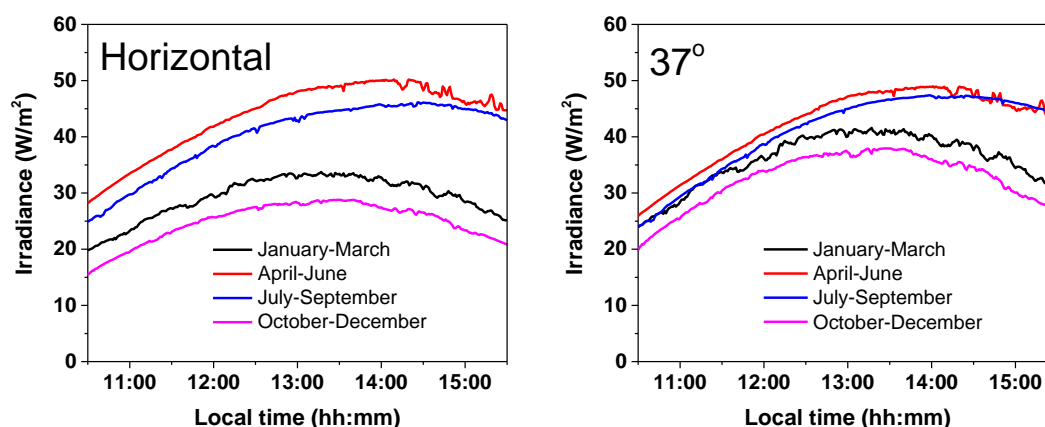
Figure 3.17. Quarterly averaged solar radiation of 2017 year (UV horizontal and UV at 37º) at PSA from 10:30 am to 15:30 pm.

3.7. Water characterization: analytical techniques

3.7.1. Ion chromatography

Ion chromatography is a technique that permits to separate ionic compounds in aqueous solution, including inorganic ions and polar organic molecules (weak and strong acids and bases), based on their affinity with a stationary phase. The sample is transferred by a mobile phase (buffered aqueous solution) onto a chromatographic column which contains the stationary phase formed by synthetic ion exchange resins which active sites are charged anchor groups. Depending on the nature of the ions (cations or anions), there are two types of ion chromatographs where the set-up for both is common and differ only on the stationary and mobile phase. The ion chromatographs used to separate and quantify cations contain a stationary phase composed by cationic ion exchange

resins with negatively charged anchor groups and the mobile phase contains an acid that competes with the analytes for the active sites on the stationary phase. In the case of anions, the stationary phase is formed by anionic ion exchange resins with positively charged anchor groups and the mobile phase usually contains carbonate ions to compete with the active sites.

The mobile phase drags the analytes at different times depending of their affinity with the stationary phase to a sensor coupled to the columns. The most common detection system is based on electric conductivity, which recorder the increase of electric conductivity of the mobile phase when the analyte pass through the detector generating Gaussian shape peaks, which area is evaluated by the software to quantify the ion content.

In this study, the ion chromatography technique was used to analyze amines, carboxylic acids, inorganic anions and cations in water samples. It was used a Metrohm ion chromatograph Model 850, that consists on two 872 extension modules (Figure 3.18): i) module for determination of anions and polycarboxylic acids through a gradient analysis in a column METROSEP A Supp 7-250 (250mm X 4.0mm ID); ii) module for determination of cations and amines through a isocratic analysis in a column METROSEP C4-250/4.0 (250mm X 4.0 mm ID). The mobile phases used were: i) an aqueous solution of sodium bicarbonate (0.53 g/L) for anions determination (inorganic anions and carboxylic acids); and ii) an aqueous solution containing acetone (9 %), pyridine (0.75 %) and nitric acid 2M (0.085 %) for cations determination (inorganic cations and amines).

Figure 3.18. Photograph of ion chromatographs.

Analytes quantification were performed by internal calibrations using straight-line calibration curves in the range 0.1-20 mg/L for inorganic anions, cations and amines and in the range of 0.1-5 mg/L for carboxylic acids. The calibration was checked before the samples measurements by standard solutions of 10 mg/L of each anion and cation analyzed.

Samples were filtered with 0.22 μm filters of nylon before injection. The run time were 23 and 47 min for cations and anions determination, respectively.

3.7.2. Turbidity, pH, temperature and conductivity

Turbidity is measured by recording the light scatter and absorption in an angle of 90° respect to the incoming source of light and is usually expressed in arbitrary NTU units (Nephelometric Turbidity Units). The equipment used was a Hach turbidimeter model 2100AN with a detection range from 0.1 to 4000 NTU. Equipment calibration was done according to the supplier using the kit Hach 2100AN (IS Stablcal® Stabilized Formazin standars). Briefly, the turbidity of water samples were measured in a cylindrical glass cuvette which water content was homogenized just before placing the sample and recording the value of turbidity immediately to avoid effects of particles precipitation.

Water pH was monitored using a pH-meter (110-K, Horiba Laqua act), water temperature by a temperature sensor Checktemp (Hanna Instruments) and conductivity using a conductivity meter GLP31 CRISON. These common devices used for water characterization are calibrated accordingly to manufacturer on the daily run-time of the laboratory.

3.7.3. Dissolved Organic Carbon (DOC)

DOC was determined to evaluate the degree of dissolve organic matter mineralisation during the water treatment processes; therefore the samples were filtered (0.22 μm nylon) before their injection into the equipment. Dissolved organic carbon (DOC), dissolved inorganic carbon (DIC) and total dissolved carbon (TDC) were analyzed using a Shimadzu TOC-V-CSN and an auto-

sampler ASI-V (Figure 3.19). DOC was calculated as the difference between the TDC and the DIC values of the same aqueous sample.

The TDC measurement is based on combustion reaction at 680 ºC in a platinum catalyst supported on aluminium oxide spheres where the carbon content is oxidized to CO_2. The CO_2 generated is transported by a carrier gas into a non-dispersive infrared detector (NDIR) where an analogue signal is converted by a standard Digital/Analog converter obtaining a peak area which is evaluated by the equipment's software. For DIC quantification, the sample reacts with phosphoric acid (25 % w/v) generating the decomposition of carbonates and bicarbonates into CO_2 which is stripped by the carrier gas and analyzed in the same detector than TDC.

The quantification of inorganic and organic carbon content requires the use of calibration lines that permits to determine the unknown carbon content of water samples. To do so, the linear relationship between the peak area and the carbon concentration obtained by the calibration lines are used for the quantification. For TDC, calibration was performed with a solution of potassium hydrogen phthalate (Panreac ACS-ISO) in ultrapure water containing sulphuric acid to avoid contamination by dissolution of atmospheric CO_2. Five calibration lines are estimated for different TDC ranges: 0-10, 10-50, 50-250, 250-1000, 1000-2500 mg/L. For DIC calibration, a solution containing sodium carbonate and sodium hydrogen carbonate in a ratio 1:1 in ultrapure water was used. In this case, five linear regression curves are also stablished (0.5 – 2.5, 2.5 – 15, 15 – 75, 75 – 250 and 250 – 1000 mg/L). The calibrations are carried out periodically to ensure the correct performance of the equipment.

Figure 3.19. Photograph of TOC-analyzer.

Each water sample in this research was measured in duplicate by two independent injections. The maximum coefficient of variance of this equipment is less than 2 %, but if this criteria is not met, automatic sample re-injection is performed. Moreover, standard solutions are injected periodically to check the correct operation of the equipment.

3.8. Reagents quantification

3.8.1. Dissolved iron

Dissolved iron (sample was pre-filtered through 0.22 μm nylon syringe-driven filter) was measured by a spectrophotometric method according to ISO 6332:1998. The ferrous iron form a chelate complex with three 1,10-phenanthroline molecules $[Fe(phen)_3]^{2+}$, which has an orange-red color as consequence of a maximum absorption peak at 510 nm. The colored solution formed follows the Lambert-Beer law in a pH range from 3 to 9 and for this reason the measurements are conducted in a buffered solution.

Briefly, the procedure consists on mixing 4 mL of the filtered sample with 1 mL of 1,10-phenantroline solution (0.1 % w/v in distilled water) and 1 mL of a buffer solution (250 g/L ammonium acetate and 700 mL/L of acetic acid in distilled water) and after a few minutes the sample absorbance at 510 nm is measured in a spectrophotometer (Unicam-II). A blank reference solution prepared in the same way but replacing only the phenantroline solution for the same quantity of the water matrix was used to avoid any colour interference. This procedure gives us the concentration of ferrous dissolved iron of the sample. Nevertheless, in water samples the total iron is commonly present as a mixture of ferrous and ferric iron. Therefore, to measure the total iron in the sample a spatula tip of ascorbic acid is also added to reduce ferric iron and avoid any other oxidant interference in the measurement.

A calibration line for total iron quantification in this equipment was performed in the range from 0.25 to 7.5 mg/L (Eq. 3.11). The limit of quantification of this method was found to be 0.1 mg/L.

$$Fe \left(\frac{mg}{L} \right) = \frac{Abs \,(510 \; nm)}{0.1328} \qquad\qquad R^2 = 0.999 \qquad\qquad \text{Eq. 3.11}$$

3.8.2. Hydrogen peroxide (H₂O₂)

Hydrogen peroxide concentration in water samples was determined by a spectrophotometric method following the DIN 38402H15 protocol. This colorimetric method is based on the formation of the complex $[Ti(O_2)(OH)(H_2O)_3]^+$ between the reagent Titanium(IV)Oxysulfate (Riedel de Haën, Germany) and the H_2O_2 in solution. This complex has a yellow coloration as consequence of a maximum absorption band at 410 nm.

The experimental procedure for H_2O_2 determination in water samples consist on the mixture of 5 mL of A filtered sample (0.22 μm) with 0.5 mL of the commercial reactive Titanium(IV)Oxysulfate. This reaction leads to the formation of the mentioned complex instantaneously which is stable during at least 10 hours. Absorbance was measured with a spectrophotometer (Unicam II) at 410 nm. The limit of quantification (LOQ) of the method was 0.1 mg/L and demineralized water was used as blank reference. To determine the unknown concentration of samples, a calibration line was performed in the range 0.5 to 60 mg/L. The H_2O_2 concentration values were obtained using the Eq. 3.12.

$$\text{H}_2O_2 \left(\frac{mg}{L} \right) = \frac{Abs \,(410 \; nm)}{0.0226} \qquad\qquad R^2 = 0.999 \qquad\qquad \text{Eq. 3.12}$$

3.8.3. Aqueous ozone

The ozone concentration in solution was also determined by the colorimetric Indigo method and it is based on the reaction between molecular ozone and the C=C bond of indigotrisulfonate [Clesceri *et al.*, 1998a].

To determine the ozone concentration in samples, two indigo solutions are used: *i)* Indigo stock solution, prepared by dissolving 770 mg of potassium

indigotrisulfonate (Sigma Aldrich) in 1 L of ultrapure acid water (0.1 % (v/v) of phosphoric acid), and storage a 4 ºC. *ii)* Indigo reagent II, prepared by dissolving 10 g of monosodium phosphate (NaH_2PO_4) in 1 L of ultrapure acid water (0.7 % (v/v) of phosphoric acid) containing a 10 % of Indigo stock solution.

The procedure for the ozone determination in samples consists on the mix of 5 mL of water sample with 10 mL of the Indigo reagent II solution in a 100-mL volumetric flask, previously filled with ultrapure water. The absorbance of the solution obtained is then measured at 600 nm in less than one hour within Unicam-II spectrophotometer. The blank was prepared and measured by the same procedure replacing the sample volume for ultrapure water.

Finally, the aqueous ozone concentration was calculated using the next equation:

$$O_3 \left(\frac{mg}{L} \right) = \frac{100 \times \Delta Abs}{f \times V}$$
Eq. 3.13

Where, 100 is the flask volume (mL), ΔAbs the difference in absorbance between the Blank and the sample absorbance (Blank Abs- sample Abs), *V* the sample volume (5 mL) and *f* a fixed factor (0.42).

3.9. Hydroxyl radicals (HO$^{\bullet}$) quantification

The generation of HO$^{\bullet}$ was determined during the photo-Fenton process with iron chelate (Fe^{3+}-EDDHA) in order to established their capability for water disinfection and decontamination. The procedure used to determine the initial formation rate of HO$^{\bullet}$ ($R_{HO\bullet}$) was previously described in literature [Vione *et al.*, 2006]. It is based on the generation of phenol by the reaction between the radicals generated and the reactive molecule benzene (used as probe). In this reaction is considered the initial formation rate of phenol and no limitation on the scavenging of HO$^{\bullet}$ by benzene. The $R_{HO\bullet}$ was calculated using the following equation [Vione *et al.*, 2006]:

$$R_{HO\cdot} = (0.95)^{-1} \times \frac{d[Phenol]}{dt} \qquad\qquad \text{Eq. 3.14}$$

The experimental procedure consists on the mixing of a solution of benzene (2.95×10^{-3} M) prepared in ultrapure water and homogenized overnight in a close glass bottle. After that, the initial sample was taken, the reagents (iron chelate and H_2O_2) were added to the benzene solution and the reactor was immediately exposed to solar radiation taking samples every 30 min during 180 min. The concentration of phenol in samples was analyzed by UPLC-UV-DAD with a C-18 column (XDB-C18 Agilent 1.8 μm, 4.6x50 mm), flow rate of 1 mL/min and 100 μL of injection volume. The elution method was isocratic with 20-80 % of ACN-ultrapure acid water (25 mM formic acid) during 5 min where phenol was detected at 268 nm and 1.9 min of retention time. The concentration of phenol was calculated according to a calibration line from 25 to 1000 μg/L (Eq. 3.15) performed previously using phenol with high purity grade (>99 %, Sigma-Aldrich) as analytical standard.

$$Phenol\ \left(\frac{\mu g}{L}\right) = \frac{peak\ area}{0.0837} \qquad R^2 = 0.999 \qquad \text{Eq. 3.15}$$

3.10. Chlorophyll content quantification

The chlorophyll content in lettuce leaves (as summation of chlorophyll a and b) was determined by a spectrophotometric method with a previous sample extraction according to the quantification procedure described for phytoplankton [Clesceri *et al.*, 1998b].

The chlorophyll from lettuce was extracted using an organic solution acetone:water (90:10). Briefly, 5 mL of this solution was mixed with 1 g of sample cut in small (<1 mm^2) pieces in a plastic centrifuge tube. The tube was placed in the fridge during 24 h for the extraction step. After that, the green solution generated was centrifuged and filtered (0.22 μm) (Figure 3.20).

Figure 3.20. Photograph of chlorophyll extract and the corresponding diluted sample.

Finally, the transmittance of the filtered solution was measured at 630, 647, 664 and 750 nm in a spectrophotometer to determine the optical density (OD) of the solution at each wavelength (OD=log T). If the optical density was not in the interval between 0.1 and 1.0, the sample was diluted using the organic solution. The OD value at 750 nm is a correction for the sample turbidity and its value was subtracted for each OD values before use them for the chlorophyll calculation in the next equations where C_a and C_b are the concentrations of chlorophyll a and b, respectively:

$$C_a \left(\frac{mg}{L}\right) = 11.85(OD664) - 1.54(OD647) - 0.08(OD630) \qquad \text{Eq. 3.16}$$

$$C_b \left(\frac{mg}{L}\right) = 21.03(OD647) - 5.43(OD664) - 2.66(OD630) \qquad \text{Eq. 3.17}$$

Finally, once the chlorophyll content of the extract (summation of C_a and C_b) is known, the amount of pigment per unit of mass was calculated considering the volume of extract (5 mL) and the sample weight.

3.11. Experimental procedures and control tests

Different types of experimental tests have been performed in this research. The detailed procedures will be widely explained below; nevertheless there are some common aspects in all of them:

- Both types of targets were spiked in the water matrix under evaluation to reach the desired initial concentration: ca. 10^6 CFU/mL of each bacteria and 100 µg/L of each OMC.

- Prior to start any experiment, a homogenization time in the dark was set to ensure the correct homogenization (order of addition: bacteria and/or OMCs, and then reagents) of the water sample. This time depends on the reactor scale (5 to 15 min), starting the experiment immediately after the initial sample (Time 0) was taken-out.

- Water samples along the experimental tests were taken at regular intervals (depending on the total treatment time and the type of experiment) for bacterial enumeration and/or OMCs analysis by UPLC-UV-DAD.

- In all experiments with H_2O_2 presence (dark, solar and ozonation), its residual concentration was eliminated by adding a bovine liver catalase solution (0.1 g/L) at ratio catalase:sample of 1:50 to each water sample taken out, to avoid any post-effect of oxidation during the laboratory procedure to quantify both bacteria and OMCs.

- All the operational conditions were carried out at least in duplicate. Therefore, results are represented as the average of replicated experiments (with standard deviation as error bar in graphs) against treatment time, solar UV-dose or Q_{UV}. Results were in all cases highly reproducible, showing *P-value* <0.05 (ANOVA).

3.11.1. Dark experiments

Prior to any solar processes and ozonation tests, the impact of some physic-chemical parameters, the presence of reagents and operational conditions on the bacterial viability were investigated. Different dark tests in order to determine the mere effect of temperature, pH, H_2O_2 concentration as well as the impact of mixing bacteria and OMCs were done in isotonic water and at laboratory scale.

Thermal test

This study was performed using a cool-hotter dry incubator (UniEquip GmbH) which permits to maintain the temperature constant and controlled with an accuracy of ±0.2 °C in the range 10-100 ºC. The experimental procedure was as follow: a suspension of both bacterial strains at ca. 10^6 CFU/mL in isotonic water was prepared and dispenser in 2 mL sterile containers type Eppendorf (2 replicates of each sampling time) and introduced in the incubator.

The effect of typical outdoor water temperature (30, 35 and 40 °C) reached during solar processes was analyzed, and thermal profiles obtained are shown in Figure 3.21.
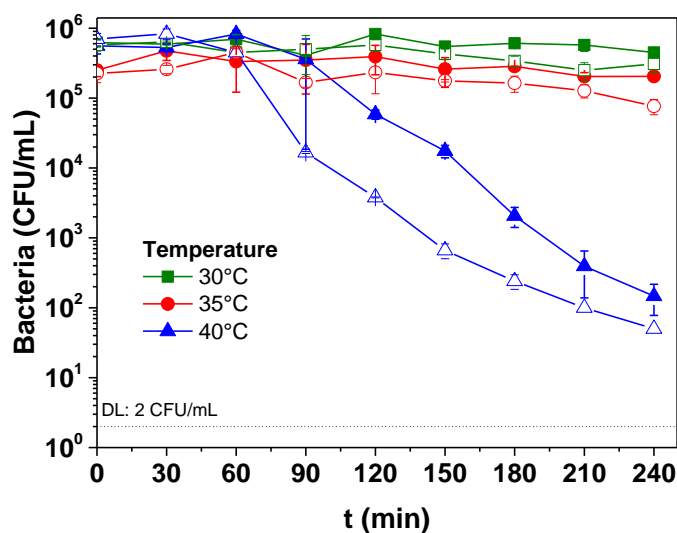
Figure 3.21. Thermal effect on *E. coli* O157:H7 (full symbols) and *S. enteritidis* viability (empty symbols) in the dark.

These results showed that only temperature higher than 40 °C may determine a detrimental effect after 120 and 90 min of thermal exposure for *E. coli* and *S. enteritidis*, respectively. Nevertheless, in this research, the thermal effect on bacteria inactivation was discarded as this temperature or higher was only sporadically reached and not significant influence was observed in the inactivation during solar experiments.

Dark effect of water pH was also investigated in 200 mL-solar reactor under magnetic agitation (set at 450 rpm) during 4 hours. Three values of water pH were analyzed by adding H_2SO_4 (2M) in IW: 3, 4 and 5. Bacterial concentration profiles obtained are showed in Figure 3.22. Results showed a detrimental bacteria effect for pH 3; nevertheless, in any case investigate in this research, water pH values lower than 6 were recorded, discarding therefore this water parameter as factor of bacterial inactivation.
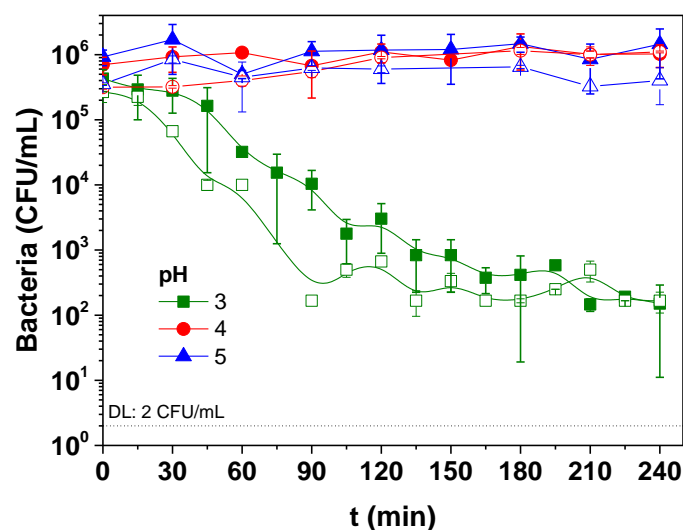
Figure 3.22. pH effect on *E. coli* O157:H7 (full symbols) and *S. enteritidis* viability (empty symbols) in the dark.

H₂O₂ concentration tests

The oxidative effect of H_2O_2 concentration in the dark over bacteria and OMCs was also investigated in 200 mL-solar reactor under magnetic agitation (set at 450 rpm) during 4 hours in IW. To reach the desired initial H_2O_2 concentration (ranged from 5 to 50 mg/L), an appropriate quantity of a stock solution prepared at 10 g/L was directly diluted in the sample.

Regarding H_2O_2 effect in dark (Figure 3.23), both pathogens showed loss of viability, being the detrimental effect higher by increasing the oxidant concentration and more significant in *E. coli* than in *S. enteritidis*. Therefore, the mere effect of H_2O_2 on the bacterial inactivation will be considered and taking

into account during the evaluation of the water treatment capability investigated in this research. The inactivation mechanisms by H_2O_2 will be deeply explained in the section 4.1.2.2. (Bacterial inactivation by H_2O_2/solar).

The OMCs was also exposed to H_2O_2 concentrations (20 and 50 mg/L) in dark in order to determine the potential oxidative effect on the targets compounds. The results did not show a significant OMCs oxidation (2 and 7 % for 20 and 50 mg/L, respectively) (Figure 3.24). Therefore, the use of this range of H_2O_2 cannot be considered as factor of OMCs degradation.

(a)

(b)
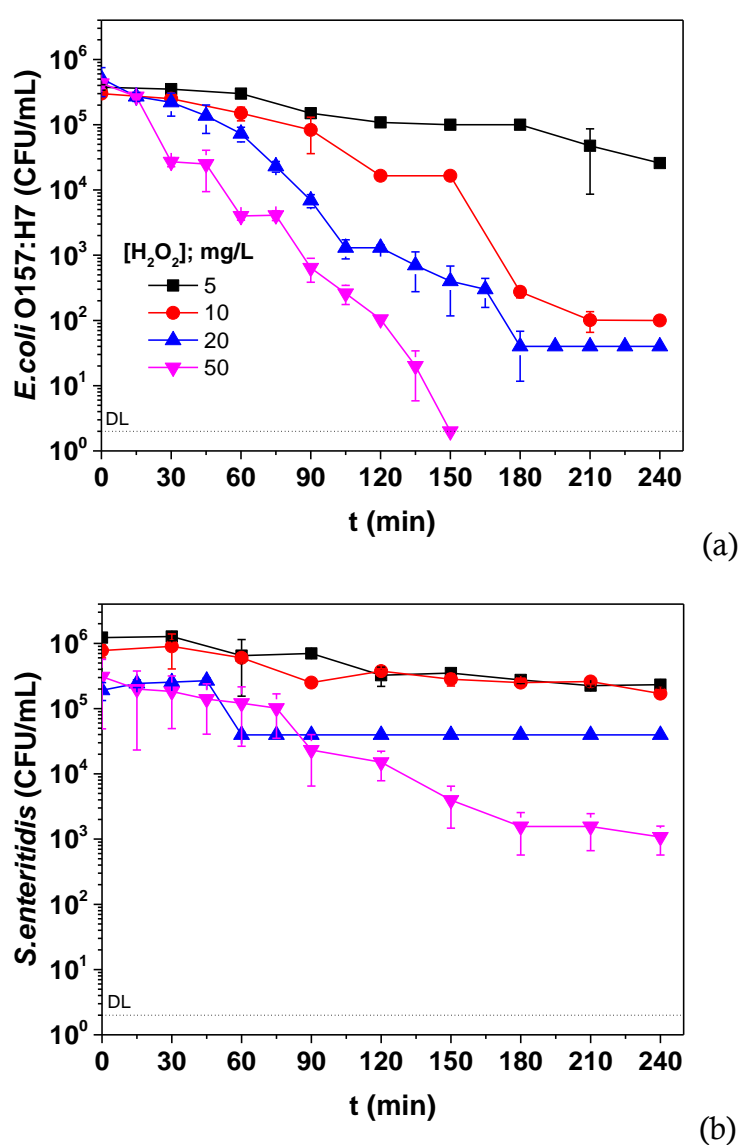
Figure 3.23. Effect of different H_2O_2 concentrations on *E. coli* O157:H7 (a) and *S. enteritidis* viability (b) in the dark.
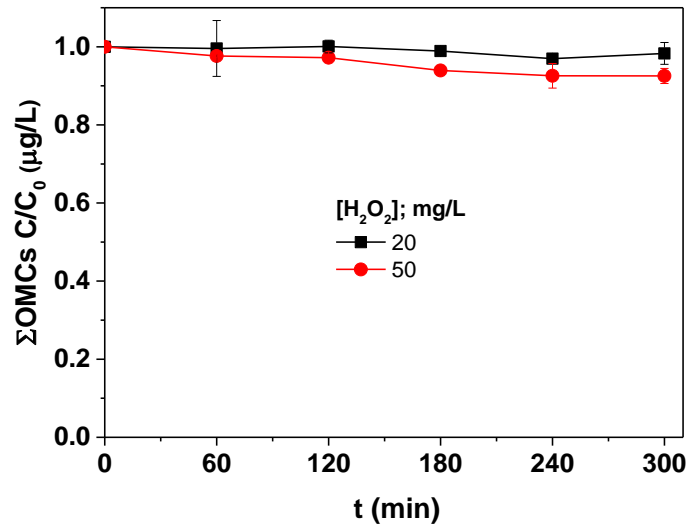
Figure 3.24. Degradation profile of the ΣOMCs oxidation by 20 and 50 mg/L of H_2O_2 in the dark.

Toxic effect of OMCs over bacteria

The potential detrimental effect of the OMCs mix presence (at 100 µg/L each) on bacterial viability was also evaluated in dark during 4 hours and results showed any viability loss for both pathogens (Figure 3.25). This result is important due to indicate the suitability to perform disinfection and decontamination experiments simultaneously.
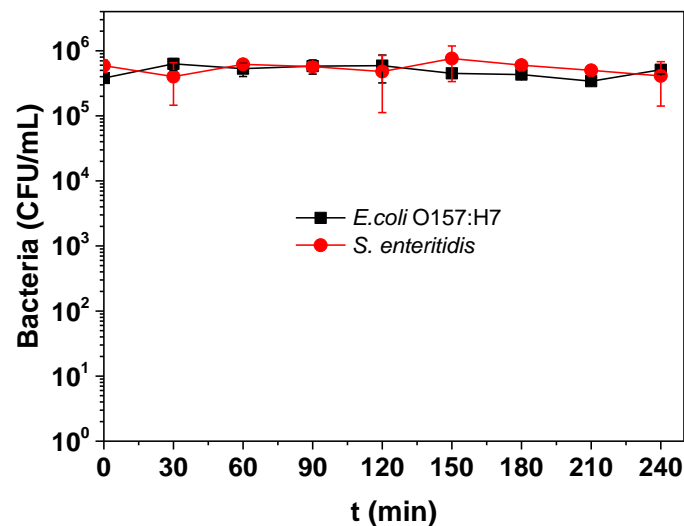
Figure 3.25. *E. coli* O157:H7 and *S. enteritidis* viability in the dark and in the presence of OMCs mix.

3.11.2. Solar experiments at lab-scale

Solar experiments at lab scale were performed in 200 mL solar-reactors under constant agitation (at 450 rpm) in completely sunny days at Plataforma Solar de Almeria. Experiments started between 10:30-11:00 am local time lasting 3 to 5 hours of solar exposure. The pH, water temperature and solar UV-irradiance were monitored throughout the experiments using the equipments previously described.

3.11.3. Solar simulator experiments

Assays under controlled conditions (constant UV-A irradiance from 10 to 50 W/m^2) were performed in a 700 mL Simulated-solar reactor (explained in the Section 3.5.1.1) with 700 mL of SFCWW. All the solar tests were carried out at a controlled temperature below 30 ºC to avoid any thermal effect on the bacterial viability.

Once the solar reactor and water samples were prepared, i.e., reagents and microbial suspension spiked properly and the first sample was taken (Time 0), the reactor was exposed to the artificial irradiation by switch on the lamp, which is automatically switch off if the door of the chamber is opened. Therefore, and to avoid irradiance interruption during the artificial solar test, the sampling in this system was done taking the samples from outside with a flexible tube and a syringe. Both were carefully disinfected before the experiment (washed with a H_2O_2 solution and rinsed at least three times with demineralized water). For each sample, the flexible tube and the syringe were rinsed with the sample itself by discarding the first sample volume (5 mL) and taking the next one.

3.11.4. Solar experiments in CPC reactors

Solar experiments at pilot plant scale were performed using the solar CPC photo-reactor previously explained (Section 3.5.2.2). Experiments started between 10:30-11:00 am local time lasting 3 to 5 hours of solar exposure.

Between experiments and before to fill the reactor with the water intended to treat, the CPC reactor was carefully cleaned and disinfected to avoid any risk of contamination. For this aim, after each experiment the reactor was filled with demineralized water (60 L) and a high H_2O_2 concentration was added (ca. 50 mL of H_2O_2 at 30 % p/v) and recirculated during at least 45 min. After that, the pilot plant was rinsed 3 times with demineralized water.

Once CPC reactor was clean, reagents, OMCs and microbial suspensions were directly diluted in the reactor, and kept the system in recirculation in the dark (using a plastic opaque sheet) for 15 minutes. After that, the first sample was taken (Time 0) and immediately the reactor was exposed to sunlight.

3.11.5. Ozonation experiments

The operational conditions of the ozone pilot plant used in the ozonation experiments of this study was 10 L of total volume of water, a constant inlet air flow of 0.06 Nm^3/h and two different initial ozone production of 0.9 and 1.5 gO_3/h, resulting from the ozone generator working at 10 or 20 % power, respectively.

The experimental procedure was similar to previous system. For test at basic pH (11), a NaOH solution 2 M was used to modify the SFCWW pH. For Peroxone tests, an initial dose of H_2O_2 (20 mg/L) was added and when concentration of H_2O_2 was lower than ca. 1.5 mg/L, additional doses were added to avoid limitations of the reagent during the experiment. In this case, prior to start with the ozonation test, the water solution was kept recirculating for 10 min in the dark for homogenization purpose.

In all samples, the residual ozone concentration was immediately removed with N_2 and for peroxone tests the residual H_2O_2 was also eliminated with catalase as was explained previously.

The ozone consumption of each sample was calculated by a mass balance taking into account the ozone measurements at the sample time (inlet, outlet and in solution) and the ozone consumption of the previous sample.

3.11.6. Irrigation experiments

The irrigation assays were performed under controlled conditions at Plataforma Solar de Almeria using a 30 m²-experimental greenhouse (Figure 3.26) divided in 4 individual areas of 7.5 m² (Suministros D.R., Spain). This experimental design allows growing plants under controlled conditions of temperature, humidity and irradiance. For this aim, each area is equipped with temperature, humidity and light sensors connected with a software of control (Ambitrol®). This software allows the adjustment and control of these parameters by cooling (Fisair, Spain) and heating (Gabarrón, Spain) systems, automatic windows located in the roof slope of each individual area and a double tarps system. Averaged temperature during solar tests was 25±5 °C and humidity varied daily from 50 to 90 %.

Romaine lettuce (*Lactuca sativa var. longifolia*) and radish (*Raphanus sativus L.*) vegetables were selected as representative leaves and fruit raw-eaten vegetables with relative fast growing, i.e., 10-12 and 4-6 weeks from seeded to harvested, respectively. Both seeds were obtained from a local provider and grown on propylene pots (9x9x10 cm) filled with commercial and regular peat as substrate. According to the manufacturer, peat contains 67 % of organic matter and 1 g of fertilizer per litter at an N-P-K ratio of 15-15-15. pH 7.25 and 75 mS/cm of conductivity. Peat was autoclaved (121 °C during 15 min) prior to use it, to avoid any possible source of faecal bacteria contamination.

Figure 3.26. Experimental greenhouse located at the PSA.

Lettuce and radish irrigation tests were done simultaneously, with similar growing conditions. 100 pots per each type of crop and irrigation condition were placed in an individual area of the greenhouse to avoid potential risk of cross contamination between the different conditions evaluated. Each pot was regularly watered with 50 mL of the corresponding type of water by simulating the sprinkle irrigation technique (Figure 3.27) during 12 weeks and 6 weeks for lettuce and radish, respectively. After that, crops were aseptically harvested for bacteria, OMCs and chlorophyll content quantification according to procedures described in sections 3.2, 3.3 and 3.10, respectively.

Figure 3.27. Image of the crops irrigation technique used.

3.12. Toxicity evaluation

OMCs and their sub-products generated after a water treatment can affect the ecological status of the receiving ecosystems by declining its biodiversity and/or some essentials functions. Therefore, a toxicity assessment of the final treated wastewater represents an important parameter to assess the environmental impact generated by the final destination of the treated wastewater.

As a first toxicity assessment approach, two standardized tests were selected: *Vibrio fischeri* (acute toxicity) to assess the potential environmental impact of treated wastewater discharge in water effluents and *Lactuca sativa* seeds (phytotoxicity) to evaluate the suitability of the treated water intended for reuse purposes.

To this aim, the initial and final sample of each water treatment evaluated in this research were tested joint with the specific negative and positive toxicity controls specific for each type of test. The samples were collected in washed glass flasks, when necessary their pH was adjusted to a value of 6~7. Samples were analyzed immediately or stored at -20 ℃ for a maximum of 1 month until the tests were performed.

3.12.1. *Vibrio fischeri* test

V. fischeri is a widely used organism for the initial screening of environmental samples with unknown eco-toxicological characteristics [Menz *et al.*, 2013; Rizzo, 2011]. This marine bacterium is frequently found in symbiotic relationships with aquatic animals (mainly marines). Its bioluminescent is generated by a chemical reaction in their *lux* operon catalysed by the luciferase enzyme (Eq. 3.18):

$$FMNH_2 + RCHO + O_2 \xrightarrow{LuxAB} FMN + H_2O + RCOOH + hv\ (493\ nm) \qquad \text{Eq. 3.18}$$
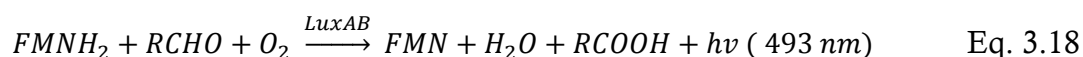
The reaction between reduced luciferin (FMNH$_2$), the long-chain fatty aldehyde tetradecanal (RCHO), and molecular oxygen as substrates is catalyzed by the luciferase enzyme (LuxAB) leading to luciferin (FMN), an acid generated by the oxidation of the aldehyde (RCOOH), water and the releasing of free energy as photons at 493 nm (blue-green light).

Based on its bioluminescent generation, the differences in the amount of light produced can be correlated with the organism's metabolism. And a decrease in the amount of light emitted by the bacteria in contact with a specific water samples is an indicative of the negative eco-toxicological impact of the water sample components.

In this study, the assessment of acute toxicity was carried out using the commercial kit BioFix$^®$ Lumi-10 by monitoring changes in the bacteria bioluminescence after 30 min exposure of the samples following the standard ISO 11348-3 method [ISO, 1998].

The freeze-dried bacterium (-20 °C) was activated by hydration according to the standard procedure of the commercial kit. Prior to the test, the samples were filtered with 0.2 μm syringe-driven filters (Millex$^®$, Millipore) to avoid interferences in luminometer measurements and salinity adjusted to 2 % (w/v) with NaCl to avoid bacterial stress conditions. Solutions of NaCl (2 % (w/v)) and K$_2$CrO$_7$ (18.7 mg/L Cr^{+6}) were used as negative and positive toxicity controls, respectively.

All the samples (including control test) were tested in triplicate and kept on at 15°C (in a thermostatic plate) along the test duration. The bioluminescence of *V. fischeri* was measured using the BioFix$^®$ Lumi-10 luminometer (Macherey-Nagel GmbH & Co. KG, Duren, Germany) after 30 min of sample exposure. Samples toxicity results were expressed as bioluminescence inhibition percentage (BI %) considering the untreated SFCWW as control, i.e., normalizing the results obtained respect to this value. Additionally, the samples were classified in different ecotoxicity levels considering its discharge in an aquatic environment: [Persoone *et al.*, 2003].

3.12.2. *Lactuca sativa* test

Phytotoxicity was assessed using the seed germination and root elongation test of *Lactuca sativa* as this specie is one of the most important terrestrial plant from a horticulture point of view and also one of the main vegetables processed by the fresh-cut sector [Priac *et al.*, 2017]. Phytotoxicity tests were performed following standard procedures [USEPA, 1989; Young *et al.*, 2012]. Commercial romaine lettuce seeds (*Lactuca sativa*) obtained from a local provider (Ramiro Arnedo S. A) were used. Tests were carried out in 90-mm-diameter Petri dishes lined with filter paper. On each plate, 13 seeds were placed on the moistened filter paper with 4 mL of each water sample. Demineralised water was used as negative toxicity control and $ZnSO_4 \cdot 7\ H_2O$ (100 mg/L) as positive toxicity control of seeds germination (Figure 3.28). All samples (including controls) were tested in triplicate. After 5 days (120 h) of incubation in the darkness at 22±2 °C the germinated seeds were counted and the root length (cm) was measured to calculate the germination rate (G %, rate between germinated and total seeds) and the relative growth index (RGI) according to the following equation [Young *et al.*, 2012]:

$$RGI = \frac{RLS}{RLC}$$

Eq. 3.19

Where RLS is the radicle length of the sample plants and RLC is the radicle length in the negative control. RGI was divided into three categories according to the toxicity effects observed: Inhibition of the root elongation (I): 0 < RGI < 0.8; No significant effects (NSE): 0.8 ≤ RGI ≤ 1.2; and Stimulation of the root elongation (S): RGI > 1.2 [Sobrero and Ronco, 2004; Young *et al.*, 2012]. Seeds were considered germinated when the root elongation was higher than 0.3 cm. The tests were accepted as valid when the G % was higher than 90 % and the coefficient of variation of the root elongation lower than 30 % in the negative control.

Before incubation   After 120 h
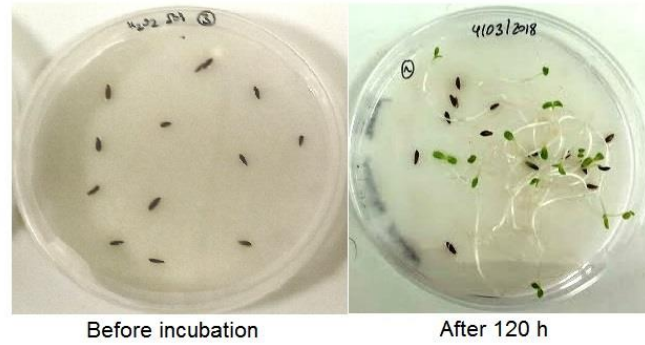
Figure 3.28. Photograph of an example of a phytotoxicity test before and after incubation time.

Statistical data evaluation was performed using Graph Pad Prism (GraphPad® Software, San Diego, California, USA). Results were analyzed by D'Agostino & Pearson omnibus normality test. Since data were normally distributed they were submitted to one-way variance analysis (ANOVA) followed by Dunnett´s multiple comparison test ($p < 0.05$).

3.13. Kinetic models

Inactivation kinetic constants of each bacterium in disinfection experiments were calculated and used to compare the efficiency of the different treatments and conditions studied. Kinetic constants were calculated considering Q_{UV} parameter (or the treatment time) in function of the bacterial inactivation. The constants were obtained by several mathematical models (Eq. 3.20-3.24) according to the higher R^2 value fitting the experimental data:

- Model 1: A log-linear decay according to the Chick´s law (Eq. 3.20).

$$Log\left(\frac{N}{N_0}\right) = -k \cdot Q_{UV} \qquad \text{Eq. 3.20}$$

- Model 2: A 'shoulder phase' characterized by a constant bacteria concentration or a very smooth decay followed by a log-linear decay, attributed to the accumulation of oxidative damages ending in the loss of cells viability (Eq. 3.21).

$$Log\left(\frac{N}{N_0}\right) = -k \cdot Q_{UV} \quad \begin{cases} 0 & ; Q_{UVt} \geq Q_{UV} \\ -k \cdot Q_{UV} & ; \quad Q_{UVt} < Q_{UV} \end{cases} \qquad \text{Eq. 3.21}$$

- Model 3: A double log-linear kinetic characterized by a fast inactivation in the first stage (k_1) followed by a slow second inactivation stage (k_2) (Eq. 3.22).

▪

$$Log\left(\frac{N}{N_0}\right) = -k_1 \cdot Q_{UV} ; Q_{UV} = [0, Q_{UV1}];$$

$$Log\left(\frac{N}{N_0}\right) = -k_2 \cdot Q_{UV} ; Q_{UV} = [Q_{UV1}, Q_{UV2}]$$

Eq. 3.22

- Model 4: A log-linear decay followed by a 'tail' (Q_{UVres}) (Eq. 3.23). The 'tail' represents the bacterial population that remains at the end of the experiment due to the presence of a resistant population.

$$Log\left(\frac{N}{N_0}\right) = -k \cdot Q_{UV} \quad \begin{cases} -k \cdot Q_{UV} & ; \quad Q_{UVt} \leq Q_{UV} \\ 0 & ; \quad Q_{UVt} \leq Q_{UVres} \end{cases} \qquad \text{Eq. 3.23}$$

- Model 5: A 'shoulder phase' followed by a log-linear decay and a 'tail' (Eq. 3.24).

$$Log\left(\frac{N}{N_0}\right) = -k \cdot Q_{UV} \quad \begin{cases} 0 & ; \quad Q_{UVt} \geq Q_{UV} \\ -k \cdot Q_{UV} & ; \quad Q_{UVres} < Q_{UVt} < Q_{UV} \\ 0 & ; \quad Q_{UVt} \leq Q_{UVres} \end{cases} \qquad \text{Eq. 3.24}$$

Where N/N_0 represents bacteria concentration reductions, k is the disinfection kinetic constant and Q_{UVres} the energy value with a residual bacterial population density.

3.14. Risk assessment

The chemical risk assessment of the harvested crops was performed by the estimation of the dietary risk assessment for the combined exposure of OMCs. The estimation was performed according to Standard United States Environmental Protection Agency (USEPA) and European Food Safety Authority (EFSA) methods using the hazard index (HI) to estimate the potential risk of adverse health effects as a long-term risk assessment for the mixture of OMCs.

On the other hand, the quantitative microbial risk assessment of the harvested crops (QMRA) was estimated using the web-based and free software FDA-iRISK®. This software is a modelling tool enables users a relative rapid quantitative risk assessment based on mathematical equations and Monte Carlo simulations. The software requires the specification of the risk scenario and hazard characterization through the input of several data. Figure 3.29 summarizes the main inputs and outputs for a food-hazard risk scenario and the calculation process.
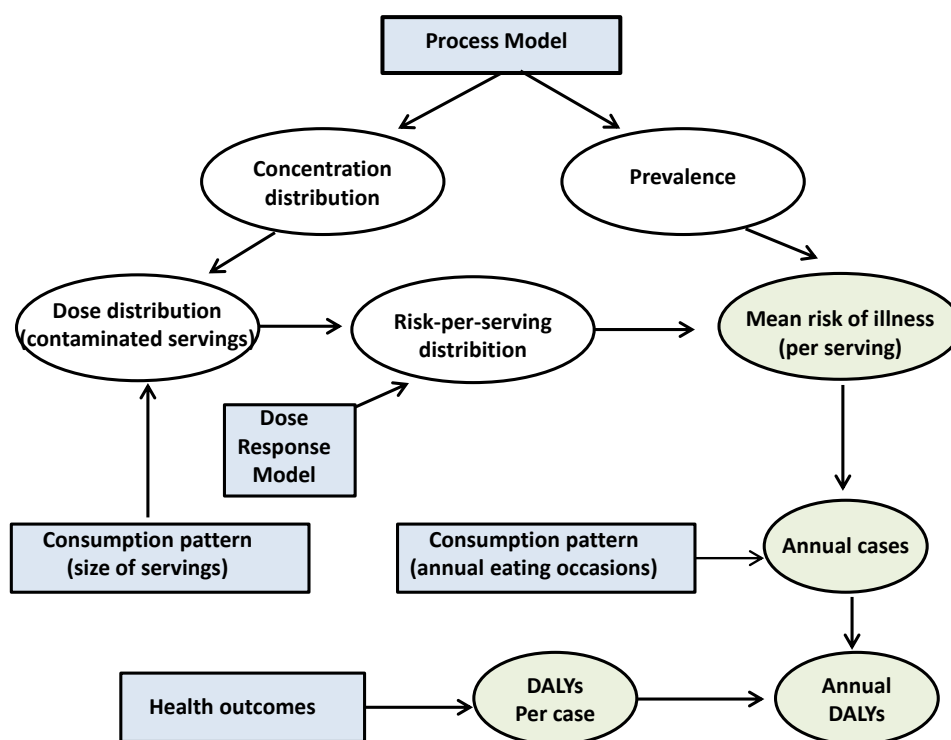
Figure 3.29. iRISK model inputs and outputs for a food-hazard risk scenario (microbial hazards). Inputs are indicated by blue square nodes and model outputs by oval green nodes.

The main input parameters are:

- The process model which describes the impact of the different food process stages on the concentration and prevalence of the hazard requiring the specification of the food, the hazard, and the data of the prevalence and concentration of the hazard per unit of mass.

- The dose-response model per each hazard.

- The consumption pattern including both, the size of serving per each eating occasion and the number of eating occasions per year.

- The health outcome which is based on the specific health impact metric for each hazard and integrate information of severity and duration of illness to estimate the disease burden.

With all of the data inputs, the software generates the data outputs for the specified risk scenario:

- Mean risk of illness per serving calculated from the risk-per-serving distribution which is obtained multiplying the mean of risk per contaminated serving (generated through Monte Carlo simulation) by the prevalence of contaminated units.

- Annual cases of illness by multiplying the mean risk of illness per serving by the annual number of eating occasions.

- DALYs (Disability-Adjusted Life Year) per case which is estimated taking into account the health metric specified for the hazard.

- Annual DALYs by multiplying the annual cases of illness by the DALYs per case.

CHAPTER 4

DEVELOPMENT OF A SYNTHETIC FRESH-CUT WASTEWATER MODEL. EVALUATION OF SOLAR TREATMENTS DISINFECTION EFFICIENCY

4. DEVELOPMENT OF A SYNTHETIC FRESH-CUT WASTEWATER MODEL. EVALUATION OF SOLAR TREATMENTS DISINFECTION EFFICIENCY

In this chapter, a synthetic fresh-cut wastewater (SFCWW) model has been developed with the aim to use this water matrix to obtain more realistic results under standardized conditions. Using the developed recipe, the disinfection capability of four solar treatments: photo-Fenton, photo-inactivation and photo-inactivation assisted with iron or H_2O_2 at near-neutral pH were evaluated. The influence of solar UV-irradiance (ranged from 10 to 50 W/m^2) and reagent concentrations (2.5 mg/L of iron; 2.5 to 20 mg/L of H_2O_2) in the inactivation of two foodborne bacteria (*E. coli* O157:H7 and *S. enteritidis*) has been experimentally determined under controlled conditions.

4.1. Synthetic fresh-cut wastewater: recipe development

The variability on the harvested vegetables, in terms of the presence of dirt, soil, and pesticides, provokes fluctuations in the physic-chemical characteristics of fresh-cut wastewater (FCWW). Although some standardized methods to simulate FCWW from vegetable extracts has been reported [López-Gálvez *et al.*, 2012], the variability mentioned above cannot be avoided by these methods due the vegetable characteristics variance and, therefore, the development of a synthetic fresh-cut wastewater (SFCWW) recipe that allows a realistic comparison between treatments and operational conditions is crucial.

The SFCWW recipe developed in this research is based on the wastewater sample characterization obtained from the local fresh-cut industry 'Verdifresh' (Málaga, Spain). The water disinfection treatment applied in this local industry, like most of the fresh-cut industries, was chlorination by the addition of sodium hypochlorite. Samples from two different washing-tanks (lettuce and spinach) were collected and analyzed at PSA laboratory. A total of 8 water samples were collected in the same journey from 06:20 am to 22:00 pm, the period of time that the washed water from each tank is used before to be discharged in this industry. Figure 4.1 shows the samples collected from the two processing lines.

Figure 4.1. Real wastewater samples collected from two washing lines (lettuce and spinach) at different processing times: from the beginning (6:20 am) to the end of the washing process (22:00 pm) in the same journey.

The detailed characterization of all samples is shown in Annex . To summarize the obtained data, the averaged chemical characterization of the initial and final

samples of a daily washing process from the two processing lines is shown in Table 4.1. Significant differences between spinach and lettuce wash water were observed, and as expected, a significant accumulation of ions along the washing time was detected. This is explained due to the high amount of vegetables washed during this process per tank (around 24 ton) in the volume ratio of amount vegetable:water of ca. 1kg:1L. A constant pH value around 6.2 was measured in both washing lines. This value was kept constant by the addition of phosphoric acid due to play a key role on the effectiveness of the chlorination process mainly based on the oxidative power of the hypochlorous acid which predominates at this pH value [Mercer and Somers, 1957]. The addition of sodium hypochlorite and phosphoric acid obviously determine also high values of phosphate and sodium ions in this type of wastewaters.

Table 4.1. Summary of main physic-chemical characterization of real samples (initial and final wash-water samples from the 'Verdifresh' company) and detailed synthetic FCWW recipe.

Parameter	Lettuce Washing water		Spinach Washing water		Proposed Values*	Measured Values**
	6:20 am	22:00 pm	6:20 am	22:00 pm		
DOC (mg/L)	20.1	530.4	3.3	109.2	25	25.4±0.4
Turbidity (NTU)	2.9	45.5	6	360	100	100.1±0.4
pH	6.37	6.34	6.26	6.2	6.2	6.25±0.06
Conductivity (µS/cm)	334	951	381	1239	1000	1209.6±14.8
Ionic composition (mg/L)						
F^-	<0.1	0.2	<0.1	0.3	0.25	0.14±0.05
Cl^-	28.7	269.9	47.7	318.4	280	282.5±6.4
NO_2^-	<0.1	0.2	<0.1	0.2	0.2	0.15±0.03
Br^-	1.1	12.9	2.3	12.4	12	10.2±0.3
NO_3^-	10.2	40.9	13	66.2	50	51.6±1.1
PO_4^{3-}	232.2	407.1	309.8	542.3	-	0.7±0.1
SO_4^{2-}	7.1	14.6	9.8	145.9	50	51.0±1.8
Na^+	18.1	158.6	31.7	178.2	165	87.7±3.2
NH_4^+	1.7	0.6	<0.1	0.7	0.7	1.05±0.20
K^+	2.7	97.9	2.1	128.4	110	109.5±1.6
Mg^{2+}	5	9.6	6.3	24.5	10	9.6±0.2
Ca^{2+}	40.2	53.2	47.2	44.3	50	46.7±1.0

*Proposed chemical concentration values to simulate the fresh-cut wastewater considering real sample analysis and literature data (Selma *et al.*, 2008b; Gómez-López *et al.*, 2014; Van Haute *et al.*, 2015; Gil *et al.*, 2016). **Averaged values of five measures of the formulated chemical recipe. The reagents used to simulate the FCWW characteristics was detailed in the Section 3.2.2.

It should be remarked the high turbidity measured in real samples, which is attributed to the suspended material accumulated during the washing cycles mainly from soils and vegetables. Significant differences between final turbidity values in both vegetable washing-lines were observed showing the spinach

wastewater much higher turbidity. This difference can be explained due to this crop are more sensitive to mechanical damages and grown closer to the soil.

Moreover, several carboxylic ions including glycolate, propionate, pyruvate or maleate were detected, which must proceed from cellular exudation of vegetables and reactions with chlorine. It is also remarkable the detection of dichloroacetic acid (0.2-0.8 mg/L) in these samples, a disinfection by-product generated as a result of the reaction between chlorine and organic matter [COT, 2007].

The chemical results from the real samples analyzed in this work are in agreement with some contributions found in literature about the chemical composition of different fresh-cut wastewaters (pH: 6.9-8; Turbidity: 88-153 NTU; DOC: 20-300 mg/L) [Selma *et al.*, 2008b; Gómez-López *et al.*, 2014; Van Haute *et al.*, 2015; Gil *et al.*, 2016].

Regarding microbiological characterization, no faecal or coliform bacteria were detected in the real samples analyzed, as expected due to the chlorination process. Nevertheless, the presence of aerobic microorganisms with a concentration ≈100 and 10 CFU/mL for spinach and lettuce respectively was detected, which may be attributed to the presence of microorganisms with high resistance to chlorine as some bacterial spores [Tonney *et al.*, 1928]. However, these microorganisms were discarded in this research due to its low concentration and the low or no risk for vegetables consumption.

Taking into account the data obtained from the analysis of real samples, a chemical recipe was formulated to simulate the fresh-cut wastewater. Nevertheless, some parameters were selected taking into account the treatment application: the DOC content (25 mg/L) was selected as a low-intermediate value in the first stage of the washing process where the treatment should be applied and the phosphate ions was not considered due to, as it was mentioned previously, its added during the chlorination process.

The proposed values to simulate the characterization of the FCWW and the results obtained after the chemical formulation of the synthetic recipe with the standard deviation of five measures are also shown in Table 4.1. As was detailed previously (Section 3.4.2), different reagents were added to demineralized water to simulate the main physic-chemical parameters and ionic composition of FCWW. Briefly, malt extract to simulate the vegetal organic matter, Kaolin (aluminum silicate hydroxide) as turbidity agent and different inorganic salts to obtain the desired ionic composition were used.

To investigate the capability of solar processes to treat this type of water, a compromise between a high level of turbidity and optical light effects was assumed. Therefore, 100 NTU was selected as one of the worse scenarios due to values higher than 100 NTU can be considered as a detrimental effect on solar processes (based on optical capabilities) and a pre-treatment to reduce water turbidity must be considered [Meierhofer *et al.*, 2002].

In line with this, the solar UV income reduction in the sample due to the presence of 100 NTU in SFCWW was determined experimentally by measuring their UV transmittance against demineralized water. To do so, a constant irradiance of 30 W/m^2 was applied to both water samples using the solar simulator. Figure 4.2 shows the absolute transmittance measured from 300 to 400 nm wavelength range with a spectrophotometer. Results showed an average irradiance intensity reduction of 28.4 % through 3 cm of optical pathway (water depth of the solar vessel reactor) in SFCWW compared with demineralized water (< 0.5 NTU). Therefore, it is important to keep in mind that all the solar processes and the inactivation results obtained in this water matrix are affected by this solar UV income reduction due to the presence of turbidity (100 NTU).
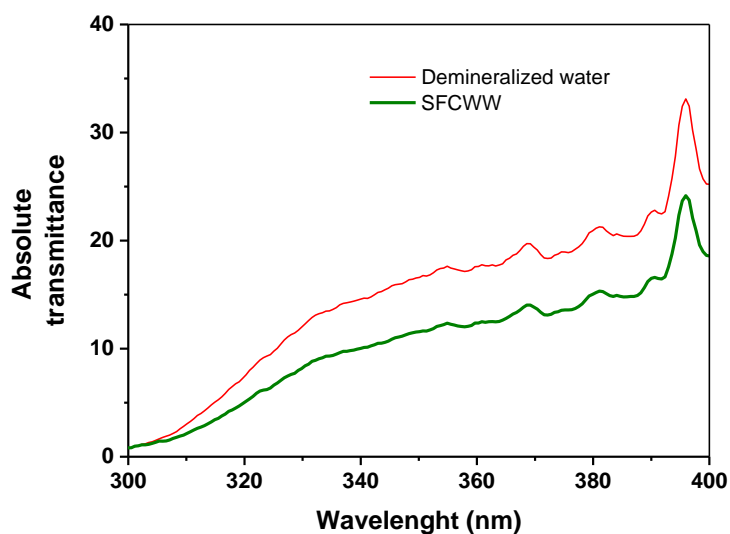
Figure 4.2. Absolute transmittance of demineralized water and SFCWW in the solar UVA range.

4.2. Comparative analysis of bacteria inactivation by solar processes: inactivation mechanisms description

The effect of several solar processes widely investigated for water and wastewater disinfection, such as solar photo-inactivation, H_2O_2/solar, Fe^{2+} or Fe^{3+}/solar and solar photo-Fenton has been assessed on the viability of *E.coli* O157:H7 and *S. enteritidis* as proof-of-principle under controlled conditions (constant solar UV-irradiance) in a solar simulator and using for the first time the complex water matrix developed (SFCWW).

The solar UV-irradiance of 30 W/m^2 was selected since this irradiance is considered a mean value of global UV irradiance under clear skies in sunny countries [Malato *et al*., 2009]. The reagent concentrations used in this research was selected based on previous works of water disinfection by solar photo-Fenton at near neutral pH ([Fe]: 1-5 mg/L and [H_2O_2] at a ratio 1:2 of Fe:H_2O_2) [Polo-López *et al.,* 2013]. In this first study, the concentration of reagents used was: 2.5 mg/L of iron for Fe^{2+} or Fe^{3+}/solar; 2.5/5 mg/L of Fe^{2+} or Fe^{3+}/H_2O_2 for solar photo-Fenton and 10 mg/L of H_2O_2 for H_2O_2/solar process. The

inactivation profiles of *E. coli* O157:H7 and *S. enteritidis* by all the solar processes are shown in Figure 4.3 (a) and (b), respectively.

Regarding the disinfection efficiency of the solar processes tested, in general, no significant differences in treatment times and kinetic rate constants were observed for both pathogens. Detection limit from an initial concentration ca. 10^6 CFU/mL (6-LRV) was achieved in all cases in less than 45 min of solar treatment. Nevertheless, the best inactivation results were obtained with H_2O_2/solar process. In this case, inactivation kinetic constants of *E. coli* O157:H7 (*k*: 0.40±0.04 min^{-1}) and *S. enteritidis* (*k*: 0.20±0.02 min^{-1}) were higher compared to those obtained by the mere effect of solar radiation (*E. coli* O157:H7; *k*: 0.23±0.03 min^{-1} and *S. enteritidis*; *k*: 0.13±0.02 min^{-1}). Although, in terms of treatment time, only 8 minutes of difference at the DL were observed between both solar processes.

Comparing these results with the inactivation profiles with Fe/solar and solar photo-Fenton treatment with both Fe^{2+} and Fe^{3+}, it is clearly observed a no enhancement on the bacterial inactivation kinetics and even more, a slight increase in the inactivation times compared to solar photo-inactivation was obtained.

It is very well known that the disinfection efficiency depends, among other parameters, on the nature of each microorganism [Giannakis *et al.*, 2016a]. In line with this, it can also highlights that from the inactivation kinetics obtained by all solar processes, *S. enteritidis* showed a higher resistance to be inactivated in comparison with *E. coli* O157:H7 considering the treatment time required to reach a similar level of log-concentration reduction. This behaviour is in agreement with other reported works [Berney *et al.*, 2006; Evison, 1988] and can be explained by different responses of each microorganism to the oxidative stress generated by each particular solar process investigated in this study which will be deeply discussed in the next sub-sections.
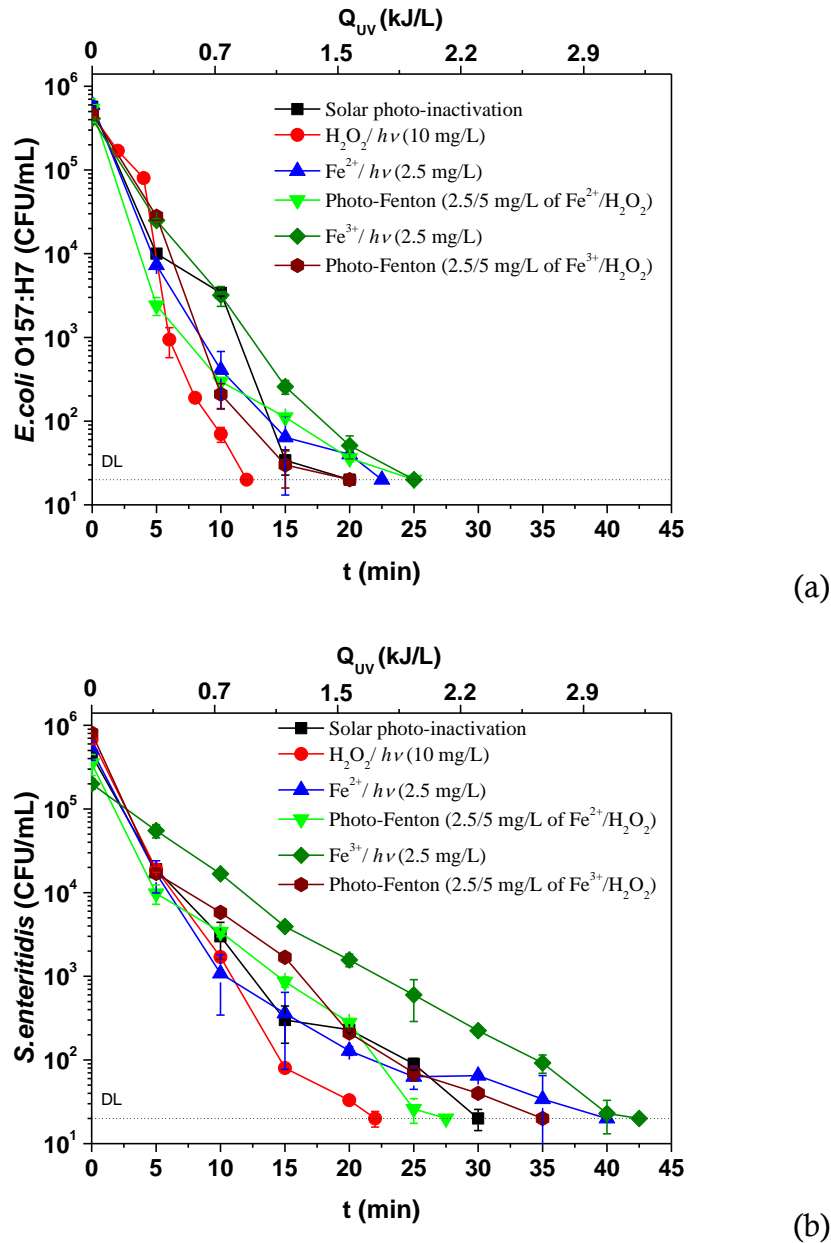
Figure 4.3. *E. coli* O157:H7 (a) and *S. enteritidis* (b) inactivation by H_2O_2/solar, solar photo-Fenton and photo-assisted processes under a constant solar UVA-irradiance of 30 W/m^2. (Solar simulator).

4.2.1. Photo-inactivation process

The inactivation of bacteria by the synergistic effect of solar radiation in the UV range and the water temperature is very well known. The solar radiation reach the Earth surface with a distribution of around 97 % of UVA and a 3 % of UVB. Therefore the bacterial injuries are provoked by both solar radiation ranges,

although mainly by the major one (UVA). The damage pathways provoked inside bacterial cells are summarized as follow:

The shortest wavelengths of UVB range slightly overlap with the DNA absorption spectrum and therefore may damage it. The main DNA alterations generated by UVB light are: the formation of dimers (cyclobutane pyrimidine dimers (CPDs) and pyrimidine-pyrimidone dimers) and cytosine and purine photoproducts [Giannakis *et al.,* 2016a]. Moreover, some proteins and siderophores also suffer alterations by absorption of UVB radiation.

In the case of UVA, although its UV range can also damage the DNA directly, the bacterial damages and inactivation are mainly provoked by indirect pathways. In general, these indirect pathways consist on the generation of Reactive Oxygen Species (ROS) through intracellular reduction-oxidation processes in the presence of oxygen and initiate by light absorption of bacterial chromophores. The ROS are generated by two types of reactions:

• Type I Reactions, based on the generation of superoxide radicals ($O_2^{\bullet-}$) by one-electron oxidation processes which DNA bases as electron donors.

• Type II reactions, formation of singlet oxygen ($^1O_2$) and conversion of DNA bases in unstable stereoisomers.

These oxidative species (ROS) are considered the main responsible of solar inactivation due to induce several damages in vital components as DNA, proteins oxidation (especially proteins of respiration process), lipids and enzymes among others [Goodsell, 2001]. Although the generation of ROS is accelerated by solar radiation, these species are naturally generated in bacterial metabolic processes and therefore defence mechanisms against ROS are present in bacterial cells. The most important cellular defence mechanisms against oxidative stress are the scavenger action of specific enzymes and the expression and activation of several genes and proteins. The key enzymes against oxidative stress are the superoxide dismutase (SOD) and catalase (CAT) which act in the decomposition of $O_2^{\bullet-}$ and H_2O_2, respectively. Nevertheless, these enzymes can be also damaged

by solar radiation generating an important alteration in bacterial defence and therefore increasing the oxidative damage by the ROS generated [Castro-Alférez *et al.,* 2017].

Among the different genes and proteins responsible of the oxidative defence in the solar inactivation process stand out the RNA polymerase sigma factor (*RpoS*) and the *SoxRS* proteins. The *SoxRS* proteins regulate the main cellular defence against the intracellular superoxide radicals and *RpoS* is the regulator of the stationary phase and the general stress response which help the bacterial cell adaptation to adverse conditions as oxidative stress or bacterial nutrient deprived state, among other. One important action of this regulator in the stationary phase is the induction of the *sodC*, which encodes the periplasmic SOD.

In this regard, although both strains are closely related bacteria, i.e., gram-negative, facultative anaerobic, rod-shaped, non-forming spores, and motile, they clearly showed phenotypic differences which are attributed to genetic divergences. As an example, Winfield and Groisman (2004) reported that the difference between *S. enterica* and *E. coli* in their resistance to the antibiotic polymyxin B relies on the divergence ability to produce Lipopolysaccharides (LPS) modifications in their cell wall. This divergence is associated with the differential regulation of homologous genes *PmrA-PmrB* [Winfield and Groisman, 2004]. Moreover, the higher resistance of *Salmonella* has been also correlated with the differential survival of these two enteric species in a host and non-host environments. In general, *Salmonella spp*. shows a high survival rate in clean water and soil (nutrient-poor/non-host environments) meanwhile *E. coli* has a net negative growth rate in these environments [Winfield and Groisman, 2003]. More specifically for radiation effects, some studies suggest that the gene *RpoS* which controls the expression of genes involved in the prevention of oxidative damage can be relevant in the photodynamic action of the radiation in *S. typhimurium*. However, this aspect is not clear today and to understand the sunlight response of *Salmonella spp*. it is necessary to investigate deeply the influence of other related genes [Oppezzo *et al.*, 2011].

4.2.2. H₂O₂/solar process

The disinfection enhancement observed by the presence of H_2O_2 compared to solar photo-inactivation process is attributed to a synergistic effect between the visible light effects mentioned above and the photo-Fenton internal cell reactions, which end in the cell death [Polo-López *et al.*, 2013]. The H_2O_2 can passively diffuse across the bacterial cell (small size and uncharged molecule) increasing its cytoplasmic concentration and reaching toxic levels. The potential toxic effects of mM concentrations of H_2O_2 can be explained by its oxidative power that can affect the outer bacterial membrane changing it permeability, and mainly, due to it is the precursor of other species with higher oxidant power (mainly HO˙) which disrupt the catabolic and biosynthesis functions of bacterial cells.

The toxic effects of high cellular H_2O_2 concentrations can be scavenge based on the action of peroxidases and catalases which acts in function of the H_2O_2 concentration. The alkyl hydroperoxide reductase (*Ahp*) is the primary H_2O_2 scavenger which function permit maintains intracellular concentrations below 0.1 μM, above this concentration the enzyme is saturated and the *OxyR* protein is activated expressing the genes that induce the catalase activity (*katG* and *katE*) [Imlay and Hassett, 2011].

On the other hand, the high H_2O_2 concentration combined with the solar light action provides conditions for the generation of HO˙ by internal photo-Fenton reactions, for which the bacteria do not have any scavenger system and therefore this process is the main responsible of the final bacteria inactivation.

The cytoplasmic iron release from iron containing biomolecules represents the main source of the intracellular iron involved in the mentioned photo-Fenton reactions. The iron releases ways into the cell can be by direct (H_2O_2) or indirect oxidation (mediated by ROS or UVA light) of iron contain compounds. The oxidation of the ferric uptake regulator (complex Fe^{2+}/Fur) by H_2O_2 increase the import of iron and represent the main source of iron by direct oxidation

[Varghese *et al.*, 2007]. For the iron release by indirect oxidation, UVA light are able to degrade storage substances of "free iron" as ferritin and ferritin-like substances and the superoxide radicals generated by the UVA action oxidize Fe/S clusters of Dehydratases releasing iron and additional H_2O_2 molecules [Giannakis *et al.*, 2016a].

In response to certain oxidative stress caused by the dose of H_2O_2, it has been reported different regulation of oxidative stress-inducible genes in *S. typhimurium* and *E. coli* as well as different related-proteins like:

i)   The so-called peroxide stimulon (including locus *Oxy-R* and *Oxy-R* regulon) includes eight proteins in *E. coli* and at least nine proteins in *S. typhimurium* [Farr and Kogoma, 1991; Christman *et al.*, 1985].

ii) A moderate induction level of the enzyme Mn-containing SOD in *S. typhimurium* with H_2O_2, while no significant induction in *E. coli* has been reported [Touati, 1988].

iii) The *ahpF* gene is induced by heat shock in an *OxyR*-dependent mode in *S. typhimurium*, whereas this gene cannot be induced by heat in *E. coli*, suggesting that the gene in *S. typhimurium* has a cis-acting heat shock element that is not present in *E. coli* [Storz *et al.*, 1989].

All these differences demonstrated that both strains have different responses to the same oxidative stress and it may also help to explain the different inactivation resistance between both types of bacteria to the same oxidative stress (solar process), supporting the higher resistance of *S. enteritidis* observed compare to *E. coli* O157: H7.

4.2.3. Fe/solar and solar photo-Fenton processes

It is widely accepted that the bactericidal power of the solar photo-inactivation process can be also enhanced by the combination with only iron salts. About the inactivation mechanism, it is different depending of the iron oxidation state and a combination of both mechanisms is accepted. For the Fe^{2+}, the inactivation

mechanism is based on internal oxidative damages due to the Fe^{2+} is able to diffuse into bacteria cell generating ROS by Fenton and photo-Fenton reactions. As for the H_2O_2 solar process, the ROS generated by the photocatalytic reactions produced additional oxidative damages improving the inactivation kinetic of the solar photo-inactivation process. Whereas for the Fe^{3+}, the inactivation mechanism is based on external oxidative damages. The Fe^{3+} in solution or in suspension can interact with macromolecules of the microorganism surface using the bacterial membrane as a ligand and generating iron-bacteria aggregates. As Fe^{3+} can be reduced by fast electron transfer processes to Fe^{2+}, the iron-bacteria aggregates formed are exciplexes which can act as a photosensitizer. Therefore, under solar irradiation an electronic transition from the ligand (microorganism surface) to the ferric iron (ligand-to-metal charge-transfer, LMCT) can occur leading to iron reduction and ligand oxidation [Spuhler *et al.*, 2010]. This reduction process may contribute to the bacterial inactivation by direct oxidation of the membrane constituents (ligand in the process) or by indirect oxidation through the generation of ROS near to the cell wall [Ruales-Lonfat *et al.*, 2014].

Regarding solar photo-Fenton process, the inactivation mechanism of this process is based on external cell membrane degradation by the high quantity of $HO^\bullet$ generated in the very well-known photo-catalytic cycle [Giannakis *et al.*, 2016a]. Nevertheless, although the bacterial membrane oxidation by the external homogenous process are the main responsible of the inactivation, all the internal and external oxidative damages explained previously for solar photo inactivation process alone and in combination with H_2O_2 or iron salts are also responsible of the microorganism inactivation. Therefore, the bacterial inactivation mechanism by solar photo-Fenton process can be defined as a complex combination between internal and external bacterial components oxidation by ROS generated through diverse chemical and bio-chemical reactions.

In spite of the high oxidation power of Fe/solar and solar photo-Fenton process, the results obtained in Figure 4.3 revealed a very low disinfection capability of both processes at the selected operational conditions. These results may be explained by several reasons:

i) The low oxidative conditions as very low amounts of reagents were used.

ii) The near neutral pH of SFCWW, which, as is widely explained in Section 1.6.2.2., strongly affects the speciation of iron in water, being the most important limitation factor on the photo-Fenton efficiency due to the iron precipitates formed (oxyhydroxides) have much less photocatalytic activity compared with the same concentration of iron in solution [Pignatello *et al.*, 2006]. In these experimental conditions, dissolved iron measured at the beginning of the photo-Fenton process was almost one fifth (0.48 mg/L) than the iron initially added (2.5 mg/L).

iii) The turbid effect of the iron precipitated may result in a worse light penetration in the sample hinders the disinfection processes based mainly on solar radiation effects.

iv) The presence of organic matter in SFCWW (DOC: 25 mg/L) that can act as scavengers of the possible $HO^•$ generated during the photo-Fenton process, and therefore, the competition between bacteria and DOC for radicals may also limit or reduce the inactivation efficiency.

For all these reasons, the efficiency of solar photo-Fenton and Fe/solar was lower compared to H_2O_2/solar, and therefore, the H_2O_2/solar process has demonstrated to be a promising option to disinfect SFCWW.

4.3. Kinetic analysis of parameters influence in H_2O_2/solar process: oxidant concentration and UV irradiance

The inactivation of the two target pathogens (*E. coli* O157:H7 and *S. enteritidis*) by solar photo-inactivation and H_2O_2/solar process at five levels of solar UVA-irradiances (10, 20, 30, 40 and 50 W/m^2) and three H_2O_2 concentrations (5, 10 and 20 mg/L) was deeply studied in SFCWW. The H_2O_2 concentrations selected did not affect the bacteria viability in dark (Dark controls, Section 3.1.1.1),

demonstrating that the bacterial inactivation obtained under solar radiation can only be attributed to the effect of the solar processes investigated.
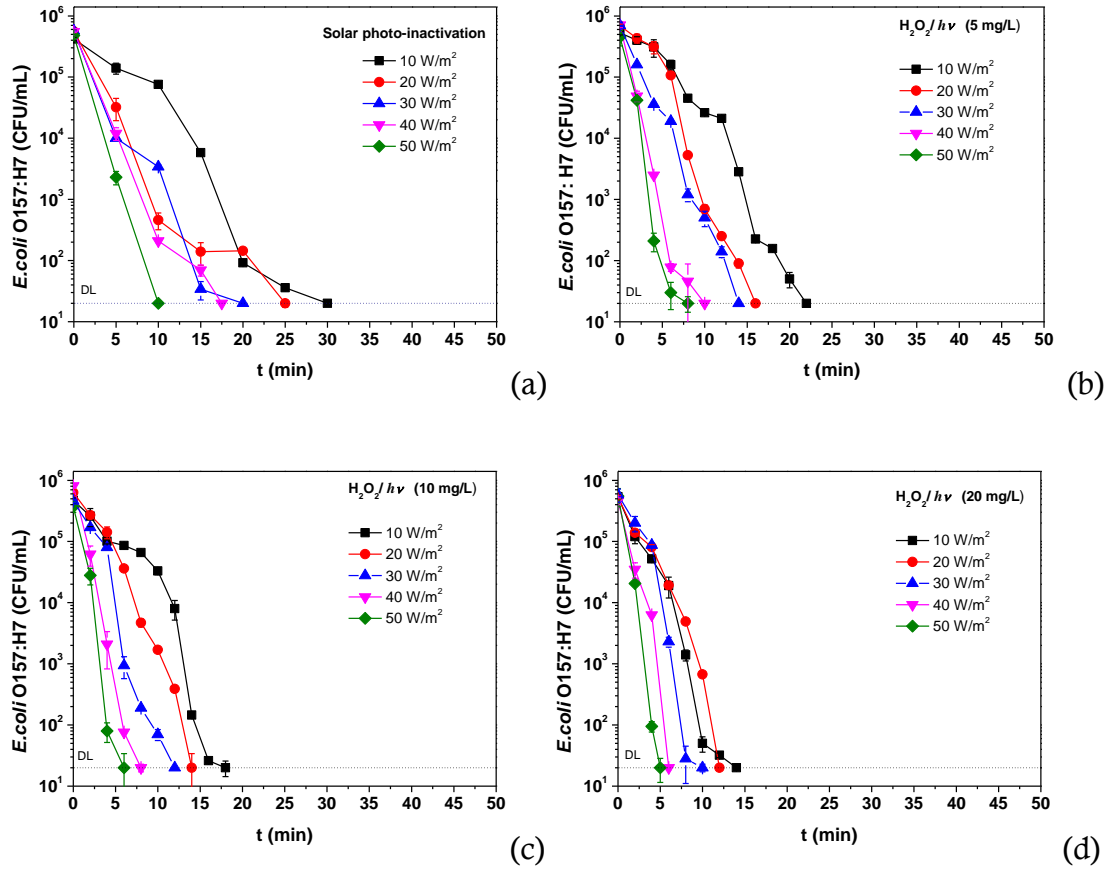
Figure 4.4. *E. coli* O157:H7 abatement by solar photo-inactivation (a) and H_2O_2/solar with 5 mg/L (b), 10 mg/L (c) and 20 mg/L (d) of H_2O_2 at several solar UV- irradiances. (Solar simulator).

Figures 4.4 and 4.5 show the inactivation results obtained in all the experimental conditions tested for *E. coli* O157:H7 and *S. enteritidis*, respectively. Results showed that the inactivation times of *E. coli* O157:H7 were slightly affected by increasing H_2O_2 concentrations (from 5 to 20 mg/L) and/or solar UVA-irradiance. This result agrees with other works reported in literature, where the increase of the oxidative conditions generates faster microorganisms inactivation [Ubomba-Jaswa *et al.*, 2009; Fisher *et al.*, 2007]. In line with this, best inactivation results were obtained with 20 mg/L of H_2O_2, where detection limit (20 CFU/mL) was attained in less than 15 min of solar treatment.
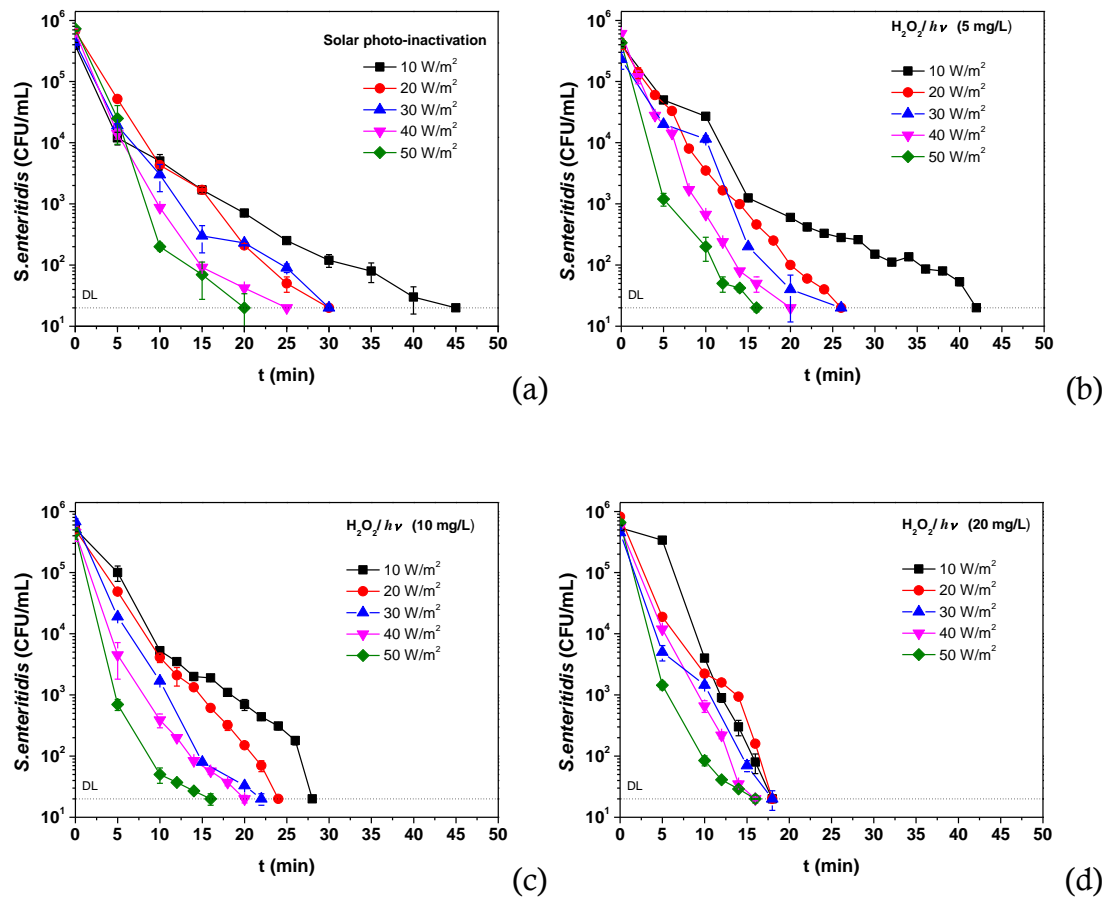
Figure 4.5. *S. enteritidis* abatement by solar photo-inactivation (a) and H_2O_2/solar with 5 mg/L (b), 10 mg/L (c) and 20 mg/L (d) of H_2O_2 at several solar UV-irradiances. (Solar simulator).

The inactivation results obtained for *S. enteritidis* are shown in Figure 4.5 with a similar behaviour observed for *E. coli* O157:H7, i.e., the higher the H_2O_2 concentration, the higher the inactivation rate. In this case, best inactivation results were also obtained with 20 mg/L of oxidant, although detection limit was achieved in a few mins more of solar exposure (less than 20 min). These results also confirm, as was observed previously, the higher resistance of *S. enteritidis* compared to *E. coli* O157:H7 to be inactivated by this solar process.

Table 4.2. Kinetic constants of *E. coli* O157:H7 abatement by solar photo-inactivation (0 mg/L of H_2O_2) and H_2O_2/solar at several solar irradiances. (Solar simulator).

Irradiance	0 mg/L-H_2O_2		5 mg/L-H_2O_2		10 mg/L-H_2O_2		20 mg/L-H_2O_2	
	k (min^{-1})	R^2	k (min^{-1})	R^2	k (min^{-1})	R^2	k (min^{-1})	R^2
10 W/m^2	0.16±0.02	0.94	0.22±0.02	0.95	0.26±0.03	0.87	0.35±0.03	0.95
20 W/m^2	0.17±0.03	0.89	0.31±0.02	0.96	0.31±0.02	0.96	0.34±0.04	0.93
30 W/m^2	0.23±0.03	0.94	0.32±0.01	0.98	0.40±0.04	0.95	0.51±0.07	0.93
40 W/m^2	0.25±0.03	0.95	0.48±0.06	0.93	0.61±0.04	0.98	0.69±0.13	0.93
50 W/m^2	0.44±0.01	0.99	0.59±0.10	0.91	0.77±0.13	0.94	0.92±0.07	0.98

The influence of H_2O_2 concentration as a function of solar UVA-irradiance on the inactivation kinetic rate was analyzed for each bacterial strain. The kinetic rates obtained for all the conditions tested are shown in Table 4.2 and Table 4.3 for *E. coli* O157:H7 and *S. enteritidis*, respectively. Table 4.2 shows that the *E. coli* O157:H7 inactivation rate constant, k, increased with solar UVA-intensity at each H_2O_2 concentration tested. Furthermore, this favourable effect of increasing irradiance was enhanced at higher H_2O_2 concentrations, as is clearly observed by the response surface analysis of the kinetic constants shown in Figure 4.6.

The analysis indicates that the *E. coli* O157:H7 inactivation by H_2O_2/solar process was both photo- and chemical- limited, meaning that the higher the irradiance and/or H_2O_2 concentration, the higher the inactivation rate.
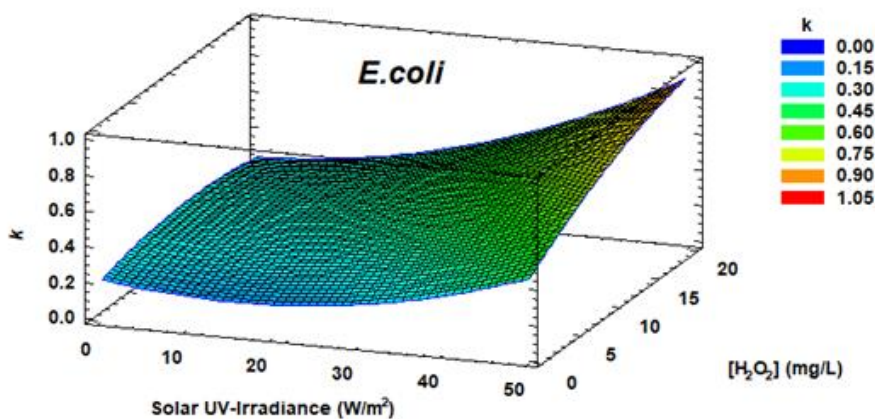
Figure 4.6. Response surface of *E. coli* O157:H7 inactivation kinetic rates (k) as a function of solar UV-irradiance and H_2O_2 concentration.

In the case of *S. enteriditis* (Table 4.3), the inactivation rate constant increases linearly with increase H_2O_2 concentration and/or solar UVA-irradiance but with no significant differences. In this case, the inactivation rate constant stabilizes around 0.26–0.28 min^{-1} suggesting that the inactivation efficiency did not increase with increased H_2O_2 concentration and/or solar UVA-irradiance once it has been achieved the optimal condition and no requiring higher oxidative conditions.

Table 4.3. Kinetic constants of *S. enteritidis* abatement by solar photo-inactivation (0 mg/L of H_2O_2) and H_2O_2/solar at several solar irradiances. (Solar simulator).

Irradiance	0 mg/L-H_2O_2		5 mg/L-H_2O_2		10 mg/L-H_2O_2		20 mg/L-H_2O_2	
	k (min^{-1})	R^2	k (min^{-1})	R^2	k (min^{-1})	R^2	k (min^{-1})	R^2
10 W/m²	0.08±0.01	0.92	0.09±0.01	0.92	0.14±0.01	0.95	0.24±0.01	0.99
20 W/m²	0.15±0.01	0.97	0.17±0.01	0.98	0.17±0.01	0.99	0.23±0.02	0.96
30 W/m²	0.13±0.02	0.93	0.17±0.02	0.94	0.20±0.02	0.96	0.23±0.02	0.96
40 W/m²	0.18±0.03	0.91	0.23±0.02	0.96	0.21±0.02	0.93	0.28±0.01	0.99
50 W/m²	0.23±0.04	0.92	0.26±0.04	0.91	0.26±0.05	0.86	0.28±0.04	0.90

This trend is also clearly observed by the response surface analysis of the kinetic constants shown in Figure 4.7, suggesting that S. *enteritidis* inactivation by H_2O_2/solar process wasn´t either photo- and/or chemically limited at high H_2O_2 concentrations and high solar UVA-irradiances, respectively.
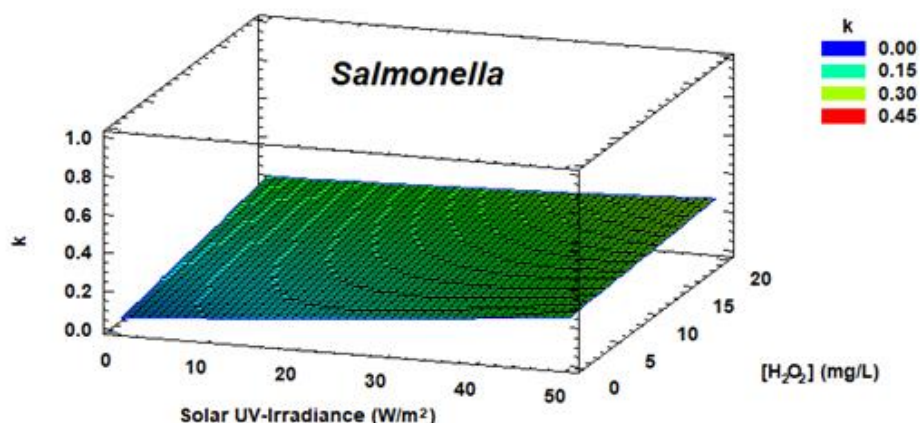
Figure 4.7. Response surface of *S. enteritidis* inactivation kinetic rates (k) as a function of solar UV-irradiance and H_2O_2 concentration.

These results show that H_2O_2/solar process represents a good alternative to disinfect fresh cut wastewater. To save cost of operation, this process may be also adjusted to reach an effective disinfection level (> 5 LRV or < 20 CFU/mL) varying the amount of H_2O_2 added considering the level of solar UVA-irradiance (seasonal fluctuation of solar UVA-intensity): 10 mg/L of H_2O_2 at high solar UVA-irradiance (>30 W/m²) or 20 mg/L at low solar UVA-irradiance (<30 W/m²).

4.4. Conclusions of Chapter 4

A synthetic fresh-cut wastewater recipe was developed taking into account the physical and chemical characterization of real fresh cut wastewater samples.

The capability of the solar processes studied to disinfect SFCWW, which has high turbidity (100 NTU), has been demonstrated at laboratory scale and under controlled conditions of UV-irradiance with the abatement of >5-LRV of two human pathogenic bacteria in less than 1 h of solar treatment.

S. *enteritidis* showed higher resistance than *E. coli* O157:H7 to be inactivated by all the solar processes investigated.

The best inactivation kinetic rate has been obtained with H_2O_2/solar process for both *E. coli* O157:H7 and *S. enteritidis* in SFCWW compared with solar photo-Fenton, Fe/solar and solar photo-inactivation at near neutral pH using low reagents concentrations.

E. coli O157:H7 inactivation by H_2O_2/solar process was both photo- and chemical- limited, while the *S. enteritidis* inactivation was not limited at high H_2O_2 concentrations or high solar irradiances.

CHAPTER 5

IRON CHELATE (Fe^{3+}-EDDHA) FOR WATER DISINFECTION UNDER NATURAL SUNLIGHT

5. IRON CHELATE (Fe^{3+}-EDDHA) FOR WATER DISINFECTION UNDER NATURAL SUNLIGHT

In this chapter the use of a commercial iron fertilizer (Fe^{3+}-EDDHA) commonly used in intensive agriculture to remediate iron chlorosis has been evaluated for the first time as a bactericidal agent in solar water disinfection processes. Proof-of-principle was investigated in isotonic water (IW) and synthetic fresh-cut wastewater (SFCWW) at neutral pH and at laboratory scale (200 mL solar open reactor) under natural solar radiation. In addition, the photostability of the iron chelate as well as its capability to generate HO$^{\bullet}$ have been investigated in this chapter.

The comparative analysis of *E. coli* O157:H7 and *S. enteritidis* inactivation kinetics by Fe^{3+}-EDDHA/solar and Fe^{3+}-EDDHA/H$_2$O$_2$/solar with other very

well-known solar processes including solar photo-inactivation, H_2O_2/solar, Fe^{3+}/solar and traditional solar photo-Fenton process (Fe^{3+}/H_2O_2/solar) with iron salts has been carried in order to establish the suitability of the commercial fertilizer as alternative source of iron for wastewater disinfection using natural sunlight.

The experiments shown in this chapter started between 10:30−11:00 am local time lasting 4 h of solar exposure. Water temperature was monitored and ranged from 24.3±1.9 °C to 38.6±2 °C, discarding any thermal effect on bacterial inactivation. Water pH was 6.9±0.1 in all solar processes investigated in both IW and SFCWW. The initial water pH value remained constant along the treatment time. DOC concentration was measured at the beginning and at the end of each solar experiment. An increase of ≤ 2, 9 and 18 mg/L in the DOC concentration was observed by the addition of 0.5, 2.5 and 5 mg/L of Fe^{3+}-EDDHA, respectively. Nevertheless, in any case, the initial DOC values in IW (only supplied by Fe^{3+}-EDDHA) neither in SFCWW showed any change along the treatment time. Solar UV radiation was measured, and it ranged from 25.9±1.7 to 47±5.7 W/m² along the experimental time.

5.1. Photostability analysis of Fe³⁺-EDDHA in water

The concentration of fertilizer selected to analyze the photostability was 100 mg/L according to the data provided by the manufacturer which contains a maximum iron concentration of ≈7 % and chelate iron of ≈6.2 %. A physic-chemical characterization of this solution, including the quantification of iron content was performed. Data obtained are shown in Table 5.1. The iron analysis results showed a total iron content of 7.5 mg/L and 6.2 mg/L in solution, i.e., as Fe^{3+}-EDDHA. These results were in concordance with the commercial data provided by the manufacturer.

In the dark, the fertilizer solution alone and in the presence of H_2O_2 did not show any significant change on both parameters. Under irradiance, the UV–vis

spectrum of the commercial fertilizer solution alone and with H_2O_2 (at Fe/H_2O_2 concentration ratio of 1:2) is shown in Figure 5.1.

Table 5.1. Physic-chemical characteristic of Fe^{3+}-EDDHA in solution at 6.2 mg/L of chelate concentration.

Parameter	Initial values
DOC	27.8 mg/L
Turbidity	5.7 NTU
pH	7.3
Conductivity	73 μS/cm
Ionic composition (mg/L)	
NO_3^-	0.2
Cl^-	17
SO_4^{2-}	0.4
Na^+	14
K^+	0.2
Glycolate	0.2
Formiate	0.2
Trimethylamine	0.2
Oxalate	0.1
Dissolved Fe	6.2

The photo-stability of this Fe^{3+}-EDDHA solution (6.2 mg/L) was investigated by following the concentration of dissolved iron ([Fe]$_{ds}$) and the UV–vis absorbance spectrum at 0, 60, 120 and 180 min in the dark and exposure to 30 W/m^2 of constant UVA irradiance with and without H_2O_2 in the solar simulator.

In general, with and without H_2O_2, at time 0 min, the UV–vis spectrum of the iron chelate solution exhibits the typical ligand absorptions bands around 200 nm (benzene ring), 281 nm (ortho substitution in the ring) and 482 nm (Fe-phenolate bond) [Gómez-Gallego *et al.*, 2002]. Throughout irradiance time, the ligand peaks absorbance (200 and 281 nm) increases whereas the peak corresponding to Fe-ligand binding (482 nm) decreases; even in the presence of H_2O_2 this last peak suffers a hypsochromic shift of 4 nm (varying from 482 to 478 nm). These changes are attributed to the decomposition mechanisms (deferration process) of the iron chelate, where the photoexcitation of the complex generates a redox reaction by a single electron transfer from one carboxylate group of the ligand to the Fe^{3+}. This leads the reduction of Fe^{3+} to Fe^{2+} and the formation of carboxylate radical cation species that generate photo-fragmentation products,

ending in the formation of Fe^{2+} and the partially decomposed organic ligands. In addition, the $[Fe]_{ds}$ measured supports this affirmation as it decreased 15 % and 24.8 % after 180 min of irradiation for iron chelate solution alone and with H_2O_2, respectively. This behaviour agrees with previous studies reporting the photosensitivity of Fe^{3+}-EDDHA [Hernández-Apaolaza *et al.,* 2011]. On the other hand, the shift of the Fe-phenolate band can be attributed to the photodegradation of the less stable diastereoisomer (meso) present in the fertilizer [García-Marco *et al.,* 2006; Laghi *et al.*, 2009].
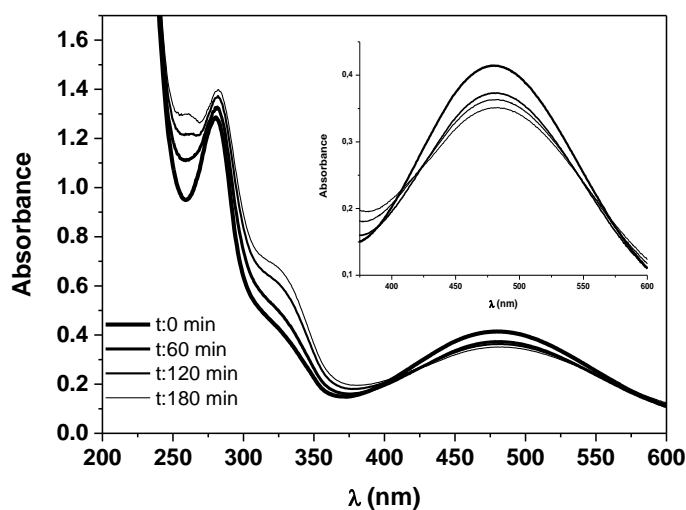
(a)
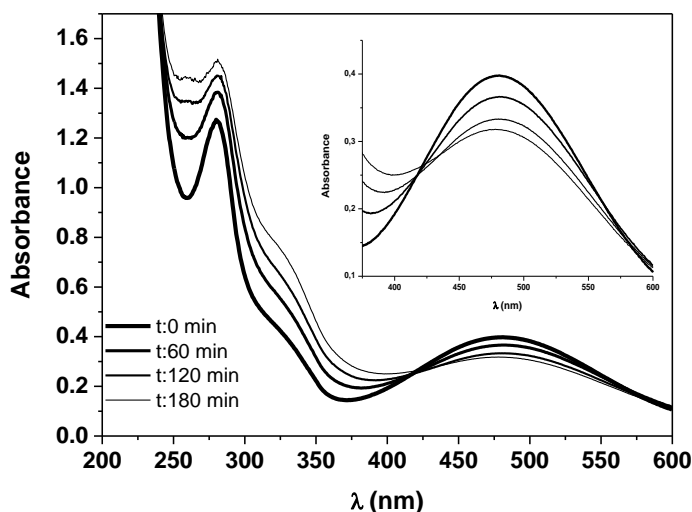
(b)

Figure 5.1. Absorbance spectrums of Fe^{3+}-EDDHA (a) and Fe^{3+}-EDDHA/H_2O_2 (b) exposure for 180 min at 30 W/m² of solar irradiance in the solar simulator. Insert graphs shown an extended view of the absorbance spectrum in the range 400–600 nm.

5.2. Bacterial inactivation by solar photo-inactivation, Fe^{3+}/solar and Fe^{3+}-EDDHA/solar

Prior to solar experiments, dark tests were performed to determine the effect of the reagents used in this chapter, Fe^{3+}-EDDHA or Fe^{3+} and H_2O_2 on the viability of both bacteria. Results obtained with the highest reagent combination, i.e., 5 mg/L of iron (for both sources) and 10 mg/L of H_2O_2 did not show any effect on the bacterial viability as bacteria concentration remained constant (ca. 10^6 CFU/mL) during 3 hours.

5.2.1. Isotonic water

The inactivation profiles and kinetic rate constants of *E. coli* O157:H7 and *S. enteritidis* by solar photo-inactivation alone, Fe^{3+} from iron salt (Fe^{3+}/solar) and the commercial fertilizer (Fe^{3+}-EDDHA/solar) under natural solar radiation in IW are shown in Figure 5.2 and Table 5.2. The iron concentrations investigated were: 0.5, 2.5 and 5 mg/L.

Best bacterial inactivation rate was obtained with 0.5 mg/L of Fe^{3+}-EDDHA/solar. DL was achieved with a solar UVA-Dose of 25.5 and 21.3 Wh/m² (35 and 30 min of treatment time) and an energy of 2.70 and 2.22 kJ/L, for *E. coli* O157:H7 and *S. enteritidis*, respectively, which means a two and four times reduction compared to solar photo-inactivation (*E. coli*: 75 min, 59.3 Wh/m² and 4.63 kJ/L; *S. enteritidis*: 120 min, 96.4 Wh/m² and 6.37 kJ/L).
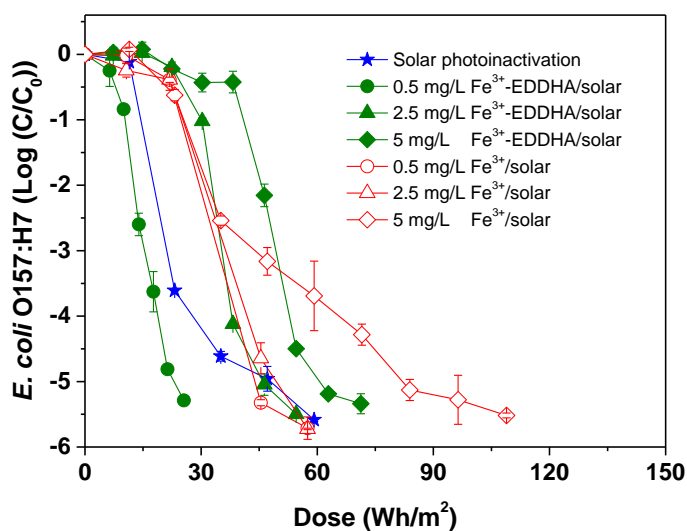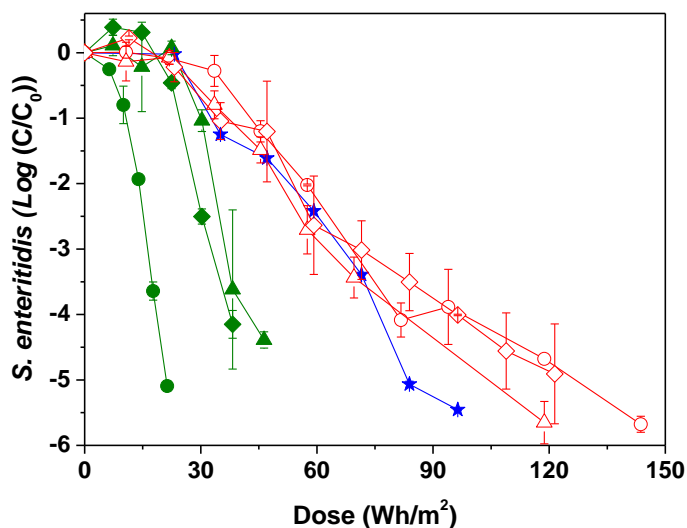
Figure 5.2. *E. coli* O157:H7 (a) and *S. enteritidis* (b) inactivation by Fe^{3+}-EDDHA/solar and Fe^{3+}/solar in IW under natural sunlight in 200-mL solar reactor.

The inactivation profiles of both bacteria showed a similar trend regarding to the following conditions: i) at same iron concentration tested, the use of chelated iron reached faster inactivation kinetics compared with traditional iron salt and ii) the higher the Fe^{3+} concentration added to the sample, the slower the bacterial inactivation, showing a marked limitation compared with solar photo-inactivation process.

Table 5.2. Inactivation kinetic constants of both pathogens for all the experimental conditions studied in 200-mL solar reactor under natural sunlight.

Treatment	Fe^{3+}:H_2O_2 (mg/L)	*E. coli* O157:H7				*S. enteritidis*			
		k (min⁻¹)	R^2	t_{lag} * (min)	Dose (Wh/m²)	k (min⁻¹)	R^2	t_{lag} * (min⁻¹)	Dose (Wh/m²)
Fig. 5.2a/2b IW									
photo-inactivation	-	0.150±0.050	0.907	15	59.3	0.061±0.004	0.979	30	96.4
Fe³⁺-EDDHA/ solar	0.5	0.218±0.016	0.978	10	25.5	0.250±0.026	0.970	10	21.3
	2.5	0.146±0.025	0.918	30	54.5	0.160±0.024	0.957	30	46.3
	5	0.166±0.023	0.963	50	71.3	0.154±0.018	0.972	20	38.2
Fe³⁺/solar	0.5	0.109±0.020	0.939	15	57.5	0.039±0.004	0.939	45	143.7
	2.5	0.122±0.017	0.982	30	57.5	0.048±0.003	0.984	30	118.7
	5	0.047±0.005	0.936	15	108.9	0.038±0.002	0.981	15	121.4
Fig. 5.3a/3b SFCCW									
photo-inactivation	-	0.077±0.005	0.995	60	89.7	0.033±0.004	0.964	60	169.9
Fe³⁺-EDDHA/ solar	0.5	0.060±0.008	0.925	40	90.9	0.040±0.005	0.885	-	116.4
	2.5	0.058±0.011	0.929	30	90.9	0.033±0.004	0.893	-	116.4
	5	0.034±0.006	0.925	30	142.8	0.021±0.002	0.955	30	195.7
Fe³⁺/solar	0.5	0.066±0.009	0.968	30	71.2	0.025±0.002	0.947	-	137.4
	2.5	0.051±0.006	0.964	30	92.5	0.031±0.005	0.906	60	160.6
	5	0.043±0.007	0.901	-	92.5	0.017±0.002	0.904	-	205.5
Fig. 5.4a/4b IW									
H₂O₂/solar	1	0.133±0.025	0.906	10	39.4	0.060±0.007	0.927	20	81.6
	5	0.176±0.016	0.983	10	17.9	0.081±0.010	0.932	-	28.2
	10	0.122±0.007	0.991	-	19.0	0.089±0.006	0.976	-	29.8
Fe³⁺-EDDHA/ H₂O₂/solar	0.5:1	0.205±0.022	0.957	5	23.0	0.136±0.021	0.895	-	23.0
	2.5:5	0.176±0.043	0.892	-	23.2	0.166±0.033	0.928	-	23.2
	5:10	0.273±0.027	0.972	10	23.2	0.364±0.051	0.963	10	19.2
Fe³⁺/H₂O₂/ solar	0.5:1	0.079±0.009	0.950	-	57.5	0.064±0.004	0.977	15	81.7
	2.5:5	0.060±0.007	0.929	-	69.6	0.049±0.006	0.916	-	93.9
	5:10	0.098±0.012	0.956	-	47.1	0.064±0.005	0.965	-	71.5
Fig. 5.5a/5b SFCCW									
H₂O₂/solar	1	0.091±0.011	0.959	-	41.1	0.041±0.004	0.959	-	89.7
	5	0.122±0.017	0.962	-	30.1	0.070±0.006	0.987	30	64.6
	10	0.118±0.009	0.989	-	30.1	0.056±0.006	0.961	-	64.6
Fe³⁺-EDDHA/ H₂O₂/solar	0.5:1	0.086±0.020	0.947	30	66.1	0.083±0.017	0.959	-	42.5
	2.5:5	0.173±0.011	0.996	15	31.1	0.150±0.033	0.953	15	31.1
	5:10	0.171±0.022	0.984	15	30.1	0.106±0.006	0.993	-	30.1
Fe³⁺/H₂O₂/ solar	0.5:1	0.107±0.009	0.992	30	53.3	0.053±0.010	0.910	-	65.4
	2.5:5	0.073±0.010	0.960	-	53.3	0.067±0.001	0.999	30	65.3
	5:10	0.069±0.005	0.991	-	53.3	0.052±0.006	0.955	-	65.3

*Values of k and t_{lag} correspond to data fitted to Model 2 (Chapter 3, section 3.13).

These observations can be explained simultaneously by the amount of dissolved iron concentration ($[Fe]_{ds}$) remained in the water in both processes which is shown in Table 5.3. At the end of the solar process, the $[Fe]_{ds}$ was in all cases <0.1 mg/L; meanwhile, for Fe³⁺-EDDHA/solar process the 50, 62 and 82 % of the initial added iron was kept dissolved for 0.5, 2.5 and 5 mg/L, respectively.

It is widely accepted that the combination of solar radiation with ferric iron can increase the inactivation rate through the formation of exciplexes between Fe³⁺

and some organic compounds of the cell wall, which may contribute to the bacterial inactivation by direct oxidation of the membrane constituents or indirect oxidation by the generation of Fe^{2+}, H_2O_2 and $HO^{\bullet}$ near to the cell wall [Giannakis *et al.*, 2016a].

Table 5.3. Dissolved iron ($[Fe]_{ds}$) and H_2O_2 concentrations for all the experimental conditions studied in 200-mL solar reactor under natural sunlight.

Treatment	$[Fe^{3+}:H_2O_2]$ (mg/L)	$[Fe^{3+}]_i$ (mg/L)	$[Fe^{3+}]_f$ (mg/L)	% Fe dissolved	$[H_2O_2]_i$ (mg/L)	$[H_2O_2]_f$ (mg/L)	% H_2O_2 decomposed
Fig. 5.2 (a)/(b) IW							
Fe³⁺-EDDHA/solar	0.5	0.5	0.25	50	-	-	-
	2.5	2.5	1.54	62	-	-	-
	5	5	4.12	82	-	-	-
Fe³⁺/solar	0.5	0.5	Nd	0	-	-	-
	2.5	2.5	Nd	0	-	-	-
	5	5	Nd	0	-	-	-
Fig. 5.3 (a)/(b) SFCCW							
Fe³⁺-EDDHA/solar	0.5	0.5	0.19	38	-	-	-
	2.5	2.5	1.46	58	-	-	-
	5	5	4.66	93	-	-	-
Fe³⁺/solar	0.5	0.5	Nd	0	-	-	-
	2.5	2.5	Nd	0	-	-	-
	5	5	Nd	0	-	-	-
Fig. 5.4 (a)/(b) IW							
H₂O₂/solar	1	-	-	-	1	0.97	3
	5	-	-	-	5	4.78	4
	10	-	-	-	10	9.49	5
Fe³⁺-EDDHA/ H₂O₂/solar	0.5:1	0.5	0.47	94	1	0.56	44
	2.5:5	2.5	1.28	51	5	2.90	42
	5:10	5	4.41	88	10	7.10	29
Fe³⁺/H₂O₂/solar	0.5:1	0.5	Nd	0	1	0.85	15
	2.5:5	2.5	Nd	0	5	4.16	17
	5:10	5	Nd	0	10	9	10
Fig. 5.5 (a)/(b) SFCCW							
H₂O₂/solar	1	-	-	-	1	0.73	27
	5	-	-	-	5	3.40	32
	10	-	-	-	10	7.26	27
Fe³⁺-EDDHA/ H₂O₂/solar	0.5:1	0.5	0.23	46	1	0.06	94
	2.5:5	2.5	1.48	59	5	2.46	51
	5:10	5	3.32	66	10	5.46	45
Fe³⁺/H₂O₂/solar	0.5:1	0.5	Nd	0	1	0.86	14
	2.5:5	2.5	Nd	0	5	4.61	8
	5:10	5	Nd	0	10	9.70	3

Nd: non-detected; - No presence

Nevertheless, this inactivation enhancement was not observed in the case of Fe^{3+}/solar process for both pathogens. This effect may be explained by the absence of dissolved iron in solution. In addition, although there is some controversy about the activity of iron oxyhydroxides for bacterial disinfection [Rodríguez-Chueca *et al.,* 2014], in our experimental conditions and reagent´s concentrations it is possible that the precipitated iron reduced the light

penetration and acted as a protective screen for bacteria against solar photons, limiting therefore the bacterial inactivation [Giannakis *et al.*, 2016a].

5.2.2. Synthetic fresh-cut wastewater

Figure 5.3 shows the inactivation of *E. coli* O157:H7 and *S. enteritidis* in SFCWW by solar photo-inactivation, Fe^{3+}/solar and Fe^{3+}-EDDHA/solar. In this case, solar UVA-dose and treatment time required to achieve the DL was higher for both pathogens compared to inactivation results in IW, which is attributed to the presence of organic matter (25 mg/L of DOC) and turbidity (100 NTU), conditions that limit or reduce the efficiency in photo-disinfection processes and reinforce the need to investigate the efficiency of these processes under near real conditions. Regarding $[Fe]_{ds}$, a similar behaviour was observed in SFCWW compared to IW (Table 5.3).

The inactivation kinetics of *E. coli* (Figure 5.3 (a)), did not show a significant enhancement for all the processes and conditions tested regarding solar photo-inactivation. Nevertheless, *S. enteritidis* results (Figure 5.3 (b)) showed that inactivation by Fe^{3+}-EDDHA/solar process (0.5 mg/L) was significantly faster than Fe^{3+}/solar and solar photo-inactivation, which suggest a different susceptibility between both bacteria against Fe^{3+}-EDDHA. This different response on the inactivation resistance between both bacteria can be explained by structural differences which could play a role in the inactivation mechanism. This aspect will be deeply discussed in the next sections where it is proposed the inactivation mechanisms by Fe^{3+}-EDDHA.
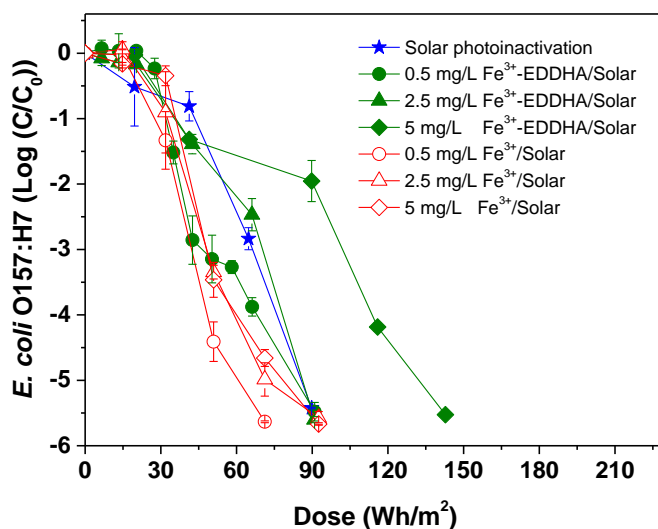
(a)
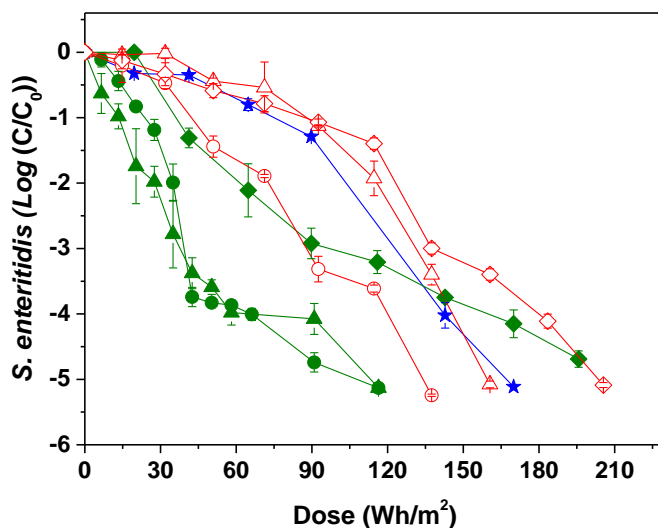
(b)

Figure 5.3. *E. coli* O157:H7 (a) and *S. enteritidis* (b) inactivation by Fe^{3+}-EDDHA/Solar and Fe^{3+}/solar in SFCWW under natural sunlight in 200-mL solar reactor.

5.3. Bacterial inactivation by Fe^{3+}-EDDHA/H_2O_2/solar, Fe^{3+}/H_2O_2/solar and H_2O_2/solar

5.3.1. Isotonic water

The comparative analysis of inactivation profiles and kinetics of both bacteria by Fe^{3+}-EDDHA/H_2O_2/solar, Fe^{3+}/H_2O_2/solar and H_2O_2/solar in IW are shown in Figure 5.4 and Table 5.2, respectively. The trend of inactivation regarding Fe^{3+}/H_2O_2/solar and Fe^{3+}-EDDHA/H_2O_2/solar was similar to the obtained in

Figure 5.2, but reaching DL with lower solar UVA-dose (or treatment time) and showing a marked decreased of the lag stage attributed to the presence of H_2O_2 (Table 5.2).

In fact, H_2O_2/solar was investigated herein in order to determine the effect of this well-known process on the bacteria viability to discard and/or discuss the overlapping effects on the interpretation mechanisms of bacterial inactivation by Fe^{3+}-EDDHA system. In IW, best inactivation rate was obtained with H_2O_2/solar process with 5 mg/L of reagent, reaching DL with 17.9 Wh/m^2 (1.89 kJ/L and 40 min) for *E. coli* O157:H7 and Fe^{3+}-EDDHA/H_2O_2/solar with 5/10 mg/L of reagents for *S. enteritidis* (19.2 Wh/m^2, 3.29 kJ/L, 40 min). Conventional photo-Fenton process showed lower inactivation kinetics compared with Fe^{3+}-EDDHA/H_2O_2/solar and H_2O_2/solar for all concentrations tested in IW.

This result agrees with other works reporting bacterial inactivation by solar photo-Fenton at near neutral pH using a low amount of added iron in the solution (< 20 mg/L) [Rodriguez-Chueca *et al.,* 2014; García-Fernandez *et al.,* 2019]. In these cases, the limited inactivation of solar photo-Fenton at neutral pH was attributed to the low amount of iron added, the almost zero $[Fe]_{ds}$ remaining in the sample (Table 5.3), the lower activity of precipitated iron as oxyhydroxides compared with dissolved iron and the possible reduction of solar photons incoming in the sample by the turbidity generated. All these parameters acting together determine a notable reduction on the capability of solar photo-Fenton for bacterial inactivation.
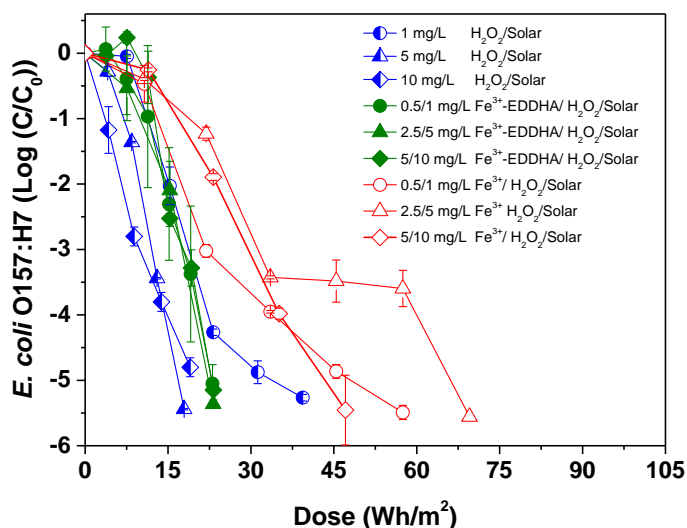
(a)
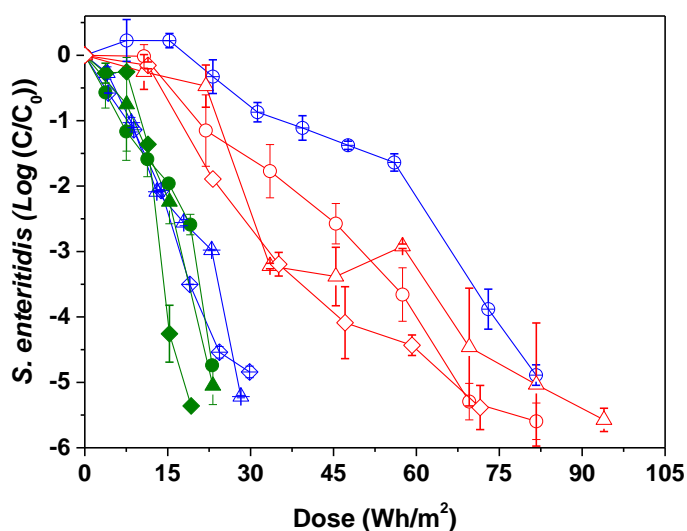
(b)

Figure 5.4. *E. coli* O157:H7 (a) and *S. enteritidis* (b) inactivation by Fe^{3+}-EDDHA/H_2O_2/solar, Fe^{3+}/H_2O_2/solar and H_2O_2/solar in IW under natural sunlight in 200-mL solar reactor.

Therefore, if inactivation efficiencies are compared with H_2O_2/solar under similar H_2O_2 concentrations, it has been observed the same or even lower inactivation kinetics for solar photo-Fenton than for H_2O_2/solar [Giannakis *et al.*, 2016a; García-Fernandez *et al.,* 2019]. This effect can be attributed to the no limitations of H_2O_2 to generated damages on bacteria in the H_2O_2/solar process, as the efficiency of the process depends mainly on the capability of each bacterium to resist the internal damages induced by this solar process [Giannakis *et al.*, 2016a].

5.3.2. Synthetic fresh-cut wastewater

The inactivation results in SFCWW (Figure 5.5) showed that DL (i.e.,> 5-LRV) was achieved in all cases but with a slight delay compared with IW, which can be also attributed to the presence of DOC and turbidity.
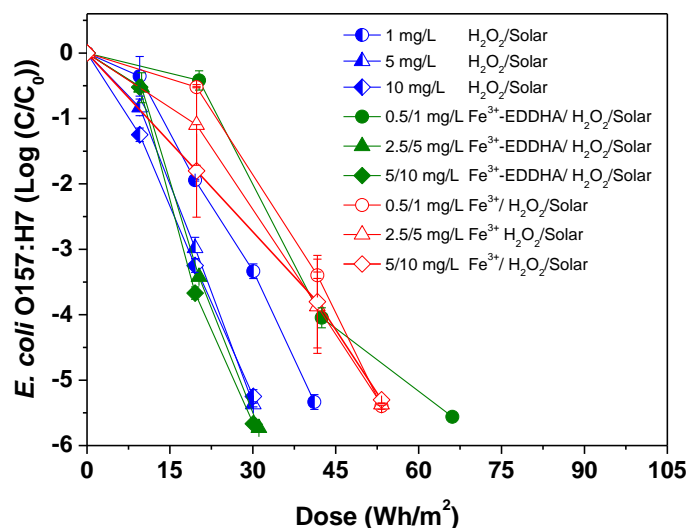
(a)
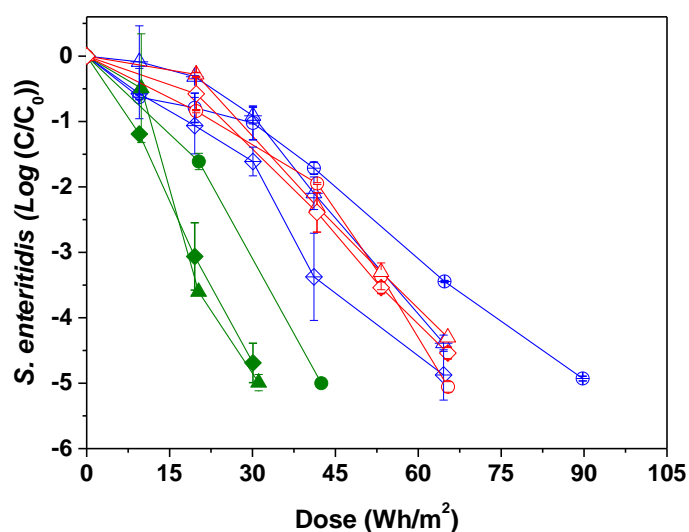
(b)

Figure 5.5. *E. coli* O157:H7 (a) and *S. enteritidis* (b) inactivation by Fe^{3+}-EDDHA/H_2O_2/solar, Fe^{3+}/H_2O_2/solar and H_2O_2/solar in SFCWW under natural sunlight in 200-mL solar reactor.

A clear enhancement in bacterial inactivation was obtained from the process Fe^{3+}-EDDHA/H_2O_2, reaching the faster inactivation kinetics rate ($k_{E.coli\ O157:H7}$:

0.173±0.011 min^{-1} and $k_{S.enteritidis}$:0.150±0.033 min^{-1}) with 2.5/5 mg/L of reagents concentration, requiring 45 min of treatment time (31.1 Wh/m^2 of solar UVA-dose or 4.06 kJ/L)

In both water matrix, again a high [Fe]$_{ds}$ still remained detected in the sample during Fe^{3+}-EDDHA/H$_2$O$_2$/solar process while with Fe^{3+}/H$_2$O$_2$/solar, [Fe]$_{ds}$ was lower than 0.1 mg/L. In addition, the increase of iron and H$_2$O$_2$ concentrations did not showed a significant inactivation enhancement neither one nor the other pathogen.

5.4. Interpretation of the bacterial inactivation mechanisms by Fe^{3+}-EDDHA

The inactivation of bacteria by solar photons, H$_2$O$_2$/solar and Fe^{3+}/solar was widely explained in Chapter 4.1. Briefly, these mechanisms are based on DNA damage for a combination of direct photo-oxidative damage (solar photo-inactivation) with internal oxidative damage by reactive oxygen species (ROS) generated by internal photo-Fenton reactions between bacterial iron and H$_2$O$_2$ from internal presence (metabolic activity and natural occurring iron) or freely diffusing inside of the cell when added to the sample [Giannakis *et al.*, 2016a]. All these damages are also occurring during the inactivation by Fe^{3+}-EDDHA/H$_2$O$_2$/solar process.

The proposed mechanisms to explain the enhanced bacterial inactivation by Fe^{3+}-EDDHA/solar process are summarized in Figure 5.6. On one hand (Figure 5.6 (a)), it is widely demonstrated that aminopolycarboxylic acid ligands including EDTA provoke changes in the permeability of the outer membrane altering the homeostasis of the cell and eventually end on cell death [Vaara *et al.,* 1992]. Briefly, this change is attributed to the chelation of cations (Ca^{2+} and Mg^{2+}), which purpose is to stabilize electrostatically the different parts of the lipopolysaccharides (LPS) present in the surface of the outer membrane, negatively charged by its polyanionic nature. Recently, a functional complexation study reported values of EDDHA affinity for Ca^{2+} and Mg^{2+}

higher than other aminopolycarboxylic acid ligands [Pesonen *et al.,* 2007]. Moreover, Hernández-Apaolaza et al. reported that salicylaldehide, salicylic acid and salicylaldehydeethylenediaminediimine are Fe^{3+}-EDDHA photodegradation products that can chelate iron [Hernández-Apaolaza and Lucena, 2011].

Previous studies reported the ability of acetilylsalicylate to disrupt the outer membrane and changes it permeability [Hancock and Wong, 1984]. Therefore, in these results, although not experimentally determined, it cannot be discard that the free EDDHA or any other subproducts with chelating capacity may affect the membrane permeability making the bacteria more susceptible to be inactivated by solar radiation.

The increase of iron-chelate concentration (from 0.5 to 5 mg/L), did not show an increase in inactivation rates for any of the pathogens. This effect can be explained by the screen effect of solar photons (higher at raised concentration of reagent) and also by the limited concentration of Ca^{2+} and Mg^{2+} available in the membrane (10^{-3} - 10^{-4} fg/fg in *E. coli*), and therefore, the increase of chelate concentration will not determine an increased effect on the bacterial susceptibility [Hernández-Apaolaza and Lucena, 2011; Heldal *et al.,* 1985]. Moreover, considering the limitation of cations, in SFCWW, the presence of Ca^{2+} and Mg^{2+} can also reduce the efficiency of the Fe^{3+}-EDDHA/solar process through a competition for the chelating agent with the membrane metals [Alakomi *et al.,* 2007].

S. enteritidis has been reported to show a higher resistance to be inactivated under stress conditions than *E. coli* (Chapter 4). In this work, the inactivation results showed same behaviour except when Fe^{3+}-EDDHA is added to the sample. This curious behaviour could be also explained by the proposed mechanism, considering different membrane stability between both pathogens. Ciesielski et al., reported that the dissociation constant (K_d) of LPS on *E. coli* is a higher order of magnitude than on *S. enteritidis* [Ciesielski *et al.,* 2012]. The higher membrane stability of *E. coli* may explain its higher resistance to be affected or inactivated in particular by the presence of Fe^{3+}-EDDHA. Therefore,

the different resistance of both bacteria reinforces the currently approach suggested in literature about the need to tests other microorganisms apart from *E. coli* to determine the efficiency of a water disinfection treatment [Giannakis *et al.,* 2016b].
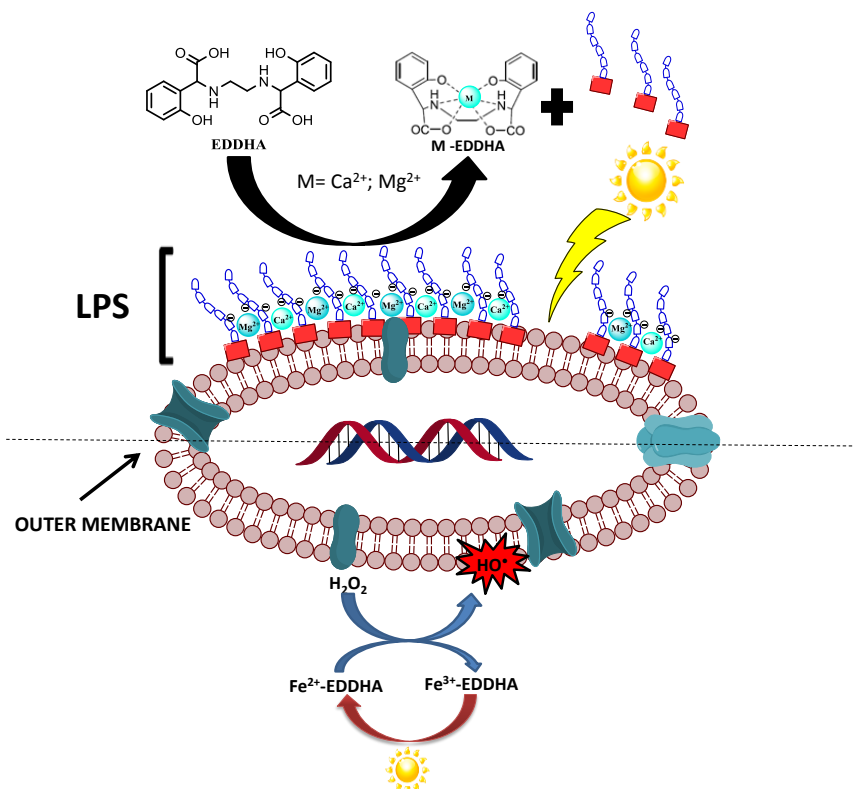
Figure 5.6. Proposed inactivation mechanism of bacteria by Fe^{3+}-EDDHA/solar (a) and Fe^{3+}-EDDHA/H_2O_2/solar processes (b).

In the case of Fe^{3+}-EDDHA/H_2O_2/solar there is some controversy about the photochemically or chemically induced electron transfer processes due to low reduction potential (E: -0.560 V) in comparison with Fenton reagents (E: +0.460 V) and Fe^{3+}-EDTA (E: +0.120 V) [Gómez-Gallego *et al.,* 2005]. Nevertheless, a recent study, reported the use of Fe^{2+}-EDDHA/H_2O_2 as Fenton treatment for degradation of polychlorinated biphenyls (PCBs) in contaminated soils [Ma *et al.,* 2018], and concluded that the oxidation mechanism of this chelate is based on a catalytic cycle according to Eqs. 5.1 and 5.2.

In addition, in these experimental conditions, the presence of light will favors the reduction of Fe^{3+} to Fe^{2+}, closing the cycle (Eq. 5.3) similarly to the mechanism

of other iron chelates (EDDS) reported previously and based in the generation of the oxidant species, mainly HO• and also other ROS like $O_2^{•-}$ [Giannakis *et al.,* 2016a; García-Fernandez *et al.,* 2019].

$$Fe^{2+} - EDDHA + H_2O_2 \rightarrow Fe^{3+} - EDDHA + HO^- + HO^• \qquad \text{Eq. 5.1}$$

$$Fe^{3+} - EDDHA + H_2O_2 \rightarrow Fe^{2+} - EDDHA + 2H^+ + O_2^{•-} \qquad \text{Eq. 5.2}$$

$$Fe^{3+} - EDDHA + h\nu \rightarrow Fe^{2+} - EDDHA^• \qquad \text{Eq. 5.3}$$

To demonstrate this possible explanation, appart from the photo-degradation of the chelate already showed in Figure 5.1, the generation of HO• in the Fe^{3+}-EDDHA/H_2O_2/solar process was also investigated using benzene as probe molecule. The results obtained confirm the generation of HO• by the new photo-Fenton like process (Fe^{3+}-EDDHA/H_2O_2/solar). Moreover, the initial rate of HO• generation ($R_{HO•}$) (Figure 5.7) for the reagents combination that showed the highest disinfection efficiency (2.5/5 mg/L of Fe/ H_2O_2) was also investigated in the solar photo-Fenton process with both iron sources at neutral pH, i.e., Fe^{3+}/H_2O_2/solar and Fe^{3+}-EDDHA/H_2O_2/solar processes. The $R_{HO•}$ value obtained for the Fe^{3+}-EDDHA/H_2O_2/solar process ($R_{HO•}$: 1.93 x 10^{-9} M/s) was higher than the value observed for the use of the conventional iron salts ($R_{HO•}$: 3.49 x 10^{-10} M/s) which is in concordance with the higher disinfection efficiency observed for this new solar process. Moreover, the $R_{HO•}$ observed for the new chelate is in line with the $R_{HO•}$ value reported for the EDDS chelate ($R_{HO•}$: 10^{-8}-10^{-9} M/s), which is one of the agents most investigated to treat water at neutral pH [Huang *et al.*, 2012b]. On the other hand, and as it was expected due to the lower [Fe]$_{ds}$, the $R_{HO•}$ obtained for the conventional solar photo-Fenton process at neutral pH was also significantly lower than the initial rate at acidic pH (ca. 10^{-6} M/s) [Lindsey and Tarr, 2000].
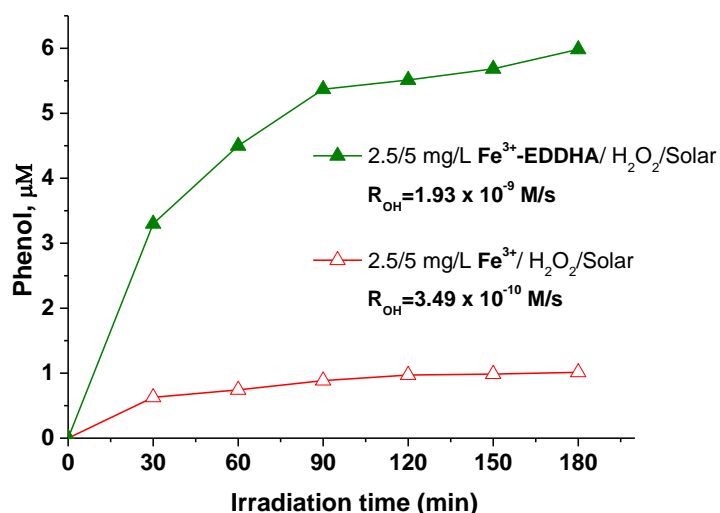
Figure 5.7. Comparison of phenol generation during solar exposure in the presence of 2.5/5 mg/L of Fe^{3+} or Fe^{3+}-EDDHA and H_2O_2 at neutral pH.

On the other hand, a complete physic-chemical characterization of the initial and final samples from Fe^{3+}-EDDHA/H_2O_2/solar process with the highest reagent combination (5/10 mg/L of Fe^{3+}-EDDHA/H_2O_2) was also evaluated in order to determine possible variation on the matrix characteristics. The results obtained are shown in Table 5.4, and no significant variations are observed. This result also permits to discard any water matrix effect on the bacterial viability, and therefore in the inactivation mechanism proposed.

Table 5.4. Physic-chemical characteristics of the initial and final samples from Fe^{3+}-EDDHA/H_2O_2/solar process with 5/10 mg/L of Fe^{3+}-EDDHA/H_2O_2.

Parameter	Initial values	Final values
DOC	19.9 mg/L	20.5 mg/L
Turbidity	5.8 NTU	11.1NTU
pH	7.09	6.94
Conductivity	77.7 µS/cm	80.4 µS/cm
Ionic composition (mg/L)		
NO_3^-	0.1	0.1
Cl^-	15.54	15.59
SO_4^{2-}	2.09	2.11
Na^+	11.05	11.09
K^+	0.16	0.33
Glycolate	<0.1	<0.1
Formiate	<0.1	<0.1)
Trimethylamine	0.17	<0.1
Oxalate	<0.1	<0.1

Summarizing, the main inactivation mechanisms of both bacteria by Fe^{3+}-EDDHA/H$_2$O$_2$/solar could be attributed to the accumulative damages on the external-cell membrane by i) the HO$^{\bullet}$ generated during the solar process and ii) the presence of the chelating agent (EDDHA) that changes membrane permeability leading to its degradation and accelerating the bacterial inactivation (Figures 5.4 and 5.5) compared to Fe^{3+}-EDDHA/solar (Figures 5.2 and 5.3).

5.5. Conclusions of Chapter 5

The capability of a commercial iron chelate Fe^{3+}-EDDHA in combination with natural solar radiation as promoter of wastewater disinfection has been demonstrated.

E. coli O157:H7 and *Salmonella sub enteritidis* have been successfully inactivated in IW after 35 min of solar exposure requiring very low concentration of Fe^{3+}-EDDHA (0.5 mg/L) and reducing the treatment time two and four times compared to solar photo-inactivation process.

The presence of organic carbon and high turbidity (100 NTU) in SFCWW delays the bacterial inactivation rate compared with their absence in terms of treatment time and solar UVA dose but reaching DL (> 5-LRV) in all cases.

Employing the commercial fertilizer as Fenton reagent is more efficient than the conventional use of iron salts for the two water matrix studied: IW and SFCWW. The combination of the iron chelate with H$_2$O$_2$ (Fe^{3+}-EDDHA/H$_2$O$_2$/solar) clearly improves the inactivation efficiency respect to all the treatments tested obtaining very successful inactivation rates (> 5-LRV). Best bacterial inactivation was obtained in only 45 min using low reagent concentrations (2.5/5 mg/L of Fe^{3+}-EDDHA/H$_2$O$_2$).

CHAPTER 6

SOLAR-DRIVEN PROCESSES TO RECLAIM SFCWW AT PILOT PLANT SCALE

6. SOLAR-DRIVEN PROCESSES TO RECLAIM SFCWW AT PILOT PLANT SCALE

In this chapter the capability of three solar processes to simultaneously inactivate two bacterial pathogens (*E. coli* O157:H7 and *S. enteritidis*) and remove five OMCs (Atrazine, Azoxystrobin, Buprofezin, Procymidone and Terbutryn) has been evaluated in synthetic fresh-cut wastewater (SFCWW). The processes have been performed at pilot plant scale (60L) using tubular reactors provided with Compound Parabolic Collectors.

A comparative analysis of the treatment efficiency of H_2O_2/solar, Fe^{3+}-EDDHA/solar and Fe^{3+}-EDDHA/H_2O_2/solar with reagent´s concentrations ranging from 0.5 to 5 mg/L of Fe^{3+}-EDDHA and 2.5-40 mg/L of H_2O_2 has been

carried out. In addition, the bacterial regrowth after each solar process has also been assessed.

The averaged day-profile of water temperature and solar UVA radiation registered during this testing campaign of solar treatments at pilot plant scale is shown in Figure 6.1. The water temperature was monitored during the experiments and ranged from 25±4 ºC to 41±6 ºC for all the experiments, discarding therefore thermal inactivation of bacteria [García-Fernández *et al.,* 2015]. Maximum and minimum solar UV irradiances were 26±3 and 49±3 W/m^2, respectively.

In addition, DOC content was measured throughout all solar processes, with a very slight DOC degradation (lower than 10 %).
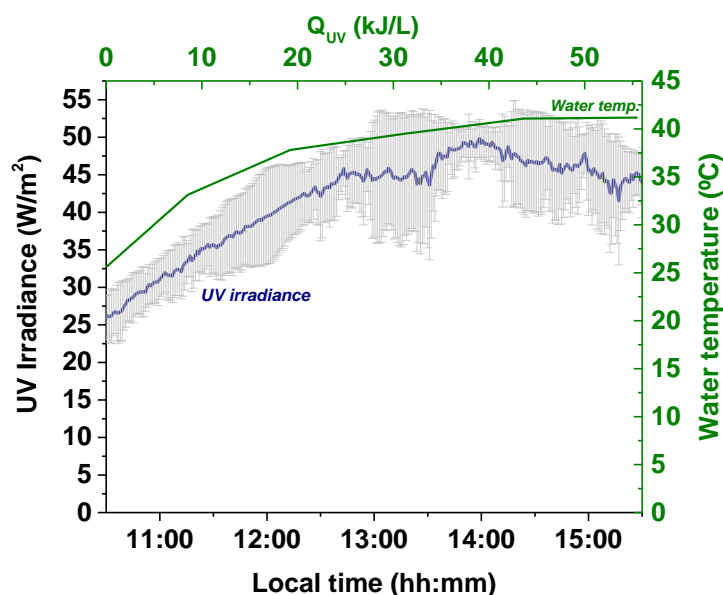
Figure 6.1. Averaged solar UV Irradiance and water temperature of all solar treatments carried out at pilot-plant scale (CPC reactor).

6.1. Bacterial inactivation by solar processes

6.1.1. Solar photo-inactivation and H$_2$O$_2$/solar processes

The inactivation profiles of *E. coli* O157:H7 and *S. enteritidis* by solar photo-inactivation and H$_2$O$_2$/solar processes at several oxidant concentrations (2.5, 5,

10, 20 and 40 mg/L) are shown in Figure 6.2 (a) and 6.2 (b), respectively. The corresponding inactivation kinetic constants are summarized in Table 6.1.

The solar photo-inactivation process leads in both pathogens a similar kinetic behaviour characterized by an initial log-linear decay followed by a residual concentration of bacteria, not attaining a complete removal (DL: 2 CFU/mL) after 300 min of solar exposure. This type of inactivation profile obtained by solar photo-inactivation has been reported previously [Ubomba-Jaswa *et al.,* 2009] and it has been attributed to the interrupted delivered solar UV radiation in the sample due to the re-circulation of the water through the dark and illuminated areas of the solar CPC reactor during the solar exposure. This influence of the reactor geometry and operational procedure may favor the activation of the self-defense mechanism of bacteria to repair in the dark the oxidative damages generated by the mild oxidative effect of solar photo-inactivation process, keeping as result a residual population in the sample [Ubomba-Jaswa *et al.,* 2009].

Nevertheless, this effect can be avoided by applying a more oxidative solar process, such as the H_2O_2/solar process, which results clearly show an enhancement of the bacterial inactivation profiles (Figure 6.2 (a,b)) and kinetic constants (Table 6.1) compared with the solar photo-inactivation process. In this case, DL was achieved for both pathogens with all the H_2O_2 concentrations tested. In general, it was observed for both pathogens that the higher the H_2O_2 concentration, the higher the inactivation kinetics. This improvement was marked at H_2O_2 concentration values > 10 mg/L (Table 6.2) in both pathogens, especially in *S. enteriditis* where the inactivation kinetics change from double log-linear decay to a log-linear decay. The slight differences showed by *S. enteritidis* by increasing the oxidant concentration from 20 to 40 mg/L are in line with the lab-scale results shown in Chapter 4, where it was stated that the inactivation of *S. enteritidis* by H_2O_2/solar process was not-chemically limited by the reagent´s concentration.

(a)

(b)
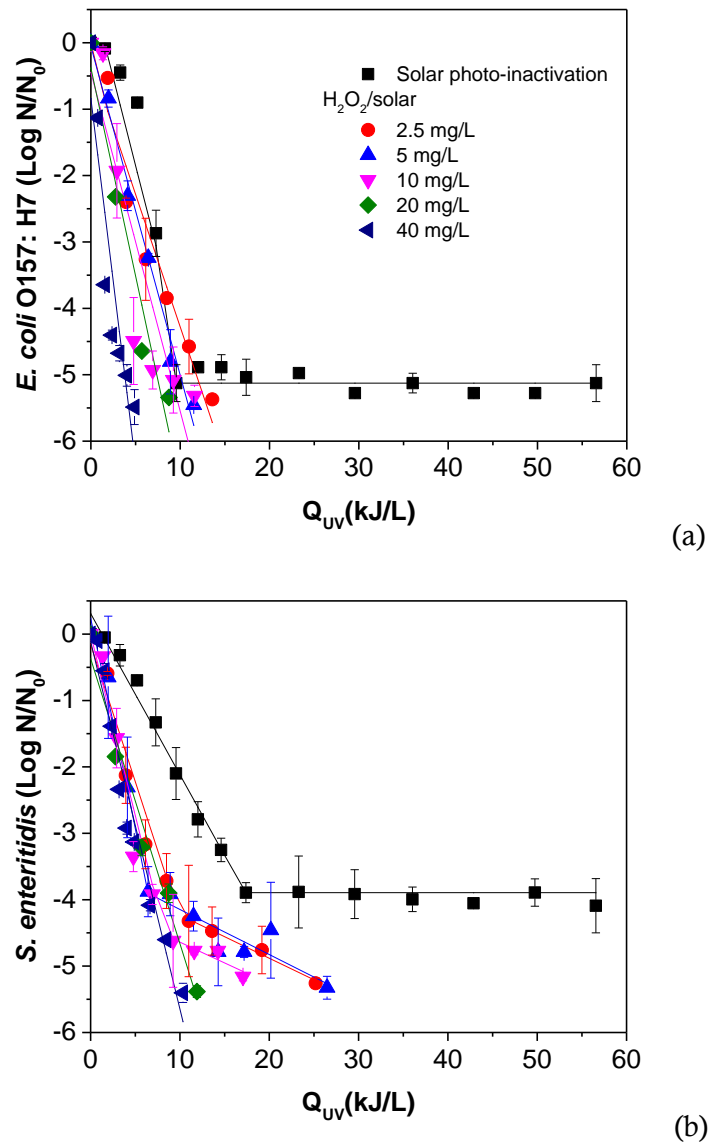
Figure 6.2. *E. coli* O157:H7 (a) and *S. enteritidis* (b) inactivation by H_2O_2/solar in CPC reactor.

Therefore, considering the overall data obtained from this solar process and the concentrations of H_2O_2 tested, the best bacteria inactivation rate was obtained with 20 mg/L of reagent for both bacteria.

In addition, at this concentration, *S. enteritidis* showed a higher resistance to be inactivated (DL reached in 60 min of treatment time and 11.9 kJ/L of Q_{UV}) than *E. coli* O157:H7 (DL reached in 45 min of treatment time and 8.7 kJ/L of Q_{UV}).

Table 6.1. Bacterial inactivation kinetic constants obtained for all the experimental conditions tested in CPC reactor.

Treatment	$[Fe^{3+}:H_2O_2]$ (mg/L)	k (L/kJ)	R^2	SL (kJ/L)	Q_{UV} (kJ/L)
E. coli O157:H7					
Fig. 6.2 (a)					
Solar photo-inactivation*	-	0.529±0.104	0.832	-	56.56
H$_2$O$_2$/solar	2.5	0.400±0.038	0.947	-	13.60
	5	0.495±0.028	0.984	-	11.52
	10	0.510±0.103	0.796	-	11.60
	20	**0.626±0.105**	**0.920**	**-**	**8.75**
	40	1.099±0.203	0.825	-	4.89
Fig. 6.3 (a)					
Fe^{3+}-EDDHA/solar	0.5	k$_1$:0.331±0.078 k$_2$:0.031±0.002	0.850 0.960	8.23	56.82
	2.5	**0.417±0.026**	**0.992**	**19.12**	**31.41**
	5	0.244±0.026	0.954	17.05	40.78
Fig. 6.4 (a)					
Fe^{3+}-EDDHA/H$_2$O$_2$/solar	0.5:2.5	0.195±0.021	0.881	-	30.82
	2.5:20	**0.706±0.093**	**0.876**	**-**	**8.41**
	5:40	0.805±0.131	0.840	-	6.33
S. enteritidis					
Fig. 6.2 (b)					
Solar photo-inactivation*	-	0.243±0.011	0.983	1.57	56.56
H$_2$O$_2$/solar	2.5	k$_1$:0.413±0.043 k$_2$:0.065±0.005	0.948 0.979	-	25.20
	5	k$_1$:0.623±0.063 k$_2$:0.068±0.015	0.970 0.768	-	26.46
	10	k$_1$:0.543±0.061 k$_2$:0.062±0.020	0.940 0.754	-	17.05
	20	**0.429±0.040**	**0.965**	**-**	**11.91**
	40	0.554±0.040	0.954	-	10.34
Fig. 6.3 (b)					
Fe^{3+}-EDDHA/solar	0.5	0.090±0.006	0.949	3.78	56.82
	2.5	**0.229±0.029**	**0.939**	**13.51**	**37.81**
	5	0.191±0.022	0.938	17.05	47.11
Fig. 6.4 (b)					
Fe^{3+}-EDDHA/H$_2$O$_2$/solar	0.5:2.5	0.142±0.015	0.856	-	43.67
	2.5:20	**0.673±0.082**	**0.893**	**-**	**8.41**
	5:40	0.527±0.022	0.984	-	11.35

*Inactivation kinetic according to model 4 (Chapter 3, section 3.13), where residual bacteria population (N$_{res}$) for *E. coli* and *S. enteritidis* was 4 and 50 CFU/mL respectively.
Bold type data means the best results obtained in each experimental condition tested.

6.1.2. Fe^{3+}-EDDHA/solar process

Figure 6.3 (a,b) shows the inactivation profile of *E. coli* O157:H7 and *S. enteritidis* by Fe^{3+}-EDDHA/solar process at three different chelate concentrations: 0.5, 2.5

and 5 mg/L. The inactivation results showed an improvement for iron chelate concentration increased from 0.5 (no DL reached in any pathogen) to 2.5 mg/L; meanwhile, an opposite behaviour occurred when the Fe^{3+}-EDDHA concentration raised from 2.5 to 5 mg/L appearing a detrimental effect on the inactivation of both pathogens (increasing the Q_{UV} need to reach the DL).

(a)

(b)
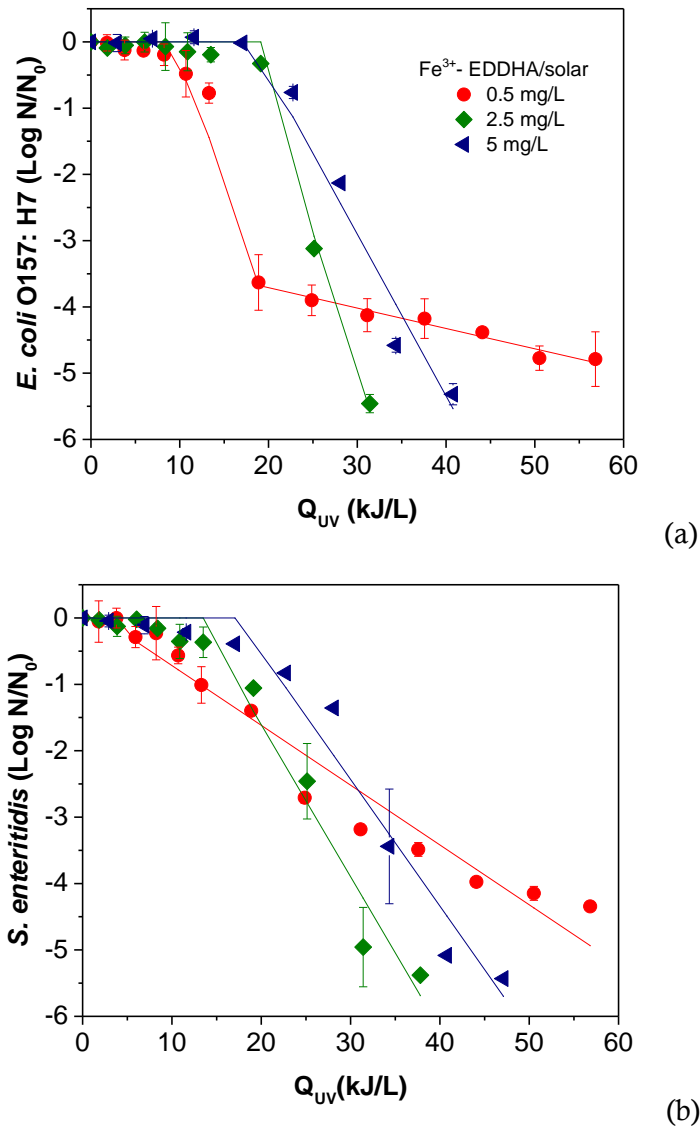
Figure 6.3. *E. coli* O157:H7 (a) and *S. enteritidis* (b) inactivation by Fe^{3+}-EDDHA/solar in CPC reactor.

The best inactivation results were therefore obtained with 2.5 mg/L of Fe^{3+}-EDDHA concentration, where *S. enteritidis* (*k*: 0.229±0.029 L/kJ) showed again

a higher resistance to be inactivated than *E. coli* O157:H7 (k: 0.417±0.026 L/kJ), requiring 30 min of treatment time and 6 kJ/L more to reach the DL (Table 6.1).

Additionally, the presence of the iron chelate provoked the appearance of a shoulder phase and lower kinetic constants compared with the effect of solar photo-inactivation (Fig. 6.2 (a,b), Table 6.1). The appearance of the lag phase delaying the inactivation of both bacteria can be attributed to the mild oxidative capability of Fe^{3+}-EDDHA/solar process and the concentration of chelated investigated. However, the addition of Fe^{3+}-EDDHA at a higher concentration than 2.5 mg/L benefits the SFCWW disinfection as it is able to reach the DL avoiding the non-desired residual concentration of bacteria observed for the solar photo-inactivation process.

On the other hand, the lower efficiency showed by increasing the iron chelate concentration from 2.5 to 5 mg/L can be explained by an increase of the light scattering effect at high Fe^{3+}-EDDHA concentrations [Hernández-Apaolaza *et al.,* 2011]. These results and behaviour agree with the previously reported at laboratory scale for similar Fe^{3+}-EDDHA concentrations in Chapter 5.

6.1.3. Fe^{3+}-EDDHA/H_2O_2/solar process

The inactivation of *E. coli* O157:H7 and *S. enteritidis* in SFCWW by the Fe^{3+}-EDDHA/ H_2O_2/solar process are shown in Figure 6.4 (a, b), respectively.

In general, the inactivation kinetic was improved by the combination of the iron chelate with H_2O_2 showing the non-presence of a shoulder phase in the first stage of the process and reducing the treatment time required to achieve the DL in all cases.
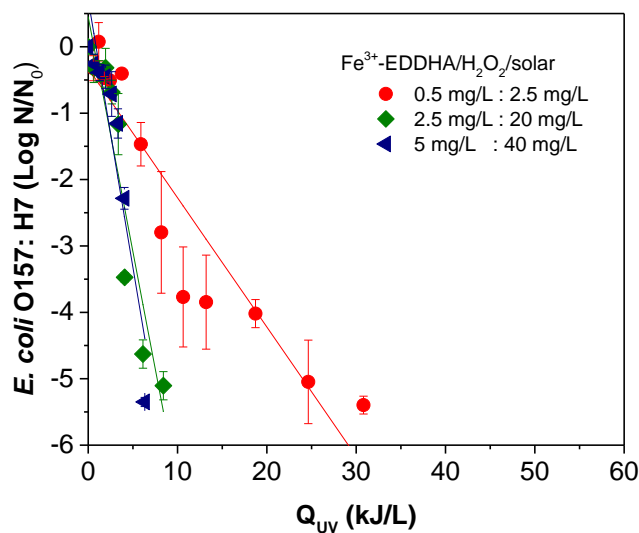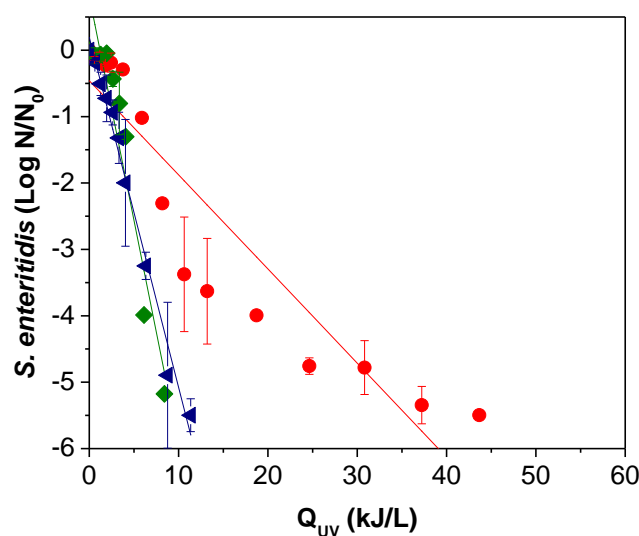
Figure 6.4. *E. coli* O157:H7 (a) and *S. enteritidis* (b) inactivation by Fe^{3+}-EDDHA/ H_2O_2/solar in CPC reactor.

As for the Fe^{3+}-EDDHA/solar process, by increasing the Fe^{3+}-EDDHA concentration from 0.5 to 2.5 mg/L the disinfection efficiency was enhanced, while no improvement was observed for bacterial inactivation when increasing the concentration from 2.5 to 5 mg/L. Therefore, the faster kinetic inactivation was obtained with 2.5/20 mg/L of Fe^{3+}-EDDHA/H_2O_2 for both bacteria, where the DL was achieved after 60 min and 8.41 kJ/L of Q_{UV}. Moreover, this operational condition was the only one that improved the efficiency of the other solar processes studied employing the same reagents concentrations separately

(H_2O_2/solar: 20 mg/L; Fe^{3+}-EDDHA/solar: 2.5 mg/L). Specifically, the cumulative UVA energy required for SFCWW disinfection by this process (8.41 kJ/L) was 30 % and 78 % less than the required for H_2O_2/solar process (11.91 kJ/L) and Fe^{3+}-EDDHA/solar (37.81 kJ/L), respectively.

6.1.4. Profiles of H_2O_2 and dissolved iron concentration

The H_2O_2 concentration and the dissolved iron along all the solar experimental time was measured in all samples. The profiles of data measured are shown in Figure 6.5 (a) and (b), respectively.

Regarding the H_2O_2 concentration, it was observed a very low reduction on H_2O_2/solar processes at all reagent concentrations, reaching at the end of the treatment a decomposition ranged from 37 to 23 % of the initially added in all cases. Comparing the residual H_2O_2 concentration between laboratory and pilot plant scale in SFCWW at 5 and 10 mg/L (Chapter 4, Table 4.3), no significant differences were obtained, being slightly higher in the case of pilot plant scale experiments. These results and decomposition trend agree with other results previously reported in literature for different water matrices [Polo-López *et al.*, 2011]. In this research, it was concluded the following order of H_2O_2 decomposition: simulated urban WW > well water > isotonic water at both scale laboratory and pilot plant, with slightly higher rate of decomposition at pilot plant scale and also under sunlight exposure than in the dark [Polo-López *et al.*, 2011].

It is very well known that H_2O_2 is auto-decomposed in water and oxygen according to Eq. 6.1 [Jones, 1999].

$$2\,H_2\,O_2 \rightarrow 2\,H_2\,O\,+\,O_2 \qquad \text{Eq. 6.1}$$

Nevertheless, the H_2O_2 decomposition rate is accelerated by the following parameters: i) the water temperature increases the decomposition rate 2.3-fold with a rise of 10 ºC [Jones, 1999; ii) the alkalinity of the solution affect the H_2O_2

ionization in H^+ and OOH^- due to it is a weak acid ($pKa = 11.62$). The ionization is favored at basic water pH [Phibbs y Giguere, 1951]; iii) the presence of chemical organic and inorganic compounds, like humic substances, tannin, ligninolytic compounds, cyanide, formaldehyde, carbonates, sulfate, thiosulfate, nitrate, chloride and phosphate [Jones, 1999]; iv) and the use of catalysts (photocatalysis), where H_2O_2 is a consumed reagent in the catalytic cycle, as it is shown in Fe^{3+}-EDDHA/H_2O_2/solar process, where H_2O_2 was almost completely consumed during the treatment (90 %) in all the tested conditions.
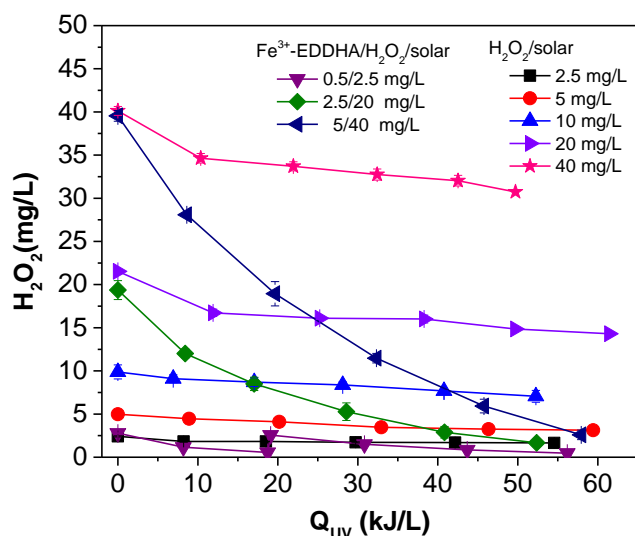
(a)
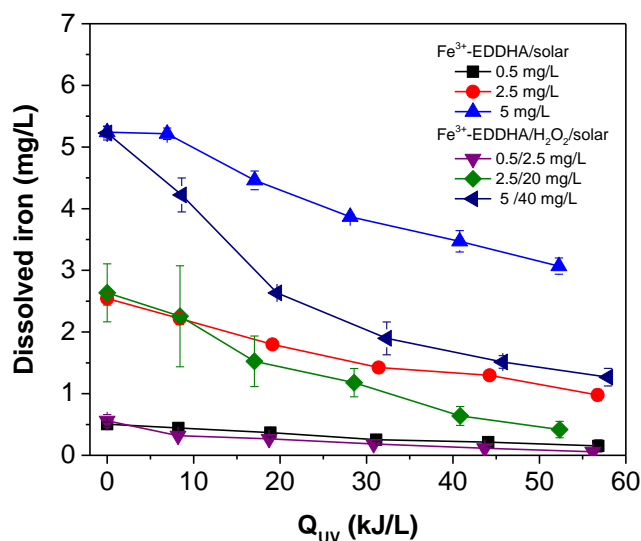
(b)

Figure 6.5. H_2O_2 (a) and dissolved iron (b) measured along all solar treatments and conditions tested at pilot plant solar reactor.

Regarding the dissolved iron concentration at the end of the solar test, it was detected at concentrations higher than the 30 % of the initially iron chelate added to the sample in Fe^{3+}-EDDHA/solar process. In the case of Fe^{3+}-EDDHA/H_2O_2/solar process, the residual iron in solution showed a concentration percentage ranged from 12 to 25 % after the solar process, for 0.5 to 5 mg/L of the iron chelated initially added, respectively.

Comparing these dissolved iron values with the data reported in Chapter 5 at laboratory scale (values measured ranged between 46 to 66 % for Fe^{3+}-EDDHA/H_2O_2/solar process, Table 4.3), a significant reduction is therefore observed at pilot plant scale. This effect can be attributed to the higher amount of solar energy (Q_{UV}) accumulated in the sample in the case of the CPC reactor test which favour the photodegradation of the iron chelate.

Finally, it is important to remark that the residual concentration of reagents is a factor to take into account for the proper selection of a suitable water treatment, in order to avoid any effect of regrowth of bacteria during storage and distribution time in real applications.

6.1.5. Post-treatment bacterial regrowth

The efficiency of the solar processes investigated was assessed in terms of bacterial regrowth after 24 h. The concentration of *E. coli* O157:H7 and *S. enteritidis* detected in those operational conditions where DL was reached is shown in Figure 6.6.

According to Spanish RD 1620/2007, the limit of *E. coli* concentration in wastewater for irrigation is established at 100 CFU/100 mL (RD 1620/2007). These results showed that after all the solar processes and reagent´s concentration tested, the bacterial concentration was less than this limit for both pathogens in the treated SFCWW, except for 2.5 mg/L of reagent in H_2O_2/solar process (for both pathogens) and 0.5/2.5 mg/L of Fe^{3+}-EDDHA/H_2O_2 process (only for *E. coli* O157:H7).

Therefore, the use of very low reagents concentrations (< 5 mg/L of H_2O_2 and 2.5 mg/L of Fe^{3+}-EDDHA) may not be appropriate to ensure efficient water disinfection. On the other hand, in the new European proposal for the regulation of wastewater reuse for irrigation, the presence of *E. coli* is more restrictive and its concentration is reduced to 10 CFU/100mL (Procedure 2018/0169/COD). Considering this regulation, the suitable solar processes for SFCWW reuse in irrigation are H_2O_2/solar at concentrations higher than 10 mg/L of H_2O_2 and Fe^{3+}-EDDHA/H_2O_2 at 2.5/20 and 5/40 mg/L of reagents concentration; while lower concentrations as well as the Fe^{3+}-EDDHA/solar process can be discarded as appropriated treatments for SFCWW reclamation.
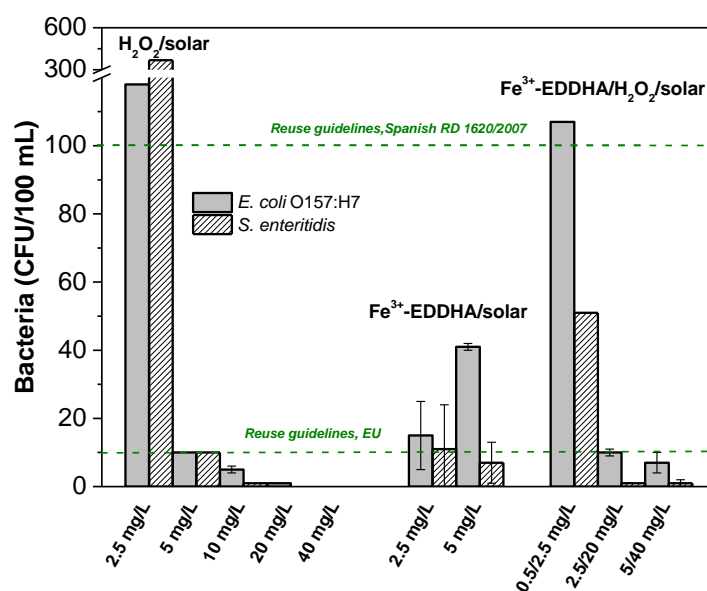
Figure 6.6. Analysis of bacteria concentration in treated SFCWW after 24 h of storage in the dark.

6.2. OMCs removal by solar processes

Simultaneously to the analysis of bacterial inactivation, the degradation of each OMC was also investigated in SFCWW. Figure 6.7 shows a comparison of the ΣOMCs removal profile obtained along the solar treatments, and the degradation of each individual OMC is shown in Figure 6.8. It should be noted that Fe^{3+}-EDDHA/solar has proven not to be capable to degrade OMCs for any of the

Fe^{3+}-EDDHA concentrations tested, and therefore these results have not been included in Figure 6.7. The non-degradation observed in this case is in agreement with the non-generation of oxidant species proposed for this solar process and described in Chapter 5.
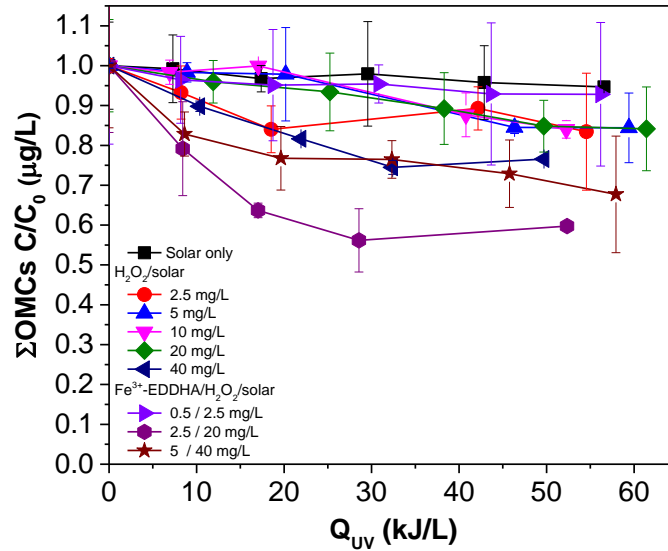
Figure 6.7. Degradation profiles of ΣOMCs by H_2O_2/solar and Fe^{3+}-EDDHA/H_2O_2/solar processes in CPC reactor.

In general, non-significant removal differences were obtained in solar only and H_2O_2/solar process at any reagent concentration tested. The percentage of ΣOMCs removal varied from 10 to 20 % in these cases, which is a very modest efficiency. These low efficiencies were expected due to the high energy required for the cleavage of the O-O bond into $HO^{\bullet}$ and therefore, their dissociation will be generated only under shortwave wavelengths (<290 nm) which are in a very small extent in the solar spectrum. The removal % obtained is in line with a previous study where degradation of ca. 20 % was reported for the antibiotic chloramphenicol by the H_2O_2/solar process when it was exposed to similar cumulative energy (60 kJ/L) [Rizzo *et al.,* 2018b].
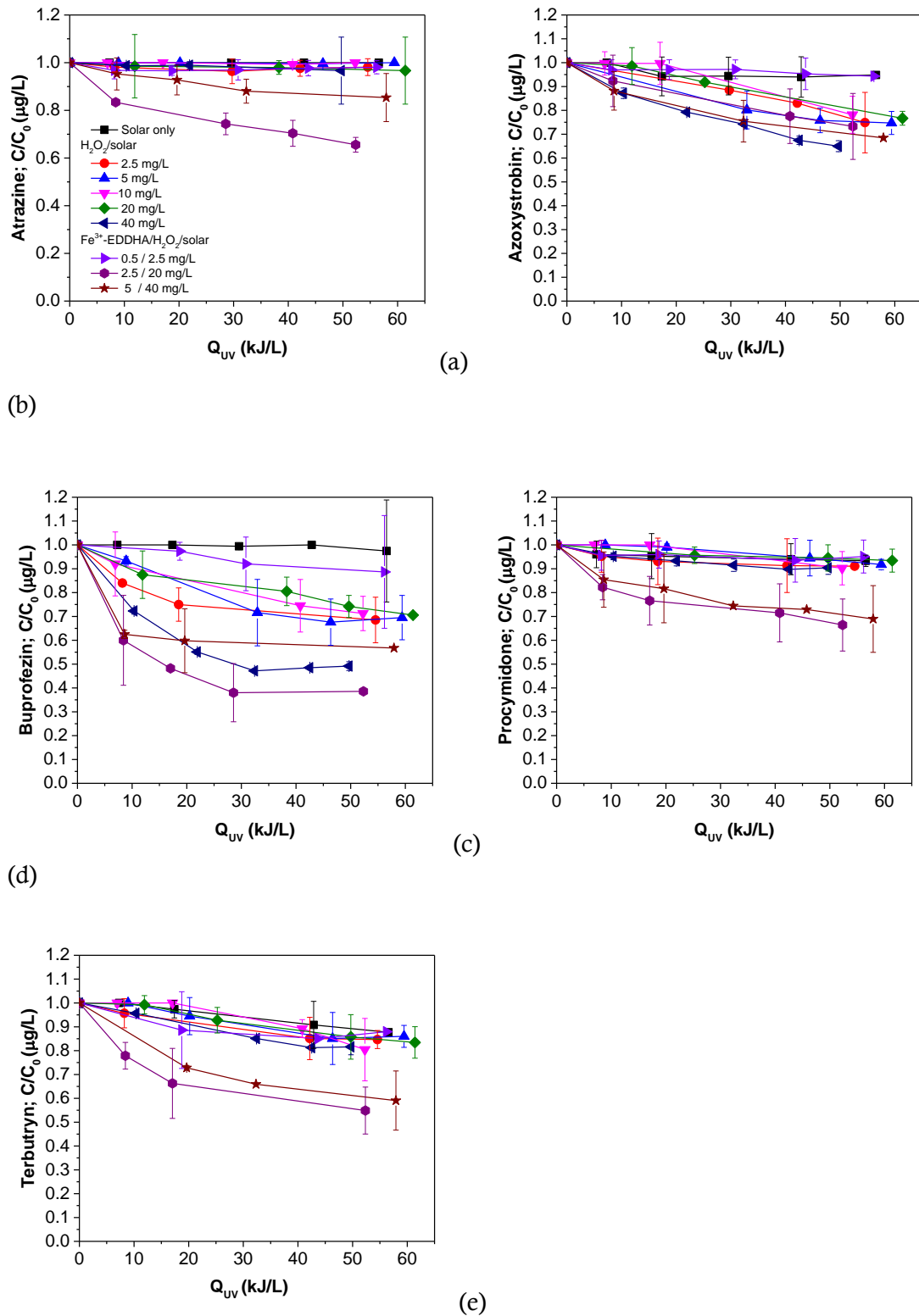
Figure 6.8. Degradation profile of each OMC by all solar treatment and conditions tested in this chapter in CPC reactor.

Nevertheless, better OMCs degradation performance was observed for the Fe^{3+}-EDDHA/H_2O_2/solar process. The higher ΣOMCs degradation (42 %) was attained with 2.5/20 mg/L of Fe^{3+}-EDDHA/H_2O_2, attributed mainly to the $HO^{\bullet}$ generation capability of this process demonstrated previously at laboratory scale in Chapter 5. The OMCs degradation profiles (Figure 6.7) observed for this solar process in the two most oxidant conditions were non-linear and were characterized by a fast degradation in the first stage of the process followed by a smooth decay until the end of the treatment time. The low chelate concentration employed and its self-degradation by the generated $HO^{\bullet}$ might explain the low efficiencies and the double kinetic degradation observed as was reported previously for other iron chelates, like EDDS agent [Huang *et al.,* 2012b].

In summary, as for disinfection, the highest ΣOMCs removal efficiency was also attained by the Fe^{3+}-EDDHA/H_2O_2/solar process using 2.5 and 20 mg/L of iron micronutrient and oxidant, respectively.

6.3. Conclusions of Chapter 6

The capability of the three solar processes studied (H_2O_2/solar, Fe^{3+}-EDDHA/solar and Fe^{3+}-EDDHA/H_2O_2/solar) to disinfect SFCWW at pilot scale has been demonstrated.

The Fe^{3+}-EDDHA/H_2O_2/solar process using low reagents concentrations (2.5/20 mg/L of Fe^{3+}-EDDHA/H_2O_2) showed the highest treatment capability reducing ca. 30% the OMCs load and reaching the DL (i.e.,> 5-LRV) for both pathogens in 60 min.

Additionally, the high disinfection efficiency obtained by the three solar processes at the best treatment conditions (H_2O_2/solar: 20 mg/L; Fe^{3+}-EDDHA/solar: 2.5 mg/L and Fe^{3+}-EDDHA/ H_2O_2/solar: 2.5/20 mg/L) satisfied the microbiological quality established in Spanish urban wastewater reuse Royal decree 1620/2007 (<100 CFU/100 mL).

Moreover, H_2O_2/solar and Fe^{3+}-EDDHA/H_2O_2/solar processes also satisfied the new European proposal (Procedure 2018/0169/COD) (<10 CFU/100 mL).

These results have significant implications due to their capability of enabling the intended treated wastewater reuse for irrigation in agriculture with the incorporation of the iron micronutrient as an advantage.

CHAPTER 7

OZONATION AND PEROXONE PROCESS AT PILOT SCALE TO RECLAIM SFCWW

7. OZONATION AND PEROXONE PROCESS AT PILOT SCALE TO RECLAIM SFCWW

In this chapter, the capability of ozonation and peroxone treatment for the simultaneous disinfection and decontamination of wash water from the fresh-cut industry has been investigated at pilot plant scale (10 L).

The removal efficiency of six organic microcontaminants (OMCs) (four of them priority substances) and the inactivation *E. coli* O157:H7 and *S. enteritidis* in SFCWW has been assessed.

Ozonation and peroxone (O_3 with 20 mg/L of H_2O_2) process has been investigated under several operational conditions: natural SFCWW pH (6.25) and basic pH (11), and two different initial ozone productions (0.09 and 0.15 gO_3/Lh).

For peroxone tests, an initial dose of H_2O_2 (20 mg/L) was added and when concentration of H_2O_2 was lower than ca. 1.5 mg/L, additional dosages were performed to avoid reagent limitations during the experiment. The H_2O_2 dose was chosen considering a 50 % of mass transfer for the ozone-water system and to obtain a molar ratio of 0.6:1 (H_2O_2:O_3) which is very close to the optimum for peroxone process (0.5:1) according to the reaction stoichiometry.

7.1. Bacterial inactivation

The inactivation profiles of *E. coli* O157:H7 and *S. enteritidis* in SFCWW at natural (6.25) and basic pH (11) by both ozonation (O_3) and peroxone treatment (O_3/H_2O_2) are shown in Figure 7.1 (a,b), respectively. In all cases, detection limit (2 CFU/mL) was reached for both pathogens, also showing both a similar inactivation kinetic order: ozonation pH 6.25 > ozonation pH 11 > peroxone pH 6.25 > peroxone pH 11, with treatment times ranging between 2 and 20 min. Therefore, the fastest inactivation was obtained with ozonation treatment at pH 6.25, where, the concentrations of *E. coli* O157:H7 and *S. enteritidis* were reduced > 5-LRV in 2 and 4 min, respectively.

Results also showed that neither H_2O_2 addition, higher pH nor higher O_3 generation (0.15 gO_3/Lh), determined faster inactivation kinetics. Previous studies showed that the H_2O_2 concentration (20 mg/L) selected did not generate any viability loss on the two target microorganisms of this study, therefore the disinfection results observed can be only attributed to the ozonation/peroxone processes (Dark test shown in Chapter 3).

Moreover, a remarkable difference on the resistance is observed between both pathogens (Figure 7.1 and Table 7.1). *S. enteritidis* showed a higher resistance than *E. coli* O157:H7 in all the operational conditions investigated. At the best condition of this study, ozonation at pH 6.25, the first order rate constant for *E. coli* O157:H7 (*k:* 2.79±0.00 min^{-1}) was much faster than *S. enteritidis* (*k:* 1.47±0.40 min^{-1}).
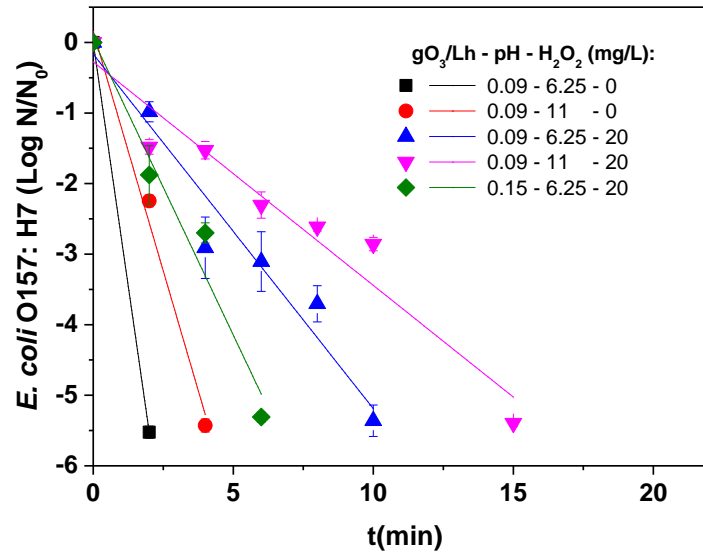
(a)
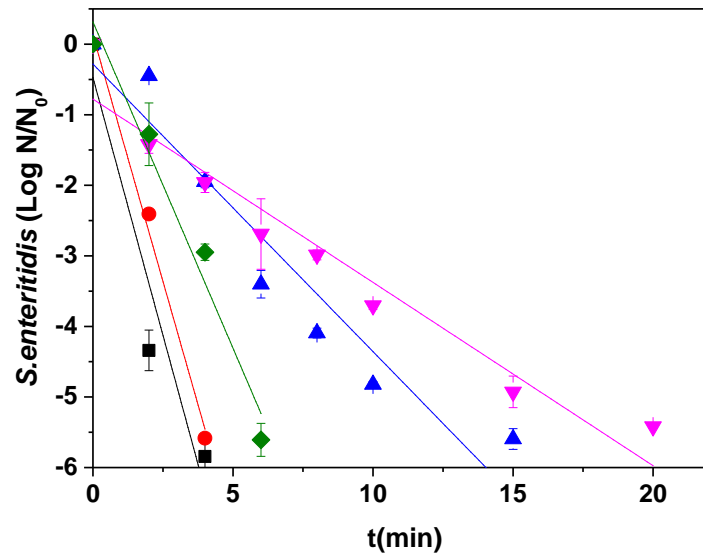
(b)

Figure 7.1. Comparison of *E. coli* O157:H7 (a) and *S. enteritidis* (b) inactivation profiles by ozone and peroxone processes.

The strong potential of ozone to both: degrade organic molecules and inactivate pathogens in water is very well known. The reaction pathways of this process is also well described in literature and already explained in Chapter 1. Nevertheless, briefly it can be explained by: i) direct oxidation, which is a selective and fast reaction between O_3 and targets with electron-rich moieties which mainly depends on the targets structure, and ii) indirect oxidation which involves the generation of reactive oxygen species (ROS), mainly non-selective

HO$^•$, by several reactions and where the water pH play a critical role [Gottschalk *et al.,* 2009]

Table 7.1. First order rate constants of OMCs removal and bacterial inactivation by ozone and peroxone process.

gO$_3$/Lh	pH	H$_2$O$_2$ (mg/L)	ΣOMCs k (min^{-1})	R^2	*E. coli* O157:H7 k (min^{-1})	R^2	*S. enteritidis* k (min^{-1})	R^2
0.09	6.25	-	0.0105±0.0005	0.97	2.79±0.00	1.00	1.47±0.40	0.93
0.09	11	-	0.0091±0.0006	0.95	1.36±0.13	0.99	1.40±0.11	0.99
0.09	6.25	20	0.0024±0.0002	0.93	0.50±0.05	0.95	0.41±0.05	0.92
0.09	11	20	0.0090±0.0006	0.94	0.32±0.03	0.94	0.26±0.02	0.95
0.15	6.25	20	0.0055 ±0.0002	0.99	0.84±0.11	0.96	0.93±0.11	0.97

The predominant reaction-path in ozonation depends on water pH which plays a critical role in the O$_3$ decomposition kinetics. At pHs lower than 8, the direct oxidation by O$_3$ predominates whereas at pHs > 8, the O$_3$ decomposition is accelerated, favoring therefore the indirect oxidation mainly by the HO$^•$ generated [Beltrán, 2003].

The microbial inactivation showed no differences in the removal kinetics between both water pHs (Fig. 7.1). This clearly evidences that in these experimental conditions, the direct attack of O$_3$ was enough to guarantee a successful performance of the process. Additionally to water pH, the O$_3$ degradation rate is also affected by other factors, including water temperature, alkalinity, and presence of DOC. Nevertheless, none of these factors suffered changes throughout the experimental conditions. Thus, the differences on degradation rates between inactivation profiles of bacteria will depend mainly of their microbiological structure.

The mechanism of bacterial inactivation by ozone is mainly based on the progressive oxidation of vital cellular components, ending in the cell's death. It is well accepted that components of cell-wall (lipoprotein and the lipopolysaccharide layers) are the first targets [Kim *et al.,* 1999]. It has been estimated that ca. 3x10^8 molecules of ozone are needed to inactivate a cell of *E. coli* [Khadre *et al.,* 2001]. In the case of the pathogens under study, although both belong to Gram negative type-bacteria (same structured cell-wall), a slight

difference between both strains were observed, showing *S. enteritidis* a higher resistance than *E. coli* O157:H7. This behaviour has been previously reported in literature, and it was attributed to the higher amount of phospholipids components in *Salmonella* cell membrane that rise up its density and rigidity and therefore increase its resistance against oxidation by ozone compared with *E. coli* [Alwi and Ali, 2014].

Moreover, the additional oxidative stress generated by other ROS produced during this process must be also considered as responsible of damage. It is reported that the regulator of the general stress response (RpoS), the superoxide response regulon (SoxRS) and the trans-activator of the response to H_2O_2 (OxyR) show an important role in bacterial protection against ozonation [Patil *et al.,* 2011]. In the previous study reported in Chapter 4, the higher resistance of *S. enteritidis* compared with *E. coli* O157:H7 was also observed towards H_2O_2/solar process, attributing the upregulation of these regulators as the possible differences between both bacteria. Therefore, the bacterial response to oxidative stress may also contribute to explain the observed high resistance (few minutes) of *S. enteritidis* to ozonation compared with *E. coli*.

A wide spectrum of results in fresh-cut wash water disinfection by ozonation can be found in literature, with disinfection results varing from 0.5-5 LRV of bacteria (*E. coli*, total coliforms, *Listeria* sp, etc) using aqueous O_3 doses from 0.5 to 25 mgO_3/L and also different treatment times (from a few minutes to 60-90 min) [Smetanska *et al.,* 2013]. Therefore, the required ozone dose and treatment time for water disinfection depend on many factors such as the target microorganism, the physic-chemical water characteristics and also the mass transfer of ozone from the gas to the liquid phase, although in all these case-studies the benefit of using ozonation is clearly demonstrated for treating FCWW.

7.2. Organic microcontaminants removal

To compare the global efficiency of each operational condition, the total load of the OMCs investigated was analyzed and results are shown in Figure 7.2 and Table 7.1.
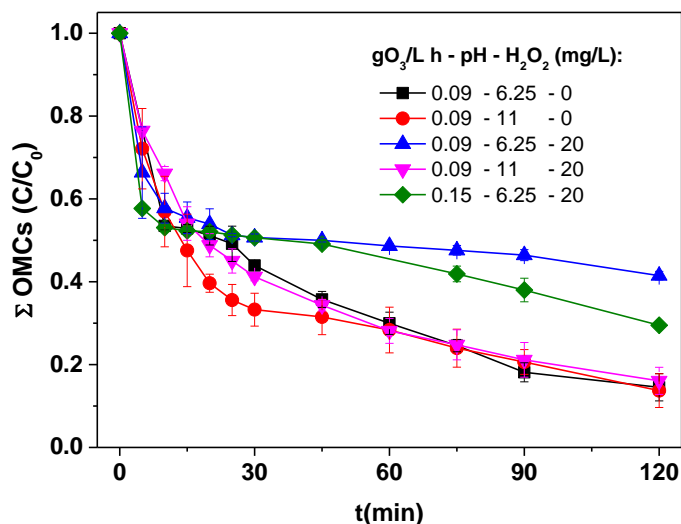
Figure 7.2. Comparison of ΣOMCs degradation profiles by ozone and peroxone processes.

For the first 15 min of treatment, results did not show any significant differences, reaching 50 % of ΣOMCs removal. After that, ozone with 0.09 gO_3/Lh at pH 6.25 and 11 and peroxone treatment with 0.09 gO_3/Lh at pH 11 reached more than 50 % of ΣOMCs degradation in 30 min; with a slightly better performance of ozone treatment with 0.09 gO_3/Lh at pH 11 (70 % of ΣOMCs removal). From 30 to 120 min, no differences were observed between these operational conditions, reaching ca. 85 % of ΣOMCs removal in all cases. Therefore, and similarly to bacterial inactivation results, it can be concluded that the best condition for ΣOMCs removal from SFCWW is the ozone treatment with 0.09 gO_3/Lh at the natural water pH (6.25), being the direct O_3 oxidation at this condition the dominant pathway for OMCs degradation.

In addition, the results of individual OMCs degradation by each ozonation operating condition are shown in Figure 7.3.
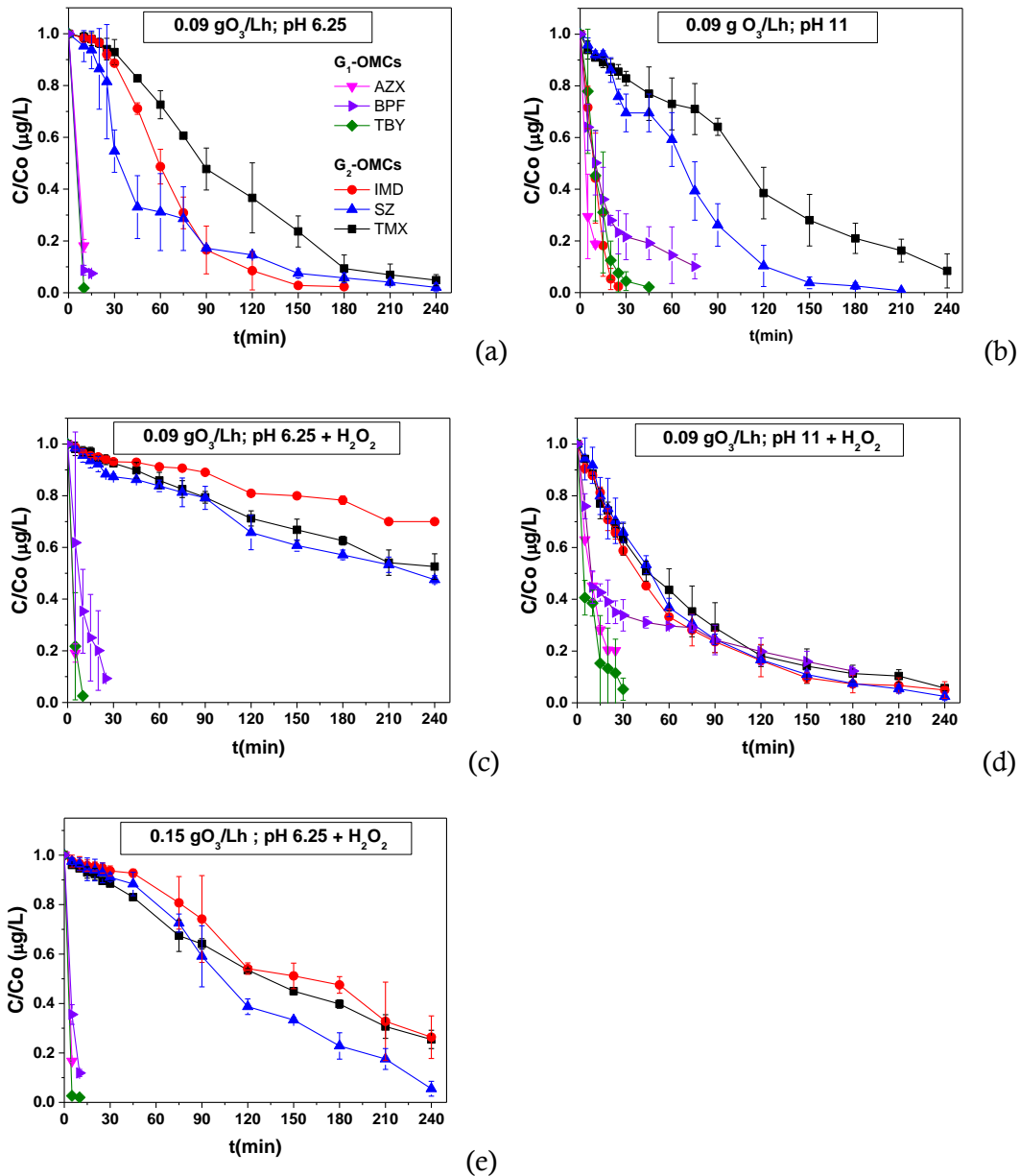
Figure 7.3. OMCs degradation by ozonation with 0.09 gO$_3$/Lh at pH 6.25 (a); pH 11 (b); and peroxone at pH 6.25 (c); at pH 11 (d); and peroxone with 0.15 gO$_3$/Lh at pH 6.25 (e).

In all cases, two groups of OMCs can be differentiated according to their degradation resistance: G$_1$-OMCs (azoxystrobin, buprofezin and terbutryn) and G$_2$-OMCs (imidacloprid, simazine, and thiamethoxam). In general, a similar trend was observed for both groups of OMCs in all operating conditions tested, G$_1$-OMCs were completely removed reaching in all cases the limit of

quantification (LOQ); while G_2-OMCs revealed different rates of degradation depending on the operating conditions.

The degradation profile of each OMC at the best operational condition, i.e., $0.09 \, gO_3/Lh$ at the natural water pH (6.25), showed a faster removal of G_1-OMCs [Terbutryn (*k:* $6.69x10^{-3}$ min^{-1}) > Buprofezin (*k:* $3.04x10^{-3}$ min^{-1}) > Azoxystrobin (*k:* $2.85x10^{-3}$ min^{-1})] compared with G_2-OMCs [Imidacloprid (*k:* $3.96x10^{-4}$ min^{-1}) > Simazine (*k:* $2.70x10^{-4}$ min^{-1}) > Thiamethoxam (*k:* $2.22x10^{-4}$ min^{-1})]. This kinetic behaviour can be explained based on the OMC chemical structures, discarding any effect based on its speciation due to the fact that all target OMCs have a pKa value below the water pH, except imidacloprid, which will be in protonated form (Table 3.2, Chapter 3). A similar behaviour was previously reported for the abatement of a mix of organophosphate esters, where two different kinetics rates were also observed for two contaminant groups depending on their chemical structure [Yuan *et al.,* 2015].

The degradation mechanism of OMCs by direct ozone attack is based on an initial electrophilic attack, and therefore the presence of electron-rich moieties (π bonds with delocalized electrons, electron-rich heteroatoms, electron withdrawing groups (EWG) and electron donating group (EDG)) in the OMC structures is the key to understand the fast degradation of G_1-OMCs [Hübner *et al.,* 2013].

In particular, for G_1-OMCs, terbutryn and buprofezin contains electron-rich heteroatoms (sulfurs and nitrogens) with hydrogen available in α position respect to the heteroatom; buprofezin also have a π system (benzene ring) [Barletta *et al.,* 2003]. Azoxystrobin contains several electron rich-moieties as the acrylate double bond and alcoxybenze groups.

For G_2-OMCs, the lower kinetic rates observed for the neonicotinoid pesticides (imidacloprid and thiamethoxam) can be explained by the presence of high oxidated groups (NO_2^-) in their structure which are resistant to ozone and radical oxidation. The higher resistance of simazine (a triazine G_2-OMCs) respect to terbutryn (other triazine G_1-OMCs) is peculiar, as both contain a triazine ring.

This can be due to the absence of sulfur in simazine side chains, while it has a electron withdrawing group (Cl^-) that confers less susceptibility to an electrophilic attack [Chen *et al.,* 2008].

On the other hand, results of the peroxone process investigated at natural and basic pH showed that in all cases, the ΣOMCs and bacterial kinetic rates were lower than the obtained for conventional ozone at natural SFCWW pH (Figure. 7.1 and 7.2 and Table 7.1). This result, although unexpected, can be explained based on several reasons. Among them, recent mechanisms studies report that the HO$^\bullet$ generation yield in this process is near to 0.5 instead to 1 (the commonly accepted yielding) [Merenyi *et al.,* 2010, Fischbacher *et al.,* 2013]. The proposed mechanism for the low yield observed is based on an adduct formation (HO_5^-) (Eq.1.4) which can decompose through 2 different ways (Eq. 1.5-1.6), of which only one yields HO$^\bullet$ (Eq. 1.5). Taking into account these latest findings, the potential treatment benefits by H_2O_2 addition during ozonation may be only based on the faster ozone decomposition into HO$^\bullet$ and not also on the higher radical yields, as accepted until now.

The detrimental effect observed by H_2O_2 addition was higher at natural pH than basic pH, which can be explained due to the reaction between O_3 and HO_2^- (Eq. 1.4) present a much lower rate constant at near-neutral pH as a consequence of the high pKa value (11.8) of H_2O_2 [Nothe *et al.,* 2009].

The lower efficiency of peroxone process observed has been previously reported in literature and can be attributed to several reasons: i) the lower O_3 concentration in solution (showed and explained in next section) which gives rise to lower removal rates of the ozone-reactive targets [Collivignarelli *et al.,* 2017; Lee *et al.,* 2014]; ii) dual role of H_2O_2 in combination with O_3, since H_2O_2 may act as scavenger of HO$^\bullet$ when is in excess in the sample [De Torres-Socías *et al.,* 2013]; and iii) the low O_3 stability (fast depletion) in complex water matrices where the O_3 react preferentially with some water constituents over H_2O_2 resulting in lower HO$^\bullet$ yields [Wang *et al.,* 2018].

In the specific case of SFCWW, the three reasons explained above can contribute to the lower efficiency observed taking into account the fast ozone depletion in this water matrix: 45 mg/L of DOC, high quantity of suspended solids (100 NTU) and presence of nitrite ions (0.15±0.03 mg/L). Therefore, the fast ozone decrease required a higher ozone concentration in solution. In fact, this observation was confirmed in this study where the efficiency of the overall process (simultaneous removal of OMC and bacteria) improved by increasing the inlet of O_3 in the peroxone process from 0.09 to 0.15 gO_3/Lh (Figure 7.1 and 7.2).

DOC was also monitored and its removal was only observed for the two processes at basic pH, where the expected major oxidant substance is HO˙, with removal percentages lower than 20 %. DOC values decreased from an initial value of 45 to 40 mg/L (11 %) and 37.5 mg/L (17 %) at the end of ozonation and peroxone processes at basic pH, respectively.

7.3. Reagents consumption and bromate generation

The profiles of ozone in the aqueous solution, and ozone and H_2O_2 consumptions along the ozonation experiments are shown in Figure 7.4 (a), (b) and (c), respectively.

Focusing on the first stage of the process (30 min of treatment), ozone consumption was similar at natural and basic pH, detecting 19 and 18 mg/L, respectively. In peroxone treatment (O_3/H_2O_2) at 0.09 gO_3/Lh, the consumption of ozone increased at both pHs, being significantly higher (40 mg/L) at natural pH.

Regarding H_2O_2 consumption, no significant differences were observed between all peroxone tests at 0.09 gO_3/Lh; while a slightly higher demand on H_2O_2 consumption was obtained when ozone generation increased to 0.15 gO_3/Lh.

All the results obtained for bacteria and OMCs removal can be correlated with ozone consumption, and although it was much higher for all the conditions

compared with ozone treatment at natural pH (Figure 7.4 (a)), these higher ozone consumptions suggest that under these operational conditions, the ROS generation is the predominant pathway, enhancing the DOC elimination but not specifically favoring the degradation of the target pollutants (bacteria and OMCs), and therefore the direct attack of ozone at natural SFCWW pH obtained the better target rate removals.

As was explained previously (Chapter 1, Section 1.6.1.1), the potential generation of the toxic by-product during wastewater ozonation represent one of the most important drawbacks of this process. Its generation depends on several factors of which the initial bromide concentration and the ozone dose applied play a key role. Previous studies reported that the bromate yields formation after wastewater ozonation is in the range of 3 to 5 %. Therefore, considering this yield conversion in the most conservative condition (i.e., 5 %), the theoretical bromate concentration expected in this water matrix (with a measured content of bromide of 0.10 ± 0.03 mg/L) will not be higher than 10 µg/L, which is below the limits recommended for the environment and similar to the maximum allowed value in drinking water legislations [Soltermann *et al.*, 2017; Rizzo *et al.*, 2019]. In this regard, bromate was measured with ionic chromatography in all the experimental conditions tested and it was never detected values above 50 µg/L (the LOD of this technique), confirming the environmental quality standard recommended, which is the objective of this research.
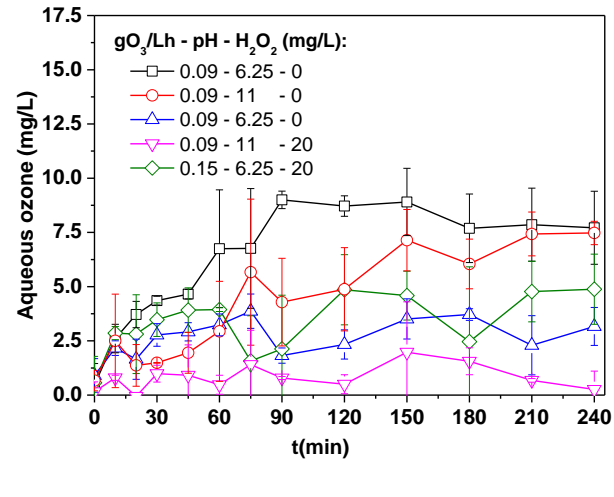
(a)
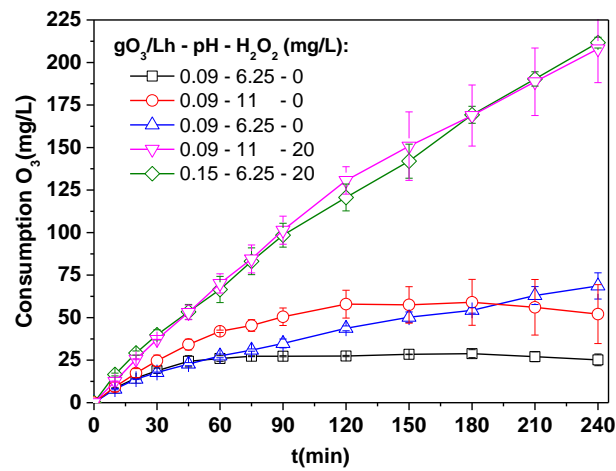
(b)
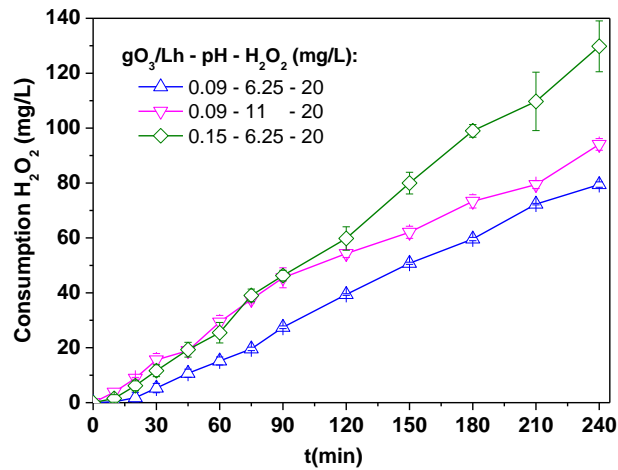
(c)

Figure 7.4. Aqueous Ozone (a), ozone consumption (b) and H_2O_2 consumption (c) obtained during ozone and peroxone processes.

7.4. Conclusions of Chapter 7

The application of ozonation treatment in agro-food wastewater has been proven to be an effective treatment and a good option for reducing high load of microbial (> 5-LRV) and OMCs (>80 % removal) from SFCWW.

From the different operational conditions tested, the simplest condition (i.e., ozonation at natural pH) leads the higher kinetics rates for both chemical and biological pollutants.

At this operational condition, the ΣOMCs were removed up to 85 % from SFCWW requiring an O_3 consumption of 27.4 mgO$_3$/L and 120 min of treatment time. For bacteria, >5-LRV of *E. coli* O157:H7 and *S. enteritidis* was achieved in less than 10 min with an ozone dose < 8.6 mg/L.

Finally, the inactivation of bacteria and OMCs degradation mechanisms have been correlated with the different oxidation ways of ozone and its chemical and biological characteristic. In general, *S. enteritidis* showed higher resistance to be inactivated than *E. coli*. Regarding OMC, the order of degradation was found to be: G_1-OMCs (Terbutryn > Buprofezin > Azoxystrobin) > G_2-OMCs (Imidacloprid > Simazine > Thiamethoxam)

CHAPTER 8

SFCWW REUSE: ASSESSMENT OF PATHOGENS AND OMCs UPTAKE IN RAW-EATEN CROPS

8. SFCWW REUSE: ASSESSMENT OF PATHOGENS AND OMCs UPTAKE IN RAW-EATEN CROPS

In this chapter, the safe reuse of treated SFCWW for irrigation in agriculture has been assessed. The presence and quantification of microbial pathogens (*E. coli* O157:H7 and *S. enteritidis*) and OMCs (atrazine, azoxystrobin, buprofezin, procymidone and terbutryn) in two raw eaten vegetables (radish and lettuce) has been studied.

Irrigation tests were conducted using treated SFCWW by the best operational conditions obtained for each treatment investigated in this research, i.e., H_2O_2/solar with 20 mg/L of oxidant, Fe^{3+}-EDDHA/H_2O_2/solar with two reagents combinations: 2.5/20 and 5/40 mg/L of Fe^{3+}-EDDHA and H_2O_2 (Chapter 6) and ozonation at natural SFCWW pH (Chapter 7).

During the crops irrigation time (maximum 3 months), several treated SFCWW batches were obtained for each water treatment. Each treated SFCWW batch was stored at 4 °C for no longer than one week, and during this storage period, OMCs, bacteria and reagents were also monitored.

In addition to the aforementioned irrigation tests, two control irrigation tests were performed in order to stablish references of crops contamination using the best ('negative control', mineral water) and worst conditions ('positive control', untreated SFCWW) in terms of chemical and microbiological contamination.

Finally, the chlorophyll content in lettuce leaves was analysed as a key parameter to determine the potential physiological benefit of the iron chelate (Fe^{3+}-EDDHA) employ in this research as source of iron for SFCWW reclamation by solar processes.

8.1. Treated SFCWW: treatment and storage monitoring

The number of SFCWW treated batches during the irrigation tests varied depending on several parameters: i) the volume of treated water obtained in each pilot plant, i.e., 10 L per ozonation treatment and 60 L per solar processes; and ii) the crops water demand during the irrigation period. The experimental procedure and the initial concentration of bacteria and OMCs were the same than that described in previous chapters. Nevertheless, during the treatment time, only the initial and final pollutant concentrations (at 240 and 300 min for ozone and solar experiments, respectively) were evaluated with the aim to control the effectiveness of each treated batch.

In the case of solar processes, a total of 7 batches (420 L of total treated water) per each solar process were performed in different days. The summarized information of the conditions and microbiological quality obtained for each solar treated SFCWW batch is shown in Table 8.1.

In the case of ozonation treatment, a total of 10 batches (100 L of SFCWW) were obtained, during which similar operational conditions were used than the

described in Chapter 7 and bacterial load were under the detection limit of the filtration technique (1CFU/100 mL) for the ozonated SFCWW batches.

Table 8.1. Summary of UV irradiance, dose, Q_{UV} and bacterial load of all solar treated SFCWW batches obtained during the crops irrigation period.

	Date*	Averaged UV-irradiance (W/m²)	Dose (Wh/m²)	Q_{UV} (kJ/L)	*E. coli* O157:H7 (CFU/100 mL)	*S. enteritidis* (CFU/100 mL)
H₂O₂/solar (20 mg/L)						
Batch 1	27/09/2018	39.3±9.2	177.5	53.1	9	0
Batch 2	03/10/2018	40.6±7.0	181.1	54.9	5	0
Batch 3	17/10/2018	35.8±9.1	159.7	48.4	8	2
Batch 4	24/10/2018	34.4±7.1	162.6	49.2	3	0
Batch 5	06/11/2018	36.0±4.4	164.4	48.4	6	0
Batch 6	27/11/2018	28.9±4.7	131.4	38.9	9	1
Batch 7	04/12/2018	30.0±4.3	137.3	40.4	7	2
Fe³⁺-EDDHA/H₂O₂/solar (2.5/20 mg/L)						
Batch 1	03/04/2019	44.0±7.9	195.6	59.4	0	1
Batch 2	09/04/2019	44.9±8.7	199.4	60.6	1	0
Batch 3	16/04/2019	42.4±9.1	192.7	57.3	0	0
Batch 4	24/04/2019	45.3±8.4	201.7	61.2	4	0
Batch 5	30/04/2019	44.5±6.7	198.3	60.1	1	0
Batch 6	07/05/2019	45.3±6.7	202.0	61.2	0	0
Batch 7	16/05/2019	44.0±6.3	196.3	59.4	1	0
Fe³⁺-EDDHA/H₂O₂/solar (5/40 mg/L)						
Batch 1	29/09/2018	42.0±7.1	187.1	56.7	0	0
Batch 2	03/10/2018	40.8±7.2	183.7	54.7	0	0
Batch 3	19/10/2018	17.7±3.9	78.4	24.0	1	0
Batch 4	25/10/2018	37.2±6.7	162.2	50.2	5	0
Batch 5	07/11/2018	35.4±4.5	162.1	47.7	2	0
Batch 6	27/11/2018	28.9±4.8	132.2	38.8	3	0
Batch 7	04/12/2018	29.9±4.6	137.5	40.2	2	0

*All solar tests were initiated at similar local time (10:30-11:00 am).

The inactivation of both bacteria obtained at the end of all treated SFCWW batches (Table 8.1) was higher than 5-LRV, reaching the limit of detection of 2 CFU/mL using the plate count technique and lower than the limit of the restrictive European proposal (10 CFU/100 mL). These results agree with previous chapters (Chapters 6 and 7) reinforcing the robustness of the water disinfection capability of the processes assessed. Nevertheless, it should be noted that in the case of the H₂O₂/solar process, the *E. coli* O157:H7 concentration detected in the treated SFCWW batches was the highest (7±2 CFU/100 mL), an

important data that must be considered to evaluate the microbiological load of the irrigated crops.

The averaged OMCs concentration of the water batches generated for each treatment is shown in Table 8.2. The ΣOMCs percentage removal in all cases agree with the results previously reported in Chapters 6 and 7, according to the following efficiency order: ozone > Fe^{3+}- EDDHA/H_2O_2/solar (2.5/20 mg/L) > Fe^{3+}-EDDHA/H_2O_2/solar (5/40 mg/L) > H_2O_2/solar (20 mg/L). It is important to note that, in general at the end of the solar processes, more than the 50 % of the initial concentration of OMCs still being detected, and procymidone and atrazine showed to be the most recalcitrant OMCs with the slightly highest residual concentrations. Therefore, these data must be considered to evaluate the crops uptake of OMCs after the irrigation period.

Table 8.2. Average of OMCs concentration in the reclaimed SFCWW by solar and ozone processes employed to crops irrigation.

Process	[OMC] after treatment (µg/L)					Total load (µg/L)	Removal %
	ATZ	AZX	BPF	PCM	TBY		
Ozone	2±1	11±8	6±4	29±8	4±3	52±24	90
H_2O_2/solar	83±20	70±13	82±18	88±12	73±33	397±96	21
Fe^{3+}- EDDHA/ H_2O_2/solar (2.5/20 mg/L)	66±3	73±14	39±33	66±11	55±10	299±71	40
Fe^{3+}- EDDHA/ H_2O_2/solar (5/40 mg/L)	77±14	61±12	55±26	65±17	68±20	327±90	35

Once a treated SFCWW batch was obtained, it was stored and used as required for crops irrigation for no longer than one week. At real or industrial scale, storage facilities are not considered a step in the treatment process, but they play a critical role between the water treatment and the irrigation system being their main functions: equalization of daily flow variations and storage water excess [FAO, 1992]. In addition, it is very well known that during storage time the water composition (chemical and microbiological) can vary especially if the

water matrix contains organic matter due to it provides nutrients for cells metabolism and consequently, microorganisms (bacteria) in reclaimed water may have the potential to reactivate and grow during the storage process [Li *et al.*, 2013]. Therefore, the monitoring of the treated SFCWW quality prior to vegetables irrigation is required considering its high DOC content: 25 mg/L in the case of SFCWW treated by ozone and H_2O_2/solar whereas 34 and 43 mg/L for reclaimed water by Fe^{3+}-EDDHA/H_2O_2/solar with 2.5 and 5 mg/L of Fe^{3+}-EDDHA, respectively.

The bacterial regrowth of the reclaimed SFCWW by all the processes studied was assessed during 3 and 7 days of water storage and the averaged results obtained are shown in Figure 8.1. In the case of *S. enteritidis*, the concentration was in all cases below the limit of detection (1 CFU/100 mL). Regarding *E. coli* O157:H7, its concentration detected was lower than the limit established by both, Spanish RD 1620/2007 (100 CFU/100mL) and the last and more restrictive European proposal (10 CFU/100mL) for wastewater reclamation [RD, 2007; COD, 2019]. Therefore, these results demonstrate the suitability of the processes for the reclamation of SFCWW for irrigation purposes.
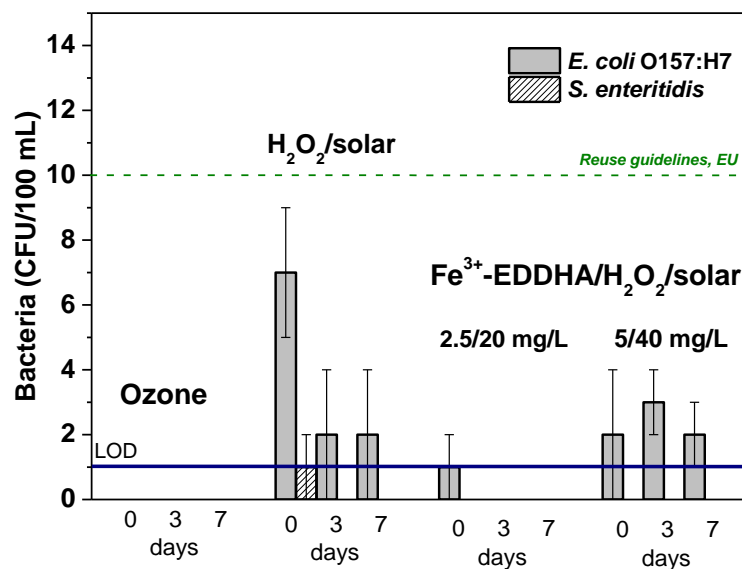
Figure 8.1. Monitoring of bacteria concentration in treated SFCWW by all processes (solar and ozone) after 3 and 7 storage days.

Regarding OMCs, no significant variations in their concentration were observed for any process during the SFCWW storage for a week compared with the data obtained in Table 8.2. This effect indicates also that any oxidative process after the treatment occurs during the storage time, effect that is related with the residual reagents concentration in the case of the solar processes.

Therefore, the analysis of the residual H_2O_2 concentration is important due to avoid a possible bacterial regrowth during the storage of reclaimed water [LeChevallier, 1999]. On the other hand, the monitoring during storage time can also provide important information about the suitability of the processes studied, mainly in the case of the Fe^{3+}-EDDHA processes which objective is water reclamation providing at the same time the iron needed for the vegetables metabolism.

The profile of dissolved iron and H_2O_2 concentration during water storage is shown in Figure 8.2. In general, both reagent concentrations decrease along the storage time for all the conditions tested.

The trend observed for the H_2O_2 concentration for the three solar conditions studied was similar: a H_2O_2 concentration decrease of 26±2 and 37±2 % after 3 and 7 storage days, respectively. As was explained previously (Chapter 6), the H_2O_2 decomposition observed is mainly caused by its interaction with the water matrix constituents which did not varied significantly for the different processes. Nevertheless, and although the residual H_2O_2 concentration decrease during storage, in view of the results discussed above its residual concentration appears to be enough to avoid bacteria regrowth during the storage time.

Nevertheless, no significant decrease on dissolved iron was observed during the storage time for Fe^{3+}-EDDHA/H_2O_2/solar process at the two conditions tested of 2.5 and 5 mg/L of Fe^{3+}-EDDHA, which ranged from 0.36 to 0.32 mg/L and from 1.52 to 1.46 mg/L, respectively.
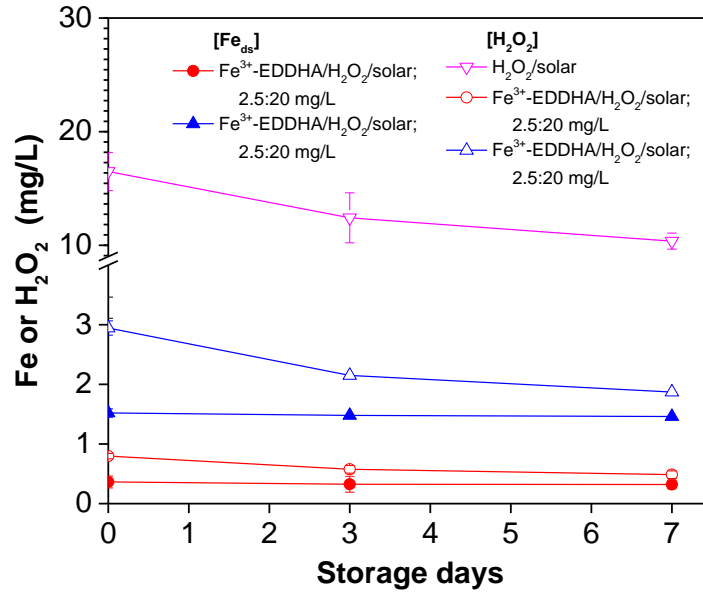
Figure 8.2. H_2O_2 (empty symbols) and dissolved iron (full symbols) measured during treated water SFCWWstorage time.

8.2. Microbiological assessment of peat and irrigated crops

The microbiological results obtained for the harvested crops including corresponding peat irrigated with the negative control (mineral water) showed, as expected, total absence of both pathogens in all samples analyzed. These results confirm the no cross-contamination by any external factor, ensuring the accuracy and reliability of the results.

The presence/absence of *E. coli* O157:H7 and *S. enteritidis* in the crop samples and peat irrigated with untreated SFCWW (positive control) and treated SFCWW by all the processes and conditions studied is shown in Table 8.3.

The samples irrigated with untreated SFCWW showed the presence of both bacteria at high concentrations in all the samples analysed of lettuce leaves, radish and peat. These results confirmed the high health and environmental risk associated with the direct reuse of SFCWW without a previous treatment. And although these results were expected, the following general findings can be noted:

i) In all samples analysed (crops and peat) a higher concentration of *S. enteritidis* compared with *E. coli* O157:H7 were obtained. In literature, it has been reported that *Salmonella* genus has a higher survival capability in nutrient-poor and non-host environments compared with *E. coli* [Winfield and Groisman, 2003], which may explain the higher detection observed also in this study. Moreover, the survival of *S. typhimurium* in soils has been reported previously as ca. 1.39 times longer than the survival time of *E. coli* O157:H7 [Semenov *et al.*, 2009].

On the other hand, the higher presence observed for *S. enteritidis* in both crops are also in concordance with a previous study where the association of *Salmonella* with plant stomata was ca. 1.8 times higher in comparison with *E. coli* O157 [Van der Linden *et al.*, 2016].

ii) The presence of high bacterial load in peat compares with the results obtained in crops. The watering favors the accumulation of water (humidity) in the crops rhizosphere, favoring therefore the survival of microorganism and the transmission of pathogens contamination in this environment.

These high bacterial load concentrations observed in peat samples increase the risks of crop contamination as the transmission of *E. coli* O157:H7 and *S. enteritidis* from contaminated soil to lettuce plants has been previously demonstrated through both: adsorption and absorption. Several studies have reported the capability of microbial pathogens to penetrate in the internal crops tissues through roots absorption and their subsequent translocation and survival in the edible plant tissues up to the harvesting time [Ávila-Quezada *et al.*, 2010; Chitarra *et al.,* 2014; Murphy *et al.,* 2016].

iii) Regarding the differences observed between both crops, a higher bacterial load was observed in the root vegetable (radish) as consequence of its higher contact with the contaminated peat.

iv) On the other side, the irrigation practice using water with a high microbiological contamination has also associated an environmental risk due to the microorganisms present in soils are able to move through the soil profile

(percolation) after rainfall or irrigation events; reaching the groundwater and contaminated it. This percolation capability and therefore the associated environmental risk has been demonstrated for several pathogens included *E.coli* O157:H7 and *S. Typhimurium* [Semenov *et al.*, 2009].

Table 8.3. Detection of *E. coli* O157:H7 and *S. enteritidis* in lettuce and radish crops and peat irrigated with untreated SFCWW (positive control) and treated SFCWW by all selected water treatments.

Sample	Pathogen	Untreated	Ozone	H_2O_2/solar	Fe^{3+}-EDDHA/H_2O_2/solar (2.5/20 mg/L)	Fe^{3+}-EDDHA/H_2O_2/solar (5/40 mg/L)
Lettuce						
Leaves	*E. coli*	**33/33 (60 CFU/g)**	0/33	**1/33 (LOD)**	0/33	0/33
	S. enteritidis	**33/33 (75 CFU/g)**	0/33	0/33	0/33	0/33
Peat	*E. coli*	**33/33 (1060 CFU/g)**	0/33	0/33	**3/33 (54CFU/g)**	0/33
	S. enteritidis	**33/33 (1384 CFU/g)**	0/33	0/33	0/33	0/33
Radish						
Fruit	*E. coli*	**33/33 (296 CFU/g)**	0/33	0/33	0/33	0/33
	S. enteritidis	**33/33 (754 CFU/g)**	0/33	0/33	0/33	0/33
Peat	*E. coli*	**33/33 (818 CFU/g)**	0/33	0/33	**1/33 (81CFU/g)**	0/33
	S. enteritidis	**33/33 (1228CFU/g)**	0/33	0/33	0/33	0/33

* Number of positive detected samples / Total samples analized, i.e., 33.
In all the positive detected samples, the bacterial concentration measured is included in brackets.
Limit of detection (LOD): 1 CFU/3g for lettuce, 1 CFU/8g for radish and 1 CFU/5g of peat.

The microbiological results from the analysis of lettuce and radish irrigated with treated SFCWW by ozone and solar processes show the absence of *E. coli* O157:H7 and *S. enteritidis* in all the analysed samples in peat and plant tissues with exception of one positive sample in lettuce leaves by *E. coli* O157:H7 in the case of H_2O_2/solar process detected at the LOD (Table 8.2) and two positives by *E. coli* O157:H7 in peat samples irrigated with Fe^{3+}-EDDHA/H_2O_2/solar process with 2.5/20 mg/L of reagents.

The detection of *E. coli* in these samples were unexpected due to the high susceptibility demonstrated during the solar treatments, nevertheless during the storage time, *E. coli* was still being detected at very low concentration and even

below the European legislation for WW reuse. Therefore, these results demonstrate that the water treatment applied to reclaim SFCWW must accomplish one of the following statements, i.e., a strong oxidative capability (as is the case of o zonation) and/or to keep residual oxidative reagents (as in the case of the Fe^{3+}-EDDHA/H_2O_2/solar process with high reagents concentrations, i.e., with 5/40 mg/L.

Regarding the solar photo-Fenton treatments, it should be noted that the addition of iron and its subsequent accumulation in peat during the irrigation may alsoreact with the residual H_2O_2 through Fenton and Fenton-like reactions generating an additional bactericidal effect in the rhizosphere environment. In fact, in this study, enough residual concentration of reagents must to be present in the peat and accumulated during irrigation to permit these possible reactions. To investigate this effect, the iron content in the peat irrigated with treated SFCWW from each solar process was measured. Results showed that in the case of 2.5/20 mg/L of reagents no iron concentration was detected (<LOD; 0.045 mg/kg); while 0.19±0.11 and 0.39±0.10 mg/kg for lettuce and radish peat was measured in the case of 5/40 mg/L of reagents, and no presence of any bacteria was detected in peat in this case. In this regard, a recent study also reports the capability of the Fenton-like process with Fe^{2+}-EDDHA as source of iron for the decontamination of soils [Ma *et al.,* 2018].

In general, the results obtained show the absence of the two pathogens studied when the SFCWW was previously treated until achieve the bacterial concentration allowed for the irrigation of raw-eaten crops according to the European legislation. Moreover these results are in agreement with previous studies reported in literature for the reuse of wastewater treated by H_2O_2/solar and the solar photo-Fenton processes, where complete absence of bacteria in crops irrigated with treated wastewater was demonstrated [Bichai et al., 2012; Ferro et al., 2015b; Aguas et al., 2019].

8.3. OMCs uptake and accumulation in crops and peat

Crops irrigation with reclaimed wastewater may allows the entry of the OMCs present in the irrigation source into the food chain as most of them are able to be taken up by the crops. The potential effect of these OMCs on human health is an issue of growing concern and therefore the assessment of OMCs uptake in crops irrigated with reclaimed wastewater is crucial to assess human exposure to these pollutants.

The most significant OMCs plant uptake pathways are root uptake and further diffusion through deposition on plant surfaces. OMCs enter in the growing roots through their tips epidermis, after that their pass through the cortex and endodermis reaching the vascular tissues (xylem and/or phloem). Finally, they are distributed forced by the transpiration derived mass flow and translocated to aboveground tissues (mainly to transpiring organs as leaves) [Christou *et al.,* 2019].

Although the plant uptake and the subsequent translocation appears to be a simple process, there are several factors involved in both processes as biotic and abiotic parameters such as crop's genotype, soil characteristics, irrigation method and cultivation conditions, among others. However, as the irrigation essays of this study were performed under controlled conditions with the same biotic and abiotic parameters, the OMCs plant uptake will be mainly related with the physic-chemical properties of the target OMCs and the type of crops. The most important OMCs properties involved in their root uptake and subsequent transport through transpiration system are electrical charge and compound lipophilicity [Aguas *et al*., 2019].

In general, non-ionic OMCs, i.e., neutral species in soil solution and plant tissues are more susceptible to be uptaken by roots and subsequently translocated due to they are able to cross cell membranes easier than the ions which suffer electrical repulsion and therefore their transfer across membranes is slow [Martínez-Piernas *et al*., 2018; Christou *et al.,* 2019]. The pKa values of the five target OMCs in this study varies from 0.9 to 6.7 (Chapter 3, section 3.3), the pH value

of the peat solution is 7 and the plant physiology pH values varies from 5.5 (vacuoles and sap xylem) to 7 (cytoplasm) [Trapp, 2000]. Thus, all the OMCs of this study are neutral species being easily absorbed and transported in the plant system.

Moreover, the other important OMCs chemical descriptor for their plant uptake and translocation is the compound polarity or lipophilicity (log Kow). Polar OMCs (-1 < log Kow < 5) have shown to be easily uptaken and transported through the vascular system [Aguas *et al.*, 2019]. The log Kow values of the OMCs range from 2.5 to 4.93 (Chapter 3, Section 3.3) and therefore, based on their lipophilicity, all of them are also susceptible to be absorbed and accumulated in plant tissues.

The OMCs concentration quantified in radish and lettuce irrigated with treated and untreated SFCWW are shown in Figure 8.3. All the OMCs present in the irrigation water have been uptaken by both vegetables, as was expected based on their physic-chemical characteristics explained below. Regarding uptake differences between OMCs, procymidone and atrazine showed the higher uptake in both vegetables. These results can be explained based on the higher plant exposure to these OMCs as they are present at the highest residual concentrations after water treatments (Table 8.2).

Furthermore, the uptake results obtained showed a higher OMCs uptake capacity of lettuce than radish roots for all the irrigation essays. This behavior is in agreement with previous studies and it is explained based on the different plant physiology of lettuce and radish crops [Martínez-Piernas *et al.*, 2018; Aguas *et al.*, 2019]. The leafy vegetables (lettuce) are the crops with the highest ability to uptake and accumulate OMCs due to the high transpiration stream to leaves which is higher than the stream to fruits or roots. Nevertheless, and although their OMCs uptake and accumulation capability is lower in root crops (radish) than in leafy crops, this vegetables type has also shown a high OMCs uptake and accumulation capability as consequence of the direct contact between the edible

parts of these crops with the OMCs present in the soil solution which enable their penetration and accumulation in the root vegetables [Christou *et al.*, 2019].
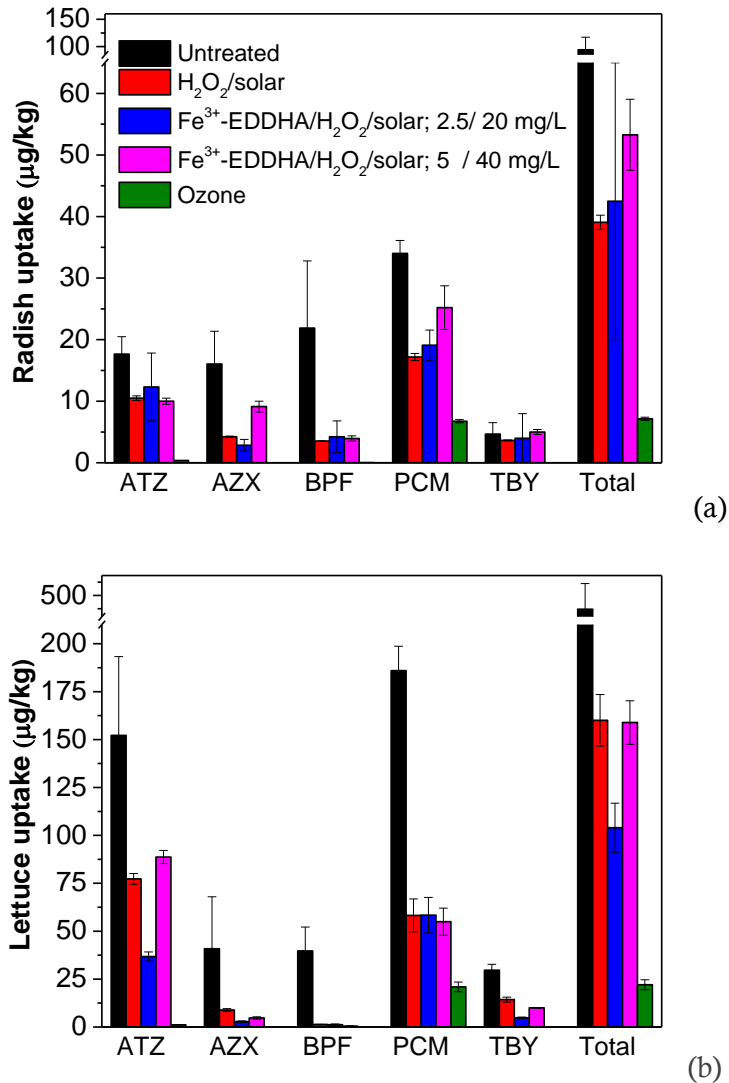
Figure 8.3. OMCs concentration (µg/kg) found in radish (a) and lettuces (b) watered with untreated and treated SFCWW.

The uptake results evidence the capability of all the processes studied (ozonation and solar processes) to reduce the OMCs crops uptake. The total OMCs uptake in lettuce leaves when irrigated with untreated SFCWW, 448 µg/kg, was reduced to 22 and to <180 µg/kg for ozone and solar processes, respectively. In radish, OMCs uptake was also reduced from 94.3 µg/kg (untreated SFCWW) to 7.1 and to <55 µg/kg for ozone and solar processes, respectively.

As expected, the higher crops uptake reductions were observed for the crops irrigated with ozonated water with reductions of 95 and 92.5 % in lettuce and radish, respectively. Regarding solar processes, non-significant uptake differences were observed for radish irrigated by H_2O_2/solar and Fe^{3+}-EDDHA/H_2O_2/solar (2.5/20 mg/L) processes whereas in lettuce the Fe^{3+}-EDDHA/H_2O_2/solar process was the most efficient. Therefore, from a general point of view taking into account both crops, the more efficient solar process to reduce crops uptake was the photo-Fenton-like process with the lower reagents combination, i.e., Fe^{3+}-EDDHA/H_2O_2/solar process with iron chelate and oxidant concentrations of 2.5 and 20 mg/L.

Furthermore, it is also important to note that the crops irrigated by the Fe^{3+}-EDDHA/H_2O_2/solar process with the highest reagents combination (5 and 40 mg/L) showed higher OMCs uptake in radish and similar in lettuce than the process H_2O_2/solar. This result is unexpected taking into account the higher treatment capability of the Fe^{3+}-EDDHA/H_2O_2/solar process and therefore the lower crops exposure to OMCs. However, it is possible that the presence of high iron micronutrient concentrations can increase the metabolic activity of the crops and their uptake capability.

On the other hand, OMCs concentration in crops is not regulated with the exception of the pesticides compounds, which are the target OMCs in this study. The maximum concentration allowed for these contaminants in vegetables is regulated by the Maximum residue levels (MRLs) according to the European Regulation (EC). No 396/ 2005 and subsequent amendments. A MRL value is '*the highest level of a pesticide residue that is legally tolerated in or on food or feed when pesticides are applied correctly*'. These values are stablished to different vegetables by the European Food Safety Authority (EFSA) according to the assessment of the consumers safety based on the compounds toxicity and the maximum levels expected in a European diet. The MLRs of the five OMCs are in general similar for lettuce and radish (10 µg/kg procimydone, terbutryn and buprofezin and 50 µg/kg for atrazine) being only different for azoxystrobin (1500 and 15000 µg/kg for radish and lettuce, respectively). A schematic summary of

compliance or not of the European MLRs for the harvested vegetables is presented in Table 8.4.

Table 8.4. Compliance (✓) or not (✗) of the European MLRs for each OMC in lettuce and radish crops irrigated with untreated SFCWW and treated SFCWW by all selected water treatments.

OMC	Untreated	Ozone	H_2O_2/solar	Fe^{3+}-EDDHA/ H_2O_2/solar (2.5/20 mg/L)	Fe^{3+}-EDDHA/ H_2O_2/solar (5/40 mg/L)
Lettuce					
ATZ	✗	✓	✗	✗	✗
AZX	✓	✓	✓	✓	✓
BPF	✗	✓	✓	✓	✓
PCM	✗	✗	✗	✗	✗
TBY	✗	✓	✗	✓	✓
Radish					
ATZ	✓	✓	✓	✓	✓
AZX	✓	✓	✓	✓	✓
BPF	✗	✓	✓	✓	✓
PCM	✗	✓	✗	✗	✗
TBY	✓	✓	✓	✓	✓

The OMCs concentration observed in the harvested lettuce irrigated with untreated SFCWW are above the MLRs for all the pesticides except for azoxystrobin (high MLR value). Although some of these limits are comply in the lettuce irrigated with reclaimed SFCWW; for ozone all the pesticides are below their MLRs except procymidone, for H_2O_2/solar process the buprofezin limit is now satisfied and for the Fe^{3+}-EDDHA/H_2O_2/solar process buprofezin and terbutryn. In radish irrigated with untreated SFCWW the concentration of buprofezin and procymidone are above their MLRs whereas both compounds are below their limits in the radish irrigated with ozonated water and finally, the radish irrigated by all the solar processes evaluated decreases the buprofezin concentration below its MLR being still detected at a concentration higher than the MLR only procymidone. In general, crops irrigation with reclaimed water is also able to decrease the OMCs uptake in both crops until satisfy the European legislation of some of the pesticides studied and therefore decrease the toxicological risk of their ingestion.

The accumulation of OMCs in soils and their persistence after crops harvested also represent an important health and environmental issue as the accumulated compounds are able to be uptaken in subsequent cultivation cycles and their percolation can contaminate aquifers. The OMC concentrations in the lettuce and radish peat were analyzed after crops harvesting and the results obtained are shown in Figure 8.4.

(a)

(b)
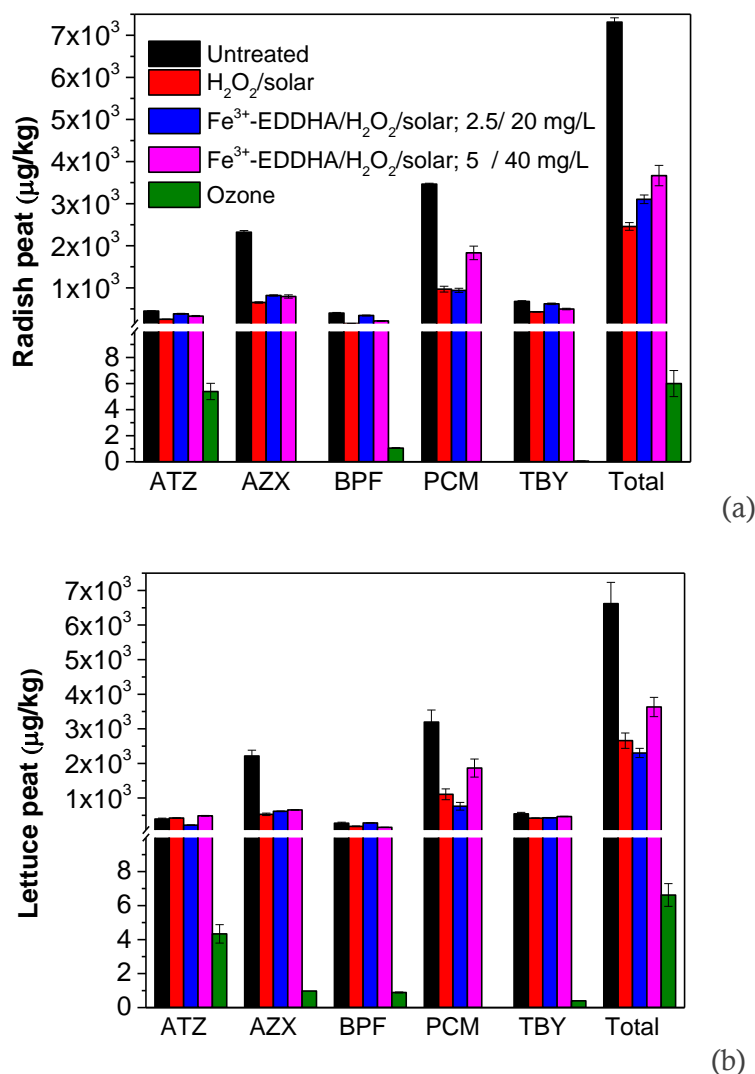
Figure 8.4. OMCs concentration (µg/kg) found in radish peat (a) and lettuces peat (b) watered with untreated and treated SFCWW.

The results obtained also showed the capability of all the processes studied to reduce the OMCs accumulation in peat for both crops of which ozone was again the more efficient process able to reduce >99 % the OMCs accumulation in the peat used for the cultivation of both crops. In the case of the solar processes, non-

significant differences were observed for the different processes neither for the different OMCs.

Additionally, and although the peat used for lettuce cultivation was watered more times than radish peat, the OMCs concentration was similar for both peats which can be explained by the higher plant uptake showed by lettuce crops and maybe by a higher OMCs degradation process in the rizosphere environment during the larger cultivation cycle.

8.4. Iron chlorosis risk: assessment of chlorophyll content

Despite the iron is present in large concentrations in most soils, its speciation in calcareous soils leads to iron precipitation not being available for plants uptake. It is estimated that approximately 30 % of the cultivable soils on Earth's surface (mainly in arid and semiarid regions) are calcareous.

On the other hand, for crops, iron is an essential micronutrient in the metabolism of photosynthetic pigments and chloroplast structures where more than 80 % of the cellular iron in leaf cells is inside them. So that, to increase the iron mobility and its uptake from soils, plants have developed different adaptive and physiological mechanisms, such as the known as Strategy I. This strategy is used by dicotyledonous plants as lettuce and radish, and it mainly consists on decreasing the rhizosphere pH to enhance Fe^{3+} reduction capacity by the roots.

Nevertheless, this physiologic mechanism is not enough in most cases to prevent iron plant deficiency or iron chlorosis. Accordingly, the iron chlorosis disease is a consequence of a chlorophyll synthesis reduction due to iron has an important role in enzymatic reactions involved in the synthesis of precursors of the chlorophyll molecule [Sbai and Haouala, 2018]. Chlorophyll is the main pigment in plants which main function is the photosynthesis process to provide plant energy. Therefore, iron chlorosis or chlorophyll deficiency is a disease that severely impact in crop healthy and consequently in the crop yield.

This important problem is ameliorated in intensive agriculture with the employ of micronutrient as chelates able to keep the iron in soluble forms enhancing its

bioavailability to the crops roots. Although there are several iron chelates Fe^{3+}-EDDHA has shown the higher efficiency in alkaline soils [Ylivainio, 2009]. Moreover, crops irrigation using iron chelates instead of iron salts has also the advantage to avoid the problems related to clogging in drip irrigation systems as consequence of iron precipitation.

An efficient use of iron chelate micronutrients is based on maximizing the plants iron uptake while minimizing the applied iron chelate dosage to avoid excessive costs and environmental impact by accumulation of chemicals. Consequently, the determination of chlorophyll concentration of the samples irrigated with the iron chelate is a tool that allows assessing the fertigation efficiency.

Therefore, to determine the dual benefit of using the Fe^{3+}-EDDHA as chelate agent for photo-Fenton treatment as well as to avoid the risk of chlorosis on crops, the foliar chlorophyll content was analysed in the harvested lettuces irrigated by all the processes studied. The quantified chlorophyll values are shown in Figure 8.5. The mean chlorophyll a/b ratio was 3±0.3 for all the samples analysed which is in line with the expected value of a C_3 plant type as the lettuce plant [Parry *et al.*, 2014].

The chlorophyll content in the lettuce irrigated with the reclaimed SFCWW that incorporate the iron micronutrient, i.e., treated by Fe^{3+}-EDDHA/H_2O_2/solar process, was almost twice than the value of the lettuces irrigated by the other two processes (ozone and H_2O_2/solar). The foliar chlorophyll content in leafy vegetables can varies significantly in function of several parameters as the growing site, agricultural practices, cultivation cycle duration, weather, soil composition, and different sub-species, among others. In the case of lettuce, Both et al reported very different foliar chlorophyll contents depending of the sub-specie type: 245 and 29 mg/kg in lettuce and iceberg lettuce, respectively [Both *et al.,* 2014]. Slamet et al reported foliar chlorophyll contents of ca. 700 mg/kg [Slamet *et al.*, 2017]. Therefore, is not possible to stablish a rigorous comparison between the data obtained in this study and the reported in literature being only plausible to perform rough comparisons. In line with this, the chlorophyll values

measured in this study (ca. 100-200 mg/kg) are in the same order of magnitude than the reported values in other studies [Both *et al.,* 2014; Slamet *et al.*, 2017].
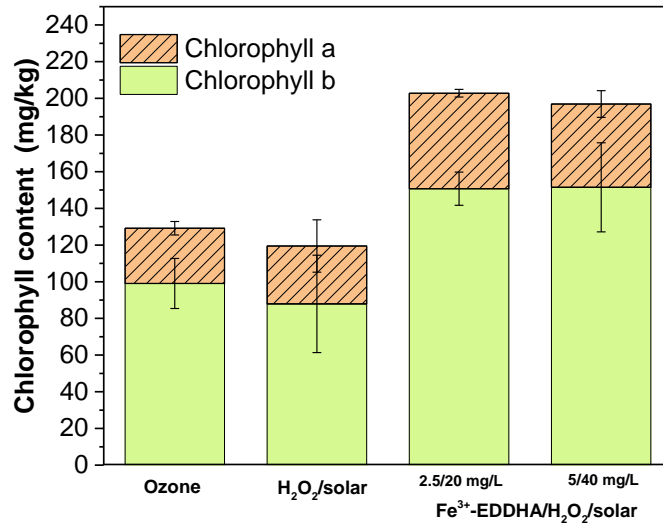
Figure 8.5. Foliar chlorophyll content of lettuce irrigated by all the processes assessed.

Moreover, non-significant differences were observed in the chlorophyll content of the two Fe^{3+}-EDDHA/H_2O_2/solar irrigation tests: 202.8±11.1 and 196.9±26.7 mg/L for 2.5 and 5 mg/L of Fe^{3+}- EDDHA, respectively. Therefore, in spite of the iron chelate dose used for the treatment, no differences were observed in the chlorophyll content of the two conditions. This indicate that the lower iron supplied (2.5 mg/L of Fe^{3+}-EDDHA) should be enough to garantee a good chlorophyll content, decreasing the risk of iron chlorosis.

8.5. Conclusions of Chapter 8

The reclamation of SFCWW by ozone or solar processes for vegetable irrigation was able to improve the microbiological and chemical quality of both SFCWW and raw-eaten vegetables. Ozone showed the best performance followed by the Fe^{3+}-EDDHA/H_2O_2/solar process with 2.5/20 mg/L of Fe^{3+}-EDDHA/H_2O_2.

The no bacterial regrowth observed along with the low variation of chemical water characteristics during the treated water storage point out the suitability of

the processes studied for the reclamation of SFCWW and its subsequent reuse for irrigation purposes.

The results obtained confirm the physiologic plant benefit of the employ of Fe^{3+}-EDDHA as iron source for solar water treatment and its subsequent reuse. Crops irrigation with SFCWW treated by the more efficient treatment condition (Fe^{3+}-EDDHA/H_2O_2/solar process with 2.5/20 mg/L of Fe^{3+}-EDDHA/H_2O_2) has also demonstrated to be the best operational condition to decrease the risk of iron chlorosis from the physiologic, cost and environmental point of view.

CHAPTER 9

SFCWW RECLAMATION AND REUSE: TECHNO-ECONOMIC, ENVIRONMENTAL AND HEALTH ASSESSMENT

9. SFCWW RECLAMATION AND REUSE: TECHNO-ECONOMIC, ENVIRONMENTAL AND HEALTH ASSESSMENT

In this chapter, the implementation viability of the global process, i.e., from fresh-cut wastewater treatment to its reuse for agricultural irrigation, was evaluated from the techno-economic, environmental and health point of view with the aim to evaluate the suitability of the processes studied to replace the commonly used industrial chlorination process (with 100 mg/L of chlorine).

The assessment was performed for the best operational conditions and treatments found in this study: H_2O_2/solar (20 mg/L); Fe^{3+}-EDDHA/H_2O_2/solar (2.5/20 and 5/40 mg/L) and ozone (0.09 gO_3/Lh at natural SFCWW pH).

The techno-economic assessment was performed through the estimation of the cost for each process to treat SFCWW taking into account investment, operational and maintenance costs (C_I, C_O and C_M).

Regarding the environmental evaluation, an ecotoxicity study of the treated SFCWW to estimate the impact of reclaimed SFCWW discharge with *Vibrio fischeri* and the suitability of the reclaimed SFCWW for its reuse in crops irrigation using *Lactuca sativa* was carried out.

Finally, a chemical and a microbiological health risk assessment of the harvested crops irrigated with untreated and treated SFCWW were also performed.

9.1. Industrial FCWW treatment costs

The economic analysis was performed considering the following assumptions:

- A volume of FCWW generated of 50 m^3/day (corresponding to a small or medium sized fresh-cut industry).

- The operation of the industry 365 days/year, which lead to the generation of 18250 m^3 of FCWW per year.

- A serviceable life of the equipment of 20 years and a 5 % interest rate, which leading to a capital recovery factor (CRF) of 8 %.

- The annual total cost was calculated considering the investment cost (C_I), operational cost (C_O) and maintenance cost (C_M).

- The treatment costs for ozonation and solar treatment of SFCWW were estimated according to the experimental data obtained (Chapters 6 and 7) for both: to comply with the current reuse regulations (SFCWW disinfection) and also for a simultaneous OMCs removal.

9.1.1. Chlorination costs

Industrial chlorination is a simple process and consists on the addition of a chlorination agent (normally a solution of sodium hypochlorite, NaOCl) and a

commercial buffering acid (normally H_3PO_4) to maintain the water pH between 6 and 7. This pH favors the chemical state of chlorine as hypochlorous acid (HOCl⁻), the highest antimicrobial power. Therefore, for the C_I estimation two pumps with alarm systems (3000 €/each) to dispense chlorine and acid solutions are required. The maintenance cost (C_M) of this pumping system is 1 % of the annual C_I. The C_O of the chlorination process was estimated considering:

- The cost of both reagents with a food grade quality: 0.29 €/L of a NaOCl 10 % (w/v) solution and 1.69 €/L of a H_3PO_4 85 % (w/v) solution.

- The volume to treat 1 m^3 of SFCWW: 1 L of NaOCl to reach the common chlorine concentration of 100 mg/L and 0.25 L of H_3PO_4 due to the buffering acid is usually added as a quarter of the NaOCl volume [Garret *et al.*, 2003].

A breakdown of the cost estimated for SFCWW chlorination is shown in Table 9.1.

Table 9.1. Breakdown of chlorination costs to treat 1m^3 of SFCWW.

Chlorination cost	€ /year	€/ m^3
C_I Pumps	480	0.03
C_O Reagents	13003	0.71
C_M 1 % of annual C_I	48	<0.01
Total cost	13531	**0.74**

The total unitary cost obtained to treat 1 m^3 of SFCWW was 0.74 €/ m^3. The reagents represent the main cost of the chlorination process, 96 %. The cost estimated are in agreement with a previous study where the estimated cost was ca. 0.6 €/m^3 [Garret *et al.*, 2003].

9.1.2. Ozonation costs

The C_I for the ozonation treatment was calculated considering the cost of the equipment including reactor and ozone generator costs (*PC*, plant cost, Eq. 9.1)

which represent the 17.6 % of the investment cost according to previous studies [Cañizares *et al.*, 2009].

$$PC = 1719.5 \cdot q^{0.6143}$$

Eq. 9.1

Where the required ozone production per hour (*q*) is the sizing parameter for the ozonation system and it is calculated according to Eq. 9.2 [Cañizares *et al.*, 2009].

$$q\left(\frac{gO_3}{h}\right) = \frac{C_{O3}(kg/m^3) \cdot (1.000 \; kg/g) \cdot f_r(m^3/d)}{24 \; h/d}$$

Eq. 9.2

Where C_{O3} is the ozone consumption (0.0086 kg O_3/m^3 for SFCWW disinfection, Chapter 7) and f_r is the daily treatment flow rate (50 m^3). The *q* value obtained for SFCWW disinfection was 17.92 gO_3/h.

Therefore, cost of the ozonation plant (*PC*) estimated for SFCWW disinfection was 10123 €, and the total C_I 57602 €. The annual C_M was considered to be 2.5% of the annual C_I. The C_O was calculated based on the electric consumption of the ozonation plant considering an electricity price of 0.155 €/kWh. The electric consumption was estimated using the figure of merit Electrical Energy per Order (EEO) according to Eq. 9.3:

$$EEO\left(\frac{kWh}{m^3}\right) = \frac{P(kW) \times t(h) \times 1000}{V(L) \times \log\left(\frac{C_i}{C_f}\right)}$$

Eq. 9.3

where *P* is the rated power, *t* the treatment time (0.16 h; 10 min), *V* is the volume of water treated per experimental batch (10 L) and C_i and C_f the initial and final concentration of the target (10^6 and 0.01 CFU/mL). The rate power (*P*) was calculated considering the electric consumption supplied by the manufacturer (7.5 and 18 kWh/kg for ozone generation and oxygen concentration,

respectively) and the ozone flow used in our experimental conditions (0.0009kg/h). The resultant EEO obtained in our experimental conditions was 0.05 kWh/m^3.

The total ozonation costs estimated for SFCWW disinfection according to the calculations explained below is summarized in Table 9.2. The total cost estimated for SFCWW disinfection by ozonation was 0.27 €/m^3, where C_I represents more than 90 % of the total costs and C_O and C_M have lower and similar contributions to the total cost (3%).

Table 9.2. Breakdown of ozonation costs to treat 1m^3 of SFCWW.

Ozonation cost	€ /year	€/ m^3
Disinfection		
C_I 57602 €	4608	0.25
C_O Electric consumption: 0.05 kWh/m^3	141	0.01
C_M 2.5 % of annual C_I	115	0.01
Total cost	4864	**0.27**
Disinfection + OMCs removal		
C_I 117362 €	9389	0.51
C_O Electric consumption: 5.6 kWh/m^3	11753	0.64
C_M 2.5 % of annual C_I	235	0.01
Total cost	21377	**1.16**

For the simultaneous disinfection and OMCs removal in SFCWW, the *q* value obtained was 57.08 gO$_3$/h (C_{O3}: 0.0274 kg O$_3$/m^3, Chapter 7). Accordingly, the cost of the ozonation plant (*PC*) was 20626 €, and the total C_I 117362 €. The EEO obtained for this case was 5.6 kWh/m^3, considering 2 h of treatment time to achieve ca. 85 % degradation of the ΣOMCs (C_i: 600 µg/L and C_f: 90 µg/L).

The total ozonation costs estimated for the simultaneous disinfection and decontamination of SFCWW was 1.16 €/m³ (Table 9.2), of which C_I (44%) and C_O (55%) have similar contributions to the total cost whereas C_M represent only the 1% of it. This estimated cost are in line with the cost reported in literature (ca. 1.2 €/m³) for a small or medium sized fresh-cut industry [Garret *et al.*, 2003].

9.1.3. Solar treatments cost

The economic analysis was carried out for the solar processes at the operational conditions investigated in Chapter 8 for crops irrigation, i.e., H_2O_2/solar (20mg/L) and Fe^{3+}-EDDHA/H_2O_2/solar (2.5/20 and 5/40 mg/L of reagents).

The annual C_I for solar processes was estimated based on the cost of the CPC field required for each condition, which represents the main investment cost for solar-driven systems. The CPC field (A_{CPC}, m²), was calculated according to the Eq. 9.4 [Malato *et al.*, 2009]:

$$A_{CPC} = \frac{Q_{UV} \cdot V_{tot}}{T_S \cdot UV_G}$$

Eq. 9.4

For SFCWW disinfection the following assumptions were taking into account:

- The UVA energy values needed to inactivate the more resistant pathogen, i.e., considering the inactivation of *S. enteritidis* (Q_{UV}, J/L): 11.91×10^3, 8.41×10^3 and 11.35×10^3 J/L for H_2O_2/solar, Fe^{3+}-EDDHA/ H_2O_2/solar with 2.5/20 mg/L and Fe^{3+}-EDDHA/H_2O_2/solar with 5/40 mg/L, respectively (Chapter 6, Table 6.1).

- The annual volume of treated water (V_{tot}, L): 18250×10^3 L/year.

- An annual operation time (T_s, s) of 157.68×10^5 s, considering 12 h of operation per day.

- The average of local solar UVA radiation (UV_G, W/m²): 36.8 W/m².

In this cost, the Q_{UV} value is the parameter that determines the CPC field in each case: H_2O_2/solar (374.6 m²) > Fe^{3+}-EDDHA/ H_2O_2/solar with 5/40 mg/L (357 m²) > Fe^{3+}-EDDHA/ H_2O_2/solar with 2.5/20 mg/L (264.5 m²). The C_I was then calculated based on a price of CPC reactor reported on previous studies performed in the EU CADOX Project, 816 €/m².

The C_M was considered to be 2.5 % of the annual C_I and the C_O were calculated based on the reagents and electricity costs. For the reagents cost estimation, only the H_2O_2 cost (industrial grade price of 0.43 €/L for a 35 % (w/v) solution) were considered due to the iron micronutrient cost can be considered an agriculture cost and not a treatment cost. Electricity costs were estimated considering a price of 0.155 € kW/h in Spain and the power required for two water centrifugal pumps: for reactor filling (0.22 kWh/m³) and water recirculation during the treatment (0.44 kWh/m³).

The estimated total cost to disinfect 1 m³ of SFCWW by the three solar conditions studied is shown in Table 9.3. Non-significant differences were observed for the C_O of each solar process (0.13-0.16 €/m³) and neither for the C_M (0.02-0.03 €/m³), being therefore the C_I (cost of CPC field) the determinant parameter of the different costs obtained for each solar treatment.

Similar treatment costs were obtained for H_2O_2/solar and Fe^{3+}-EDDHA/ H_2O_2/solar process with 5/40 mg/L as consequence of their similar efficiency (Q_{UV} value) and thus similar C_I costs. However, the Fe^{3+}-EDDHA/H_2O_2/solar process with 2.5/20 mg/L showed, as was expected, the lower estimated C_I (0.95 €/m³) and consequently the lower total cost as a result of the higher efficiency of this solar condition. The estimated price to disinfect 1 m³ of SFCWW by this solar process and condition was 1.10 €, ca. 30 % lower than the estimated for the H_2O_2/solar and Fe^{3+}-EDDHA/solar process with 5/40 mg/L.

Table 9.3. Breakdown of cost of solar processes to treat 1m³ of SFCWW.

	H_2O_2/solar (20 mg/L)		Fe^{3+}-EDDHA/ H_2O_2/solar (2.5/20 mg/L)		Fe^{3+}EDDHA/ H_2O_2/solar (5/40 mg/L)	
	€/year	€/m³	€/year	€/m³	€/year	€/m³
Disinfection						
C_I	24453	1.34	17267	0.95	23303	1.28
C_O Electricity	1867	0.10	1867	0.10	1867	0.10
Reagents	523	0.03	523	0.03	1045	0.06
C_M 2.5 % of annual C_I	611	0.03	432	0.02	583	0.03
Total costs	30599	**1.50**	23234	**1.10**	29943	**1.47**
Disinfection + OMCs						
C_I	38373	2.10	26367	1.44	32380	1.77
C_O Electricity	1867	0.10	1867	0.10	1867	0.10
Reagents	523	0.03	523	0.03	1045	0.06
C_M 2.5 % of annual C_I	959	0.05	659	0.04	809	0.04
Total costs	44867	**2.28**	32561	**1.61**	39246	**1.97**

On the other hand, if the simultaneous disinfection and decontamination are taking into account, the cumulative UVA energy obtained for 2 h of treatment must be considered as the time where maximum OMCs removal were obtained. Higher exposure times will not led to a high improvement (Chapter 6, Fig.6.7).

The UVA energy values considered were (Q_{UV}, J/L): 25.24x10³, 17.03x10³ and 19.64x10³ J/L for H_2O_2/solar, Fe^{3+}-EDDHA/ H_2O_2/solar with 2.5/20 mg/L and Fe^{3+}-EDDHA/H_2O_2/solar with 5/40 mg/L, respectively (Chapter 6, Figure 6.7). The CPC field needed for each case follows the same order as for SFCWW disinfection: H_2O_2/solar (793.8 m²) > Fe^{3+}-EDDHA/ H_2O_2/solar with 5/40 mg/L (617.7 m²) > Fe^{3+}-EDDHA/ H_2O_2/solar with 2.5/20 mg/L (535.6 m²). In this case, C_I was calculated by scaling the price based on the CPC field and costs obtained for SFCWW disinfection and applying the rule of the six-tenths factor (Eq. 9.5):

$$C_I = C_D \; x \; \left(\frac{CPC_T}{CPC_D}\right)^{0.6}$$

Eq. 9.5

Where C_D and CPC_D are the cost and CPC field needed for SFCWW disinfection and CPC_T the CPC field needed for the simultaneous disinfection and OMCs removal.

The estimated total costs to disinfect and remove OMCs simultaneously by the three conditions studied (Table 9.3) also showed that the C_I, i.e., cost of CPC field is the determinant parameter of the cost obtained for each condition as non-significant differences for the C_O and neither for the C_M were observed.

The Fe^{3+}-EDDHA/H_2O_2/solar process with 2.5/20 mg/L showed again, as was expected, the lower estimated C_I (1.44 €/m³) and therefore the lower total cost, 1.61 €/m³.

9.2. Ecotoxicity evaluation of treated SFCWW

9.2.1. *Vibrio fischeri*

Toxicity test with *V. fischeri* was used to evaluate the potential environmental impact associated with the discharge of reclaimed SFCWW with the best operational conditions of each process investigated, i.e., ozone (0.09 gO_3/Lh at pH 6.25), H_2O_2/solar (20 mg/L), Fe^{3+}-EDDHA/H_2O_2/solar (2.5/20 and 5/40 mg/L) and chlorination (100 mg/L). Additionally, the mere effect of Fe^{3+}-EDDHA (2.5 and 5 mg/L) was also investigated as control tests due to no studies dealing with the ecotoxicity of this chelating agent in wastewater samples are found in literature. The bioluminiscense results for all these samples are shown in Figure 9.1.
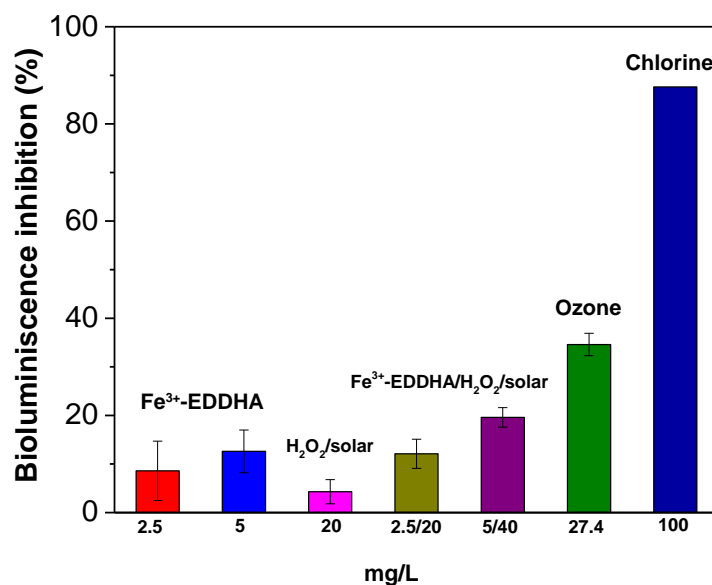
Figure 9.1. Ecotoxicity detected by *V. fischeri* in test controls and treated SFCWW.

The percentage of bioluminescence inhibition (BI) by the presence of Fe^{3+}-EDDHA was found to be 8.6±6.1 and 12.6±4.4 BI % for 2.5 and 5 mg/L of chelate, respectively. These results indicate that the presence of the commercial iron-chelate or any sub-product generated during its synthesis, somehow affected *V. fischeri* metabolism, not being possible to discard the effect of each one in this study. Nevertheless, the treated SFCWW samples by Fe^{3+}-EDDHA/H_2O_2/solar process showed an increase of the BI of ca. 30 % respect to their corresponding baseline controls: 12.1±3 and 19.6±2 BI % for 2.5/20 and 5/40 mg/L, respectively. This higher BI % could be related with the formation of photodegraded products such as salicylaldehide, salicylic acid, salicylaldehyde ethylenediamine diimine or similar subproducts, which have been already reported in literature [Hernández-Apaolaza and Lucena, 2011] and some of them have been also reported to be harmful to aquatic microorganisms [Milovac *et al.*, 2014].

Regarding the toxicity generated by the H_2O_2/solar process, the luminescence emitted by the marine bacteria was not significantly affected (4.3±2.5 BI %), as expected due to the low oxidant capability of this solar process. However,

significant toxicity towards *V. fischeri* was observed for the ozonated (34.6±2.3 BI %) and chlorinated (87.6±0 BI %) samples.

The increase in the acute toxicity observed for the ozonated samples can be attributed to the possible formation of toxic by-products generated from the partial oxidation of the organic matter content (45 mg/L of DOC) into lower molecular and toxic compounds in the mg/L range such as carboxylic acids or aldehydes or unknown OMCs intermediates in the μg-ng/L range [Carbajo *et al*., 2015; and Park *et al*., 2016]. On the other hand, the generation of bromate during ozonation was also investigated. An additional toxicity test with a high bromate concentration (1.5 mg/L) was performed, and results showed no-toxicity on *V. fischeri*, discarding therefore the undesired bromate generation as factor of toxicity in this study.

Regarding results of chlorinated samples, the toxic effect may be due to both, the effect of residual free chlorine and/or the undesired formation of DBPs [Bayo *et al*., 2009]. To discard the effect of residual free chlorine on *V. fischery* toxicity, additional test in the presence of sodium thiosulphate (quencher of free chlorine) was performed. The BI % observed for both samples (chlorinated and dechlorinated) was similar, indicating that free chlorine exhibit no-effect or very smooth effect on the cell viability, and at the same time, attributing the toxic effect observed as a consequence of substances such as chlorinated DBPs.

According to the toxicity classification system for waste discharged into the aquatic environment proposed by Persoone et al., the treated SFCWW belongs to Class I (non-acute toxicity) for all the solar processes, Class II for ozonation (slight acute toxicity) and Class III for chlorination (acute toxicity) [Persoone *et al*., 2003].

The toxicity generated during ozonation and chlorination processes could be reduced by including a subsequent stage in the treatment line based on biologically activated carbon filter (BAC) or sand filters [Rizzo *et al*., 2019]. Nevertheless, the application of this strategy will obviously lead to an increase in the treatment cost.

9.2.2. *Lactuca sativa*

The potential toxic effects of reuse treated SFCWW for irrigation was assessed by seed germination/root elongation test with *Lactuca sativa*. The results of root elongation average, germination rate (G %) and relative growth index (RGI) are shown in Table 9.4.

Table 9.4. Results of *Lactuca sativa* toxicity obtained for untreated and treated SFCWW.

	G (%)	Root length (mean, cm)	RGI	Toxicity effect
Negative control	95	1.5±0.4	-	-
Untreated SFCWW	98	1.7±0.3	1.07	NSE
Treated SFCWW				
H_2O_2/solar	95	1.9±0.4	1.23	S
Fe^{3+} EDDHA/H_2O_2/solar (2.5/20 mg/L)	100	1.8±0.4	1.20	NSE
Fe^{3+} EDDHA/H_2O_2/solar (5/40 mg/L)	97.4	1.7±0.4	1.10	NSE
Ozonation	94.4	1.6±0.3	1.20	NSE
Chlorination	92.3	1.2±0.2	0.79	I

S = stimulation; I= inhibition; NSE = non- significant effect.

Initially, the phytotoxicity of untreated SFCWW was assessed. The obtained results showed a higher G % for the seeds exposed to untreated SFCWW (98 %) than the exposed to the negative control, i.e., ultrapure water (95 %). This slight difference might be explained by the presence of salts such as nitrates in the SFCWW matrix able to favors the germination of *L. sativa* seeds [Hendricks and Taylorson, 1974]. On the other hand, non-significant effect was observed for the value of root elongation: 1.7±0.3 and 1.5±0.4 cm for the negative control and untreated SFCWW, respectively. These results are in agreement with previous studies in which no significant effects were detected neither for root elongation nor for germination in lettuce seeds exposed to pesticides in a concentration range similar than the pesticides concentration of this study (100 μg/L) [Margenat *et al.*, 2017; Utzig *et al.*, 2019].

Non-significant toxic effects were observed for the seeds exposed to SFCWW reclaimed by ozone and the Fe^{3+}-EDDHA/H_2O_2/solar processes at the two

reagents combinations studied (1.1-1.2 RGI % and G % > 95). These results, on contrary to the *V. fischeri*, seem to indicate a non-phytotoxicity effect of the subproducts generated during the ozonation and solar treatment of SFCWW.

Lettuce seeds exposed to SFCWW treated by the H_2O_2/solar process showed the highest elongation compared with the negative control, being this effect categorized as stimulation (RGI value > 1.2). The presence of H_2O_2 can play a double role towards lettuce seeds germination depending of its concentration: at H_2O_2 concentration higher than 2.5 mM, has a toxic effect [Moraes *et al.*, 2018], whereas lower concentrations could help to weak the endosperm cap of *L. sativa* seeds accelerating their germination [Wojtyla *et al.*, 2016]. Additionally, the presence of a residual H_2O_2 concentration might protect the emerging seedlings to potential microbial infections and its decomposition in O_2 and H_2O could provide to the plantlets higher oxygen concentrations favoring their germination process [Liu *et al.*, 2012]. In this study, it is possible that the combination of these three reasons (low H_2O_2 concentrations (0.41 mM), protection against infections and oxygenation) could be responsible of the stimulation effect observed in this test when lettuce seeds were exposed to SFCWW treated by the H_2O_2/solar process.

Finally, an inhibition effect (phytotoxicity) was observed for the chlorinated SFCWW. This toxic effect towards lettuce seeds observed could be due to the presence of toxic chlorinated DPBs.

In summary, from the toxicity point of view, the results obtained indicate the suitability of solar processes and ozonation for the intended further reuse of FCWW for crops irrigation, discarding in this approach the use of chlorination for the same purpose.

9.3. Risk assessment of crops irrigated with treated SFCWW

A chemical and microbiological risk assessment was performed to study the potential health risk associated with the consumption of the crops irrigated by

untreated and treated SFCWW (Chapter 8). The following assumptions were considered:

- A standard body weight (bw) for an average adult of 60 kg.

- 150 eating occasions of both vegetables per year.

- A serving size of 100 g for lettuce according to WHO recommendations [WHO, 2006], and 8 g for radish according to the data of chronic exposure of EFSA for GEMS/Food Cluster diets relevant for the EU Member States (G15) [EFSA,2018].

9.3.1. Chemical health risk assessment

There are different methods to assess the long-term (chronic) human risk associated with the consumption of vegetables contaminated with chemical compounds such as the evaluation through the Threshold of Toxicological Concern (TTC) and the comparison of the acceptable daily intakes (ADI) of the contaminants (EFSA). The TTC method is recommended and commonly used for compounds without an ADI value already assigned. This method is suitable for new or recent chemical compounds. Moreover, the risk assessment by TTC values consist on the risk estimation based on the chemical structure of the contaminant and normally led to a risk over or underestimation [Evans *et al.*, 2015]. In this study, the OMCs investigated are pesticides with ADI values already established for all of them. Therefore, the chemical risk assessment was performed according to the EFSA recommendations.

The ADI values, given by the European Commission and the EFSA, can be defined as '*the estimated maximum amount of a contaminant, expressed based on body mass, to which a consumer may be exposed daily over its lifetime without an appreciable health risk'*. Based on its definition, some studies based the risk assessment by the comparison of ADI value with the known or estimated daily intake (EDI).

The EDI value can be easily calculated according to Eq. 9.6 [Camara *et al.*, 2017]:

$$EDI = C \ x \ \left(\frac{L}{bw}\right)$$

Eq. 9.6.

Where C is the average pesticide residue concentration of each pesticide at harvest (mg/kg), L is the food consumption rate (kg/day). The reference ADI values and the EDI estimated for each OMC in the harvested radishes and lettuces are shown in Table 9.5 and Table 9.6, respectively.

Table 9.5. Estimated daily dietary intakes (EDI) of harvested radishes irrigated by untreated and reclaimed SFCWW.

Radish		EDI (mg/kg bw day)				
OMC	ADI (mg/kg bw day)	Non-treated	Ozone	H_2O_2/solar	Fe^{3+}EDDHA/ H_2O_2/solar (2.5/20 mg/L)	Fe^{3+}EDDHA/ H_2O_2/solar (5/40 mg/L)
ATZ	2.00×10^{-2}	2.35×10^{-5}	4.93×10^{-7}	1.45×10^{-5}	2.35×10^{-5}	1.33×10^{-5}
AZX	2.00×10^{-1}	2.14×10^{-5}	-	5.64×10^{-6}	2.14×10^{-5}	1.22×10^{-5}
BPF	1.00×10^{-2}	2.92×10^{-5}	2.67×10^{-8}	4.69×10^{-6}	2.92×10^{-5}	5.25×10^{-6}
PCM	2.80×10^{-3}	4.53×10^{-5}	9.00×10^{-8}	2.27×10^{-5}	4.53×10^{-5}	3.33×10^{-5}
TBY	2.70×10^{-2}	6.21×10^{-6}	-	4.85×10^{-6}	6.21×10^{-6}	6.67×10^{-6}

Table 9.6. Estimated daily dietary intakes (EDI) of harvested lettuces irrigated by untreated and reclaimed SFCWW.

Lettuce		EDI (mg/kg bw day)				
OMC	ADI (mg/kg bw day)	Non-treated	Ozone	H_2O_2/solar	Fe^{3+}EDDHA/ H_2O_2/solar (2.5/20 mg/L)	Fe^{3+}EDDHA/ H_2O_2/solar (5/40 mg/L)
ATZ	2.00×10^{-2}	2.54×10^{-4}	1.86×10^{-6}	1.29×10^{-4}	6.13×10^{-5}	1.48×10^{-4}
AZX	2.00×10^{-1}	6.81×10^{-5}	-	1.48×10^{-5}	4.67×10^{-6}	7.87×10^{-6}
BPF	1.00×10^{-2}	6.62×10^{-5}	-	2.20×10^{-6}	2.00×10^{-6}	8.17×10^{-5}
PCM	2.80×10^{-3}	3.10×10^{-4}	3.84×10^{-5}	9.71×10^{-5}	9.07×10^{-5}	9.16×10^{-5}
TBY	2.70×10^{-2}	4.94×10^{-5}	-	2.39×10^{-5}	8.00×10^{-6}	1.67×10^{-5}

The EDI values obtained for all the OMCs and harvested crops, i.e., radishes and lettuces irrigated with untreated and treated SFCWW, were several orders of magnitude lower than the ADI values. Moreover, the EDI values of the lettuces crops were higher than radishes, as expected due to the higher serving size and OMCs uptake of this vegetable taking into account that the EDI value is proportional to the OMCs concentration.

On the other hand, the estimation of the chemical risk for a mixture of contaminants in vegetables (the most common scenario) is estimated by the calculation of EDI/ADI quotient values for each compound, also known as hazard quotient values (HQ). The sum of the HQ values is known as hazard index (HI), this parameter is an indicator of the potential chemical risk associated to the consumption of a mixture of contaminants (usually pesticides) [Yu *et al.*, 2016]. HI values <1 are considered acceptable and HI values >1 are considered a health risk.

The HQ values for each pesticide and the combined risk (HI) values calculated for the harvested radishes and lettuce are shown in Table 9.7 and Table 9.8, respectively.

Table 9.7. Potential health risk for the consumption of the harvested radishes: risk of each OMC residue (HQ) and combined risk (HI).

Radish	HQ				
OMC	**Non-treated**	**Ozone**	**H_2O_2/solar**	**Fe^{3+}EDDHA/ H_2O_2/solar (2.5/20mg/L)**	**Fe^{3+}EDDHA/ H_2O_2/solar (5/40 mg/L)**
ATZ	1.18×10^{-3}	2.47×10^{-5}	6.99×10^{-4}	8.21×10^{-4}	6.70×10^{-4}
AZX	1.07×10^{-4}	-	2.82×10^{-5}	1.09×10^{-5}	6.00×10^{-5}
BPF	2.92×10^{-3}	2.67×10^{-6}	4.69×10^{-4}	5.64×10^{-4}	5.30×10^{-4}
PCM	1.62×10^{-2}	3.21×10^{-3}	8.09×10^{-3}	9.09×10^{-3}	1.19×10^{-2}
TBY	2.30×10^{-4}	-	1.80×10^{-4}	1.97×10^{-4}	2.50×10^{-4}
HI	**2.06×10^{-2}**	**3.24×10^{-3}**	**9.47×10^{-3}**	**1.07×10^{-2}**	**1.34×10^{-2}**

The HQ values obtained for all the OMCs and samples evaluated were very low: range of 10^{-4} to 10^{-2} in the vegetables irrigated with untreated SCWW and range of 10^{-6} to 10^{-4} for all the compounds (except procymidone) in the samples irrigated with treated SFCWW. The values observed are in agreement with the values reported (10^{-5} to 10^{-4}) in a previous study of the risk associated to the presence of several pesticides in fresh-cut lettuce samples [Camara *et al.*, 2017].

Table 9.8. Potential health risk for the consumption of the harvested lettuces: risk of each OMC residue (HQ) and combined risk (HI).

Lettuce	HQ				
OMC	Non-treated	Ozone	H_2O_2/solar	Fe^{3+}EDDHA/ H_2O_2/solar (2.5/20mg/L)	Fe^{3+}EDDHA/ H_2O_2/solar (5/40 mg/L)
ATZ	1.27×10^{-2}	9.29×10^{-5}	6.44×10^{-3}	3.01×10^{-3}	7.39×10^{-3}
AZX	3.40×10^{-4}	-	7.40×10^{-5}	2.33×10^{-5}	3.93×10^{-5}
BPF	6.61×10^{-3}	-	2.20×10^{-4}	2.00×10^{-4}	8.17×10^{-5}
PCM	1.11×10^{-1}	1.24×10^{-2}	3.47×10^{-2}	3.24×10^{-2}	3.27×10^{-2}
TBY	1.83×10^{-3}	-	8.83×10^{-4}	2.96×10^{-4}	6.18×10^{-4}
HI	$\mathbf{1.32 \times 10^{-1}}$	$\mathbf{1.25 \times 10^{-2}}$	$\mathbf{4.23 \times 10^{-2}}$	$\mathbf{3.60 \times 10^{-2}}$	$\mathbf{4.09 \times 10^{-2}}$

Respect to the estimated risk obtained for the combined exposure of the 5 OMCs, i.e., HI, their value was less than 0.05 for all the samples evaluated except for the lettuce samples irrigated with untreated SFCWW (HI: 1.32×10^{-1}). It is also important to note that the risk associated to the consumption of these vegetables is mainly provided by the procymidone compound as its HQ represent ≈80 % of the HI for the crops irrigated by untreated and solar treated water and the 99 % for the crops irrigated by ozonated SFCWW, being almost irrelevant the risk associated with the other 4 OMCs.

In general, the HI obtained for all the harvested crops were lower than one indicating that the consumption of these vegetables does not pose significant human health risk. Moreover, their value were significant lower for the crops irrigated with reclaimed SFCWW than the crops irrigated by untreated SFCWW and therefore, the chemical risk associated with their consumption was also reduced by the cultivation with reclaimed SFCWW: risk reductions of an order of magnitude for the lettuce samples and at least a reduction of 50 % for the harvested radishes.

Overall, it can be concluded that today, any harvested sample represent a risk for the consumer. Nonetheless, it is important to note that actually the OMCs concentrations do not represent a risk but, it is possible that in a near future will represent as the assessment methods and the toxicological technologies change with the time increasing its sensitivity.

9.3.2. Microbiological health risk assessment

The contribution of the irrigation water to vegetables contamination and the subsequent foodborne infection outbreaks, mainly in raw-eaten vegetables represent an important global concern. For this reason, the number of studies about the microbiological risk associated to irrigation has been increased in the last years. Nevertheless, most of the risk assessment studies were performed by the estimation of the cross-contamination between water and the vegetables, being very scarce the number of studies in real exposure scenarios and with experimental data, as the study performed in this work (Chapter 8).

The most widely used methodology for the estimation of a microbiological risk is the quantitative microbial risk assessment (QMRA). This process estimates the risk associated to pathogens exposure using the environmental concentration of the microorganism as the main input data and generating the associated risk as output data [Rasheduzzaman *et al.*, 2019].

A QMRA is performed by four established parameters: (i) hazard identification, (ii) hazard characterization, (iii) exposure assessment and (iv) risk characterization [FAO/WHO, 2016]. The microbiological assessment performed for the harvested samples of this study was performed according to these parameters as follow:

(i) <u>Hazard identification</u>; the high infective *E. coli* O157:H7 and *S. enteritidis* bacteria, commonly associated to several foodborne infections outbreaks (Chapter 1, section 1.4.1.2), are the microbiological hazards of this assessment.

(ii) <u>Hazard characterization</u>; the health metric used for this assessment were 0.143 and 0.049 disability-adjusted life year (DALYs) for *E.coli* O157:H7 and *S. enteritidis*, respectively [Havelaar *et al.*, 2012]. The DALY value is a measure of overall disease burden, expressed as the number of years lost due to ill-health, disability or early death and along with the annual infection risk is the main health-based risk metrics.

(iii) <u>Exposure assessment</u>; the experimental data of *E. coli* O157:H7 and *S. enteritidis* concentration obtained from the microbiological analysis of the harvested samples (Chapter 8) was employed as the hazard characterization. The LOD (1 CFU/99 g of lettuce and 1 CFU/8 g of radish) was used as the bacterial concentration detected in crops irrigated with reclaimed SFCWW.

The prevalence of the hazard were 1 for the crops irrigated with untreated SFCWW (all the samples were positive in both pathogens) and 0.01 for the crops irrigated with reclaimed SFCWW (only a positive sample was detected in lettuce irrigated by H_2O_2/solar process).

The serving sizes and eating occasions per year was the same explained above: 100 g of lettuce, 8 g of radish and 150 eating occasions per year.

Finally, the dose-response model used for both pathogens was the β-poisson dose-response model, where the risk of infection/illness (R_{ill}) is estimated based on Eq. 9.7:

$$R_{ill} = 1 - \left(1 + \frac{D}{\beta}\right)^{-\alpha}$$

<div align="right">Eq. 9.7.</div>

Where *D* is the hazard dose and α/β the dose-response parameters. The dose-response parameters used for this assessment were:

- *E. coli* O157:H7; α: 0.248; β: 48.8 [Teunis *et al.,* 2008].
- *S. enteritidis;* α: 0.3126; β: 2884 [Haas, 1999].

Finally, the probability of adverse effect was considered 100 %, for a conservative approach.

(iv)   <u>Risk characterization</u>; the results obtained from the quantitative analysis performed for both pathogens and samples analyzed with all the parameters explained above is presented in Table 9.9 and discussed below.

The output data obtained were the number of total illnesses per 150 eating occasions per year (i.e., the annual risk of illness), the mean risk of illness per eating occasions (R_{ill}) and the DALYs per person per year. The accepted values

for the annual risk of illness and DALYs per person per year are 10^{-4} and 10^{-6}, respectively [Rasheduzzaman *et al.*, 2019].

Table 9.9. QMRA results obtained for the consumption of harvested radishes and lettuces irrigated by untreated and reclaimed SFCWW.

Radish		
***E.coli* O157:H7**	**Untreated**	**Treated**
Total illnesses	93	7.58×10^{-3}
Mean risk of illness	0.62	5.05×10^{-5}
Total DALYs per year	13.3	$\mathbf{1.08 \times 10^{-3}}$
S. enteritidis	**Untreated**	**Treated**
Total illnesses	42.40	1.64×10^{-4}
Mean risk of illness	0.295	1.09×10^{-6}
Total DALYs per year	2.17	$\mathbf{8.02 \times 10^{-6}}$
Lettuce		
***E.coli* O157:H7**	**Untreated**	**Treated**
Total illnesses	104	7.7×10^{-3}
Mean risk of illness	0.696	5.13×10^{-5}
Total DALYs per year	14.9	$\mathbf{1.10 \times 10^{-3}}$
S. enteritidis	**Untreated**	**Treated**
Total illnesses	49.2	1.66×10^{-4}
Mean risk of illness	0.328	1.11×10^{-6}
Total DALYs per year	2.41	$\mathbf{8.15 \times 10^{-6}}$

In general, the data obtained from the QMRA analysis indicated a very high risk associated with the consumption of the crops irrigated with untreated SFCWW for both pathogens. The number of illness per 150 eating occasions is ca. 95 for crops contaminated by *E. coli* O157:H7 and almost half (ca. 45) for *S. enteritidis.* The higher risk associated with *E. coli* O157:H7 can be explained based on the higher value of health metric for this highly infective pathogen.

However, the microbiological risk associated to the consumption of the crops irrigated by reclaimed SFCWW was reduced significantly (more than 4 orders of magnitude), which indicate the suitability of the processes studied to also reduce the microbiological risk of the consumer. The results obtained for *S. enteritidis* in both crops are in agreement with the acceptable value of the two main health risk metrics: annual risk of illness (10^{-4}) and DALYs per person per year (10^{-6}), whereas the risk values observed for *E .coli* O157:H7 (10^{-3} for both parameters) are higher than the acceptable values. These results may be due to the higher

infectivity of *E .coli* O157:H7 (0.143 DALYs) than *S. enteritidis* (0.049 DALYs) and maybe also due to the conservative conditions implemented (100 % of adverse effect probability).

9.4. Conclusions of Chapter 9

The treatment costs estimated for SFCWW disinfection by ozone (0.27 €/m^3), H_2O_2/solar process (1.50 €/m^3) and the Fe^{3+}-EDDHA/H_2O_2/solar process at the best operational condition (1.10 €/m^3) indicated the suitability of the ozonation process as an economically viable alternative to the conventional chlorination process (0.74 €/m^3). Whereas, the treatment cost obtained for SFCWW disinfection by the solar processes were almost twice the estimated for chlorination.

The treatment costs estimated for SFCWW disinfection and a simultaneous OMCs removal by ozone (1.16 €/m^3) and by the Fe^{3+}-EDDHA/H_2O_2/solar process (1.61 €/m^3) may be economically competitive with the conventional chlorination process taking into account the advantage of these processes which are able to also degrade OMCs.

The ecotoxicity results obtained with *V. fischeri* test point out a high toxic effect for chlorinated SFCWW, a slight effect for ozonated water and non-toxic effects for solar treated SFCWW.

The phytotoxicity results with *L. sativa* showed non-toxic effects for ozonated and solar treated SFCWW and a toxic effect for chlorinated SFCWW. These results highlight the non-suitability of chlorinated water for its reuse in agricultural irrigation and the suitability of the water processes studied as potential chlorine alternatives.

Finally, the chemical and microbiological risk assessment of the harvested crops showed a high capability of ozone and the solar processes to reduce significantly the human risk associated with the consumption of radishes and lettuces irrigated by untreated SFCWW.

CHAPTER 10
CONCLUSIONS

10. CONCLUSIONS

1. The treatment of fresh-cut wastewater has been experimentally demonstrated in this study using a synthetic recipe developed taking into account the physical and chemical characterization of real fresh-cut wastewater samples, and allowing a realistic evaluation and comparison of different water treatment processes.

2. The H_2O_2/solar process represents a promising environmentally friendly alternative to chlorine for fresh-cut wastewater treatment due to the good disinfection performance obtained with low amounts of oxidant (20 mg/L of H_2O_2) regardless of the year season. The application of this process in the fresh-cut industry has important advantages, including low

cost, easy to use, absence of residual toxic chemicals in the final product (vegetables) and wastewater as it is decomposed into oxygen and water.

3. Ozonation treatment showed the higher inactivation kinetic and OMCs degradation rates obtained in this study. The best operational condition for this treatment was obtained at natural pH not requiring either additional reagents or pH modification.

4. In spite of ozonation proving to be a feasible process for decontamination and disinfection of SFCWW, the results obtained by the toxicity analysis of ozonated samples indicates that this process may not be recommended for the fresh-cut industry.

5. The capability of a commercial iron chelate Fe^{3+}-EDDHA in combination with natural solar radiation as promoter of bacterial inactivation and OMC degradation in SFCWW has been demonstrated in this study for the first time.

6. The use of low amounts of the commercial fertilizer (0.5-5 mg/L of Fe^{3+}-EDDHA) for solar photo-Fenton process at natural SFCWW pH (6.25) (Fe^{3+}-EDDHA/H_2O_2/solar) showed significant better disinfection and decontamination efficiencies than the conventional use of iron salts; while slightly enhanced results were obtained when compared with H_2O_2/solar process.

7. The analysis of bacterial inactivation rates revealed that *S. enteritidis* showed higher resistance than *E. coli* O157:H7 to be inactivated by all the processes investigated. Regarding OMCs, two different groups were observed based on their degradation profiles, showing G_1-OMC (terbutryn, buprofezin, azoxystrobin) lower resistance to be removal than G_2-OMC (imidacloprid, simazine, thiamethoxam, atrazine, procymidone).

8. These results support the need to amplify the microbial spectrum analysis as well as the selection of organic pollutants as indicators or targets in

guidelines and regulations, especially if a potential human infection risk exists by cross-contamination, like may occur in the fresh-cut industry.

9. The disinfection efficiency obtained by all the treatments studied satisfied the microbiological quality (<100 CFU/100 mL) established by the Spanish reuse law (Royal decree 1620/2007) and the new European proposal with restricted value (<10 CFU/100 mL) related with the wastewater reuse for irrigation of raw-eaten vegetables.

10. The results obtained by the chemical and microbial risk assessment have proven to reduce significantly the human risk associated to the consumption of the vegetables when lettuce and radish crops are irrigated with SFCWW treated by all the processes tested in this study.

11. The estimated treatment cost for all the processes studied (ozonation and solar processes) seems to be high, nevertheless the possibility of reusing the treated SFCWW directly for irrigation with an iron micronutrient may contribute to the reduction of the water footprint of the fresh-cut industry and the reduction of water scarcity (including iron chlorosis in crops) in arid or semi-arid regions, making these treatments promising alternatives to the wide spread use of chlorination.

CHAPTER 11

REFERENCES

11. REFERENCES

Abeledo-Lameiro, M. J.; Reboredo-Fernández, A.; Polo-López, M. I.; Fernández-Ibáñez, P.; Ares-Mazás, E.; Gómez-Couso, H. Photocatalytic Inactivation of the Waterborne Protozoan Parasite Cryptosporidium Parvum Using TiO_2/H_2O_2 under Simulated and Natural Solar Conditions. *Catal. Today.* **2017**, *280*, 132–138. https://doi.org/10.1016/j.cattod.2016.05.046.

Aguas, Y.; Hincapie, M.; Fernández-Ibáñez, P.; Polo-López, M. I. Solar Photocatalytic Disinfection of Agricultural Pathogenic Fungi (*Curvularia* Sp.) in Real Urban Wastewater. *Sci. Total Environ.* **2017**, *607–608*, 1213–1224. https://doi.org/10.1016/j.scitotenv.2017.07.085.

Aguas, Y.; Hincapie, M.; Martínez-Piernas, A. B.; Agüera, A.; Fernández-Ibáñez, P.; Nahim-Granados, S.; Polo-López, M. I. Reclamation of Real Urban Wastewater Using Solar Advanced Oxidation Processes: An Assessment of Microbial Pathogens and 74 Organic Microcontaminants Uptake in Lettuce and Radish. *Environ. Sci. Technol.* **2019**, *53 (16)*, 9705-9714. https://doi.org/10.1021/acs.est.9b00748.

Agüero, M. V.; Jagus, R. J.; Martín-Belloso, O.; Soliva-Fortuny, R. Surface Decontamination of Spinach by Intense Pulsed Light Treatments: Impact on Quality

Attributes. *Postharvest Biol. Technol.* **2016**, *121*, 118–125. https://doi.org/10.1016/j.postharvbio.2016.07.018.

Agulló-Barceló, M.; Polo-López, M. I.; Lucena, F.; Jofre, J.; Fernández-Ibáñez, P. Solar Advanced Oxidation Processes as Disinfection Tertiary Treatments for Real Wastewater: Implications for Water Reclamation. *Appl. Catal. B Environ.* **2013**, *136–137*, 341–350. https://doi.org/10.1016/j.apcatb.2013.01.069.

Alakomi, H. L.; Puupponen-Pimiä, R.; Aura, A. M.; Helander, I. M.; Nohynek, L.; Oksman-Caldentey, K. M.; Saarela, M. Weakening of Salmonella with Selected Microbial Metabolites of Berry-Derived Phenolic Compounds and Organic Acids. *J.Agric. Food Chem.* **2007**, *55* (10), 3905-3912. https://doi.org/10.1021/jf070190y.

Alcalde-Sanz, L.; Gawlik, B. M. Minimum Quality Requirements for Water Reuse in Agricultural Irrigation and Aquifer Recharge Towards a Legal Instrument on Water Reuse at EU Level. **2017**. https://doi.org/10.2760/887727.

Alkan, U.;engül Topaç, B.; Denizli, N. Efficiencies of Solar Light, Solar/H2O2 and Solar Photo-Fenton Processes for Disinfection of Turbid Wastewaters. *Desalin. Water Treat.* **2017**, *80*, 149–155. https://doi.org/10.5004/dwt.2017.21003.

Allende, A.; Monaghan, J. Irrigation Water Quality for Leafy Crops: A Perspective of Risks and Potential Solutions. *Int. J. Environ. Res. Public Health.* **2015**, *12* (7), 7457–7477. https://doi.org/10.3390/ijerph120707457.

Alwi, N. A.; Ali, A. Reduction of Escherichia Coli O157, Listeria Monocytogenes and Salmonella Enterica Sv. Typhimurium Populations on Fresh-Cut Bell Pepper Using Gaseous Ozone. *Food Control.* **2014**, *46*, 304–311. https://doi.org/10.1016/j.foodcont.2014.05.037.

Ananthaswamy, H. N.; Eisenstark, A. Near-UV-Induced breaks in phage DNA: sensitization by hydrogen peroxide (a tryptophan photoproduct). *Photochem. Photobiol.* **1976**, *24* (5), 439-442. https://doi.org/10.1111/j.1751-1097.1976.tb06851.x.

Arevalos-Sánchez, M.; Regalado, C.; Martin, S. E.; Domínguez-Domínguez, J.; García-Almendárez, B. E. Effect of Neutral Electrolyzed Water and Nisin on Listeria Monocytogenes Biofilms, and on Listeriolysin O Activity. *Food Control.* **2012**, *24*, 116-122. https://doi.org/10.1016/j.foodcont.2011.09.012.

Artés-Hernández, F.; Martínez-Hernández, G. B.; Aguayo, E.; Gómez, P. A.; Artés, F. Fresh-Cut Fruit and Vegetables: Emerging Eco-Friendly Techniques for Sanitation and Preserving Safety. *Postharvest Handling*; InTech, **2017**, *2*, 7-45. https://doi.org/10.5772/intechopen.69476.

Arzate, S.; Pfister, S.; Oberschelp, C.; Sánchez-Pérez, J. A. Environmental Impacts of an Advanced Oxidation Process as Tertiary Treatment in a Wastewater Treatment Plant. *Sci. Total Environ.* **2019,** *694*, 133572. https://doi.org/10.1016/j.scitotenv.2019.07.378.

ASTM. **2005.** ASTM G159-98, Standard Tables for References Solar Spectral

Irradiance at Air Mass 1.5: Direct Normal and Hemispherical for a 37° Tilted Surface, ASTM International, West Conshohocken, PA. https://doi.org/10.1520/G0159-98.

ASTM. **2014**. ASTM E490-00a, Standard Solar Constant and Zero Air Mass Solar Spectral Irradiance Tables, ASTM International, West Conshohocken, PA. https://doi.org/10.1520/E0490-00AR14.

Aurioles-López, V.; Polo-López, M. I.; Fernández-Ibáñez, P.; López-Malo, A.; Bandala, E. R. Effect of Iron Salt Counter Ion in Dose-Response Curves for Inactivation of *Fusarium Solani* in Water through Solar Driven Fenton-like Processes. *Phys. Chem. Earth.* **2016**, *91*, 46–52. https://doi.org/10.1016/j.pce.2015.10.006.

Ávila-Quezada, G.; Sánchez, E.; Gardea-Béjar, A. A.; Acedo-Félix, E. *Salmonella* Spp. and *Escherichia Coli*: Survival and Growth in Plant Tissue. *New Zeal. J. Crop Hortic. Sci.* **2010**, *38* (2), 47–55. https://doi.org/10.1080/01140671003767834.

Bandala, E. R.; González, L.; Sanchez-Salas, J. L.; Castillo, J. H. Inactivation of *Ascaris* Eggs in Water Using Sequential Solar Driven Photo-Fenton and Free Chlorine. *J. Water Health.* **2012**, *10* (1), 20–30. https://doi.org/10.2166/wh.2011.034.

Barletta, B.; Bolzacchini, E.; Meinardi, S.; Orlandi, M.; Rindone, B. The Kinetics and the Mechanism of the Reaction of 2-Chloro-4,6-Dialkylamino-1,3,5-Triazines with Ozone. *Ozone Sci. Eng.* **2003**, *25* (2), 81–94. https://doi.org/10.1080/713610663.

Bayo, J.; Angosto, J. M.; Gómez-López, M. D.; Oleaga, I.; García, C. Toxicity Assessment of Chlorinated Secondary Effluents by the *Vibrio Fischeri* Bioluminescence Assay. *WIT Trans. Biomed. Heal.* **2009**, *14*, 329–340. https://doi.org/10.2495/EHR090321.

Belletti, N.; Lanciotti, R.; Patrignani, F.; Gardini, F. Antimicrobial Efficacy of Citron Essential Oil on Spoilage and Pathogenic Microorganisms in Fruit-Based Salads. *J. Food Sci.* **2008**, *73* (7), 331–338. https://doi.org/10.1111/j.1750-3841.2008.00866.x.

Beltran, F. Ozone Reaction Kinetics for Water and Wastewater Systems; *crc press*, **2003**. https://doi.org/10.1201/9780203509173.

Berney, M.; Weilenmann, H. U.; Simonetti, A.; Egli, T. Efficacy of Solar Disinfection of *Escherichia Coli*, *Shigella Flexneri*, *Salmonella Typhimurium* and *Vibrio Cholerae*. *J. Appl. Microbiol.* **2006**, *101* (4), 828–836. https://doi.org/10.1111/j.1365-2672.2006.02983.x.

Bhilwadikar, T.; Pounraj, S.; Manivannan, S.; Rastogi, N. K.; Negi, P. S. Decontamination of Microorganisms and Pesticides from Fresh Fruits and Vegetables: A Comprehensive Review from Common Household Processes to Modern Techniques. *Compr. Rev. Food Sci. Food Saf.* **2019**, *18* (4), 1003–1038. https://doi.org/10.1111/1541-4337.12453.

Bianco, A.; Polo−López, M. I.; Fernández−Ibáñez, P.; Brigante, M.; Mailhot, G. Disinfection of Water Inoculated with *Enterococcus Faecalis* Using Solar/Fe(III)EDDS-H_2O_2 or $S_2O_8^{2-}$ Process. *Water Res.* **2017**, *118*, 249–260. https://doi.org/10.1016/j.watres.2017.03.061.

Biasone, A.; Cianci, G.; Di Tommaso, D.; Piaggesi, A.; Tagliavini, E.; Galletti, P.; Moretti, F. Characterization and Quantification of Racemic and Meso-Ethylenediamine-N,N'-Bis(2-Hydroxy-5-Sulfophenylacetic) Acid/Iron (III) by Ion-Pair Ultra-High Performance Liquid Chromatography Coupled with Diode Array Detector and Electrospray Tandem Mass Spectrometry. *J. Chromatogr. A.* **2013**, *1282*, 142–152. https://doi.org/10.1016/j.chroma.2013.01.083.

Bichai, F.; Polo-López, M. I.; Fernández Ibañez, P. Solar Disinfection of Wastewater to Reduce Contamination of Lettuce Crops by Escherichia Coli in Reclaimed Water Irrigation. *Water Res.* **2012**, *46* (18), 6040–6050. https://doi.org/10.1016/j.watres.2012.08.024.

Bilek, S. E.; Turantas, F. Decontamination Efficiency of High Power Ultrasound in the Fruit and Vegetable Industry, a Review. *Int. J. of Food Microbiol.* **2013**, 155–162. https://doi.org/10.1016/j.ijfoodmicro.2013.06.028.

Blanco, J. Desarrollo de colectores solares sin concentración para aplicaciones fotoquímicas de degradación de contaminantes persistentes en agua. (Doctoral thesis). Universidad de Almería, **2002**.

Blanco, J.; Malato, S.; Fernández, P.; Vidal, A.; Morales, A.; Trincado, P.; Oliveira, J. C.; Minero, C.; Musci, M.; Casalle, C.; et al. Compound Parabolic Concentrator Technology Development to Commercial Solar Detoxification Applications. *Sol. Energy.* **1999**, *67* (4–6), 317–330. https://doi.org/10.1016/s0038-092x(00)00078-5.

BME. **2019.** Boletin Nacional de estadística, Ministerio de Agricultura, Pesca y Alimentación, Gobierno de España, Enero 2019.

Bohn, T.; Walczyk, T.; Leisibach, S.; Hurrell, R. F. Chlorophyll-Bound Magnesium in Commonly Consumed Vegetables and Fruits: Relevance to Magnesium Nutrition. *J. Food Sci.* **2006**, *69* (9), S347–S350. https://doi.org/10.1111/j.1365-2621.2004.tb09947.x.

BREF. **2006**. Integrated Pollution Prevention and Control Reference Document on Best Available Techniques in the Food, Drink and Milk Industries, 1-638. https://eippcb.jrc.ec.europa.eu/reference/BREF/fdm_bref_0806.pdf (accessed July 27, 2019).

Burek, P.; Satoh, Y.; Fischer, G.; Kahil, M. T.; Scherzer, A.; Tramberend, S.; Nava, L. F.; Wada, Y.; Eisner, S.; Flörke, M.; Hanasaki, N.; Magnuszewski, P.; Cosgrove, B.; Wiberg, D. Water Futures and Solution: Fast Track Initiative. (Final Report). *IIASA*, Laxenburg, Austria, **2016**.

Burt, S. Essential Oils: Their Antibacterial Properties and Potential Applications in Foods - A Review. *Int. J. of Food Microbiol.* **2004**, *94* (3), 223-253. https://doi.org/10.1016/j.ijfoodmicro.2004.03.022.

Callejón, R. M.; Rodríguez-Naranjo, M. I.; Ubeda, C.; Hornedo-Ortega, R.; Garcia-Parrilla, M. C.; Troncoso, A. M. Reported Foodborne Outbreaks Due to Fresh Produce in the United States and European Union: Trends and Causes. *Foodborne Pathog. Dis.* **2015**, *12* (1), 32–38. https://doi.org/10.1089/fpd.2014.1821.

Camara, M. A.; Barba, A.; Cermeño, S.; Martinez, G.; Oliva, J. Effect of Processing on the Disappearance of Pesticide Residues in Fresh-Cut Lettuce: Bioavailability and Dietary Risk. *J. Environ. Sci. Heal. - Part B Pestic. Food Contam. Agric. Wastes.* **2017**, *52* (12), 880–886. https://doi.org/10.1080/03601234.2017.1361767.

Campos-Mañas, M. C.; Plaza-Bolaños, P.; Martínez-Piernas, A. B.; Sánchez-Pérez, J. A.; Agüera, A. Determination of Pesticide Levels in Wastewater from an Agro-Food Industry: Target, Suspect and Transformation Product Analysis. *Chemosphere.* **2019**, *232*, 152–163. https://doi.org/10.1016/j.chemosphere.2019.05.147.

Cañizares, P.; Paz, R.; Sáez, C.; Rodrigo, M. A. Costs of the Electrochemical Oxidation of Wastewaters: A Comparison with Ozonation and Fenton Oxidation Processes. *J. Environ. Manage.* **2009**, *90* (1), 410–420. https://doi.org/10.1016/j.jenvman.2007.10.010.

Carbajo, J. B.; Petre, A. L.; Rosal, R.; Herrera, S.; Letón, P.; García-Calvo, E.; Fernández-Alba, A. R.; Perdigón-Melón, J. A. Continuous Ozonation Treatment of Ofloxacin: Transformation Products, Water Matrix Effect and Aquatic Toxicity. *J. Hazard. Mater.* **2015**, *292*, 34-43. https://doi.org/10.1016/j.jhazmat.2015.02.075.

Castro-Alférez, M.; Polo-López, M. I.; Marugán, J.; Fernández-Ibáñez, P. Mechanistic Model of the Escherichia Coli Inactivation by Solar Disinfection Based on the Photo-Generation of Internal ROS and the Photo-Inactivation of Enzymes: CAT and SOD. *Chem. Eng. J.* **2017**, *318*, 214–223. https://doi.org/10.1016/j.cej.2016.06.093.

Castro-Ibáñez, I.; Gil, M. I.; Allende, A. Ready-to-Eat Vegetables: Current Problems and Potential Solutions to Reduce Microbial Risk in the Production Chain. *LWT - Food Sci. Technol.* **2017**, *85*, 284–292. https://doi.org/10.1016/j.lwt.2016.11.073.

CDC. **2018**. Centers for Disease Control and Prevention, Multistate Outbreak of E. coli O157:H7 Infections Linked to Romaine Lettuce (Final Update). (Accessed, 15 July 2019)

CEN. European Committee for Stantarization, P. Lebensmittel, Q. Aliments, Foods of plant origin-Determination of pesticide residues using GC-MS and/or LCMS/MS following acetonitrile extraction/partitioning and cleanup by dispersive SPE-QuEChERS-method, **2007**, *24*, 1-83.

CFA. **2010**. Protocol for produce washing. Chilled Food Association.

Chen, W. R.; Wu, C.; Elovitz, M. S.; Linden, K. G.; Suffet, I. H. Reactions of Thiocarbamate, Triazine and Urea Herbicides, RDX and Benzenes on EPA Contaminant Candidate List with Ozone and with Hydroxyl Radicals. *Water Res.* **2008**, *42* (1–2), 137–144. https://doi.org/10.1016/j.watres.2007.07.037.

Chinnici, G., Di Grusa, A., D'Amico, M. (2019). The consumption of fresh-cut vegetables: features and purchasing behaviour. *Quality-Access to Success.* **2019**, *20*, 178-185.

Chitarra, W.; Decastelli, L.; Garibaldi, A.; Gullino, M. L. Potential Uptake of *Escherichia Coli* O157:H7 and *Listeria Monocytogenes* from Growth Substrate into Leaves

of Salad Plants and Basil Grown in Soil Irrigated with Contaminated Water. *Int. J. Food Microbiol.* **2014**, *189*, 139–145. https://doi.org/10.1016/j.ijfoodmicro.2014.08.003.

Cho, M.; Lee, Y.; Chung, H.; Yoon, J. Inactivation of *Escherichia Coli* by Photochemical Reaction of Ferrioxalate at Slightly Acidic and Near-Neutral PHs. *Appl. Environ. Microbiol.* **2004**, *70* (2), 1129–1134. https://doi.org/10.1128/AEM.70.2.1129-1134.2004.

Cho, M.; Yoon, J. Measurement of OH Radical CT for Inactivating *Cryptosporidium Parvum* Using Photo/Ferrioxalate and Photo/TiO2 Systems. *J. Appl. Microbiol.* **2008**, *104* (3), 759–766. https://doi.org/10.1111/j.1365-2672.2007.03682.x.

Christman, M. F.; Morgan, R. W.; Jacobson, F. S.; Ames, B. N. Oxidative Stress and Some Heat-Shock Proteins in *Salmonella Typhimurium. Cell.* **1985**, *41*, 753–762. https://doi.org/10.1016/S0092-8674(85)80056-8.

Christou, A.; Papadavid, G.; Dalias, P.; Fotopoulos, V.; Michael, C.; Bayona, J. M.; Piña, B.; Fatta-Kassinos, D. Ranking of Crop Plants According to Their Potential to Uptake and Accumulate Contaminants of Emerging Concern. *Environ. Res.* Academic Press Inc., 2019, 422–432. https://doi.org/10.1016/j.envres.2018.12.048.

Ciesielski, F.; Davis, B.; Rittig, M.; Bonev, B. B.; O'Shea, P. Receptor-Independent Interaction of Bacterial Lipopolysaccharide with Lipid and Lymphocyte Membranes; the Role of Cholesterol. *PLoS One.* **2012**, *7* (6), 1–9. https://doi.org/10.1371/journal.pone.0038677.

Clarizia, L.; Russo, D.; Di Somma, I.; Marotta, R.; Andreozzi, R. Homogeneous Photo-Fenton Processes at near Neutral PH: A Review. *Appl. Catal. B Environ.* **2017**, *209,* 358–371. https://doi.org/10.1016/j.apcatb.2017.03.011.

Clesceri, L.S., Greenberg, A.E., Eaton, A.D. (Eds.) Standard Methods for the Examination of water and Wastewater, 20th edition, United Book Press Inc., American Public Health Association; American Waterworks Association; Water Environment Federation, Baltimore, Maryland, **1998a,** 4500-O3, 4-137.

Clesceri, L.S., Greenberg, A.E., Eaton, A.D.(Eds.) Standard Methods for the Examination of water and Wastewater, 20th edition, United Book Press Inc., American Public Health Association; American Waterworks Association; Water Environment Federation, Baltimore, Maryland, **1998b**, 10200-H, 10-18.

COD. **2019**. Ordinary legislative procedure. Minimum requirements for water reuse, 2018/0169(COD), Awaiting Council 1st reading position / budgetary conciliation convocation.https://oeil.secure.europarl.europa.eu/oeil/popups/ficheprocedure.do?lang=en&reference=2018/0169(COD). (Accessed July 08, 2019).

Collazo, C.; Noguera, V.; Aguiló-Aguayo, I.; Abadias, M.; Colás-Medà, P.; Nicolau, I.; Viñas, I. Assessing Water-Assisted UV-C Light and Its Combination with Peroxyacetic Acid and *Pseudomonas Graminis* CPA-7 for the Inactivation and Inhibition of *Listeria Monocytogenes* and *Salmonella Enterica* in Fresh-Cut 'Iceberg' Lettuce and Baby Spinach Leaves. *Int. J. Food Microbiol.* **2019**, *297*, 11–20.

https://doi.org/10.1016/j.ijfoodmicro.2019.02.024.

Collivignarelli, M. C.; Abbà, A.; Benigna, I.; Sorlini, S.; Torretta, V. Overview of the Main Disinfection Processes for Wastewater and Drinking Water Treatment Plants. *Sustain.* **2018**, *10* (1). https://doi.org/10.3390/su10010086.

Cossu, A.; Ercan, D.; Wang, Q.; Peer, W. A.; Nitin, N.; Tikekar, R. V. Antimicrobial Effect of Synergistic Interaction between UV-A Light and Gallic Acid against *Escherichia Coli* O157:H7 in Fresh Produce Wash Water and Biofilm. *Innov. Food Sci. Emerg. Technol.* **2016**, *37*, 44–52. https://doi.org/10.1016/j.ifset.2016.07.020.

Cossu, A.; Huang, K.; Cossu, M.; Tikekar, R. V.; Nitin, N. Fog, Phenolic Acids and UV-A Light Irradiation: A New Antimicrobial Treatment for Decontamination of Fresh Produce. *Food Microbiol.* **2018**, *76*, 204–208. https://doi.org/10.1016/j.fm.2018.05.013.

COT. **2007**. Committee on Toxicity of Chemicals in Food, Consumer Products and the Environment. COT statement on a survey investigating disinfection by-products in prepared salads. https://cot.food.gov.uk/sites/default/files/cot/cotstatementwashaids200614.pdf. (Accessed July 05, 2019).

Cuervo Lumbaque, E.; Salmoria Araújo, D.; Moreira Klein, T.; Lopes Tiburtius, E. R.; Argüello, J.; Sirtori, C. Solar Photo-Fenton-like Process at Neutral PH: Fe(III)-EDDS Complex Formation and Optimization of Experimental Conditions for Degradation of Pharmaceuticals. *Catal. Today.* **2019**, *328*, 259–266. https://doi.org/10.1016/j.cattod.2019.01.006.

Davididou, K.; Chatzisymeon, E.; Perez-Estrada, L.; Oller, I.; Malato, S. Photo-Fenton Treatment of Saccharin in a Solar Pilot Compound Parabolic Collector: Use of Olive Mill Wastewater as Iron Chelating Agent, Preliminary Results. *J. Hazard. Mater.* **2019**, *2010*, 137–144. https://doi.org/10.1016/j.jhazmat.2018.03.016.

De la Obra, I.; Ponce-Robles, L.; Miralles-Cuevas, S.; Oller, I.; Malato, S.; Sánchez Pérez, J. A. Microcontaminant Removal in Secondary Effluents by Solar Photo-Fenton at Circumneutral PH in Raceway Pond Reactors. *Catal. Today.* **2017**, *287*, 10–14. https://doi.org/10.1016/j.cattod.2016.12.028.

De Luca, A.; Dantas, R. F.; Esplugas, S. Assessment of Iron Chelates Efficiency Forphoto-Fenton at Neutral PH. *Water Res.* **2014**, *61*, 232–242. https://doi.org/10.1016/j.watres.2014.05.033.

De Torres-Socías, E.; Fernández-Calderero, I.; Oller, I.; Trinidad-Lozano, M. J.; Yuste, F. J.; Malato, S. Cork Boiling Wastewater Treatment at Pilot Plant Scale: Comparison of Solar Photo-Fenton and Ozone (O_3 , O_3 /H_2O_2). Toxicity and Biodegradability Assessment. *Chem. Eng. J.* **2013**, *234*, 232–239. https://doi.org/10.1016/j.cej.2013.08.072.

Delaquis, P. J.; Fukumoto, L. R.; Toivonen, P. M. A.; Cliff, M. A. Implications of Wash Water Chlorination and Temperature for the Microbiological and Sensory Properties of Fresh-Cut Iceberg Lettuce. *Postharvest Biol. Technol.* **2004**, *31* (1), 81–91. https://doi.org/10.1016/S0925-5214(03)00134-0.

Deng, L.-Z.; Mujumdar, A. S.; Pan, Z.; Vidyarthi, S. K.; Xu, J.; Zielinska, M.; Xiao, H.-W. Emerging Chemical and Physical Disinfection Technologies of Fruits and Vegetables: A Comprehensive Review. *Crit. Rev. Food Sci. Nutr.* **2019**, *0* (0), 1–28. https://doi.org/10.1080/10408398.2019.1649633.

Ding, Q.; Alborzi, S.; Bastarrachea, L. J.; Tikekar, R. V. Novel Sanitization Approach Based on Synergistic Action of UV-A Light and Benzoic Acid: Inactivation Mechanism and a Potential Application in Washing Fresh Produce. *Food Microbiol.* **2018**, *72*, 39–54. https://doi.org/10.1016/j.fm.2017.11.004.

Ding, Q.; Tikekar, R. V. The Synergistic Antimicrobial Effect of a Simultaneous UV-A Light and Propyl Paraben (4-Hydroxybenzoic Acid Propyl Ester) Treatment and Its Application in Washing Spinach Leaves. *J. Food Process Eng.* **2019**, 1–9. https://doi.org/10.1111/jfpe.13062.

Dong, W.; Jin, Y.; Zhou, K.; Sun, S. P.; Li, Y.; Chen, X. D. Efficient Degradation of Pharmaceutical Micropollutants in Water and Wastewater by FeIII-NTA-Catalyzed Neutral Photo-Fenton Process. *Sci. Total Environ.* **2019**, *688*, 513–520. https://doi.org/10.1016/j.scitotenv.2019.06.315.

Doyle, M. P.; Erickson, M. C. Summer Meeting 2007 - The Problems with Fresh Produce: An Overview. *J. Appl. Microbiol.* **2008**, *105* (2), 317–330. https://doi.org/10.1111/j.1365-2672.2008.03746.x.

Drewes, J. E.; Hübner, U.; Zhiteneva, V.; Karakurt, S. Characterization of Unplanned Water Reuse in the EU; **2017**. https://doi.org/10.2779/597701.

EEA, **2016**. European Environmental Agency. Guidelines on Integrating Water Reuse into Water Planning and Management in the context of the WFD, Policy Document, Common Implementation Strategy for the Water Framework Directive. https://www.eea.europa.eu/policy-documents/guidelines-on-integrating-water-reuse (accessed July 08, 2019).

EFSA. **2011**. Urgent Advice on the Public Health Risk of Shiga-Toxin Producing Escherichia Coli in Fresh Vegetables. *EFSA J.,* *9* (6), 2274. https://doi.org/10.2903/j.efsa.2011.2274.

EFSA. **2018**. Guidance on use of EFSA Pesticide Residue IntakeModel (EFSA PRIMo revision 3). EFSA Journal, 16(1):5147, 43. https://doi.org/10.2903/j.efsa.2018.5147.

Eleren, S. Ç.; Alkan, U.; Teksoy, A. Inactivation of *E. Coli* and *B. Subtilis* by Solar and Solar/H_2O_2 Processes in Humic Surface Waters. *Fresenius Environ. Bull.* **2014**, *23* (6), 1397–1406.

Elizaquível, P.; Sánchez, G.; Selma, M. V.; Aznar, R. Application of Propidium Monoazide-QPCR to Evaluate the Ultrasonic Inactivation of *Escherichia Coli* O157:H7 in Fresh-Cut Vegetable Wash Water. *Food Microbiol.* **2012**, *30* (1), 316–320. https://doi.org/10.1016/j.fm.2011.10.008.

Ercan, D.; Cossu, A.; Nitin, N.; Tikekar, R. V. Synergistic Interaction of Ultraviolet

Light and Zinc Oxide Photosensitizer for Enhanced Microbial Inactivation in Simulated Wash-Water. *Innov. Food Sci. Emerg. Technol.* **2016**, *33*, 240–250. https://doi.org/10.1016/j.ifset.2015.11.015.

European Commission. **2000**. Directive 2000/60/EC of the European Parliament and of the Council of 23 October 2000 establishing a framework for Community action in the field of water policy, *Off. J. Eur. Communities*. 327, 1–72.

European Commission. **2001**. Decision 2001/2455/EC of the European Parliament and of the Council of November 2001 establishing the list of priority substances in the field of water policy and amending Directive 2000/60/EC, *Off. J. Eur. Communities*. 331, 1–5.

European Commission. **2004**. Regulation (EC) No 850/2004 of the European Parliament and of the Council of 29 April 2004 on persistent organic pollutants and amending Directive 79/117/EEC, 158, 7–49.

European Commission. **2008**. Directive 2008/105/EC of the European Parliament and of the Council of 16 December 2008 on environmental quality standards in the field of water policy, *Off. J. Eur. Union*. 348, 84–97.

European Commission. **2013**. Directive 2013/39/EU of the European Parliament and of the Council of 12 August 2013 amending Directives 2000/60/EC and 2008/105/EC as regards priority substances in the field of water policy, *Off. J. Eur. Union*. 226, 1–17.

European Commission. **2015**. Decision 2015/495/EU of 20 March 2015 establishing a watch list of substances for Union-wide monitoring in the field of water policy pursuant to Directive 2008/105/EC of the European Parliament and of the Council, *Off. J. Eur. Union.* 78, 40–42.

European Commission. **2018**. Decision 2018/840/EU of 5 June 2018 establishing a watch list of substances for Union-wide monitoring in the field of water policy pursuant to Directive 2008/105/EC of the European Parliament and of the Council and repealing Decision 2015/495/EU, *Off. J. Eur. Union*. 141, 9–12.

EUROSTAT. **2019**. Pesticides sales.Online data code: aei_fm_salpest09.

Evans, R. M.; Scholze, M.; Kortenkamp, A. Examining the Feasibility of Mixture Risk Assessment: A Case Study Using a Tiered Approach with Data of 67 Pesticides from the Joint FAO/WHO Meeting on Pesticide Residues (JMPR). *Food Chem. Toxicol.* **2015**, *84*, 260–269. https://doi.org/10.1016/j.fct.2015.08.015.

Evison, L. M. Comparative Studies on the Survival of Indicator Organisms and Pathogens in Fresh and Sea Water. *Water Sci. Technol.* **1988**, *20* (11–12), 309–315. https://doi.org/10.2166/wst.1988.0300.

FAO WATER. **2010**. The wealth of waste: the economics of wastewater use in agriculture. *Water Reports*, 35, 1-129.

FAO. **2011**. The state of the world's land and water resources for food and agriculture (SOLAW) – Managing systems at risk. Food and Agriculture Organization

of the United Nations, Rome and Earthscan, London.

FAO. **2015**. Towards a Water and Food Secure Future: Critical Perspectives for Policy-Makers. World Water Counc. I4560, 62.

FAO. **2017**. Water for Sustainable Food and Agriculture: A Report Produced for the G20 Presidency of Germany.

FAO/WHO. **2008**. Microbiological hazards in fresh leafy vegetables and herbs: Meeting Report. Microbiological Risk Assessment Series No. 14. Rome.1-151.

FAO/WHO. **2016**. Codex Alimentarius commission. Procedural Manual, 25th ed. Rome.

FAO-AQUASTAT. **2016**. Main Database, Food and Agriculture Organization of the United Nations (FAO). http://www.fao.org/nr/water/aquastat/data/query/index.html?lang=en (accessed July 11, 2019).

Farr, S. B.; Kogoma, T. Oxidative Stress Responses in *Escherichia Coli* and *Salmonella Typhimurium*. *Microbiol. Rev*. **1991**, *55* (4), 561–585.

FDA. **1998**. Guidance for Industry. Guide to minimize microbial food safety hazards for fresh fruits and vegetables, Food Safety Initiative Staff, HFS-32. U.S. Food and Drug Administration, Center for Food Safety and Applied Nutrition,Washington DC.

Fenton, H. J. H. Oxidation of Tartaric Acid in Presence of Iron. *J. Chem Soc*. **1894**, *65*, 899-910. https://doi.org/10.1039/CT8946500899.

Ferro, G.; Fiorentino, A.; Alferez, M. C.; Polo-López, M. I.; Rizzo, L.; Fernández-Ibáñez, P. Urban Wastewater Disinfection for Agricultural Reuse: Effect of Solar Driven AOPs in the Inactivation of a Multidrug Resistant *E. Coli* Strain. *Appl. Catal. B Environ.* **2015a**, *178*, 65–73. https://doi.org/10.1016/j.apcatb.2014.10.043.

Ferro, G.; Polo-López, M. I.; Martínez-Piernas, A. B.; Fernández-Ibáñez, P.; Agüera, A.; Rizzo, L. Cross-Contamination of Residual Emerging Contaminants and Antibiotic Resistant Bacteria in Lettuce Crops and Soil Irrigated with Wastewater Treated by Sunlight/H_2O_2. *Environ. Sci. Technol.* **2015b**, *49* (18), 11096–11104. https://doi.org/10.1021/acs.est.5b02613.

Fiorentino, A.; Ferro, G.; Alferez, M. C.; Polo-López, M. I.; Fernández-Ibañez, P.; Rizzo, L. Inactivation and Regrowth of Multidrug Resistant Bacteria in Urban Wastewater after Disinfection by Solar-Driven and Chlorination Processes. *J. Photochem. Photobiol. B Biol.* **2015**, *148*, 43–50. https://doi.org/10.1016/j.jphotobiol.2015.03.029.

Fischbacher, A.; Von Sonntag, J.; Von Sonntag, C.; Schmidt, T. C. The •OH Radical Yield in the H_2O_2 + O_3 (Peroxone) Reaction. *Environ. Sci. Technol.* **2013**, *47* (17), 9959–9964. https://doi.org/10.1021/es402305r.

Fisher, M. B.; Keenan, C. R.; Nelson, K. L.; Voelker, B. M. Speeding up Solar

Disinfection (SODIS): Effects of Hydrogen Peroxide, Temperature, PH, and Copper plus Ascorbate on the Photoinactivation of *E. Coli*. *J. Water Health.* **2007**, *6* (1), 35–51. https://doi.org/10.2166/wh.2007.005.

Flynn, C. M. Hydrolysis of Inorganic Iron (III) Salts. **1984**, *84 (1)*, 31–41. https://doi.org/10.1021/cr00059a003.

Formisano, F.; Fiorentino, A.; Rizzo, L.; Carotenuto, M.; Pucci, L.; Giugni, M.; Lofrano, G. Inactivation of *Escherichia Coli* and *Enterococci* in Urban Wastewater by Sunlight/PAA and Sunlight/H_2O_2 Processes. *Process Saf. Environ. Prot.* **2016**, *104*, 178–184. https://doi.org/10.1016/j.psep.2016.09.003.

Gallard, H.; Laat, J.; Legube, B. Influence Du PH Sur La Vitesse D´oxydation de Composes Organiques Par Fe^{II} / H_2O_2 . Mecanismes Reactionnels et Modelisation. *New journal of chemistry*, **1998**, *22*, 263–268. https://doi.org/10.1039/A708335A.

Gallego-Schmid, A.; Tarpani, R. R. Z.; Miralles-Cuevas, S.; Cabrera-Reina, A.; Malato, S.; Azapagic, A. Environmental Assessment of Solar Photo-Fenton Processes in Combination with Nanofiltration for the Removal of Micro-Contaminants from Real Wastewaters. *Sci. Total Environ.* **2019**, *650*, 2210–2220. https://doi.org/10.1016/j.scitotenv.2018.09.361.

García-Fernández, I.; Fernández-Calderero, I.; Inmaculada Polo-López, M.; Fernández-Ibáñez, P. Disinfection of Urban Effluents Using Solar TiO_2 Photocatalysis: A Study of Significance of Dissolved Oxygen, Temperature, Type of Microorganism and Water Matrix. *Catal. Today.* **2015**, *240*, 30–38. https://doi.org/10.1016/j.cattod.2014.03.026.

García-Fernández, I.; Miralles-Cuevas, S.; Oller, I.; Malato, S.; Fernández-Ibáñez, P.; Polo-López, M. I. Inactivation of *E. Coli* and *E. Faecalis* by Solar Photo-Fenton with EDDS Complex at Neutral PH in Municipal Wastewater Effluents. *J. Hazard. Mater.* **2019**, *372*, 85–93. https://doi.org/10.1016/j.jhazmat.2018.07.037.

García-Fernández, I.; Polo-López, M. I.; Oller, I.; Fernández-Ibáñez, P. Bacteria and Fungi Inactivation Using Fe^{3+}/Sunlight, H_2O_2/Sunlight and near Neutral Photo-Fenton: A Comparative Study. *Appl. Catal. B Environ.* **2012**, *121–122*, 20–29. https://doi.org/10.1016/j.apcatb.2012.03.012.

García-Marco, S.; Torreblanca, A.; Lucena, J. J. Chromatographic Determination of Fe Chelated by Ethylenediamine-N-(o-Hydroxyphenylacetic)-N′-(p-Hydroxyphenylacetic) Acid in Commercial EDDHA/Fe^{3+} Fertilizers. *J. Agric. Food Chem.* **2006**, *54* (4), 1380–1386. https://doi.org/10.1021/jf051745x.

Garrett, E. H.; Gorny, J. R.; Beuchat, L. R.; Farber, J. N.; Harris, L. J.; Parish, M. E.; Suslow, T. V.; Busta, F. F. Microbiological Safety of Fresh and Fresh-Cut Produce: Description of the Situation and Economic Impact. *Compr. Rev. Food Sci. Food Saf.* **2003**, *2* (s1), 13–37. https://doi.org/10.1111/j.1541-4337.2003.tb00029.x.

Garrido, Y.; Marín, A.; Tudela, J. A.; Allende, A.; Gil, M. I. Chlorate Uptake during Washing Is Influenced by Product Type and Cut Piece Size, as Well as Washing Time and Wash Water Content. *Postharvest Biol. Technol.* **2019**, *151*, 45–52.

https://doi.org/10.1016/j.postharvbio.2019.01.014.

Giannakis, S.; López, M. I. P.; Spuhler, D.; Pérez, J. A. S.; Ibáñez, P. F.; Pulgarin, C. Solar Disinfection Is an Augmentable, in Situ-Generated Photo-Fenton Reaction-Part 2: A Review of the Applications for Drinking Water and Wastewater Disinfection. *Appl. Catal. B Environ.*, **2016b**, *198*, 431–446. https://doi.org/10.1016/j.apcatb.2016.06.007.

Giannakis, S.; Polo López, M. I.; Spuhler, D.; Sánchez Pérez, J. A.; Fernández Ibáñez, P.; Pulgarin, C. Solar Disinfection Is an Augmentable, in Situ-Generated Photo-Fenton Reaction—Part 1: A Review of the Mechanisms and the Fundamental Aspects of the Process. *Appl. Catal. B Environ.*, **2016a**, *199,* 199–223. https://doi.org/10.1016/j.apcatb.2016.06.009.

Giannakis, S.; Watts, S.; Rtimi, S.; Pulgarin, C. Solar Light and the Photo-Fenton Process against Antibiotic Resistant Bacteria in Wastewater: A Kinetic Study with a Streptomycin-Resistant Strain. *Catal. Today.* **2018**, *313,* 86-93. https://doi.org/10.1016/j.cattod.2017.10.033.

Gil, M. I.; Gómez-López, V. M.; Hung, Y. C.; Allende, A. Potential of Electrolyzed Water as an Alternative Disinfectant Agent in the Fresh-Cut Industry. *Food Bioprocess Technol.* **2015**, *8* (6), 1336–1348. https://doi.org/10.1007/s11947-014-1444-1.

Gil, M. I.; López-Gálvez, F.; Andújar, S.; Moreno, M.; Allende, A. Disinfection By-Products Generated by Sodium Hypochlorite and Electrochemical Disinfection in Different Process Wash Water and Fresh-Cut Products and Their Reduction by Activated Carbon. *Food Control.* **2019**, *100*, 46–52. https://doi.org/10.1016/j.foodcont.2018.12.050.

Gil, M. I.; Marín, A.; Andujar, S.; Allende, A. Should Chlorate Residues Be of Concern in Fresh-Cut Salads? *Food Control.* **2016**, *60*, 416–421. https://doi.org/10.1016/j.foodcont.2015.08.023.

Gil, M. I.; Selma, M. V. Overview of Hazards in Fresh-Cut Produce Production: Control and Management of Food Safety Hazards. In Microbial Hazard Identification in Fresh Fruits and Vegetables; John Wiley and Sons Inc, **2006**, 155–219. https://doi.org/10.1002/0470007761.ch6.

Gómez-Gallego, M.; Pellico, D.; Ramírez-López, P.; Mancheño, J. M.; Romano, S.; De La Torre, M. C.; Sierra, M. A. Understanding of the Mode of Action of FeIII-EDDHA as Iron Chlorosis Corrector Based on Its Photochemical and Redox Behavior. *Chem. - A Eur. J.* **2005**, *11* (20), 5997–6005. https://doi.org/10.1002/chem.200500286.

Gómez-Gallego, M.; Sherra, M. A.; Alcázar, R.; Ramírez, P.; Piñar, C.; Mancheño, M. J.; García-Marco, S.; Yunta, F.; Lucena, J. J. Synthesis of o,p-EDDHA and Its Detection as the Main Impurity in o,o-EDDHA Commercial Iron Chelates. *J. Agric. Food Chem.* **2002**, *50*, 6395-6399. https://doi.org/10.1021/jf025727g.

Gómez-López, V. M.; Lannoo, A. S.; Gil, M. I.; Allende, A. Minimum Free Chlorine Residual Level Required for the Inactivation of *Escherichia Coli* O157: H7 and

Trihalomethane Generation during Dynamic Washing of Fresh-Cut Spinach. *Food Control .* **2014**, *42*, 132–138. https://doi.org/10.1016/j.foodcont.2014.01.034.

Goodsell D. S., The molecular perspective: ultraviolet light and pyrimidine dimmers. Oncologist, **2001**, *6*, 298–299.

Gottschalk, C., Libra, J.A., Saupe, A., Ozonation of Water and Waste Water: A Practical Guide to Understanding Ozone and its Applications. **2009**. John Wiley & Sons.

Haas, C.N., Rose, J.B. and Gerba, C.P. Quantitative Microbial Risk Assessment. John Wiley and Sons, Inc., New York, NY, USA, **1999**.

Hadjok, C.; Mittal, G. S.; Warriner, K. Inactivation of Human Pathogens and Spoilage Bacteria on the Surface and Internalized within Fresh Produce by Using a Combination of Ultraviolet Light and Hydrogen Peroxide. *J. Appl. Microbiol.* **2008**, *104* (4), 1014–1024. https://doi.org/10.1111/j.1365-2672.2007.03624.x.

Hancock, R. E. W.; Wong, P. G. W. Compounds Which Increase the Permeability of the *Pseudomonas Aeruginosa* Outer Membrane. *Antimicrob. Agents Chemother.* **1984**, *26* (1), 48–52. https://doi.org/10.1128/AAC.26.1.48.

Hansen, K. M. S.; Spiliotopoulou, A.; Cheema, W. A.; Andersen, H. R. Effect of Ozonation of Swimming Pool Water on Formation of Volatile Disinfection By-Products A Laboratory Study. *Chem. Eng. J.* **2016**, *289*, 277–285. https://doi.org/https://doi.org/10.1016/j.cej.2015.12.052.

Harris, L. J.; Farber, J. N.; Beuchat, L. R.; Parish, M. E.; Suslow, T. V.; Garrett, E. H.; Busta, F. F. Outbreaks Associated with Fresh Produce: Incidence, Growth, and Survival of Pathogens in Fresh and Fresh-Cut Produce. *Compr. Rev. Food Sci. Food Saf.* **2003**, *2* , 78–141. https://doi.org/10.1111/j.1541-4337.2003.tb00031.x.

Hartman, P. S.; Eisenstark, A. Killing of Escherichia Coli K-12 by near-Ultraviolet Radiation in the Presence of Hydrogen Peroxide: Role of Double-Strand DNA Breaks in Absence of Recombinational Repair. *Mutat. Res. - Fundam. Mol. Mech. Mutagen.* **1980**, *72*(1), 31-42. https://doi.org/10.1016/0027-5107(80)90217-1.

Hassenberg, K.; Idler, C.; Molloy, E.; Geyer, M.; Plöchl, M.; Barnes, J. Use of Ozone in a Lettuce-Washing Process: An Industrial Trial. *J. Sci. Food Agric.* **2007**, *87* (5), 914–919. https://doi.org/10.1002/jsfa.2815.

Havelaar, A. H.; Haagsma, J. A.; Mangen, M. J. J.; Kemmeren, J. M.; Verhoef, L. P. B.; Vijgen, S. M. C.; Wilson, M.; Friesema, I. H. M.; Kortbeek, L. M.; van Duynhoven, Y. T. H. P.; et al. Disease Burden of Foodborne Pathogens in the Netherlands, *Int. J. Food Microbiol.* **2012**, *156* (3), 231–238. https://doi.org/10.1016/j.ijfoodmicro.2012.03.029.

Heldal, M.; Norland, S.; Tumyr, O. X-Ray Microanalytic Method for Measurement of Dry Matter and Elemental Content of Individual Bacteria. *Appl. Environ. Microbiol.* **1985**, *50* (5), 1251–1257.

Hendricks, S. B.; Taylorson, R. B. Promotion of Seed Germination by Nitrate,

Nitrite, Hydroxylamine, and Ammonium Salts. *Plant Physiol.* **1974**, *54* (3), 304–309. https://doi.org/10.1104/pp.54.3.304.

Herman, K. M.; Hall, A. J.; Gould, L. H. Outbreaks Attributed to Fresh Leafy Vegetables, United States, 1973-2012. *Epidemiol. Infect.* **2015**, *143* (14), 3011–3021. https://doi.org/10.1017/S0950268815000047.

Hernández-Apaolaza, L.; Lucena, J. J. Influence of Irradiation Time and Solution Concentration on the Photochemical Degradation of EDDHA/Fe^{3+}: Effect of Its Photodecomposition Products on Soybean Growth. *J. Sci. Food Agric.* **2011**, *91* (11), 2024–2030. https://doi.org/10.1002/jsfa.4414.

Hu, Z.; Chen, X.; Chen, D.; Li, J.; Wang, S.; Zhou, Q.; Yin, G.; Guo, M. "Dry Gets Drier, Wet Gets Wetter": A Case Study over the Arid Regions of Central Asia. *Int. J. Climatol.* **2019**, *39* (2), 1072–1091. https://doi.org/10.1002/joc.5863.

Huang, W.; Brigante, M.; Wu, F.; Hanna, K.; Mailhot, G. Effect of Ethylenediamine-N,N-Disuccinic Acid on Fenton and Photo-Fenton Processes Using Goethite as an Iron Source: Optimization of Parameters for Bisphenol A Degradation. *Environ. Sci. Pollut. Res.* **2012b**, *20* (1), 39–50. https://doi.org/10.1007/s11356-012-1042-6.

Huang, Y.; Ye, M.; Chen, H. Efficacy of Washing with Hydrogen Peroxide Followed by Aerosolized Antimicrobials as a Novel Sanitizing Process to Inactivate *Escherichia Coli* O157:H7 on Baby Spinach. *Int. J. Food Microbiol.* **2012a**, *153* (3), 306–313. https://doi.org/10.1016/j.ijfoodmicro.2011.11.018.

Hübner, U.; Keller, S.; Jekel, M. Evaluation of the Prediction of Trace Organic Compound Removal during Ozonation of Secondary Effluents Using Tracer Substances and Second Order Rate Kinetics. *Water Res.* **2013**, *47* (17), 6467–6474. https://doi.org/10.1016/j.watres.2013.08.025.

Ignat, A.; Manzocco, L.; Bartolomeoli, I.; Maifreni, M.; Nicoli, M. C. Minimization of Water Consumption in Fresh-Cut Salad Washing by UV-C Light. *Food Control* **2015**, *50*, 491–496. https://doi.org/10.1016/j.foodcont.2014.09.036.

Ikehata, K. Hazardous Agents in Wastewater: Public Health Impacts and Treatment Options for Safe Disposal and Reuse. In *Wastewater Reuse and Management*; Springer Netherlands, **2013**, 165–191. https://doi.org/10.1007/978-94-007-4942-9_6.

Imlay, J. A.; Hassett, D. J. Oxidative and Nitrosative Stress Defence Systems in *Escherichia Coli* and *Pseudomonas Aeruginosa*: A Model Organism of Study versus a Human Opportunistic Pathogen. *Stress response in pathogenic bacteria*; **2011**. https://doi.org/10.1079/9781845937607.0003.

Inyinbor, A. A.; Bello, O. S.; Oluyori, A. P.; Inyinbor, H. E.; Fadiji, A. E. Wastewater Conservation and Reuse in Quality Vegetable Cultivation: Overview, Challenges and Future Prospects. *Food Control*, **2019**, 489–500. https://doi.org/10.1016/j.foodcont.2018.12.008.

ISO, **1998**. ISO 11348-3:1998 - Water quality -- Determination of the inhibitory effect of water samples on the light emission of *Vibrio fischeri* (Luminescent bacteria test).

Johnston, A. E.; Poulton, P. R.; Fixen, P. E.; Curtin, D. Phosphorus : Its Efficient Use in Agriculture, 1st ed.; *Elsevier Inc.*, **2014**; Vol. 123. https://doi.org/10.1016/B978-0-12-420225-2.00005-4.

Jones, C.W. Applications of hydrogen peroxide and derivates. James H. Clark (Ed). *Royal Society of chemistry*, Cambrigde, UK, ISBN 0-85404-536-8, **1999**, 264.

Kaczmarek, M.; Avery, S. V.; Singleton, I. *Microbes Associated with Fresh Produce: Sources, Types and Methods to Reduce Spoilage and Contamination*, 1st ed.; Elsevier Inc., **2019**; Vol. 107. https://doi.org/10.1016/bs.aambs.2019.02.001.

Khadre, M. A.; Yousef, A. E.; Kim, J.-G. Microbiological Aspects of Ozone Applications in Food: A Review. **2001**, *66*.

Kim, J.-G.; Yousef, A. E.; Dave, S. Application of Ozone for Enhancing the Microbiological Safety and Quality of Foods: A Review. *J. Food Prot.* **1999**, *62* (9), 1071–1087. https://doi.org/10.4315/0362-028X-62.9.1071.

Kim, J.-G.; Yousef, A. E.; Dave, S. Application of Ozone for Enhancing the Microbiological Safety and Quality of Foods: A Review. *J. Food Prot.* **1999**, *62* (9), 1071–1087. https://doi.org/10.4315/0362-028X-62.9.1071.

Kiwi, J. Lopez, A. Nadtochenko, V. Mechanism and Kinetics of the OH-Radical Intervention during Fenton Oxidation in the Presence of a Significant Amount of Radical Scavenger (Cl⁻). **2000**, *34* (11), 2162–2168. https://doi.org/10.1021/es991406i.

Klamerth, N.; Malato, S.; Agüera, A.; Fernández-Alba, A.; Mailhot, G. Treatment of Municipal Wastewater Treatment Plant Effluents with Modified Photo-Fenton as a Tertiary Treatment for the Degradation of Micro Pollutants and Disinfection. *Environ. Sci. Technol.* **2012**, *46* (5), 2885–2892. https://doi.org/10.1021/es204112d.

Kowalska, K.; Maniakova, G.; Carotenuto, M.; Sacco, O.; Vaiano, V.; Lofrano, G. Chemosphere Removal of Carbamazepine , Diclofenac and Trimethoprim by Solar Driven Advanced Oxidation Processes in a Compound Triangular Collector Based Reactor : A Comparison between Homogeneous and Heterogeneous Processes. *Chemosphere.* **2020**, *238*, 124665. https://doi.org/10.1016/j.chemosphere.2019.124665.

Laghi, L.; Alcaniz, S.; Cerdán, M. A. R.; Gomez-Gallego, M. A. R.; Sierra, M. A.; Placucci, G.; Cremonini, M. A. Facile Deferration of Commercial Fertilizers Containing Iron Chelates for Their NMR Analysis. *J. Agric. Food Chem.* **2009**, *57* (12), 5143–5147. https://doi.org/10.1021/jf900116z.

LeChevallier, M. W. Case for Maintaining a Disinfectant Residual. *J. Am. Water Work. Assoc.* **1999**, *91* (1), 86–94. https://doi.org/10.1002/j.1551-8833.1999.tb08573.x.

Lee, W. N.; Huang, C. H. Formation of Disinfection Byproducts in Wash Water and Lettuce by Washing with Sodium Hypochlorite and Peracetic Acid Sanitizers. *Food Chem. X.* **2019**, *1*, 100003 https://doi.org/10.1016/j.fochx.2018.100003.

Lee, Y.; Kovalova, L.; McArdell, C. S.; von Gunten, U. Prediction of Micropollutant Elimination during Ozonation of a Hospital Wastewater Effluent. *Water Res.* **2014**, *64*, 134–148. https://doi.org/10.1016/j.watres.2014.06.027.

Lewis, K. A.; Tzilivakis, J.; Warner, D. J.; Green, A. An International Database for Pesticide Risk Assessments and Management. *Hum. Ecol. Risk Assess.* **2016**, *22* (4), 1050–1064. https://doi.org/10.1080/10807039.2015.1133242.

Li, D.; Zeng, S.; Gu, A. Z.; He, M.; Shi, H. Inactivation, Reactivation and Regrowth of Indigenous Bacteria in Reclaimed Water after Chlorine Disinfection of a Municipal Wastewater Treatment Plant. *J. Environ. Sci.* **2013**, *25* (7), 1319–1325. https://doi.org/10.1016/S1001-0742(12)60176-4.

Lindsey, M. E.; Tarr, M. A. Quantitation of Hydroxyl Radical during Fenton Oxidation Following a Single Addition of Iron and Peroxide. *Chemosphere.* **2000**, *41* (3), 409–417. https://doi.org/10.1016/S0045-6535(99)00296-9.

Liu, G.; Marshall Porterfield, D.; Li, Y.; Klassen, W. Increased Oxygen Bioavailability Improved Vigor and Germination of Aged Vegetable Seeds. *HortScience* **2012**, *47* (12), 1714–1721. https://doi.org/10.21273/hortsci.47.12.1714.

Loeb, B. L.; Thompson, C. M.; Drago, J.; Takahara, H.; Baig, S. Worldwide Ozone Capacity for Treatment of Drinking Water and Wastewater: A Review. *Ozone Sci. Eng.* **2012**, *34* (1), 64–77. https://doi.org/10.1080/01919512.2012.640251.

López-Gálvez, F.; Posada-Izquierdo, G. D.; Selma, M. V.; Pérez-Rodríguez, F.; Gobet, J.; Gil, M. I.; Allende, A. Electrochemical Disinfection: An Efficient Treatment to Inactivate *Escherichia Coli* O157:H7 in Process Wash Water Containing Organic Matter. *Food Microbiol.* **2012**, *30* (1), 146–156. https://doi.org/10.1016/j.fm.2011.09.010.

López-Vinent, N.; Cruz-Alcalde, A.; Gutiérrez, C.; Marco, P.; Giménez, J.; Esplugas, S. Micropollutant Removal in Real WW by Photo-Fenton (Circumneutral and Acid PH) with BLB and LED Lamps. *Chem. Eng. J.* **2020**, *379*, 122416. https://doi.org/10.1016/j.cej.2019.122416.

Lu, M.; Chen, J. Effect of inorganic ions on the oxidation of dichlorvos insecticide with Fenton's reagent. *Chemosfere.* **1997**, *35* (10), 2285–2293. https://doi.org/10.1016/S0045-6535(97)00307-X.

Luo, Y.; Guo, W.; Ngo, H. H.; Nghiem, L. D.; Hai, F. I.; Zhang, J.; Liang, S.; Wang, X. C. A Review on the Occurrence of Micropollutants in the Aquatic Environment and Their Fate and Removal during Wastewater Treatment. *Sci. Total Environ.* **2014**, *473*, 619–641. https://doi.org/10.1016/j.scitotenv.2013.12.065.

Lynch, M. F.; Tauxe, R. V.; Hedberg, C. W. The Growing Burden of Foodborne Outbreaks Due to Contaminated Fresh Produce: Risks and Opportunities. *Epidemiol. Infect.* **2009**, *137* (3), 307–315. https://doi.org/10.1017/S0950268808001969.

Ma, X. H.; Zhao, L.; Dong, Y. H.; Chen, H.; Zhong, M. Enhanced Fenton

Degradation of Polychlorinated Biphenyls in Capacitor-Oil-Contaminated Soil by Chelating Agents. *Chem. Eng. J.* **2018**, *333*, 370–379. https://doi.org/10.1016/j.cej.2017.09.167.

Malaj, E.; von der Ohe, P. C.; Grote, M.; Kühne, R.; Mondy, C. P.; Usseglio-Polatera, P.; Brack, W.; Schäfer, R. B. Organic Chemicals Jeopardize the Health of Freshwater Ecosystems on the Continental Scale. *Proc. Natl. Acad. Sci.* **2014**, *111* (26), 9549-9554. https://doi.org/10.1073/pnas.1321082111.

Malato, S.; Fernández-Ibáñez, P.; Maldonado, M. I.; Blanco, J.; Gernjak, W. Decontamination and Disinfection of Water by Solar Photocatalysis: Recent Overview and Trends. *Catal. Today*. **2009**, 1–59. https://doi.org/10.1016/j.cattod.2009.06.018.

Maniakova, G.; Kowalska, K.; Murgolo, S.; Mascolo, G.; Libralato, G.Lofrano, G.; Saco, O.; Guida, M.; Rizzo, L. Comparison between heterogeneous and homogeneous solar driven advanced oxidation processes for urban wastewater treatment: Pharmaceuticals removal and toxicity. *Sep. Purif. Technol.*, **2020**, 116249. https://doi.org/10.1016/j.seppur.2019.116249.

Mao, Y.; Guo, D.; Yao, W.; Wang, X.; Yang, H.; Xie, Y. F.; Komarneni, S.; Yu, G.; Wang, Y. Effects of Conventional Ozonation and Electro-Peroxone Pretreatment of Surface Water on Disinfection by-Product Formation during Subsequent Chlorination. *Water Res.* **2018**, *130*, 322–332. https://doi.org/10.1016/j.watres.2017.12.019.

MAPA. **2019**. Ministerio de Agricultura,Pesca y Alimentación, Food Consumption Report in Spain 2018. https://www.mapa.gob.es/en/alimentacion/temas/consumo-y-comercializacion-y-distribucion-alimentaria/panel-de-consumo-alimentario/ultimos-datos/. (Accessed July 29, 2019).

Margenat, A.; Matamoros, V.; Díez, S.; Cañameras, N.; Comas, J.; Bayona, J. M. Occurrence of Chemical Contaminants in Peri-Urban Agricultural Irrigation Waters and Assessment of Their Phytotoxicity and Crop Productivity. *Sci. Total Environ.* **2017**, *599–600*, 1140–1148. https://doi.org/10.1016/j.scitotenv.2017.05.025.

Margot, J.; Kienle, C.; Magnet, A.; Weil, M.; Rossi, L.; de Alencastro, L. F.; Abegglen, C.; Thonney, D.; Chèvre, N.; Schärer, M.; Barry, D.A. Treatment of Micropollutants in Municipal Wastewater: Ozone or Powdered Activated Carbon? *Sci. Total Environ.* **2013**, *461–462*, 480–498. https://doi.org/10.1016/j.scitotenv.2013.05.034.

Martínez-Piernas, A. B.; Polo-López, M. I.; Fernández-Ibáñez, P.; Agüera, A. Validation and Application of a Multiresidue Method Based on Liquid Chromatography-Tandem Mass Spectrometry for Evaluating the Plant Uptake of 74 Microcontaminants in Crops Irrigated with Treated Municipal Wastewater. *J. Chromatogr. A.* **2018**. *26*, 10-21. https://doi.org/10.1016/j.chroma.2017.12.037.

Mateo-Sagasta, J.; Burke , J. Agriculture and water quality interactions. SOLAW Background Thematic Report TR08. Rome, **2010**, FAO.

Meierhofer, R.; Wegelin, M.; Rosario Torres, X. del. Solar Water Disinfection : A Guide for the Application of SODIS; EAWAG, **2002**.

Meireles, A.; Giaouris, E.; Simões, M. Alternative Disinfection Methods to Chlorine for Use in the Fresh-Cut Industry. *Food Res. Int.*, **2016**, *82,* 71–85. https://doi.org/10.1016/j.foodres.2016.01.021.

Mekonnen, M. M.; Hoekstra, Y. A. Four Billion People Facing Severe Water Scarcity. *Am. Assoc. Adv. Sci.* **2016**, 1–7. https://doi.org/10.1126/sciadv.1500323

Menz, J.; Schneider, M.; Kümmerer, K. Toxicity Testing with Luminescent Bacteria - Characterization of an Automated Method for the Combined Assessment of Acute and Chronic Effects. *Chemosphere.* **2013**, *93* (6), 990–996. https://doi.org/10.1016/j.chemosphere.2013.05.067.

Mercer,W.A., Somers,I.I. Chlorine in food plant sanitation. *Adv. Food Res.* **1957**, *7,* 129-169.

Merényi, G.; Lind, J.; Naumov, S.; Sonntag, C. Von. Reaction of Ozone with Hydrogen Peroxide (Peroxone Process): A Revision of Current Mechanistic Concepts Based on Thermokinetic and Quantum-Chemical Considerations. *Environ. Sci. Technol.* **2010**, *44* (9), 3505–3507. https://doi.org/10.1021/es100277d.

Milovac, N.; Juretic, D.; Kusic, H.; Dermadi, J.; Bozic, A. L. Photooxidative Degradation of Aromatic Carboxylic Acids in Water: Influence of Hydroxyl Substituents. *Ind. Eng. Chem. Res.* **2014**, *53 (26),* https://doi.org/10.1021/ie501338q.

Miralles-Cuevas, S.; Oller, I.; Ruíz-Delgado, A.; Cabrera-Reina, A.; Cornejo-Ponce, L.; Malato, S. EDDS as Complexing Agent for Enhancing Solar Advanced Oxidation Processes in Natural Water: Effect of Iron Species and Different Oxidants. *J. Hazard. Mater.* **2019**, *372*, 129-136. https://doi.org/10.1016/j.jhazmat.2018.03.018.

Moraes, R. M.; Carvalho, M.; Nery, F. C.; Filho, P. R. S.; Nogueira, M. L.; Barbosa, S. Effects of Hydrogen Peroxide on Initial Growth and Enzymatic Antioxidant System of Lactuca Sativa L (Asteraceae). *Pakistan J. Bot.* **2018**, *50* (5), 1769–1774.

Moreira, N. F. F.; Narciso-da-Rocha, C.; Polo-López, M. I.; Pastrana-Martínez, L. M.; Faria, J. L.; Manaia, C. M.; Fernández-Ibáñez, P.; Nunes, O. C.; Silva, A. M. T. Solar Treatment (H_2O_2, TiO_2-P25 and GO-TiO_2 Photocatalysis, Photo-Fenton) of Organic Micropollutants, Human Pathogen Indicators, Antibiotic Resistant Bacteria and Related Genes in Urban Wastewater. *Water Res.* **2018**, *135*, 195–206. https://doi.org/10.1016/j.watres.2018.01.064.

Murphy, S.; Gaffney, M. T.; Fanning, S.; Burgess, C. M. Potential for Transfer of *Escherichia Coli* O157:H7, *Listeria Monocytogenes* and *Salmonella Senftenberg* from Contaminated Food Waste Derived Compost and Anaerobic Digestate Liquid to Lettuce Plants. *Food Microbiol.* **2016**, *59*, 7–13. https://doi.org/10.1016/j.fm.2016.04.006.

Ndounla, J.; Pulgarin, C. Solar Light (Hv) and H_2O_2/Hv Photo-Disinfection of Natural Alkaline Water (PH 8.6) in a Compound Parabolic Collector at Different Day Periods in Sahelian Region. *Environ. Sci. Pollut. Res.* **2015**, *22* (21), 17082–17094. https://doi.org/10.1007/s11356-015-4784-0.

Ng, T. W.; An, T.; Li, G.; Ho, W. K.; Yip, H. Y.; Zhao, H.; Wong, P. K. The Role and Synergistic Effect of the Light Irradiation and H_2O_2 in Photocatalytic Inactivation of *Escherichia Coli*. *J. Photochem. Photobiol. B Biol.* **2015**, *149*, 164–171. https://doi.org/10.1016/j.jphotobiol.2015.06.007.

Nöthe, T.; Fahlenkamp, H.; Von Sonntag, C. Ozonation of Wastewater: Rate of Ozone Consumption and Hydroxyl Radical Yield. *Environ. Sci. Technol.* **2009**, *43* (15), 5990–5995. https://doi.org/10.1021/es900825f.

OECD. **2012** .OECD Environmental Outlook to 2050: The Consequences of Inaction, OECD Publishing, Paris.

OECD. **2015**. Environment at a Glance 2015: OECD Indicators, OECD Publishing, Paris. http://dx.doi.org/10.1787/9789264235199-en

OECD. **2018**. OECD Workshop on Managing Contaminants of Emerging Concern in Surface Waters: Scientific Developments and Cost-Effective Policy Responses, Summary Note.

Oppezzo, O. J.; Costa, C. S.; Pizarro, R. A. Influence of RpoS Mutations on the Response of *Salmonella Enterica Serovar Typhimurium* to Solar Radiation. *J. Photochem. Photobiol. B Biol.* **2011**, *102* (1), 20–25.

Ortega-Gómez, E.; Esteban García, B.; Ballesteros Martín, M. M.; Fernández Ibáñez, P.; Sánchez Pérez, J. A. Inactivation of Enterococcus Faecalis in Simulated Wastewater Treatment Plant Effluent by Solar Photo-Fenton at Initial Neutral PH. *Catal. Today.* **2013**, *209*, 195–200. https://doi.org/10.1016/j.cattod.2013.03.001.

Ortega-Gómez, E.; Fernández-Ibáñez, P.; Ballesteros Martín, M. M.; Polo-López, M. I.; Esteban García, B.; Sánchez Pérez, J. A. Water Disinfection Using Photo-Fenton: Effect of Temperature on Enterococcus Faecalis Survival. *Water Res.* **2012**, *46* (18), 6154–6162. https://doi.org/10.1016/j.watres.2012.09.007.

Papoutsakis, S.; Miralles-Cuevas, S.; Oller, I.; Garcia Sanchez, J. L.; Pulgarin, C.; Malato, S. Microcontaminant Degradation in Municipal Wastewater Treatment Plant Secondary Effluent by EDDS Assisted Photo-Fenton at near-Neutral PH: An Experimental Design Approach. *Catal. Today* **2015**, *252*, 61–69. https://doi.org/10.1016/j.cattod.2015.02.005.

Park, K. Y.; Choi, S. Y.; Lee, S. H.; Kweon, J. H.; Song, J. H. Comparison of Formation of Disinfection By-Products by Chlorination and Ozonation of Wastewater Effluents and Their Toxicity to *Daphnia Magna*. *Environ. Pollut.* **2016**, *215*, 314–321. https://doi.org/10.1016/j.envpol.2016.04.001.

Park, S. H.; Choi, M. R.; Park, J. W.; Park, K. H.; Chung, M. S.; Ryu, S.; Kang, D. H. Use of Organic Acids to Inactivate *Escherichia Coli* O157: H7, *Salmonella Typhimurium*, and *Listeria Monocytogenes* on Organic Fresh Apples and Lettuce. *J. Food Sci.* **2011**, *76* (6), 293-298. https://doi.org/10.1111/j.1750-3841.2011.02205.x.

Parry, C.; Blonquist, J. M.; Bugbee, B. In Situ Measurement of Leaf Chlorophyll Concentration: Analysis of the Optical/Absolute Relationship. *Plant, Cell Environ.* **2014**,

37 (11), 2508–2520. https://doi.org/10.1111/pce.12324.

Patil, S.; Valdramidis, V. P.; Karatzas, K. A. G.; Cullen, P. J.; Bourke, P. Assessing the Microbial Oxidative Stress Mechanism of Ozone Treatment through the Responses of *Escherichia Coli* Mutants. *J. Appl. Microbiol.* **2011**, *111* (1), 136–144. https://doi.org/10.1111/j.1365-2672.2011.05021.x.

Payá, P.; Anastassiades, M.; MacK, D.; Sigalova, I.; Tasdelen, B.; Oliva, J.; Barba, A. Analysis of Pesticide Residues Using the Quick Easy Cheap Effective Rugged and Safe (QuEChERS) Pesticide Multiresidue Method in Combination with Gas and Liquid Chromatography and Tandem Mass Spectrometric Detection. *Anal. Bioanal. Chem.* **2007**, *389* (6), 1697–1714. https://doi.org/10.1007/s00216-007-1610-7.

Pekárek, S. DC Corona Ozone Generation Enhanced by TiO_2 Photocatalyst. *Eur. Phys. J. D.* **2008**, *50 (2)*, 171-175.https://doi.org/10.1140/epjd/e2008-00216-x.

Perini, J. A.; Perez-Moya, M.; Nogueira, R. F. P. Photo-Fenton Degradation Kinetics of Low Ciprofloxacin Concentration Using Different Iron Sources and PH. *J. Photochem. Photobiol. A Chem.* **2013**, *259*, 53–58. https://doi.org/10.1016/j.jphotochem.2013.03.002.

Perrin, A.; Basset-Mens, C.; Gabrielle, B. Life Cycle Assessment of Vegetable Products: A Review Focusing on Cropping Systems Diversity and the Estimation of Field Emissions. *Int. J. Life Cycle Assess.* **2014**, *19* (6), 1247–1263. https://doi.org/10.1007/s11367-014-0724-3.

Persoone, G.; Marsalek, B.; Blinova, I.; Törökne, A.; Zarina, D.; Manusadzianas, L.; Nalecz-Jawecki, G.; Tofan, L.; Stepanova, N.; Tothova, L.; et al. A Practical and User-Friendly Toxicity Classification System with Microbiotests for Natural Waters and Wastewaters. *Environ. Toxicol.* **2003**, *18* (6), 395–402. https://doi.org/10.1002/tox.10141.

Pesonen, H.; Aksela, R.; Laasonen, K. Density Functional Complexation Study of Metal Ions with Amino Polycarboxylic Acid Ligands: EDDHA and HBED in Comparison to EDTA, EDDS, ODS, and ISA. *J. Mol. Struct. THEOCHEM* **2007**, *804* (1–3), 101–110. https://doi.org/10.1016/j.theochem.2006.10.013.

Pietrzak, D.; Kania, J.; Malina, G.; Kmiecik, E.; Wtor, K. Pesticides from the EU First and Second Watch Lists in the Water Environment. *Clean - Soil, Air, Water.* **2019**, *47* (7), 1–13. https://doi.org/10.1002/clen.201800376.

Pignatello, J. J. Dark and Photoassisted Fe^{3+}-Catalyzed Degradation of Chlorophenoxy Herbicides by Hydrogen Peroxide. **1992**, *26* (5), 944–951. https://doi.org/10.1021/es00029a012.

Pignatello, J. J.; Oliveros, E.; MacKay, A. Advanced Oxidation Processes for Organic Contaminant Destruction Based on the Fenton Reaction and Related Chemistry. *Crit. Rev. Environ. Sci. Technol.* **2006**, *36*, 1–84. https://doi.org/10.1080/10643380500326564.

Pocostales, J. P.; Sein, M. M.; Knolle, W.; Von Sonntag, C.; Schmidt, T. C. Degradation of Ozone-Refractory Organic Phosphates in Wastewater by Ozone and Ozone/Hydrogen Peroxide (Peroxone): The Role of Ozone Consumption by Dissolved Organic Matter. *Environ. Sci. Technol.* **2010**, *44* (21), 8248–8253. https://doi.org/10.1021/es1018288.

Polo-López, M. I.; Castro-Alférez, M.; Nahim-Granados, S.; Malato, S.; Fernández-Ibáñez, P. *Legionella Jordanis* Inactivation in Water by Solar Driven Processes: EMA-QPCR versus Culture-Based Analyses for New Mechanistic Insights. *Catal. Today.* **2017**, *287*, 15–21. https://doi.org/10.1016/j.cattod.2016.10.029.

Polo-López, M. I.; Castro-Alférez, M.; Oller, I.; Fernández-Ibáñez, P. Assessment of Solar Photo-Fenton, Photocatalysis, and H_2O_2 for Removal of Phytopathogen Fungi Spores in Synthetic and Real Effluents of Urban Wastewater. *Chem. Eng. J.* **2014**, *257*, 122–130. https://doi.org/10.1016/j.cej.2014.07.016.

Polo-López, M. I.; García-Fernández, I.; Oller, I.; Fernández-Ibáñez, P. Solar Disinfection of Fungal Spores in Water Aided by Low Concentrations of Hydrogen Peroxide. *Photochem. Photobiol. Sci.* **2011**, *10* (3), 381–388. https://doi.org/10.1039/c0pp00174k.

Polo-López, M. I.; García-Fernández, I.; Velegraki, T.; Katsoni, A.; Oller, I.; Mantzavinos, D.; Fernández-Ibáñez, P. Mild Solar Photo-Fenton: An Effective Tool for the Removal of Fusarium from Simulated Municipal Effluents. *Appl. Catal. B Environ.* **2012**, *111–112*, 545–554. https://doi.org/10.1016/j.apcatb.2011.11.006.

Polo-López, M. I.; Oller, I.; Fernández-Ibáñez, P. Benefits of Photo-Fenton at Low Concentrations for Solar Disinfection of Distilled Water. A Case Study: *Phytophthora Capsici. Catal. Today.* **2013**, *209*, 181–187. https://doi.org/10.1016/j.cattod.2012.10.006.

Priac, A.; Badot, P. M.; Crini, G. Évaluation de La Phytotoxicité d'eaux de Rejets via Lactuca Sativa : Paramètres Des Tests de Germination et d'élongation. *Comptes Rendus - Biol.* **2017**, *340* (3), 188–194. https://doi.org/10.1016/j.crvi.2017.01.002.

Qadir, M.; Scott, C. A. Non-Pathogenic Trade-Offs of Wastewater Irrigation. In Wastewater Irrigation and Health: Assessing and Mitigating Risk in Low-income Countries; **2009**. https://doi.org/10.4324/9781849774666.

Qi, H.; Huang, Q.; Hung, Y. C. Efficacy of Activated Persulfate in Pathogen Inactivation: A Further Exploration. *Food Res. Int.* **2019**, *120*, 425–431. https://doi.org/10.1016/j.foodres.2019.03.012.

Rasheduzzaman, M.; Singh, R.; Haas, C. N.; Tolofari, D.; Yassaghi, H.; Hamilton, K. A.; Yang, Z.; Gurian, P. L. Reverse QMRA as a Decision Support Tool: Setting Acceptable Concentration Limits for *Pseudomonas Aeruginosa* and *Naegleria Fowleri. Water.* **2019,** *11*, 1850. https://doi.org/10.3390/w11091850.

RD. **2007**. Real Decreto 1620/2007, por el que se establece el régimen jurídico de la reutilización de las aguas depuradas. «BOE» núm. 294, de 8 de diciembre de 2007, BOE-A-2007-21092, 50639-50661. https://www.boe.es/eli/es/rd/2007/12/07/1620.

Rendueles, E.; Omer, M. K.; Alvseike, O.; Alonso-Calleja, C.; Capita, R.; Prieto, M. Microbiological Food Safety Assessment of High Hydrostatic Pressure Processing: A Review. *LWT - Food Sci. Technol.* **2011**, *44 (5)*, 1251–1260. https://doi.org/10.1016/j.lwt.2010.11.001

Rice, R. G. Applications of Ozone for Industrial Wastewater Treatment - A Review. *Ozone Sci. Eng.* **1996**, *18* (6), 477-515. https://doi.org/10.1080/01919512.1997.10382859.

Rincón, A. G.; Pulgarin, C. Comparative Evaluation of Fe^{3+} and TiO_2 Photoassisted Processes in Solar Photocatalytic Disinfection of Water. *Appl. Catal. B Environ.* **2006**, *63* (3–4), 222–231. https://doi.org/10.1016/j.apcatb.2005.10.009.

Rizzo, L. Bioassays as a Tool for Evaluating Advanced Oxidation Processes in Water and Wastewater Treatment. *Water Res.* **2011**, 45 (15), 4311-4340. https://doi.org/10.1016/j.watres.2011.05.035.

Rizzo, L.; Krätke, R.; Linders, J.; Scott, M.; Vighi, M.; de Voogt, P. Proposed EU Minimum Quality Requirements for Water Reuse in Agricultural Irrigation and Aquifer Recharge: SCHEER Scientific Advice. *Curr. Opin. Environ. Sci. Heal.* **2018a**, *2*, 7–11. https://doi.org/10.1016/j.coesh.2017.12.004.

Rizzo, L.; Lofrano, G.; Gago, C.; Bredneva, T.; Iannece, P.; Pazos, M.; Krasnogorskaya, N.; Carotenuto, M. Antibiotic Contaminated Water Treated by Photo Driven Advanced Oxidation Processes: Ultraviolet/H_2O_2 vs Ultraviolet/Peracetic Acid. *J. Clean. Prod.* **2018b**, *205*, 67–75. https://doi.org/10.1016/j.jclepro.2018.09.101.

Rizzo, L.; Malato, S.; Antakyali, D.; Beretsou, V. G.; Đolić, M. B.; Gernjak, W.; Heath, E.; Ivancev-Tumbas, I.; Karaolia, P.; Lado Ribeiro, A. R.; et al. Consolidated vs New Advanced Treatment Methods for the Removal of Contaminants of Emerging Concern from Urban Wastewater. *Sci. Total Environ.*, **2019**, *655*, 986–1008. https://doi.org/10.1016/j.scitotenv.2018.11.265.

Rodríguez-Chueca, J.; Polo-López, M. I.; Mosteo, R.; Ormad, M. P.; Fernández-Ibáñez, P. Disinfection of Real and Simulated Urban Wastewater Effluents Using a Mild Solar Photo-Fenton. *Appl. Catal. B Environ.* **2014**, *150–151*, 619–629. https://doi.org/10.1016/j.apcatb.2013.12.027.

Ruales-Lonfat, C.; Barona, J. F.; Sienkiewicz, A.; Vélez, J.; Benítez, L. N.; Pulgarín, C. Bacterial Inactivation with Iron Citrate Complex: A New Source of Dissolved Iron in Solar Photo-Fenton Process at near-Neutral and Alkaline PH. *Appl. Catal. B Environ.* **2016**, *180*, 379–390. https://doi.org/10.1016/j.apcatb.2015.06.030.

Ruales-Lonfat, C.; Benítez, N.; Sienkiewicz, A.; Pulgarín, C. Deleterious Effect of Homogeneous and Heterogeneous Near-Neutral Photo-Fenton System on Escherichia Coli. Comparison with Photo-Catalytic Action of TiO_2 during Cell Envelope Disruption. *Appl. Catal. B Environ.* **2014**, *160–161* (1), 286–297. https://doi.org/10.1016/j.apcatb.2014.05.001.

Ruíz-Delgado, A.; Roccamante, M. A.; Oller, I.; Agüera, A.; Malato, S. Natural

Chelating Agents from Olive Mill Wastewater to Enable Photo-Fenton-like Reactions at Natural PH. *Catal. Today* **2019**, *328*, 281–285. https://doi.org/10.1016/j.cattod.2018.10.051.

Sadoff, C.W., Hall, J.W., Grey, D., Aerts, J.C.J.H., Ait-Kadi, M., Brown, C., Cox, A., Dadson, S., Garrick, D., Kelman, J., McCornick, P., Ringler, C., Rosegrant, M., Whittington, D.; Wiberg, D. Securing Water, Sustaining Growth: Report of the GWP/OECD Task, Force on Water Security and Sustainable Growth, University of Oxford, UK, **2015**, 1-180.

SANTE 11813/2017 Method Validation and Quality Control Procedures for Pesticide Residues Analysis in Food and Feed, **2017.**

Santos, M. I.; Cavaco, A.; Gouveia, J.; Novais, M. R.; Nogueira, P. J.; Pedroso, L.; Ferreira, M. A. S. S. Evaluation of Minimally Processed Salads Commercialized in Portugal. *Food Control* **2012**, *23* (1), 275–281. https://doi.org/10.1016/j.foodcont.2011.06.022.

Sbai, H. Responses of Two Apiaceae Species to Direct Iron Deficiency. *Int. J. Photochem. Photobiol.* **2019**, *2* (1), 16. https://doi.org/10.11648/j.ijpp.20180201.14.

Schnabel, U.; Andrasch, M.; Stachowiak, J.; Weit, C.; Weihe, T.; Schmidt, C.; Muranyi, P.; Schlüter, O.; Ehlbeck, J. Sanitation of Fresh-Cut Endive Lettuce by Plasma Processed Tap Water (PPtW) – Up-Scaling to Industrial Level. *Innov. Food Sci. Emerg. Technol*. **2019**, *53*, 45–55. https://doi.org/10.1016/j.ifset.2017.11.014.

Schwarzenbach, R. P.; Egli, T.; Hofstetter, T. B.; von Gunten, U.; Wehrli, B. Global Water Pollution and Human Health. *Annu. Rev. Environ. Resour.* **2010**, *35* (1), 109–136. https://doi.org/10.1146/annurev-environ-100809-125342.

Schwarzenbach, R. P.; Escher, B. I.; Fenner, K.; Hofstetter, T. B.; Johnson, C. A.; von Gunten, U.; Wehrli, B. The Challenge of Micropollutants in Aquatic Systems. *Science.* **2006**, *313* (5790), 1072-1077. https://doi.org/10.1126/science.1127291.

Sciacca, F.; Rengifo-Herrera, J. A.; Wéthé, J.; Pulgarin, C. Solar Disinfection of Wild Salmonella Sp. in Natural Water with a 18L CPC Photoreactor: Detrimental Effect of Non-Sterile Storage of Treated Water. *Sol. Energy.* **2011**, *85* (7), 1399–1408. https://doi.org/10.1016/j.solener.2011.03.022.

Selma, M. V.; Allende, A.; López-Gálvez, F.; Conesa, M. A.; Gil, M. I. Disinfection Potential of Ozone, Ultraviolet-C and Their Combination in Wash Water for the Fresh-Cut Vegetable Industry. *Food Microbiol.* **2008a**, *25* (6), 809–814. https://doi.org/10.1016/j.fm.2008.04.005.

Selma, M. V.; Allende, A.; López-Gálvez, F.; Conesa, M. Á.; Gil, M. I. Heterogeneous Photocatalytic Disinfection of Wash Waters from the Fresh-Cut Vegetable Industry. *J. Food Prot.* **2008b**, 71 (2), 286–292. https://doi.org/10.4315/0362-028x-71.2.286.

Selma, M. V.; Beltrán, D.; Allende, A.; Chacón-Vera, E.; Gil, M. I. Elimination by Ozone of Shigella Sonnei in Shredded Lettuce and Water. *Food Microbiol.* **2007**, *24* (5),

492–499. https://doi.org/10.1016/j.fm.2006.09.005.

Semenov, A. V.; Van Overbeek, L.; Van Bruggen, A. H. C. Percolation and Survival of *Escherichia Coli* O157:H7 and *Salmonella Enterica Serovar Typhimurium* in Soil Amended with Contaminated Dairy Manure or Slurry. *Appl. Environ. Microbiol.* **2009**, *75* (10), 3206–3215. https://doi.org/10.1128/AEM.01791-08.

Serna-Galvis, E. A.; Vélez-Peña, E.; Osorio-Vargas, P. A.; Jiménez, J. N.; Salazar-Ospina, L.; Guaca-González, Y. M.; Torres-Palma, R. A. Inactivation of Carbapenem-Resistant Klebsiella Pneumoniae by Photo-Fenton: Residual Effect, Gene Evolution and Modifications with Citric Acid and Persulfate. *Water Res.* **2019**, *161*, 354-363. https://doi.org/10.1016/j.watres.2019.06.024.

Shiklomanov I. A., World fresh water resources, in: *Water in crisis: A guide to the world's fresh water resources*, (ed. Gleick P. H.), Oxford University Press, New York, **1993**,13–24.

Sichel, C.; Fernández-Ibáñez, P.; de Cara, M.; Tello, J. Lethal Synergy of Solar UV-Radiation and H_2O_2 on Wild *Fusarium Solani* Spores in Distilled and Natural Well Water. *Water Res.* **2009**, 43 (7), 1841-1850. https://doi.org/10.1016/j.watres.2009.01.017.

Slamet, W.; Purbajanti, E. D.; Darmawati, A.; Fuskhah, E. Leaf Area Index, Chlorophyll, Photosynthesis Rate of Lettuce (*Lactuca Sativa*) under N-Organic Fertilizer. *Indian J. Anim. Res.* **2017**, *51* (4), 365–369. https://doi.org/10.18805/ijare.v51i04.8424.

Smetanska, I., Hunaefi, D., Barbosa-Cánovas, G.V. Nonthermal technologies to extendthe shelf life of fresh-cut fruits and vegetables. In: Yanniotis, S. (Ed.), et al., Advances in Food Process Engineering Research and Applications, Food Engineering Series. **2013**, 375–412. doi:10.1007/978-1-4614-7906-2_18.

Smetanska, I.; Hunaefi, D.; Barbosa-Cánovas, G. V. Nonthermal Technologies to Extend the Shelf Life of Fresh-Cut Fruits and Vegetables. In *Food Engineering Series*; Springer, **2013**; 375–413. https://doi.org/10.1007/978-1-4614-7906-2_18.

Sobrero, M. C.; Ronco, A. Toxicity Test with Lettuce Seeds *Lactuca Sativa* L. *IMTA* **2004**, 71-79. https://doi.org/10.1017/CBO9781107415324.004.

Soltermann, F.; Abegglen, C.; Tschui, M.; Stahel, S.; von Gunten, U. Options and Limitations for Bromate Control during Ozonation of Wastewater. *Water Res.* **2017**, *116*, 76–85. https://doi.org/10.1016/j.watres.2017.02.026.

Soriano-Molina, P.; Plaza-Bolaños, P.; Lorenzo, A.; Agüera, A.; García Sánchez, J. L.; Malato, S.; Sánchez Pérez, J. A. Assessment of Solar Raceway Pond Reactors for Removal of Contaminants of Emerging Concern by Photo-Fenton at Circumneutral PH from Very Different Municipal Wastewater Effluents. *Chem. Eng. J.* **2019**, *366,141-149.* https://doi.org/10.1016/j.cej.2019.02.074.

Sousa, J. C. G.; Ribeiro, A. R.; Barbosa, M. O.; Pereira, M. F. R.; Silva, A. M. T. A Review on Environmental Monitoring of Water Organic Pollutants Identified by EU

Guidelines. *J. Hazard. Mater.* **2018**, 344, 146–162. https://doi.org/10.1016/j.jhazmat.2017.09.058.

Spricigo, D. A.; Bardina, C.; Cortés, P.; Llagostera, M. Use of a Bacteriophage Cocktail to Control *Salmonella* in Food and the Food Industry. *Int. J. Food Microbiol.* **2013**, *165* (2), 169–174. https://doi.org/10.1016/j.ijfoodmicro.2013.05.009.

Spuhler, D.; Andrés Rengifo-Herrera, J.; Pulgarin, C. The Effect of Fe^{2+}, Fe^{3+}, H_2O_2 and the Photo-Fenton Reagent at near Neutral PH on the Solar Disinfection (SODIS) at Low Temperatures of Water Containing *Escherichia Coli* K12. *Appl. Catal. B Environ.* **2010**, *96* (1–2), 126–141. https://doi.org/10.1016/j.apcatb.2010.02.010.

Stockholm Convention. **2008**. http://chm.pops.int/. (Accessed May 18, 2019).

Storz, G.; Jacobson, F. S.; Tartaglia, L. A.; Morgan, R. W.; Silveira, L. A.; Ames, B. N. An Alkyl Hydroperoxide Reductase Induced by Oxidative Stress in *Salmonella Typhimurium* and *Escherichia Coli*: Genetic Characterization and Cloning of Ahp. *J. Bacteriol.* **1989**, *171* (4), 2049–2055. https://doi.org/10.1128/jb.171.4.2049-2055.1989.

Teunis, P. F. M.; Ogden, I. D.; Strachan, N. J. C. Hierarchical Dose Response of *E. Coli* O157:H7 from Human Outbreaks Incorporating Heterogeneity in Exposure. *Epidemiol. Infect.* **2008**, *136* (6), 761–770. https://doi.org/10.1017/S0950268807008771.

Tomas, N.; Tiwari, B. K. Sustainable Cleaning and Sanitation in the Food Industry. In *Sustainable Food Processing*; Wiley Blackwell, **2013**; 363–376. https://doi.org/10.1002/9781118634301.ch15.

Tonney, F. O.; Greer, F. E.; Liebig, G. F. The Minimal "Chlorine Death Points" of Bacteria. *Am. J. Public Heal. Nations Heal.* **1928**, *20* (5), 503–508. https://doi.org/10.2105/ajph.20.5.503.

Topac, B. S.; Alkan, U. Comparison of Solar/H_2O_2 and Solar Photo-Fenton Processes for the Disinfection of Domestic Wastewaters. *KSCE J. Civ. Eng.* **2016**, *20* (7), 2632–2639. https://doi.org/10.1007/s12205-016-0416-6.

Touati, D. Transcriptional and Posttranscriptional Regulation of Manganese Superoxide Dismutase Biosynthesis in *Escherichia Coli*, Studied with Operon and Protein Fusions. *J. Bacteriol.* **1988**, *170* (6), 2511–2520. https://doi.org/10.1128/jb.170.6.2511-2520.1988.

Trapp, S. Modelling Uptake into Roots and Subsequent Translocation of Neutral and Ionisable Organic Compounds. *Pest Manag. Sci.* **2000**, *56* (9), 767–778. https://doi.org/10.1002/1526-4998(200009)56:9<767::AID-PS198>3.0.CO;2-Q.

Ubomba-Jaswa, E.; Navntoft, C.; Polo-López, M. I.; Fernandez-Ibáñez, P.; McGuigan, K. G. Solar Disinfection of Drinking Water (SODIS): An Investigation of the Effect of UV-A Dose on Inactivation Efficiency. *Photochem. Photobiol. Sci.* **2009**, *8* (5), 587–595. https://doi.org/10.1039/b816593a.

UN. **2016**. Final list of proposed Sustainable Development Goal indicators. https://sustainabledevelopment.un.org/content/documents/11803Official-List-of-

Proposed-SDG-Indicators.pdf. (Accessed July 05, 2019).

UNESCO. **2019**. WWAP (World Water Assessment Programme). The United Nations World Water Development Report 2019: Leaving No One Behind.

USEPA. **1989**. Protocols for short-term toxicity screening of hazardous waste sites.Protocols for Short Term Toxicity Screening of Hazardous Waste Sites. A.8.7. Lettuce Root Elongation (*Lactuca sativa*). Chicago, EUA.

Utzig, L. M.; Lima, R. M.; Gomes, M. F.; Ramsdorf, W. A.; Martins, L. R. R.; Liz, M. V.; Freitas, A. M. Ecotoxicity Response of Chlorpyrifos in Aedes Aegypti Larvae and Lactuca Sativa Seeds after UV/H_2O_2 and UVC Oxidation. *Ecotoxicol. Environ. Saf.* **2019**, *169*, 449–456. https://doi.org/10.1016/j.ecoenv.2018.11.003.

Vaara, M. Agents That Increase the Permeability of the Outer Membrane. *Microbiol. Rev.* **1992**, *56* (3), 395–411.

Van der Linden, I.; Avalos Llano, K. R.; Eriksson, M.; De Vos, W. H.; Van Damme, E. J. M.; Uyttendaele, M.; Devlieghere, F. Minimal Processing of Iceberg Lettuce Has No Substantial Influence on the Survival, Attachment and Internalization of *E. Coli* O157 and *Salmonella*. *Int. J. Food Microbiol.* **2016**, *238*, 40–49. https://doi.org/10.1016/j.ijfoodmicro.2016.07.029.

Van Haute, S.; Sampers, I.; Holvoet, K.; Uyttendaelea, M. Physicochemical Quality and Chemical Safety of Chlorine as a Reconditioning Agent and Wash Water Disinfectant for Fresh-Cut Lettuce Washing. *Appl. Environ. Microbiol.* **2013**, *79* (9), 2850–2861. https://doi.org/10.1128/AEM.03283-12.

Van Haute, S.; Uyttendaele, M.; Sampers, I. Coagulation of Turbidity and Organic Matter from Leafy-Vegetable Wash-Water Using Chitosan to Improve Water Disinfectant Stability. *LWT - Food Sci. Technol.* **2015**, *64* (1), 337–343. https://doi.org/10.1016/j.lwt.2015.05.063.

Varghese, S.; Wu, A.; Park, S.; Imlay, K. R. C.; Imlay, J. A. Submicromolar Hydrogen Peroxide Disrupts the Ability of Fur Protein to Control Free-Iron Levels in *Escherichia Coli. Mol. Microbiol.* **2007**, *64* (3), 822-830.https://doi.org/10.1111/j.1365-2958.2007.05701.x.

Villegas-Guzman, P.; Giannakis, S.; Torres-Palma, R. A.; Pulgarin, C. Remarkable Enhancement of Bacterial Inactivation in Wastewater through Promotion of Solar Photo-Fenton at near-Neutral PH by Natural Organic Acids. *Appl. Catal. B Environ.* **2017**, *205*, 219–227. https://doi.org/10.1016/j.apcatb.2016.12.021.

Vione, D.; Falletti, G.; Maurino, V.; Minero, C.; Pelizzetti, E.; Malandrino, M.; Ajassa, R.; Olariu, R. I.; Arsene, C. Sources and Sinks of Hydroxyl Radicals upon Irradiation of Natural Water Samples. *Environ. Sci. Technol.* **2006**,*40*, 3775-3781. https://doi.org/10.1021/es052206b.

Von Gunten, U. Ozonation of Drinking Water: Part I. Oxidation Kinetics and Product Formation. *Wat. Res.* **2003**,*37 (7),* 1443-1467. https://doi.org/10.1016/S0043-

1354(02)00457-8.

Von Sonntag, C.; Von Gunten, U. Chemistry of Ozone in Water and Wastewater Treatment: From Basic Principles to Applications, IWA Publishing, **2012**.

Wachtel, M. R.; Charkowski, A. O. Cross-Contamination of Lettuce with *Escherichia Coli* O157:H7. *J. Food Prot.* **2002**, *65* (3), 465–470. https://doi.org/10.4315/0362-028X-65.3.465.

Wadamori, Y.; Gooneratne, R.; Hussain, M. A. Outbreaks and Factors Influencing Microbiological Contamination of Fresh Produce. *J. Sci. Food Agric.*, **2017**, *97(5),* 1396–1403. https://doi.org/10.1002/jsfa.8125.

Wang, H.; Zhan, J.; Yao, W.; Wang, B.; Deng, S.; Huang, J.; Yu, G.; Wang, Y. Comparison of Pharmaceutical Abatement in Various Water Matrices by Conventional Ozonation, Peroxone (O_3/H_2O_2), and an Electro-Peroxone Process. *Water Res.* **2018**, *130*, 127–138. https://doi.org/10.1016/j.watres.2017.11.054.

Wei, C.; Zhang, F.; Hu, Y.; Feng, C.; Wu, H. Ozonation in Water Treatment: The Generation, Basic Properties of Ozone and Its Practical Application. *Rev. Chem. Eng.* **2017**, *33* (1) 49-89. https://doi.org/10.1515/revce-2016-0008.

WHO. **2004**. Guidelines for drinking water quality,Geneva.

WHO. **2005**. Diet, nutrition, and the prevention of chronic diseases. Report of a WHO Study Group. Geneva, World Health Organization, Technical Report Series, No. 916.

WHO. **2006**. Volume II of the Guidelines for the Safe Use of Wastewater, Excreta and Greywater: Wastewater Use in Agriculture; Paris, France.

WHO. **2011**. World Health Organization. Guidelines for Drinking-water Quality, 4th edition.

Winfield, M. D.; Groisman, E. A. Phenotypic Differences between *Salmonella* and *Escherichia Coli* Resulting from the Disparate Regulation of Homologous Genes. Proc. *Natl. Acad. Sci*. **2004**, *101* (49), 17162–17167. https://doi.org/10.1073/pnas.0406038101.

Winfield, M. D.; Groisman, E. A. Role of Nonhost Environments in the Lifestyles Of. **2003**, *69* (7), 3687–3694. https://doi.org/10.1128/AEM.69.7.3687.

Wojtyla, Ł.; Lechowska, K.; Kubala, S.; Garnczarska, M. Different Modes of Hydrogen Peroxide Action during Seed Germination. *Front. Plant Sci.* **2016**, *7* , 1–16. https://doi.org/10.3389/fpls.2016.00066.

Ylivainio, K. Influence of Iron-Chelates on Trace Element Uptake from Two Calcareous Soils and the Activity of Oxygen-Scavenging Enzymes in Lettuce. *J. Plant Nutr.* **2010**, *33* (1), 80–94. https://doi.org/10.1080/01904160903391107.

Young, B. J.; Riera, N. I.; Beily, M. E.; Bres, P. A.; Crespo, D. C.; Ronco, A. E. Toxicity of the Effluent from an Anaerobic Bioreactor Treating Cereal Residues on

Lactuca Sativa. *Ecotoxicol. Environ. Saf.* **2012**, 76, 182-186. https://doi.org/10.1016/j.ecoenv.2011.09.019.

Yu, R.; Liu, Q.; Liu, J.; Wang, Q.; Wang, Y. Concentrations of Organophosphorus Pesticides in Fresh Vegetables and Related Human Health Risk Assessment in Changchun, Northeast China. *Food Control.* **2016**, *60*, 353–360. https://doi.org/10.1016/j.foodcont.2015.08.013.

Yuan, X.; Lacorte, S.; Cristale, J.; Dantas, R. F.; Sans, C.; Esplugas, S.; Qiang, Z. Removal of Organophosphate Esters from Municipal Secondary Effluent by Ozone and UV/H$_2$O$_2$ Treatments. *Sep. Purif. Technol.* **2015**, *156*, 1028–1034. https://doi.org/10.1016/j.seppur.2015.09.052.

CHAPTER 12
ANNEX

Annex A. Fresh-cut wastewater characterization

In chapter 4.1 (*Synthetic water development and disinfection assessment under controlled conditions)*, it is presented the microbiological and physic-chemical characteristics of some real FCWW samples analyzed: the first and the last one of the wash cycle of each processing line. Nevertheless, all the samples collected (8 per each processing line: spinach and lettuce) were analyzed and their detailed physicochemical and microbiological characterization is presented in this annex. Moreover, the data of pesticides screening of these samples is also presented.

Physicochemical characterization

Table A.1. pH, conductivity, turbidity, total suspended soils (TSS) and total volatile soils (TVS) of real samples obtained from 'Verdifresh' company.

Spinach line	pH	Conductivity (µS/cm)	Turbidity (NTU)	TSS/TVS (mg/mL)
6:20 am	6.26	381	6.12	< 0.1/< 0.1
8:20 am	6.33	364	12	< 0.1/< 0.1
11:20 am	6.34	364	22.6	< 0.1/< 0.1
13:20 pm	6.33	478	71.9	< 0.1/< 0.1
15:20 pm	6.27	730	137	0.31/0.24
17:20 pm	6.2	1077	256	0.58/0.5
19:20 pm	6.27	1109	360	0.65/0.54
22:00 pm	6.2	1239	360	0.52/0.44
Lettuce line samples	pH	Conductivity (µS/cm)	Turbidity (NTU)	TSS/TVS (mg/mL)
6:20 am	6.37	334	2.89	< 0.1/< 0.1
8:20 am	6.44	417	2.89	< 0.1/< 0.1
11:20 am	6.33	723	26	< 0.1/< 0.1
13:20 pm	6.19	888	45	< 0.1/< 0.1
15:20 pm	6.19	906	50.1	< 0.1/< 0.1
17:20 pm	6.28	1090	76	< 0.1/< 0.1
19:20 pm	6.25	1041	58.9	< 0.1/< 0.1
22:00 pm	6.34	951	45.5	< 0.1/< 0.1

Table A.2. Total dissolved carbon (TDC), dissolved inorganic carbon (DIC), dissolved organic carbon (DOC) and chemical oxygen demand (DQO) of real samples obtained from 'Verdifresh' company.

Spinach line samples	TDC (mg/L)	IC (mg/L)	DOC (mg/L)	DQO (mg 0_2/L)
6:20 am	5.12	1.86	3.27	81.54
8:20 am	10.04	1.24	8.80	88.52
11:20 am	15.31	1.28	14.02	99.57
13:20 pm	35.27	0.99	34.28	142.21
15:20 pm	54.79	1.24	53.55	182.91
17:20 pm	79.25	0.95	78.30	308.45
19:20 pm	86.53	1.20	85.33	304.96
22:00 pm	110.50	1.34	109.20	361.56
Lettuce line samples	TDC (mg/L)	IC (mg/L)	DOC (mg/L)	DQO (mg 0_2/L)
6:20 am	21.13	1.02	20.12	338.91
8:20 am	199.50	1.29	198.70	782.76
11:20 am	344.80	0.80	344.00	1327.12
13:20 pm	456.40	0.80	455.60	1569.39
15:20 pm	490.80	0.79	490.00	1639.17
17:20 pm	583.50	0.76	582.70	1867.88
19:20 pm	551.60	0.74	550.90	1809.73
22:00 pm	531.20	0.84	530.40	1778.72

Table A.3. Ionic content: anions (mg/L) of real samples obtained from 'Verdifresh' company.

Spinach line samples	F^-	Cl^-	ClO_3^-	NO_2^-	NO_3^-	PO_4^{3-}	SO_4^{2-}
6:20 am	< 0.1	47.37	2.32	-	13.00	309.82	9.82
8:20 am	< 0.1	38.06	1.67	-	12.85	276.60	9.08
11:20 am	< 0.1	24.08	0.82	-	15.77	270.42	7.87
13:20 pm	0.16	57.71	0.87	-	30.49	294.45	25.66
15:20 pm	0.15	135.85	3.31	0.17	39.78	340.32	52.06
17:20 pm	0.20	195.87	6.28	0.19	53.25	419.63	97.89
19:20 pm	0.22	222.85	7.85	0.17	58.36	437.05	111.45
22:00 pm	0.32	318.45	12.39	0.18	66.24	542.26	145.90
Lettuce line samples	F^-	Cl^-	ClO_3^-	NO_2^-	NO_3^-	PO_4^{3-}	SO_4^{2-}
6:20 am	< 0.1	28.73	1.15	-	10.20	232.22	7.08
8:20 am	< 0.1	47.73	1.36	-	18.01	228.61	8.46
11:20 am	0.13	144.43	5.99	-	27.11	257.32	9.86
13:20 pm	0.16	207.77	8.97	-	34.91	333.14	11.64
15:20 pm	0.17	210.68	9.21	0.17	34.15	319.45	11.37
17:20 pm	0.18	259.03	11.78	0.18	43.73	343.18	12.44
19:20 pm	0.19	280.63	13.34	0.18	45.00	387.10	14.42
22:00 pm	0.21	269.94	12.88	0.18	40.88	407.15	14.58

Table A.4. Ionic content: cations (mg/L) of real samples obtained from 'Verdifresh' company.

Spinach line samples	Na$^+$	NH$_4^+$	K$^+$	Mg^{+2}	Ca^{+2}
6:20 am	31.67	-	2.16	6.26	47.23
8:20 am	21.66	-	2.90	6.06	41.09
11:20 am	12.14	-	5.50	6.53	42.36
13:20 pm	29.11	< 0.1	21.05	11.52	42.46
15:20 pm	74.07	< 0.1	42.31	17.05	40.80
17:20 pm	107.97	0.29	80.75	23.21	40.91
19:20 pm	130.55	0.27	95.26	23.97	43.31
22:00 pm	178.20	0.73	128.37	24.54	44.35
Lettuce line samples	Na$^+$	NH$_4^+$	K$^+$	Mg^{+2}	Ca^{+2}
6:20 am	18.11	1.71	2.68	5.04	40.18
8:20 am	22.04	1.61	27.04	5.57	39.04
11:20 am	77.14	0.32	48.60	6.39	34.07
13:20 pm	114.80	0.41	75.30	7.93	40.65
15:20 pm	117.92	0.40	77.98	7.77	43.26
17:20 pm	142.78	0.71	95.03	7.40	40.77
19:20 pm	167.04	3.41	101.57	9.33	48.95
22:00 pm	158.57	0.64	97.88	9.56	53.20

Table A.5. Ionic content: carboxylic acids (mg/L) of real samples obtained from 'Verdifresh' company.

Spinach line samples	Glycolate	Acetate	Propionate	Formiate	Pyruvate	DCA	Maleate	Oxalate
6:20 am	< 0.1	1.93	-	-	-	0.19	-	0.49
8:20 am	< 0.1	0.14	-	0.90	-	0.22	-	0.50
11:20 am	< 0.1	0.15	-	1.38	< 0.1	0.14	-	0.58
13:20 pm	0.14	0.19	-	1.59	< 0.1	0.13	< 0.1	1.15
15:20 pm	0.26	0.45	1.32	1.67	1.11	0.31	0.13	1.80
17:20 pm	0.85	0.40	2.87	2.31	1.63	0.46	0.59	3.08
19:20 pm	0.78	0.60	3.03	2.70	1.76	0.57	0.25	2.81
22:00 pm	1.01	0.53	2.71	2.46	2.17	0.81	0.92	4.50
Lettuce line samples*	Glycolate	Acetate	Propionate	Formiate	Pyruvate	DCA	Maleate	Oxalate
6:20 am	0.13	< 0.1	0.64	-	-	-	-	< 0.1
8:20 am	0.10	< 0.1	0.28	1.14	0.26	-	-	0.25
11:20 am	0.16	-	2.79	1.78	1.02	-	0.19	0.87
13:20 pm	0.36	-	4.68	2.37	1.41	-	1.73	2.20
15:20 pm	0.40	< 0.1	4.95	3.67	1.47	-	0.34	1.60
17:20 pm	0.17	0.17	5.69	2.37	1.93	-	0.98	2.37
19:20 pm	-	-	6.12	4.80	1.96	-	1.08	2.58
22:00 pm	0.15	0.11	6.42	4.22	2.11	0.24	0.52	2.82

In the samples taken at 19:20 and 22:00 for the lettuce line was detected methylamine at a concentration < 0.1 mg/L.

Microbiological characterization

All the samples were analyzed by the standard plate counting method

(LD: 2 CFU/mL) for the presence of :

- Total aerobic bacteria
- Total aerobic bacteria in vegetative form
- Total coliforms
- *E.coli* spp
- *Salmonella* spp
- *Enterococcus* spp

However, all samples were negative in the presence of total coliforms, *E.coli* spp, *Salmonella* spp and *Enterococcus* spp. The results obtained for total aerobic bacteria and total aerobic bacteria in vegetative form are presented in Table A.6.

Table A.6. Microbiological characterization of real samples obtained from 'Verdifresh' company.

Spinach line samples	Total aerobic bacteria (CFU/mL)	Total aerobic bacteria in vegetative form (CFU/mL)
6:20 am	LD	LD
8:20 am	LD	LD
11:20 am	LD	LD
13:20 pm	LD	LD
15:20 pm	200	50
17:20 pm	420	158
19:20 pm	60	92
22:00 pm	100	36
Lettuce line samples	Total aerobic bacteria (CFU/mL)	Total aerobic bacteria in vegetative form (CFU/mL)
6:20 am	LD	LD
8:20 am	200	LD
11:20 am	LD	LD
13:20 pm	36	LD
15:20 pm	4	LD
17:20 pm	LD	LD
19:20 pm	14	LD
22:00 pm	LD	LD

Pesticides screening

Table A.7. Pesticides screening of real samples obtained from 'Verdifresh' company.

	Spinach line samples (ng/L)				Lettuce line samples (ng/L)			
	6:20 am	**13:20 pm**	**19:20 pm**	**22:00 pm**	**6:20 am**	**13:20 pm**	**19:20 pm**	**22:00 pm**
Acetamiprid	70.9	148.3	4611.1	4099.7	644.6	2320.9	4387.2	4319.8
Azoxystrobin	9.0	25.9	412.6	480.5	-	-	-	-
Imidacloprid	-	-	911.3	1468.6	852.9	3233.2	4880.4	2896.0
Iprodione	-	1008	1583	1392	-	-	413	59
Metalaxyl	-	387.9	262.8	295.0	251.7	1044.0	1413.5	1024.6
Pirimicarb	-		26.9	54.1	-	-	-	-
Propamocarb	-	132.4	8655.0	42513.5	-	66.6	77.7	10
Simazine	-	-	196.1	131.2	-	-	74.0	10